VISUALISING MICROGLIA IN NEURODEGENERATIVE DISEASES

ERIK NUTMA

VISUALISING MICROGLIA IN NEURODEGENERATIVE DISEASES

Erik Nutma

The image on the front cover is a negative of The Bubble Nebula (NGC 7635) captured by the Hubble Space telescope. The Bubble Nebula is located 7,100 light-years away and was discovered by William Herschel in 1787. The seething star forming this nebula is 45 times more massive than our sun. Gas on the star gets so hot that it escapes away into space as a "stellar wind" moving at over 4 million miles per hour. This outflow sweeps up the cold, interstellar gas in front of it, forming the outer edge of the bubble. As the surface of the bubble's shell expands outward, it slams into dense regions of cold gas on one side of the bubble. This asymmetry makes the star appear dramatically off-center from the bubble, with its location in the 10 o'clock position in the Hubble view. The colours correspond to red for oxygen, pink for hydrogen and blue for nitrogen. I was drawn to this image because of the similarities between astronomy and visualising complex molecular processes in the human brain.

The font used for the chapter pages is a personally modified Gilbert Color Bold. The Gilbert font is a tribute font to honor the memory of Gilbert Baker, the creator of the LGBT Rainbow Flag. The Gilbert Color font was later designed to express diversity and inclusion.

The work described in this thesis was performed at the Department of Pathology of the Amsterdam UMC - location VUmc (Amsterdam, The Netherlands) under supervision of prof. dr. S. Amor and prof.dr. P. van der Valk and in collaboration with the Department of Brain Sciences of the Imperial College (London, United Kingdom) under supervision of dr. D.R.J. Owen.

Financial support for the printing of this thesis was kindly provided by the Stichting MS Research and by the Graduate School Neurosciences Amsterdam Rotterdam (ONWAR).

Printing: Ridderprint | www.ridderprint.nl

ISBN: 978-94-6458-048-8

VRIJE UNIVERSITEIT

Visualising microglia in neurodegenerative diseases

ACADEMISCH PROEFSCHRIFT

ter verkrijging van de graad Doctor of Philosophy aan
de Vrije Universiteit Amsterdam,
op gezag van de rector magnificus
prof.dr. J.J.G. Geurts,
in het openbaar te verdedigen
ten overstaan van de promotiecommissie
van de Faculteit der Geneeskunde
op donderdag 7 Juli 2022 om 11.45 uur
in een bijeenkomst van de universiteit,
De Boelelaan 1105

Door

Erik Nutma

Geboren te Leeuwarden

promotoren:	prof.dr. S. Amor prof.dr. P. van der Valk
copromotor:	dr. D.R.J. Owen
promotiecommissie:	prof.dr. J.M. Rozemuller prof.dr. M. Kipp prof.dr. D. Baker prof.dr. E.M. Hol dr. W. Scheper dr. J.J. Bajramovic dr. M. Bugiani

It has been said that the great events of the world take place in the brain.

- Oscar Wilde

Table of contents

General introduction

Adapted from:

Inflammation in CNS neurodegenerative diseases

Erik Nutma[†], Jodie Stephenson[†], Paul van der Valk, Sandra Amor

[†]shared first author

Immunology 2018; 154(2):204-219

Neuroinflammation in the central nervous system

The prevalence of neuroinflammatory and neurodegenerative diseases highly depends on the country surveyed, yet the most prevalent disease globally is dementia, with an estimated incidence of 9.33% worldwide[1]. The increase in the incidence of dementia, as with many neurodegenerative diseases, is in part due to the ageing population[3], since an ageing brain, or one following peripheral infections or other insults is 'primed' to render the central nervous system (CNS) more susceptible to damage[4]. Although neurodegenerative and neuroinflammatory diseases often have different aetiologies, a common feature is chronic activation of innate immune cells within the CNS, mainly microglia (Table 1), and in other diseases such as multiple sclerosis (MS), also the influx of peripheral immune cells across the blood-brain barrier (BBB). Microglia can be implicated as the primary cause of neuropathology in many CNS diseases and can induce neuronal cell death through both direct and indirect pathways. For example, when microglia are activated by infectious pathogens, aggregated proteins or superoxides, they can cause excitotoxic neuronal death by expressing iNOS, releasing glutamate or proteases such as cathepsins or matrix metalloproteases[5]. Additionally, activated microglia release tumor necrosis factor (TNF) increasing neuronal apoptosis[5]. Innate immunity in the CNS, and specifically microglia and astrocytes, are becoming increasingly implicated in neuropathology of CNS diseases due to the exponential increase of knowledge on microglia and astrocyte biology over the past decade. Due to this, there is an increasing need to monitor glial cell behaviour in vivo in patients during disease progression but also in response to therapies.

Innate immunity in the brain

Innate immunity is the first line of defence in infection, but also plays a key role in tissue repair, clearance of apoptotic cells and cellular debris as well as in response to tumours. While the key innate immune cells in the CNS are microglia and astrocytes, peripheral macrophages as well as oligodendrocytes contribute to innate immune responses in the CNS. Additionally, the immune system in the CNS is unique in that mostly occurs behind several CNS barriers (Figure 1).

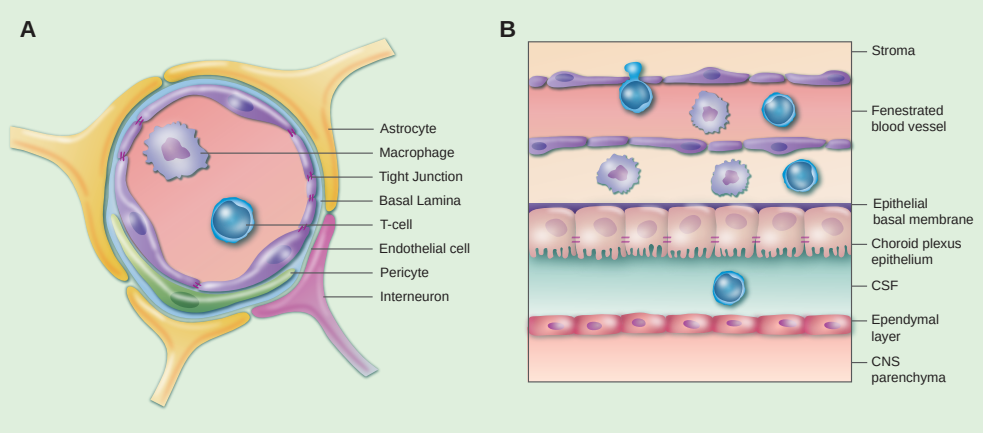

Figure 1. Blood–central nervous system (CNS) barriers. The blood–brain barrier (BBB) (a) and blood–spinal cord barrier (BSCB) limit potential immune cells, antibodies and soluble factors entering the CNS in health. Likewise, while the choroid plexus (CP) also limits cell migration, evidence suggests that regulatory T-cells enter the brain via the CP (b) during health in order to ensure surveillance of the CNS. CSF, cerebrospinal fluid.

Table 1. Current and predicted incidence of neuroinflammatory diseases

Disease	(Proposed) Aetiology	Innate immune response involvement	Adaptive immune response involvement	Incidence % or number/ 100000	Predicted change in prevalence	Ref
MS	Autoimmune Viral	Microglial and macrophage activation, ↑ROS, complement, ↑innate receptors, ↑cytokines, ↑chemokines	↑HSPs ↑neurotrophins Antibodies / T cells to CNS antigens.	9.64	↑2.4% per year	6,7
AD, other dementias	AD – misfolded and aggregated tau and Abeta	Activated and dystrophic microglia, ↑TNF-α, ↑IFN-γ, ↑chemokines, ↑complement, ↑TLRs	↑antibody and T-cell response	9.33%	↑3.3% per year (triple by 2050)	1,3,7
PD	Loss of dopaminergic neurons in SN due to α-syn-inclusions	↑TLRs, ↑CD14, activated NK cells, microglial activation, ↑IL-1β, ↑IL-6, ↑TNF-α	↑T-cells ↑antibody response	100-200	double in 25 years	7-9
HD	Expansion of CAG (Q) in huntingtin gene induces aberrant toxic protein	↑microglial proliferation, ↑complement,	not reported	0.02-9.71	↑15-20% per decade	7,10
SMA	SMN1 gene mutations	↑IL-6, ↑IL-1β	not reported	1-2	not reported	7,11
ALS (MND)	Aberrant aggregated proteins due to mutations SOD1, TDP; C9orf72 or FUS genes	↑complement, ↑CD14, ↑macrophages, ↑IL-6, ↑TNF-α	↑$CD4^+$ ↑$CD8^+$ T-cells	1.9	↑69% in 25 years	7,11, 12
Prion diseases	Infectious forms of misfolded aggregated forms of prion protein	↑microglial activation, ↑IL-1β, ↑IL-6, ↑complement, ↑ROS, mast cells expressing PrP	B cells aid transport of PrP	variable	not reported	7
Stroke	Ischemia or Haemorrhage	↑lymphopenia, ↑NK cells, ↑IL-10	↑Th2 responses	115	↑44% in 20 years	13,14
TBI	Open and head Injury, Deceleration Injuries, Chemical/Toxic, Hypoxia, Tumors,	↑pro-inflammatory cytokines, ↑TLRs	↑T-cells ↑B-cells	295	not reported	7,15
HIV/AIDS	HIV encephalopathy, toxoplasmosis, PML	↓IL-27, ↓IFN-γ, ↓CD4 cells, ↑IL-4	↓T-cells, immune-senescence	0.8%	depending on country	16
Meningitis	Bacterial and viral infections	↑IL-6, ↑TNF-α, ↑NK cells, ↑microglial activation	↑T-cells ↑B-cells	0.2-1000	outbreak dependent	17,18
Ageing	Natural event	↑proinflammatory cytokines, ↓NK cell function	↓T-cells	n/a	n/a	19
Epilepsy	Unprovoked seizures, febrile events, autoantibodies	↑proinflammatory cytokines, ↑chemokines, ↑TLRs, ↑complement	↑autoantibodies T and B-cell activation	45-81.7	↑	20-22

Table 1. Current and predicted incidence of neuroinflammatory diseases *(continued)*

Disease	(Proposed) Aetiology	Innate immune response involvement	Adaptive immune response involvement	Incidence % or number/ 100000	Predicted change in prevalence	Ref
Autism	Genetic / Environmental	↑proinflammatory cytokines	↓T-cells	425-760	variable	23-25
Depression	Multifactorial e.g. genetics, hormonal	Microglial activation, ↑ cytokines, ↑chemokines	↑ T-reg cells	3%	↑	26-28
Schizophrenia	Multifactorial	Microglial activation, ↑ROS, ↑proinflammatory cytokines, ↑chemokines, ↑TLRs, ↓NK cells	not reported	18.5	not reported	29-31
Bipolar disorder	Genetic / Environmental	Microglial activation, ↑proinflammatory cytokines, ↑complement, ↑TNF-α	↑T-cell activation	2.4%	debated	32-34

Abbreviations: AD, Alzheimer's disease; ALS, amyotrophic lateral sclerosis; APP, amyloid-β precursor protein; CD, cluster of differentiation; CNS, central nervous system; FUS, Fused in Sarcoma; HD, Huntington's disease; HIV/AIDS, human immunodeficiency virus/acquired immunodeficiency syndrome; HSP, heat shock protein; IFN, interferon, IL, interleukin; MS, multiple sclerosis; NK, natural killer; PD, Parkinson's disease; PML, progressive multifocal leukoencephalopathy; ROS, reactive oxygen species; SMA, spinal muscular atrophy; SOD1, superoxide dismutase 1; SMN, Survival of Motor Neuron protein; SN, substantia nigra; TBI, traumatic brain injury; TDP, TAR DNA-binding protein 43 kDa; TLR, toll-like receptor; TNF, tumor necrosis factor.

Neuroimmune privilege and CNS barriers

The concept of immune privilege originated from Sir Peter Medawar's studies in the mid-20th century showing that tissue grafts in the CNS were not rejected. It also takes into account the presence of the BBB which was revealed by Paul Ehrlich's studies in the late 1800s showing that solutes and molecules were excluded from the brain. However, it is now clear that entry of compounds into the CNS occurs via capillary venules, while cell migration occurs at the post-capillary venules and is controlled by adhesion molecules, cytokines, and chemokines[35]. Anatomically, the CNS is separated by three barriers: the BBB/blood spinal cord barrier (BSCB), the blood-cerebrospinal fluid barrier (BCSFB) at the choroid plexus (CP), and the arachnoid barrier. Differences in the structure of the BBB and BSCB, as well as differences in the cranial and spinal meninges, in white and grey matter, and other regional differences may explain the differential susceptibility of anatomical regions to neuroinflammatory events. For example, the BSCB has reduced levels of ZO-1, occludin, VE cadherin and P-gp (p-glycoprotein), and fewer pericytes than the BBB[36], indicating that the spinal cord may well be more susceptible to inflammatory insults than the brain. The presence of barriers originally explained why CNS antigens in the brain were ignored by the peripheral immune response. However, this dogma has been challenged recently by the identification of the glymphatic system[37] and rediscovery of lymphatic vessels in the dura mater[38,39] that are crucial to clear waste products such as Aβ peptides and tissue debris that accumulate during disease. Dysfunction of these barriers is well known to occur in neuroinflammatory disorders including MS, Parkinson's disease (PD), Alzheimer's disease (AD), stroke, epilepsy and traumatic brain injury (TBI)[40] and is associated with activated endothelial cells that display an altered pheno-

type and a decrease in tight junction proteins. These changes that are also observed during ageing[41] may explain the increase in susceptibility to neuroinflammation and neurodegenerative disorders in the elderly.

Microglia and macrophages

Historically microglia have been described as the phagocytes of the CNS, however over the last decades microglia are increasingly implicated in exerting diverse roles. Microglia comprise roughly 10% of the glial population in the CNS but unlike astrocytes or oligodendrocytes, microglia are derived from the yolk sac from which they migrate and populate the brain during embryonic development[42]. Microglia are highly motile and versatile cells, they self-renew, through proliferation, and upon damage or injury can increase their population by clonal expansion[43]. This clonal expansion is directed by cues from the micro-environment and results in microglia numbers that are dependent on the local need[43]. Activated microglia are often seen as drivers for neuropathology[44], however, loss of vital homeostatic functions of microglia has also been linked with leukodystrophies, characterised by progressive myelin damage. Initially, microglia were classified as being either classically activated (M1) or alternatively activated (M2), based on chemokine and cytokine expression in vivo[45]. More recently the field has switched to account for a plethora of microglial states recognising the microglial heterogeneity that is present within the brain parenchyma in health and disease. Several reports indicate that microglia have different transcriptomic profiles dependent on the region of the brain, the stage of development and age[46], neuropathological state[47], and the microbiome[48] (Figure 2).

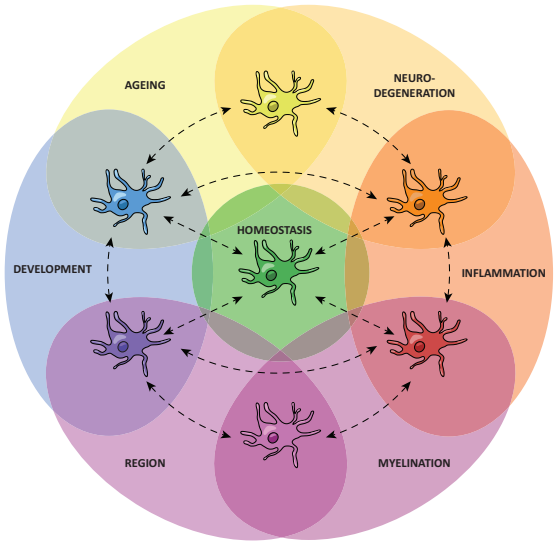

Figure 2. Kaleidoscope of microglia heterogeneity. Microglia are highly heterogeneous and can adapt to any function that is needed for the local environment which is different in health when it is compared to neuroinflammation, remyelination, as well as neurodegeneration. Additionally, microglia are influenced by extrinsic factors such as ageing, the stage of development, or the region where they reside.

Switching between microglial states is vital for processes such as remyelination and is affected by ageing[49]. Microglia secrete pro-inflammatory as well as anti-inflammatory factors which can either be beneficial or detrimental in neurodegenerative diseases[50], for example microglia depletion in a mouse model of AD reduced neuronal loss without affecting β-amyloid pathology[51]. Additionally, microglia-derived factors such as blood derived neurotrophic

factor (BDNF) are important for learning and memory processes, a process that can be affected by maternal inflammation leading to disrupted behaviour and learning in later life[52]. On the other hand, monocytes are the blood-borne precursors to macrophages and dendritic cells, and play a key role in innate immunity although their distinct roles in CNS disorders are frequently hard to distinguish from microglia. The novel markers TMEM119 and P2Y12 have helped differentiate microglia and macrophages[53], indicating that the relative contribution of these cells to neuroinflammatory diseases can be examined. However, microglia have been found to downregulate both TMEM119, and P2RY12 upon activation[53], complicating the picture. A more recent study has found the enzyme HexB has high microglial specificity, during both health and disease[54], a finding that may better clarify their role in health and disease in the future.

Astrocytes

While astrocytes were originally viewed as supportive cells for neurons, it is now clear that astrocytes perform a broad array of physiological and immunological functions in the CNS[55-59]. Similar to the M1/M2 polarization of macrophages and microglia, subpopulations of astrocytes have been reported that produce proinflammatory mediators (A1) and immunoregulatory mediators (A2). The A1 astrocytes that secrete IL-1a, TNF and C1q are considered to be neuroinflammatory, and damage neurons and oligodendrocytes in vitro as well as inducing apoptosis, suppress T helper cell activation, proliferation and function of activated T-cells, while in contrast, A2 astrocytes are neuroprotective, promoting neuronal growth, survival, and synaptic repair[60]. Astrocytes respond to a plethora of insults and are frequently observed as hypertrophic in many neurodegenerative diseases including stroke, TBI, MS, amyotrophic lateral sclerosis (ALS) and viral infections and other inflammatory conditions[60]. A1 reactive astrocytes have been suggested as having toxic effects in ALS, AD, MS, Parkinson's disease (PD), Huntington's disease (HD), schizophrenia and ageing[60,61]; whilst synapse-promoting A2 astrocytes may be responsible for unwanted synapses in epilepsy and neuropathic pain[62]. However, similar to recent advances in the microglial field, astrocytes should be considered to be more heterogeneous than A1 and A2. Multiple subtypes of astrocytes were identified using single cell RNA sequencing; each with their own distinct gene enrichment profile and physiological functions[63]. For example, different subtypes were found to contribute differentially to synaptogenesis which might be locally regulated by neuronal activity. More recently, different subtypes were identified that during LPS induced inflammation undergo distinct inflammatory transitions with defined transcriptomic profiles[64]. There is increasing evidence that astrocytes in the brain are heterogeneous in function depending on the context and time of injury and disease, similar to microglia (Figure 2), and that astrocytes interact with microglia and oligodendrocytes to exert immunological functions.

Oligodendrocytes

As well as the classical innate immune cells, i.e. microglia and astrocytes, oligodendrocytes also contribute to innate immune reactions, expressing receptors and producing immunomodulatory cytokines and chemokines. Originally, oligodendrocytes were regarded as bystanders in immunological responses. However, during CNS insults and disease, oligodendrocytes can aid in protection and regenerative processes, but can also contribute to neurodegeneration through poor production or repair of myelin. Expression of MHC Class I on oligodendrocytes was initially labelled as controversial. However, oligodendrocytes upregulate MHC class I expression after IFN-γ treatment[65]. Additionally, oligodendrocytes express pattern recognition

receptors (PRRs) such as Toll-like receptors (TLRs), as well as a range of receptors for inflammatory mediators such as IL-4, IL-6, IL-7, IL-10, IL-11, IL-12, and IL-18[66-70]. As microglia are the primary immune cells of the CNS, cross-talk between oligodendrocytes and microglia is a key area of interest in many CNS diseases[71]. Indeed, when oligodendrocytes are stressed they may be triggered to produce CXCL10, CCL2, and CCL3 to attract microglia to the area of damage[72,73]. Stressed oligodendrocytes upregulate HSPB5 (also known as αB-crystallin), a molecule that is reported to activate microglia[74], is involved in immunoregulatory functions, and reduces clinical symptoms and tissue damage[75]. While astrocytes are increasingly implicated in being involved in immune functions the cross talk between oligodendrocytes and astrocytes is a relatively unexplored field.

Imaging and monitoring neuroinflammation

Over the last decades there have been significant advances in imaging techniques to visualise the brain during health and disease. One of the main challenges with developing current therapies for neurodegenerative and neuroinflammatory diseases is to monitor the efficacy and impact of the drug on the pathological processes in the CNS. Biomarkers of neuroinflammation and innate immune processes are considered essential for monitoring disease diagnosis, progression, and response to therapy, however there is a lack of accurate and reliable biomarkers for many neurological diseases[76]. Generally, blood and CSF are commonly used to monitor neuroinflammation, however *in vivo* imaging the CNS during disease has become a more widely accepted approach due to its ability to provide region-specific information as well as being minimally invasive depending on the technique. Such techniques include magnetic resonance imaging (MRI), positron emission tomography (PET), single photon emission computed tomography (SPECT), and optical imaging[85]. These approaches allow the study of some aspects of neuroinflammation: a) monitoring activation of resident CNS immune cells e.g. microglia activation, b) BBB permeability e.g. upregulation of adhesion molecules, c) CNS infiltration of immune cells and, d) pathology as a result of neuroinflammation e.g. demyelination and cell death (Table 2).

In addition, aspects of BBB integrity, regarded as a hallmark of neuroinflammation, is imaged by leakage of gadolinium using MRI, or by nuclear imaging of P-gp and vascular cell adhesion molecule (VCAM-1), which are differentially expressed in MS[86], stroke[87], AD and vascular dementia[88]. Indicators of leukocyte function include markers of oxidative stress, such as pro-inflammatory and oxidative enzymes secreted by activated monocytes and neutrophils. One such product is myeloperoxidase (MPO) that can be detected by gadolinium (MPO-Gd) to track the oxidative activity of MPO non-invasively. Thus MPO has been used as a potential biomarker of neuroinflammation in experimental models of MS, namely experimental autoimmune encephalitis (EAE)[89], and experimental stroke[90]. Cell-labelling approaches include radiolabeled antibodies and radiolabelled cytokines, which are imaged using SPECT, PET or optical imaging. For example, anti-CD3, anti-CD4, IL-1 and IL-2 have all been used to visualise receptors on T-lymphocytes in MS[91] and rheumatoid arthritis[92]. As well as ongoing neuroinflammation, several approaches image the resultant pathology. As an example, PET ligands have been used to visualise myelin damage in MS[93,94] while many approaches are used to visualise cell death e.g. neuronal loss, such as annexin-V, caspases and ML-10 [85]. Imaging of neuro-inflammatory biomarkers is an expanding topic with the potential to expedite diagnosis and improve disease and therapeutic monitoring. While many approaches are examined in preclinical models, fewer are available for studies in humans[76].

Table 2. Biomarkers and Imaging of Neuroinflammatory Diseases

Target type	Target	Marker	Methods	Ref
Resident CNS cells	TSPO	Innate immune activation	PET, SPECT	[76]
	Monoamine oxidase-B	Reactive astrocytes	PET	[76]
	Cyclooxygenase 1	Activated microglia and astrocytes	PET	[76]
	MPO	Inflammatory mediator in leukocytes	MRI, PET	[77]
	Adenosine receptors	Cell injury	PET	[78]
	A4B2 nicotinic acetylcholine receptors	Activated microglia and astrocytes	PET	[76]
	Myo-inositol	Astrocyte hypertrophy	MRS	[76]
	N-acetyl-aspartate	Neuronal integrity	MRS	[76]
	Iron accumulation	Free radical formation, mitochondrial or neuronal dysfunction	MRI	[79]
	Myelin	Demyelination and loss of myelin integrity in white matter disorders	PET	[76]
BBB integrity	VCAM	Activation BBB	Molecular imaging	[76]
	P-gp	Alterations of expression in relation to BBB activity	PET, optical imaging	[76]
Immune markers	Cytokines	Pro or anti-inflammatory signals	CSF	[80]
	Chemokines	Pro or anti-inflammatory signals	CSF	[80]
	SPIO	SPIO-labelled phagocytic cells	MRI	[81]
Antibodies	Oligoclonal bands	IgG of unknown specificity	CSF	[82]
	Anti-aquaporin 4 antibodies	Antibodies to aquaporin 4 (water channel protein)	Blood	[82]
	Anti-NF antibodies	Neuronal damage	Blood	[82]
Free proteins	Neurofilaments	Neuronal damage	CSF	[82]
	microRNAs	Circulating microRNAs involved in inflammation	Blood	[82]
	β-amyloid	Proteins involved in disease pathology	Blood	[83]
	Tau	Proteins involved in disease pathology	Blood	[84]
	Annexin V	Apoptosis	PET, SPECT, blood	[76]
	Exosomes	A potential mechanism by which pathology is spread and/or toxic proteins are transported	CSF/blood	[84]

Abbreviations: BBB, blood brain barrier; CNS, central nervous system, CSF, cerebrospinal fluid; MRI, magnetic resonance imaging; MPO, myeloperoxidase; PET, positron emission tomography; Pgp, P-glycoprotein; SPECT, single-photon emission computed tomography; SPIO, superparamagnetic particles of iron oxide; TSPO, translocator protein; VCAM, vascular cell adhesion molecule 1.

TSPO

One protein that has been of interest as the target in PET imaging of ongoing neuroinflammation is the translocator protein (TSPO). TSPO is an outer mitochondrial membrane protein, expressed in many tissues in the body, whose exact functions are unknown[95-99]. TSPO PET signal is markedly upregulated in many neurodegenerative and neuroinflammatory diseases[95-111]. However, one of the caveats of using TSPO PET is that the exact cellular origin of the TSPO PET signal in the brain is unclear. Knowing the origin of TSPO PET is necessary for clinical meaningful decisions, e.g. whether a therapeutic intervention is having the desired *in vivo* effects on neuroinflammation. Due to the fast pace of research and development of new TSPO radiotracers many conclusions of TSPO PET have been made without proper investigation into the cellular origin[100]. This has led to the belief that the TSPO PET signal mostly originates in activated microglia[99,105,106,109,112-124]. The contribution of other cell types such as astrocytes have been largely ignored, even though there have been multiple reports of TSPO in astrocytes for many years[125-141]. Most of these studies have demonstrated astrocytic TSPO in animal models of CNS diseases[125-138], however only a few studies have investigated expression of TSPO in astrocytes in the human CNS, most of which are qualitative rather than quantitative[139-142]. Additionally, human microglia do not upregulate expression of *TSPO* after pro-inflammatory stimulation, and human macrophages even downregulate *TSPO* expression[143]. This recent finding has sparked interest into whether TSPO is a marker of all microglia or a readout on microglial density rather than activated microglia. The use of TSPO PET also allows us to investigate the efficacy of newly developed drugs on neuroinflammation *in vivo* in a preclinical setting in experimental animal models. But similar to the human conundrum, we need to know what cells express TSPO (e.g. microglia or astrocytes). Of similar importance is to find out whether the TSPO gene is regulated in a similar manner in animal models compared to humans. In contrast to the human microglia and macrophages, mouse microglia and macrophages upregulate *TSPO* after pro-inflammatory stimulation up to 10-fold, indicating that there are differences in the regulation of the TSPO gene between humans and mice[143-147]. This questions whether biological processes in animal and experimental models of human diseases truly reflect the pathological processes occurring in humans[148-150].

Due to the limitations of TSPO, other candidate markers for PET imaging of microglia have been suggested, such as cyclooxygenase-2 (COX-2), cannabinoid receptor type 2 (CB2R), purinergic ion channel receptor 7 (P2X7R). However, the radioligands for these targets each come with their own obstacles in terms of radioligand binding, sensitivity and specificity of microglia.

Multiple sclerosis

Multiple sclerosis (MS) is a chronic inflammatory demyelinating disease of the CNS, and is the most common disabling disease affecting young adults. MS most often presents itself between 20 and 40 years of age, but may occur in younger and older people. The first report of a disease with characteristics showing similar transient neurological deficits goes back as far as the 14th century, originating in the Netherlands. Despite decades of research into the aetiology of MS, the exact cause of MS is unknown, there is however evidence that the incidence of MS increases based on several environmental risk factors including the Epstein-Barr virus (EBV)[151]. EBV is present in nearly all people with MS (pwMS, > 99%), however roughly 95% of the general population has had an EBV infection during their lifetime[152]. Nevertheless, the risk of developing MS increases with EBV antibody titer[153], and is linked

to infectious mononucleosis, i.e. EBV infection in childhood and young adulthood[154]. EBV interacts with complement C2 receptors on memory B cells to infect and subsequently immortalise them[155-157]. There are reports that EBV can infect specific memory B-cells to produce anti-MOG (myelin oligodendrocyte glycoprotein) auto-antibodies[158]. These auto-antibodies induce upregulation of heat shock protein B5 (HSPB5) in oligodendrocytes, which activates microglia[159], but also activates HSPB5-reactive memory T-cells[160]. When these T-cells are activated they in turn start producing IFNγ, a pro-inflammatory cytokine with detrimental effects in MS[159], possibly initiating the development of demyelinating lesions in MS.

The latitudinal effect on risk of MS, is mainly attributed to sunlight exposure, as well as vitamin D production[161]. High vitamin D consumption in Norway, or through supplementation in the US military have protective effects against MS[162,163]. Additionally, there is a genetic risk to developing MS. Risk of developing MS increases 10-25 times for first-degree relatives, compared to the general population, where monozygotic twins have the highest risk if either one twin develops MS[164,165]. Risk of developing MS has also been linked to human leukocyte antigen (HLA) and is increased in people expressing HLA-DR*1501 common in northern Europeans. This is also supported by an increased risk people homozygous for HLA-DR1501 compared to heterozygous[166]. Additionally, regional variation revealed many haplotypes of the HLA gene that have either protective or detrimental effects on the risk of developing MS. These HLA haplotypes differ in magnitude of effect which and can either interact with each other or act on their own[167].

Clinical symptoms

The clinical presentation of MS is heterogeneous depending on the presence of lesions and extent of damage affecting the brain but also the spinal cord and optic nerve. The variety in clinical presentation is a consequence of the transient nature of focal attacks of neuroinflammatory lesions in the CNS. The location and timing of the lesions can result in clinical symptoms ranging from visual problems, if lesions arise in the optic nerve, to motor problems, when lesions arise in the motor areas. The first symptoms of MS often include signs of visual problems such as diplopia and optic neuritis, but also sensory disorders and limb weakness. During the early stages of the disease when neuronal reserve is high, pwMS may fully recover from their clinical attacks, recognised as relapsing-remitting forms of the disease (RRMS). Over time, this reserve and ability to repair the damage in the CNS is lost and pwMS develop a more progressive form of the disease: secondary progressive MS (SPMS). SPMS develops in 90% of people with RRMS over the course of 10-15 years after onset. However, up to 10% of people don't recover from their clinical attacks and have a primary progressive disease course (PPMS) with increasing disease disability.

The diagnosis of MS is made according the McDonald criteria[168] (Table 3). The McDonald criteria have been extensively revised due to increasing knowledge of the pathology of the disease, and the incorporation of rapidly advances in development of imaging modalities. However, the key requirement of a diagnosis according to the criteria is that people have experienced damage of the CNS that is disseminated in time and space, meaning that there is evidence of CNS damage at 2 or more time points and different areas of the CNS. These criteria are supported by the presence of oligoclonal bands in the CSF.

Table 3. 2017 McDonald Criteria for diagnosis of Multiple Sclerosis

Clinical presentation	What additional data is needed for an MS diagnosis?
Two or more relapses AND EITHER objective clinical evidence of two or more lesions OR objective clinical evidence of one lesion together with reasonable historical evidence of a previous relapse	None
Two or more relapses; objective clinical evidence of one lesion (shows DIT)	Dissemination in space shown by: One or more MRI detected lesions typical of MS **OR** A further relapse showing damage to another part of the CNS
One relapse; objective clinical evidence of two or more lesions (shows DIS)	Dissemination in time shown by: Oligoclonal bands **OR** MRI evidence of a new lesion since a previous scan **OR** A further relapse
One attack/relapse; objective clinical evidence of one lesion (known as 'clinically isolated syndrome')	Dissemination in space shown by: One or more MRI detected lesions typical of MS **OR** A further relapse showing activity in another part of the CNS Dissemination in time shown by: Oligoclonal bands **OR** MRI showing new lesions since a previous scan **OR** A further relapse
Insidious neurological progression suggestive of multiple sclerosis (typical for primary progressive MS)	**Continued progression for one year (from previous symptoms or by ongoing observation) plus any two of:** One or more MRI detected lesions in the brain typical of MS, Two or more MRI detected lesions in the spinal cord, Oligoclonal bands in the spinal fluid

Abbreviations: CNS, central nervous system; DIS, dissemination in space; DIT, dissemination in time; MRI, magnetic resonance imaging; MS, multiple sclerosis.

Neuropathology

The pathology of MS is primarily based on the presence of microglia and macrophages, the loss of myelin, the degree of astrogliosis and neuronal and synaptic loss (Figure 3). Histopathological, the lesions are classified as preactive, active, chronic active, or inactive. Upon histopathological examination, preactive lesions are classified as clustering microglia in the normal appearing white matter (NAWM). In the NAWM there is no myelin damage, no astrogliosis and only rarely foamy macrophages are observed[169]. The preactive lesion is a relatively new description in neuropathology and the term suggests it could be the start of the classical active lesions that are commonly described. However, the discrepancy between number of preactive lesions and the relatively lower number of active lesions suggest that a significant amount of preactive lesions do not develop into active lesions. Active lesions are characterised by myelin loss and damage, the presence of foamy macrophages and microglia, periventricular infiltrates filled with cells of the peripheral immune system, mainly lymphocytes[169]. Chronic active lesions are characterised by a rim of foamy macrophages around the area of demyelination, the centre of chronic active lesions shows signs of astrogliosis and hypertrophy and is hypocellular[169]. Inactive lesions show signs of severe myelin damage, hypertrophic astrocytes and is characterised by hypocellularity[169]. In inactive

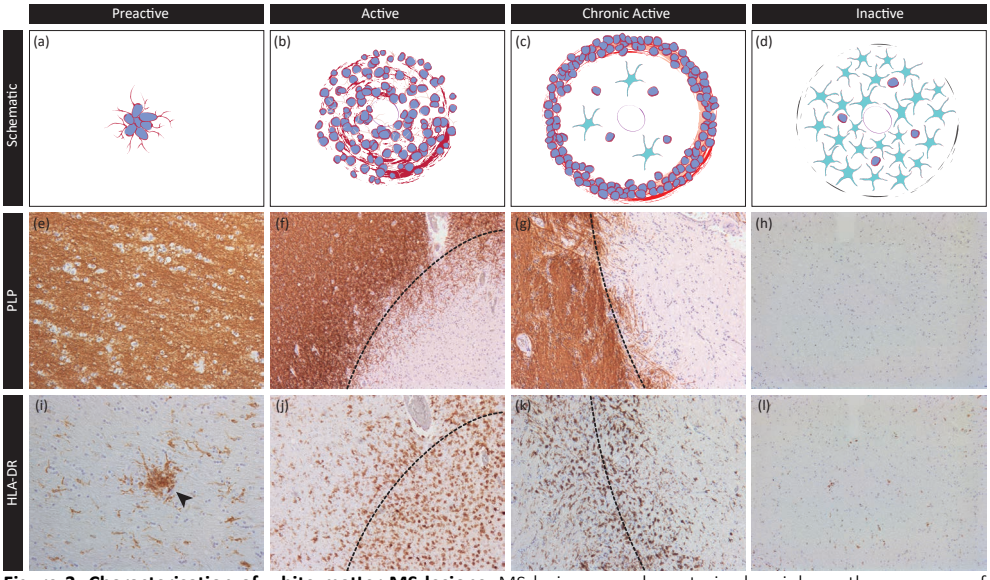

Figure 3. Characterisation of white matter MS lesions. MS lesions are characterised mainly on the presence of activated microglia/macrophages, marked by HLA-DR staining (i-l), demarcated by the dotted lines, and the preence of myelin, marked by PLP staining (e-h). Pre-active lesions (a,e,i) are microglial clusters (arrow) in the normal appearing white matter (NAWM). Active lesions (b,f,j) are characterised on absence of myelin and the presence of high numbers of activated microglia/macrophages. Chronic active lesions (c,g,k) have a demarcated rim of activated microglia/macrophages around a centre of inactivity marked by loss of myelin. In inactive lesions (d,h,l) activity subsides and the area is left with a plaque with no myelin, and astroglial scarring.

lesions there are almost no signs of inflammatory cells. Then there is some evidence that some lesions show signs of remyelination where oligodendrocyte precursor cells remyelinate naked axons, although the new myelin has other characteristics such as thinner sheaths[170]. In the grey matter of the brain MS lesions are classified based on their anatomical location rather than on their degree of inflammation due to the lack of apparent neuroinflammation that is present in the cortex of the brain[171] (Figure 4). Lesions that comprise both the white and grey matter are classified as leukocortical lesions (type I), sometimes the white matter of these lesions show clear signs of inflammation which gradually decreases when crossing to the grey matter[172]. Lesions that are purely within the grey matter are classified as intracortical lesions (type II)[172]. Areas of demyelination along the outer border of the cortex area are classified as subpial lesions (type III) and are the most commonly observed[172]. Lesions that extend from the surface of the brain to the border of the white and grey matter are classified as transcortical (type IV)[2,172].

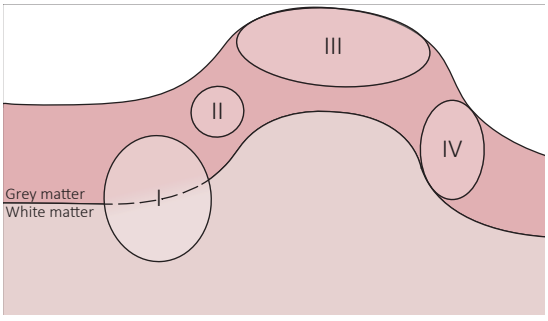

Figure 4. Grey matter lesions in MS. Lesions are classified by their location and spread in the grey matter. Type I comprises both white and grey matter. Type II lesions are surrounded by grey matter. Type III lesions are subpially located along the grey matter. Type IV lesions comprise the whole width of the grey matter but do not cross into the white matter[2].

Neuroinflammation in neurodegenerative diseases

Neuroinflammation is an apparent feature of MS, however, neuroinflammation is also present in other CNS diseases (Figure 5), as well as their experimental models, albeit in different forms and gradations. For example, while ALS is primarily a neurodegenerative disease characterised by motor neuron loss, neuroinflammation plays a critical role in the degeneration of neurons in the brainstem, spinal cord and motor cortex[173]. Recently, it was shown that 1573 out of 2637 of genes related to inflammation were differentially expressed compared to controls in the motor cortex of people with ALS. The most dysregulated signalling pathways are involved in antigen presentation, the complement system, and reactive oxygen species (ROS) production[174]. Microglia activation is correlated with disease severity in the spinal cord of ALS patients[175]. Additionally, one of the genes that has been implicated in the aetiology of ALS, C9orf72, is highly expressed in myeloid cells. Loss of C9orf functions results in lysosomal trafficking defects, and a reduced ability of microglia to clear cellular debris and aggregated proteins and aberrant microglia responses[176]. Furthermore, astrocytes are also affected in ALS showing increased expression of small heat shock protein to protect the cell against damage by refolding or promoting degradation of misfolded proteins[175,177]. TSPO PET studies of ALS have indicated that increased signal was caused by activated microglia while ignoring the contribution of other cell types such as astrocytes[106,178-180].

Over the last years, increasing insights into immunological processes in the CNS have shed light on the role of neuroinflammation in AD. The misfolded and aggregated proteins, characteristic of AD pathology in the form of Aβ plaques and neurofibrillary tangles, bind to PRRs on microglia and astrocytes, activating innate immune system cascades[181]. Microglia and astrocytes start engulfing Aβ fibrils, which is mostly resistant to degradation resulting in inefficient clearance of Aβ[182,183]. As a result, astrocytes around plaques are reactive but do not form gliotic scars. It has been suggested that astrocyte activation may even happen before microglia involvement in AD pathogenesis, where astrocyte atrophy leads to aberrant synaptic functioning resulting in cognitive deficits[184]. One of the most affected areas in AD is the hippocampus and several PET studies have found increased TSPO binding in the hippocampus[101,185,186]. However, some studies have not found differences in TSPO binding, complicating the use of TSPO PET to identify neuroinflammation in AD[187-190]. On the protein level, increased expression of TSPO is present in the cortex, but no studies have investigated TSPO expression in the hippocampus or have looked at the microglial states that were responsible for the increased expression[191].

Experimental animal models of CNS disease

MS related pathology such as inflammation, neurodegeneration and demyelination is most commonly studied in EAE. EAE is a T-cell mediated disease induced by immunising mice or rats with CNS antigens. However, the clinical severity of EAE is highly dependent on the antigen, species, age, gender and strain of animals, but also the method of induction. All these factors can influence immunological processes as well as the response to therapies tested in EAE mice[192] which unfortunately has resulted in a very low translation of therapeutic compounds for MS. For ALS, the most commonly used experimental model is the $SOD1^{G93A}$ mouse, as it was one of the first mutations discovered to be associated with ALS[193]. Whilst the $SOD1^{G93A}$ model replicates a moderate disease duration with misfolded SOD1, motor neuron loss, metabolic deficits and gliosis, most therapeutic compounds have failed to translate to humans[148].

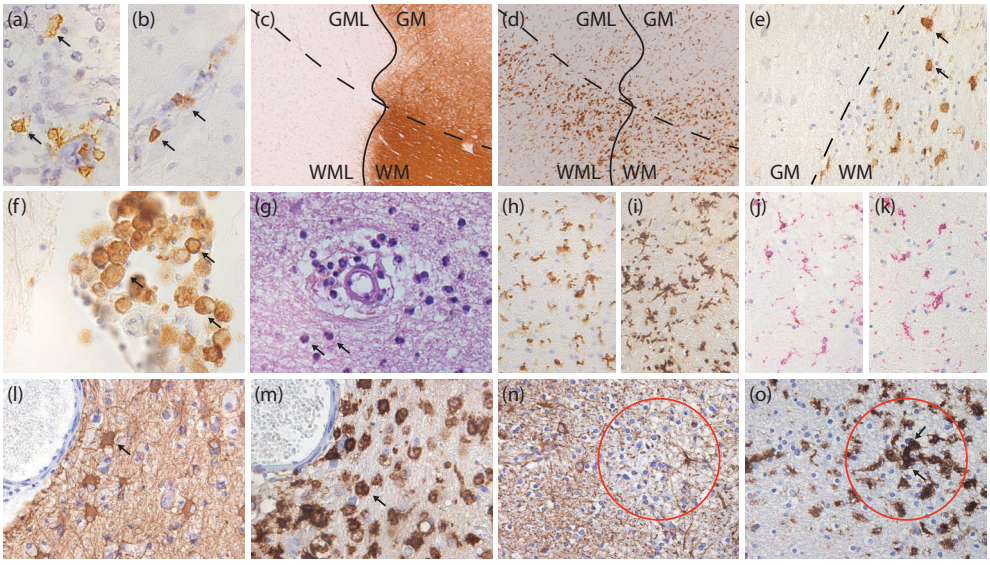

Figure 5. Immune responses in human and experimental inflammatory neurodegenerative disorders. B-cells (arrows) are observed in white (a) and grey matter lesions (b) in multiple sclerosis (MS). (c) and (d) depict an MS leucocortical lesion. The white matter (WML) is associated with HLA+ microglia (d, WML) in contrast to the lack of HLA + microglia in the grey matter (d, GML). A similar pattern of HLA+ cells is seen in the white and grey matter in an X-ALD case (e) and where peripheral macrophages infiltrate the white matter (f). Granulocytes (arrow) in suspected vasculitis cases (g). Ageing influences the activity of microglia in a mouse model of MS: microglia in the CNS of young mice (h; Iba1 staining) are less active than in aged mice (i). In MS cases microglia in NAWM express P2Y12 (j) and TMEM119 (k). In progressive multifocal leucoencephalopathy astrocytes (l, arrow) and activated microglia/ macrophages (m, arrow) are highly reactive in an area of demyelination. The paucity of astrocytic glial fibrillary acidic protein expression (red circle, n) is associated with an area of microglial activation (red circle, o) in acute haemorrhagic leucoencephalitis.

This is likely at least partly explained by the low representation (1-2%) of the mutation in people with ALS. Animal models for AD most commonly represent either amyloid pathology by increasing Aβ, or increasing the relative ratio of Aβ42 which is prone to aggregation or tau pathology by overexpressing the microtubule-associated protein tau[194]. Again, both models have relatively poor translational value when it comes to disease modifying therapies as over the last decades almost no positive clinical results have been yielded. Although experimental animal models are often used to study CNS pathology they rarely reflect the multifactorial complexity of human diseases. Failure of translation of disease modifying therapies may be attributed to varying study designs, imperfect animal models or timing of therapy. Nevertheless, TSPO PET is utilised to monitor ongoing neuroinflammation *in vivo* in experimental animals. Indeed, increases in TSPO PET signal are found in EAE, $SOD1^{G93A}$, and APP and TAU^{P301S} experimental animal models[141,195-197]. However, there is no consensus on whether this increase in TSPO is due to increased microglial density, an increase in TSPO expression, or an increase in ligand binding or whether this is disease, model or context-dependent.

Aim of thesis

Advancing techniques and increasing knowledge on cellular processes during neuroinflammation have contributed towards generating many targets for imaging neuroinflammation with PET. The aim of this thesis is to better understand the expression of TSPO in CNS diseases and respective animal models as well as investigating the role of microglia and astrocytes as innate immune cells of the brain in CNS diseases.

Hypothesis

The hypothesis tested in this thesis is that TSPO is not a marker of activated microglia in the human brain. We hypothesise that TSPO is not increased in activated microglia and there is a substantial contribution of other cell types to the TSPO PET signal. While TSPO PET might be a good marker for innate immune processes, increased TSPO PET signal might originate from multiple cell types in the CNS, and/or reflect cell density rather than phenotype of TSPO expressing cells.

Outline

Increased TSPO PET signal is widely attributed to activated pathogenic microglia in CNS diseases and the contributions of other cells, as well as the cell phenotype has been overlooked in many neuroinflammatory diseases. On this basis, the identification of the cellular expression of TSPO in MS in microglia, astrocytes and other cell types as well as their activation state was considered key to understanding the data arising from TSPO PET imaging in MS (**Chapter 2**).

Studies of multiple sclerosis (MS) lesions reveal that TSPO is not restricted to pro-inflammatory microglia/macrophages, but also present in homeostatic or reparative microglia. Here, we investigated quantitative relationships between TSPO expression and microglia/macrophage phenotypes in white matter and lesions of brains with MS pathology (**Chapter 3**).

Since TSPO PET is increasingly used as a marker for neuroinflammation in the CNS, characterisation of TSPO for PET in neurodegenerative diseases with inflammatory components, such as ALS and AD, is of importance. Additionally, many studies are done on animal models for CNS diseases but results do not translate well to humans. To identify possible phylogenetic diversity between humans and rodents in the expression and regulation of TSPO we directly compared ALS, and AD with their respective animal models, as well as EAE (**Chapter 4**).

TSPO expression is altered in many neurodegenerative, neuroinflammatory, and neuropsychiatric diseases. In PET studies, the TSPO signal is often viewed as a marker of microglial cell activity. However, there is little evidence in support of a microglia-specific TSPO expression. Therefore, we described the cellular sources and functions of TSPO in animal models of disease and human studies, in health, and in CNS diseases (**Chapter 5**).

Clinical disability of pwMS is considered primarily a result of axonal loss. Given the reported correlation between indices of spinal cord cross-sectional area (CSA) and disability, and earlier evidence suggesting axonal loss as the key driver of chronic disability. We have compared the extent of axonal loss and whether this correlates with local neuronal loss in the spinal cord of pwMS (**Chapter 6**).

Over the last decade knowledge of the role of astrocytes in CNS neuroinflammatory diseases has changed dramatically. Rather than playing a merely passive role in response to damage it is clear that astrocytes are increasingly implicated in exerting immunological relevant functions within the CNS. Whilst most astrocyte research focuses on modulating neuronal function and synaptic transmission little is known about the cross-talk between astrocytes and oligodendrocytes, the myelinating cells of the CNS. We thus reviewed evidence for the immunological roles astrocytes and oligodendrocytes play and how the two cell types interact (**Chapter 7**).

As primary innate immune cells in the CNS, microglia play critical roles in shaping the brain during development, responding to pathogens, and clearing tissue debris or protein aggregations during ageing, neuroinflammation and neurodegeneration. The last decade has given us many new insights in the heterogeneity of microglia states. However, many of the single cell/nucleus RNA-seq studies have focused on microglia in the grey matter or of the whole brain while ignoring the heterogeneity of microglia in the white matter. Therefore, we provide an update on the current knowledge of microglia heterogeneity in the white matter and how microglia are important for development of the white matter as well as how ageing affects white matter homeostasis (**Chapter 8**).

To conclude this thesis, the results of the previous chapters are summarised. The data in this thesis is discussed and put into context, which enables us to give an overview on the current knowledge of innate immune cells in the CNS, and how to monitor these cells in vivo during neuroinflammation (**Chapter 9**).

References

1. Wimo A, *et al*. The worldwide costs of dementia 2015 and comparisons with 2010. *Alzheimers Dement*. Jan 2017;13(1):1-7. doi:10.1016/j.jalz.2016.07.150
2. Bo L, *et al*. Grey matter pathology in multiple sclerosis. *Acta Neurol Scand Suppl*. 2006;183:48-50. doi:10.1111/j.1600-0404.2006.00615.x
3. Cova I, *et al*. Worldwide trends in the prevalence of dementia. *J Neurol Sci*. Aug 15 2017;379:259-260. doi:10.1016/j.jns.2017.06.030
4. Perry VH. The influence of systemic inflammation on inflammation in the brain: implications for chronic neurodegenerative disease. *Brain Behav Immun*. Sep 2004;18(5):407-13. doi:10.1016/j.bbi.2004.01.004
5. Hickman S, *et al*. Microglia in neurodegeneration. *Nat Neurosci*. Oct 2018;21(10):1359-1369. doi:10.1038/s41593-018-0242-x
6. McKenzie IA, *et al*. Motor skill learning requires active central myelination. *Science*. Oct 17 2014;346(6207):318-22. doi:10.1126/science.1254960
7. Amor S, *et al*. Inflammation in neurodegenerative diseases–an update. *Immunology*. 2014;142(2):151-166.
8. Myall DJ, *et al*. Parkinson's in the oldest old: Impact on estimates of future disease burden. *Parkinsonism Relat Disord*. Sep 2017;42:78-84. doi:10.1016/j.parkreldis.2017.06.018
9. Tysnes OB, *et al*. Epidemiology of Parkinson's disease. *J Neural Transm (Vienna)*. Aug 2017;124(8):901-905. doi:10.1007/s00702-017-1686-y
10. Rawlins MD, *et al*. The Prevalence of Huntington's Disease. *Neuroepidemiology*. 2016;46(2):144-53. doi:10.1159/000443738
11. Verhaart IEC, *et al*. Prevalence, incidence and carrier frequency of 5q-linked spinal muscular atrophy- a literature review. *Orphanet J Rare Dis*. Jul 4 2017;12(1):124. doi:10.1186/s13023-017-0671-8
12. Arthur KC, *et al*. Projected increase in amyotrophic lateral sclerosis from 2015 to 2040. *Nat Commun*. Aug 11 2016;7:12408. doi:10.1038/ncomms12408
13. Mohan KM, *et al*. Risk and cumulative risk of stroke recurrence: a systematic review and meta-analysis. *Stroke*. May 2011;42(5):1489-94. doi:10.1161/STROKEAHA.110.602615
14. Wong CH, *et al*. Prolonged Activation of Invariant Natural Killer T Cells and TH2-Skewed Immunity in Stroke Patients. *Front Neurol*. 2017/01/19 2017;8:6. doi:10.3389/fneur.2017.00006
15. Nguyen R, *et al*. The International Incidence of Traumatic Brain Injury: A Systematic Review and Meta-Analysis. *Can J Neurol Sci*. Nov 2016;43(6):774-785. doi:10.1017/cjn.2016.290
16. Zheng YH, *et al*. The Role of IL-27 and its Receptor in the Pathogenesis of HIV/AIDS and Anti-viral Immune Response. *Curr HIV Res*. 2017/08/25 2017;15(4):279-284. doi:10.2174/1570162X15666170517130339
17. Harrison LH, *et al*. Global epidemiology of meningococcal disease. *Vaccine*. Jun 24 2009;27 Suppl 2:B51-63. doi:10.1016/j.vaccine.2009.04.063
18. Ribes S, *et al*. The Early Adaptive Immune Response in the Pathophysiological Process of Pneumococcal Meningitis. *J Infect Dis*. Jan 1 2017;215(1):150-158. doi:10.1093/infdis/jiw517
19. Deeks SG. HIV infection, inflammation, immunosenescence, and aging. *Annu Rev Med*. 2011/02/18 2011;62(1):141-55. doi:10.1146/annurev-med-042909-093756
20. Amor S, *et al*. Imaging immunological processes from blood to brain in amyotrophic lateral sclerosis. *Clin Exp Immunol*. Dec 2021;206(3):301-313. doi:10.1111/cei.13660
21. Ngugi AK, *et al*. Incidence of epilepsy: a systematic review and meta-analysis. *Neurology*. Sep 6 2011;77(10):1005-12. doi:10.1212/WNL.0b013e31822cfc90
22. Singh A, *et al*. The Epidemiology of Global Epilepsy. *Neurol Clin*. Nov 2016;34(4):837-847. doi:10.1016/j.ncl.2016.06.015
23. Baxter AJ, *et al*. The epidemiology and global burden of autism spectrum disorders. *Psychol Med*. Feb 2015;45(3):601-13. doi:10.1017/S003329171400172X
24. Careaga M, *et al*. Immune Endophenotypes in Children With Autism Spectrum Disorder. *Biol Psychiatry*. Mar 1 2017;81(5):434-441. doi:10.1016/j.biopsych.2015.08.036
25. Scott JG. Environmental Contributions to Autism: Explaining the Rise in Incidence of Autistic Spectrum Disorders. *Journal of Enviromental Immunology and Toxicology*. 2013;1(2):75. doi:10.7178/jeit.7
26. Ferrari AJ, *et al*. Global variation in the prevalence and incidence of major depressive disorder: a systematic review of the epidemiological literature. *Psychol Med*. Mar 2013;43(3):471-81. doi:10.1017/S0033291712001511
27. Hidaka BH. Depression as a disease of modernity: explanations for increasing prevalence. *J Affect Disord*. Nov 2012;140(3):205-14. doi:10.1016/j.jad.2011.12.036
28. Hughes MM, *et al*. Stress-Related Immune Markers in Depression: Implications for Treatment. *Int J Neuropsychopharmacol*. Jun 2016;19(6):pyw001. doi:10.1093/ijnp/pyw001
29. Burns JK, *et al*. Income inequality and schizophrenia: increased schizophrenia incidence in countries with high levels of income inequality. *Int J Soc Psychiatry*. Mar 2014;60(2):185-96. doi:10.1177/0020764013481426
30. Karpinski P, *et al*. Reduced number of peripheral natural killer cells in schizophrenia but not in bipolar

disorder. *Brain Behav Immun*. May 2016;54:194-200. doi:10.1016/j.bbi.2016.02.005
31. Keri S, *et al*. Antipsychotics influence Toll-like receptor (TLR) expression and its relationship with cognitive functions in schizophrenia. *Brain Behav Immun*. May 2017;62:256-264. doi:10.1016/j.bbi.2016.12.011
32. Ascoli BM, *et al*. The role of macrophage polarization on bipolar disorder: Identifying new therapeutic targets. *Aust N Z J Psychiatry*. Jul 2016;50(7):618-30. doi:10.1177/0004867416642846
33. Merikangas KR, *et al*. Prevalence and correlates of bipolar spectrum disorder in the world mental health survey initiative. *Arch Gen Psychiatry*. Mar 2011;68(3):241-51. doi:10.1001/archgenpsychiatry.2011.12
34. Yutzy SH, *et al*. The increasing frequency of mania and bipolar disorder: causes and potential negative impacts. *J Nerv Ment Dis*. May 2012;200(5):380-7. doi:10.1097/NMD.0b013e3182531f17
35. Owens T, *et al*. Perivascular spaces and the two steps to neuroinflammation. *J Neuropathol Exp Neurol*. Dec 2008;67(12):1113-21. doi:10.1097/NEN.0b013e31818f9ca8
36. Wilhelm I, *et al*. Heterogeneity of the blood-brain barrier. *Tissue Barriers*. Jan-Mar 2016;4(1):e1143544. doi:10.1080/21688370.2016.1143544
37. Iliff JJ, *et al*. Is there a cerebral lymphatic system? *Stroke*. Jun 2013;44(6 Suppl 1):S93-5. doi:10.1161/STROKEAHA.112.678698
38. Aspelund A, *et al*. A dural lymphatic vascular system that drains brain interstitial fluid and macromolecules. *J Exp Med*. Jun 29 2015;212(7):991-9. doi:10.1084/jem.20142290
39. Louveau A, *et al*. Revisiting the Mechanisms of CNS Immune Privilege. *Trends Immunol*. Oct 2015;36(10):569-577. doi:10.1016/j.it.2015.08.006
40. Abbott NJ, *et al*. Structure and function of the blood-brain barrier. *Neurobiol Dis*. Jan 2010;37(1):13-25. doi:10.1016/j.nbd.2009.07.030
41. Gorle N, *et al*. The effect of aging on brain barriers and the consequences for Alzheimer's disease development. *Mamm Genome*. Aug 2016;27(7-8):407-20. doi:10.1007/s00335-016-9637-8
42. Ginhoux F, *et al*. Fate mapping analysis reveals that adult microglia derive from primitive macrophages. *Science*. Nov 5 2010;330(6005):841-5. doi:10.1126/science.1194637
43. Tay TL, *et al*. A new fate mapping system reveals context-dependent random or clonal expansion of microglia. *Nat Neurosci*. Jun 2017;20(6):793-803. doi:10.1038/nn.4547
44. Tada M, *et al*. Characteristic microglial features in patients with hereditary diffuse leukoencephalopathy with spheroids. *Ann Neurol*. Oct 2016;80(4):554-65. doi:10.1002/ana.24754
45. Sica A, *et al*. Macrophage plasticity and polarization: in vivo veritas. *J Clin Invest*. Mar 2012;122(3):787-95. doi:10.1172/JCI59643
46. Grabert K, *et al*. Microglial brain region-dependent diversity and selective regional sensitivities to aging. *Nat Neurosci*. Mar 2016;19(3):504-16. doi:10.1038/nn.4222
47. Erny D, *et al*. Host microbiota constantly control maturation and function of microglia in the CNS. *Nat Neurosci*. Jul 2015;18(7):965-77. doi:10.1038/nn.4030
48. Saederup N, *et al*. Selective chemokine receptor usage by central nervous system myeloid cells in CCR2-red fluorescent protein knock-in mice. *PLOS ONE*. Oct 27 2010;5(10):e13693. doi:10.1371/journal.pone.0013693
49. Ruckh JM, *et al*. Rejuvenation of regeneration in the aging central nervous system. *Cell Stem Cell*. Jan 6 2012;10(1):96-103. doi:10.1016/j.stem.2011.11.019
50. Wes PD, *et al*. Next generation transcriptomics and genomics elucidate biological complexity of microglia in health and disease. *Glia*. Feb 2016;64(2):197-213. doi:10.1002/glia.22866
51. Spangenberg EE, *et al*. Eliminating microglia in Alzheimer's mice prevents neuronal loss without modulating amyloid-beta pathology. *Brain*. Apr 2016;139(Pt 4):1265-81. doi:10.1093/brain/aww016
52. Schaafsma W, *et al*. Long-lasting pro-inflammatory suppression of microglia by LPS-preconditioning is mediated by RelB-dependent epigenetic silencing. *Brain Behav Immun*. Aug 2015;48:205-21. doi:10.1016/j.bbi.2015.03.013
53. Zrzavy T, *et al*. Loss of 'homeostatic' microglia and patterns of their activation in active multiple sclerosis. *Brain*. Jul 1 2017;140(7):1900-1913. doi:10.1093/brain/awx113
54. Masuda T, *et al*. Novel Hexb-based tools for studying microglia in the CNS. *Nat Immunol*. Jul 2020;21(7):802-815. doi:10.1038/s41590-020-0707-4
55. Allen NJ, *et al*. Astrocyte glypicans 4 and 6 promote formation of excitatory synapses via GluA1 AMPA receptors. *Nature*. May 27 2012;486(7403):410-4. doi:10.1038/nature11059
56. Alvarez JI, *et al*. The Hedgehog pathway promotes blood-brain barrier integrity and CNS immune quiescence. *Science*. Dec 23 2011;334(6063):1727-31. doi:10.1126/science.1206936
57. Chung WS, *et al*. Astrocytes mediate synapse elimination through MEGF10 and MERTK pathways. *Nature*. Dec 19 2013;504(7480):394-+. doi:10.1038/nature12776
58. Molofsky AV, *et al*. Astrocyte-encoded positional cues maintain sensorimotor circuit integrity. *Nature*. May 8 2014;509(7499):189-94. doi:10.1038/nature13161
59. Tsai HH, *et al*. Regional astrocyte allocation regulates CNS synaptogenesis and repair. *Science*. Jul 20 2012;337(6092):358-62. doi:10.1126/

science.1222381
60. Liddelow SA*, et al*. Reactive Astrocytes: Production, Function, and Therapeutic Potential. *Immunity*. Jun 20 2017;46(6):957-967. doi:10.1016/j.immuni.2017.06.006
61. Vilalta A*, et al*. Neurophagy, the phagocytosis of live neurons and synapses by glia, contributes to brain development and disease. *Febs j*. Oct 2018;285(19):3566-3575. doi:10.1111/febs.14323
62. Eroglu C*, et al*. Regulation of synaptic connectivity by glia. *Nature*. Nov 11 2010;468(7321):223-31. doi:10.1038/nature09612
63. Lin CCJ*, et al*. Identification of diverse astrocyte populations and their malignant analogs. *Nat Neurosci*. Mar 2017;20(3):396-405. doi:10.1038/nn.4493
64. Hasel P*, et al*. Neuroinflammatory astrocyte subtypes in the mouse brain. *Nat Neurosci*. Oct 2021;24(10):1475-1487. doi:10.1038/s41593-021-00905-6
65. Massa PT*, et al*. Cell type-specific regulation of major histocompatibility complex (MHC) class I gene expression in astrocytes, oligodendrocytes, and neurons. *Glia*. Jul 1993;8(3):201-7. doi:10.1002/glia.440080307
66. Zhang Y*, et al*. Interleukin-11 potentiates oligodendrocyte survival and maturation, and myelin formation. *J Neurosci*. Nov 22 2006;26(47):12174-85. doi:10.1523/JNEUROSCI.2289-06.2006
67. Cannella B*, et al*. Multiple sclerosis: cytokine receptors on oligodendrocytes predict innate regulation. *Ann Neurol*. Jan 2004;55(1):46-57. doi:10.1002/ana.10764
68. Chakraborty G*, et al*. Interleukin-2 receptors and interleukin-2-mediated signaling in myelin: activation of diacylglycerol kinase and phosphatidylinositol 3-kinase. *Neuroscience*. 2003;122(4):967-73. doi:10.1016/j.neuroscience.2003.09.003
69. Bsibsi M*, et al*. Broad expression of Toll-like receptors in the human central nervous system. *J Neuropathol Exp Neurol*. Nov 2002;61(11):1013-21. doi:10.1093/jnen/61.11.1013
70. Bsibsi M*, et al*. Toll-like receptors 2 and 3 agonists differentially affect oligodendrocyte survival, differentiation, and myelin membrane formation. *J Neurosci Res*. Feb 2012;90(2):388-98. doi:10.1002/jnr.22767
71. Peferoen L*, et al*. Oligodendrocyte-microglia cross-talk in the central nervous system. *Immunology*. Mar 2014;141(3):302-13. doi:10.1111/imm.12163
72. Ramesh G*, et al*. A possible role for inflammation in mediating apoptosis of oligodendrocytes as induced by the Lyme disease spirochete Borrelia burgdorferi. *J Neuroinflammation*. Apr 23 2012;9(1):72. doi:10.1186/1742-2094-9-72
73. Balabanov R*, et al*. Interferon-γ-oligodendrocyte interactions in the regulation of experimental autoimmune encephalomyelitis. *Journal of Neuroscience*. 2007;27(8):2013-2024.
74. van Noort JM*, et al*. αB-crystallin is a target for adaptive immune responses and a trigger of innate responses in preactive multiple sclerosis lesions. *Journal of Neuropathology & Experimental Neurology*. 2010;69(7):694-703.
75. van Noort JM*, et al*. Mechanisms in the development of multiple sclerosis lesions: reconciling autoimmune and neurodegenerative factors. *CNS Neurol Disord Drug Targets*. Aug 2012;11(5):556-69. doi:10.2174/187152712801661293
76. Albrecht DS*, et al*. In Vivo Imaging of Human Neuroinflammation. *ACS Chem Neurosci*. Apr 20 2016;7(4):470-83. doi:10.1021/acschemneuro.6b00056
77. Zhang Y*, et al*. Myeloperoxidase Nuclear Imaging for Epileptogenesis. *Radiology*. Mar 2016;278(3):822-30. doi:10.1148/radiol.2015141922
78. Petroni D*, et al*. Toward PET imaging of A2B adenosine receptors: a carbon-11 labeled triazinobenzimidazole tracer: Synthesis and imaging of a new A2B PET tracer. *Nucl Med Biol*. May 2016;43(5):309-17. doi:10.1016/j.nucmedbio.2016.02.005
79. Walsh AJ*, et al*. Longitudinal MR imaging of iron in multiple sclerosis: an imaging marker of disease. *Radiology*. Jan 2014;270(1):186-96. doi:10.1148/radiol.13130474
80. Kothur K*, et al*. CSF cytokines/chemokines as biomarkers in neuroinflammatory CNS disorders: A systematic review. *Cytokine*. Jan 2016;77:227-37. doi:10.1016/j.cyto.2015.10.001
81. Wang YX*, et al*. Superparamagnetic iron oxide contrast agents: physicochemical characteristics and applications in MR imaging. *Eur Radiol*. 2001/05/03 2001;11(11):2319-31. doi:10.1007/s003300100908
82. El Ayoubi NK*, et al*. Blood Biomarkers as Outcome Measures in Inflammatory Neurologic Diseases. *Neurotherapeutics*. Jan 2017;14(1):135-147. doi:10.1007/s13311-016-0486-7
83. Lue LF*, et al*. Amyloid Beta and Tau as Alzheimer's Disease Blood Biomarkers: Promise From New Technologies. *Neurol Ther*. Jul 2017;6(Suppl 1):25-36. doi:10.1007/s40120-017-0074-8
84. Croese T*, et al*. Extracellular vesicles in neurodegenerative diseases. *Mol Aspects Med*. Apr 2018;60:52-61. doi:10.1016/j.mam.2017.11.006
85. Pulli B*, et al*. Imaging Neuroinflammation - from Bench to Bedside. *J Clin Cell Immunol*. 2014;5doi:10.4172/2155-9899.1000226
86. Serres S*, et al*. VCAM-1-targeted magnetic resonance imaging reveals subclinical disease in a mouse model of multiple sclerosis. *FASEB J*. Dec 2011;25(12):4415-22. doi:10.1096/fj.11-183772
87. Gauberti M*, et al*. Ultra-sensitive molecular MRI of vascular cell adhesion molecule-1 reveals a dynamic inflammatory penumbra after strokes. *Stroke*. Jul 2013;44(7):1988-96. doi:10.1161/

STROKEAHA.111.000544
88. Montagne A, *et al*. Ultra-sensitive molecular MRI of cerebrovascular cell activation enables early detection of chronic central nervous system disorders. *Neuroimage*. Nov 1 2012;63(2):760-70. doi:10.1016/j.neuroimage.2012.07.018
89. Chen JW, *et al*. Myeloperoxidase-targeted imaging of active inflammatory lesions in murine experimental autoimmune encephalomyelitis. *Brain*. Apr 2008;131(Pt 4):1123-33. doi:10.1093/brain/awn004
90. Breckwoldt MO, *et al*. Tracking the inflammatory response in stroke in vivo by sensing the enzyme myeloperoxidase. *Proc Natl Acad Sci U S A*. Nov 25 2008;105(47):18584-9. doi:10.1073/pnas.0803945105
91. Costa GL, *et al*. Adoptive immunotherapy of experimental autoimmune encephalomyelitis via T cell delivery of the IL-12 p40 subunit. *J Immunol*. Aug 15 2001;167(4):2379-87. doi:10.4049/jimmunol.167.4.2379
92. Barrera P, *et al*. Radiolabelled interleukin-1 receptor antagonist for detection of synovitis in patients with rheumatoid arthritis. *Rheumatology (Oxford)*. Aug 2000;39(8):870-4. doi:10.1093/rheumatology/39.8.870
93. Frullano L, *et al*. A myelin-specific contrast agent for magnetic resonance imaging of myelination. *J Am Chem Soc*. Feb 16 2011;133(6):1611-3. doi:10.1021/ja1040896
94. Wang C, *et al*. Longitudinal near-infrared imaging of myelination. *J Neurosci*. Feb 16 2011;31(7):2382-90. doi:10.1523/JNEUROSCI.2698-10.2011
95. Datta G, *et al*. Translocator positron-emission tomography and magnetic resonance spectroscopic imaging of brain glial cell activation in multiple sclerosis. *Mult Scler*. Oct 2017;23(11):1469-1478. doi:10.1177/1352458516681504
96. Oh U, *et al*. Translocator protein PET imaging for glial activation in multiple sclerosis. *J Neuroimmune Pharmacol*. Sep 2011;6(3):354-61. doi:10.1007/s11481-010-9243-6
97. Rissanen E, *et al*. In Vivo Detection of Diffuse Inflammation in Secondary Progressive Multiple Sclerosis Using PET Imaging and the Radioligand (1)(1)C-PK11195. *J Nucl Med*. Jun 2014;55(6):939-44. doi:10.2967/jnumed.113.131698
98. Versijpt J, *et al*. Microglial imaging with positron emission tomography and atrophy measurements with magnetic resonance imaging in multiple sclerosis: a correlative study. *Mult Scler*. Apr 2005;11(2):127-34. doi:10.1191/1352458505ms1140oa
99. Vowinckel E, *et al*. PK11195 binding to the peripheral benzodiazepine receptor as a marker of microglia activation in multiple sclerosis and experimental autoimmune encephalomyelitis. *Journal of Neuroscience Research*. Oct 15 1997;50(2):345-353. doi:Doi 10.1002/(Sici)1097-4547(19971015)50:2<345::Aid-Jnr22>3.0.Co;2-5
100. Guilarte TR. TSPO in diverse CNS pathologies and psychiatric disease: A critical review and a way forward. *Pharmacol Ther*. Feb 2019;194:44-58. doi:10.1016/j.pharmthera.2018.09.003
101. Edison P, *et al*. Microglia, amyloid, and cognition in Alzheimer's disease: An [11C](R)PK11195-PET and [11C]PIB-PET study. *Neurobiol Dis*. Dec 2008;32(3):412-9. doi:10.1016/j.nbd.2008.08.001
102. Yasuno F, *et al*. Increased binding of peripheral benzodiazepine receptor in Alzheimer's disease measured by positron emission tomography with [11C]DAA1106. *Biol Psychiatry*. Nov 15 2008;64(10):835-41. doi:10.1016/j.biopsych.2008.04.021
103. Ouchi Y, *et al*. Microglial activation and dopamine terminal loss in early Parkinson's disease. *Ann Neurol*. Feb 2005;57(2):168-75. doi:10.1002/ana.20338
104. Banati RB, *et al*. [11C](R)-PK11195 positron emission tomography imaging of activated microglia in vivo in Rasmussen's encephalitis. *Neurology*. Dec 10 1999;53(9):2199-203. doi:10.1212/wnl.53.9.2199
105. Cagnin A, *et al*. In vivo visualization of activated glia by [11C] (R)-PK11195-PET following herpes encephalitis reveals projected neuronal damage beyond the primary focal lesion. *Brain*. Oct 2001;124(Pt 10):2014-27. doi:10.1093/brain/124.10.2014
106. Turner MR, *et al*. Evidence of widespread cerebral microglial activation in amyotrophic lateral sclerosis: an [11C](R)-PK11195 positron emission tomography study. *Neurobiol Dis*. Apr 2004;15(3):601-9. doi:10.1016/j.nbd.2003.12.012
107. Messmer K, *et al*. Increased peripheral benzodiazepine binding sites in the brain of patients with Huntington's disease. *Neurosci Lett*. Jan 23 1998;241(1):53-6. doi:10.1016/s0304-3940(97)00967-1
108. Cagnin A, *et al*. In vivo detection of microglial activation in frontotemporal dementia. *Ann Neurol*. Dec 2004;56(6):894-7. doi:10.1002/ana.20332
109. Banati RB, *et al*. The peripheral benzodiazepine binding site in the brain in multiple sclerosis: quantitative in vivo imaging of microglia as a measure of disease activity. *Brain*. Nov 2000;123 (Pt 11)(11):2321-37. doi:10.1093/brain/123.11.2321
110. Venneti S, *et al*. The peripheral benzodiazepine receptor (Translocator protein 18kDa) in microglia: from pathology to imaging. *Prog Neurobiol*. Dec 2006;80(6):308-22. doi:10.1016/j.pneurobio.2006.10.002
111. Colasanti A, *et al*. In Vivo Assessment of Brain White Matter Inflammation in Multiple Sclerosis with (18)F-PBR111 PET. *J Nucl Med*. Jul 2014;55(7):1112-8. doi:10.2967/jnumed.113.135129
112. Debruyne JC, *et al*. PET visualization of microglia in multiple sclerosis patients using [11C]PK11195. *Eur J Neurol*. May 2003;10(3):257-64. doi:10.1046/

j.1468-1331.2003.00571.x
113. Gerhard A, *et al*. [11C](R)-PK11195 PET imaging of microglial activation in multiple system atrophy. *Neurology*. Sep 9 2003;61(5):686-9. doi:10.1212/01.wnl.0000078192.95645.e6
114. Gerhard A, *et al*. In vivo imaging of microglial activation with [11C](R)-PK11195 PET in idiopathic Parkinson's disease. *Neurobiol Dis*. Feb 2006;21(2):404-12. doi:10.1016/j.nbd.2005.08.002
115. Gerhard A, *et al*. In vivo imaging of microglial activation with [11C](R)-PK11195 PET in progressive supranuclear palsy. *Mov Disord*. Jan 2006;21(1):89-93. doi:10.1002/mds.20668
116. Gerhard A, *et al*. In vivo imaging of microglial activation with [11C](R)-PK11195 PET in corticobasal degeneration. *Mov Disord*. Oct 2004;19(10):1221-6. doi:10.1002/mds.20162
117. Ghadery C, *et al*. Microglial activation in Parkinson's disease using [(18)F]-FEPPA. *J Neuroinflammation*. Jan 11 2017;14(1):8. doi:10.1186/s12974-016-0778-1
118. Groom GN, *et al*. PET of peripheral benzodiazepine binding sites in the microgliosis of Alzheimer's disease. *J Nucl Med*. Dec 1995;36(12):2207-10.
119. Henkel K, *et al*. Imaging of activated microglia with PET and [11C]PK 11195 in corticobasal degeneration. *Mov Disord*. Jul 2004;19(7):817-821. doi:10.1002/mds.20040
120. Politis M, *et al*. Increased central microglial activation associated with peripheral cytokine levels in premanifest Huntington's disease gene carriers. *Neurobiol Dis*. Nov 2015;83:115-21. doi:10.1016/j.nbd.2015.08.011
121. Tai YF, *et al*. Imaging microglial activation in Huntington's disease. *Brain Res Bull*. Apr 30 2007;72(2-3):148-51. doi:10.1016/j.brainresbull.2006.10.029
122. Tomasi G, *et al*. Novel reference region model reveals increased microglial and reduced vascular binding of 11C-(R)-PK11195 in patients with Alzheimer's disease. *J Nucl Med*. Aug 2008;49(8):1249-56. doi:10.2967/jnumed.108.050583
123. Venneti S, *et al*. PK11195 labels activated microglia in Alzheimer's disease and in vivo in a mouse model using PET. *Neurobiol Aging*. Aug 2009;30(8):1217-26. doi:10.1016/j.neurobiolaging.2007.11.005
124. Yankam Njiwa J, *et al*. Quantitative longitudinal imaging of activated microglia as a marker of inflammation in the pilocarpine rat model of epilepsy using [(11)C]-(R)-PK11195 PET and MRI. *J Cereb Blood Flow Metab*. Apr 2017;37(4):1251-1263. doi:10.1177/0271678X16653615
125. Arlicot N, *et al*. Evaluation of CLINDE as potent translocator protein (18 kDa) SPECT radiotracer reflecting the degree of neuroinflammation in a rat model of microglial activation. *Eur J Nucl Med Mol Imaging*. Dec 2008;35(12):2203-11. doi:10.1007/s00259-008-0834-x
126. Dickens AM, *et al*. Detection of microglial activation in an acute model of neuroinflammation using PET and radiotracers 11C-(R)-PK11195 and 18F-GE-180. *J Nucl Med*. Mar 2014;55(3):466-72. doi:10.2967/jnumed.113.125625
127. Domene A, *et al*. Expression of Phenotypic Astrocyte Marker Is Increased in a Transgenic Mouse Model of Alzheimer's Disease versus Age-Matched Controls: A Presymptomatic Stage Study. *Int J Alzheimers Dis*. 2016;2016:5696241. doi:10.1155/2016/5696241
128. Israel I, *et al*. Combined [(18)F]DPA-714 micro-positron emission tomography and autoradiography imaging of microglia activation after closed head injury in mice. journal article. *J Neuroinflammation*. Jun 7 2016;13(1):140. doi:10.1186/s12974-016-0604-9
129. Ji B, *et al*. Imaging of peripheral benzodiazepine receptor expression as biomarkers of detrimental versus beneficial glial responses in mouse models of Alzheimer's and other CNS pathologies. *J Neurosci*. Nov 19 2008;28(47):12255-67. doi:10.1523/JNEUROSCI.2312-08.2008
130. Lavisse S, *et al*. Reactive astrocytes overexpress TSPO and are detected by TSPO positron emission tomography imaging. *J Neurosci*. Aug 8 2012;32(32):10809-18. doi:10.1523/JNEUROSCI.1487-12.2012
131. Lavisse S, *et al*. [18F]DPA-714 PET imaging of translocator protein TSPO (18 kDa) in the normal and excitotoxically-lesioned nonhuman primate brain. *Eur J Nucl Med Mol Imaging*. Mar 2015;42(3):478-94. doi:10.1007/s00259-014-2962-9
132. Maeda J, *et al*. Phase-dependent roles of reactive microglia and astrocytes in nervous system injury as delineated by imaging of peripheral benzodiazepine receptor. *Brain Res*. Jul 9 2007;1157:100-11. doi:10.1016/j.brainres.2007.04.054
133. Mattner F, *et al*. Evaluation of [(1)(2)(3)I]-CLINDE as a potent SPECT radiotracer to assess the degree of astroglia activation in cuprizone-induced neuroinflammation. *Eur J Nucl Med Mol Imaging*. Aug 2011;38(8):1516-28. doi:10.1007/s00259-011-1784-2
134. Nguyen DL, *et al*. Longitudinal positron emission tomography imaging of glial cell activation in a mouse model of mesial temporal lobe epilepsy: Toward identification of optimal treatment windows. *Epilepsia*. Jun 2018;59(6):1234-1244. doi:10.1111/epi.14083
135. Rojas S, *et al*. Imaging brain inflammation with [(11)C]PK11195 by PET and induction of the peripheral-type benzodiazepine receptor after transient focal ischemia in rats. *J Cereb Blood Flow Metab*. Dec 2007;27(12):1975-86. doi:10.1038/sj.jcbfm.9600500
136. Serriere S, *et al*. Amyloid load and translocator protein 18 kDa in APPswePS1-dE9 mice: a longitudinal study. *Neurobiol Aging*. Apr 2015;36(4):1639-1652. doi:10.1016/j.

neurobiolaging.2014.11.023
137. Wang Y, *et al*. PET imaging of neuroinflammation in a rat traumatic brain injury model with radiolabeled TSPO ligand DPA-714. *Eur J Nucl Med Mol Imaging*. Jul 2014;41(7):1440-9. doi:10.1007/s00259-014-2727-5
138. Daugherty DJ, *et al*. A TSPO ligand is protective in a mouse model of multiple sclerosis. *EMBO Mol Med*. Jun 2013;5(6):891-903. doi:10.1002/emmm.201202124
139. Cosenza-Nashat M, *et al*. Expression of the translocator protein of 18 kDa by microglia, macrophages and astrocytes based on immunohistochemical localization in abnormal human brain. *Neuropathol Appl Neurobiol*. Jun 2009;35(3):306-28. doi:10.1111/j.1365-2990.2008.01006.x
140. Liu B, *et al*. In Vivo Detection of Age- and Disease-Related Increases in Neuroinflammation by 18F-GE180 TSPO MicroPET Imaging in Wild-Type and Alzheimer's Transgenic Mice. *J Neurosci*. Nov 25 2015;35(47):15716-30. doi:10.1523/JNEUROSCI.0996-15.2015
141. Maeda J, *et al*. In vivo positron emission tomographic imaging of glial responses to amyloid-beta and tau pathologies in mouse models of Alzheimer's disease and related disorders. *J Neurosci*. Mar 23 2011;31(12):4720-30. doi:10.1523/JNEUROSCI.3076-10.2011
142. Kaunzner UW, *et al*. Quantitative susceptibility mapping identifies inflammation in a subset of chronic multiple sclerosis lesions. *Brain*. Jan 1 2019;142(1):133-145. doi:10.1093/brain/awy296
143. Owen DR, *et al*. Pro-inflammatory activation of primary microglia and macrophages increases 18 kDa translocator protein expression in rodents but not humans. *J Cereb Blood Flow Metab*. Aug 2017;37(8):2679-2690. doi:10.1177/0271678X17710182
144. Bae KR, *et al*. Translocator protein 18 kDa negatively regulates inflammation in microglia. *J Neuroimmune Pharmacol*. Jun 2014;9(3):424-37. doi:10.1007/s11481-014-9540-6
145. Gottfried-Blackmore A, *et al*. Brain microglia express steroid-converting enzymes in the mouse. *J Steroid Biochem Mol Biol*. Mar 2008;109(1-2):96-107. doi:10.1016/j.jsbmb.2007.12.013
146. Karlstetter M, *et al*. Translocator protein (18 kDa) (TSPO) is expressed in reactive retinal microglia and modulates microglial inflammation and phagocytosis. *J Neuroinflammation*. Jan 8 2014;11:3. doi:10.1186/1742-2094-11-3
147. Wang M, *et al*. Macroglia-microglia interactions via TSPO signaling regulates microglial activation in the mouse retina. *J Neurosci*. Mar 5 2014;34(10):3793-806. doi:10.1523/JNEUROSCI.3153-13.2014
148. Stephenson J, *et al*. Modelling amyotrophic lateral sclerosis in mice. *Drug Discovery Today: Disease Models*. 2017/12/01/ 2017;25-26:35-44. doi:10.1016/j.ddmod.2018.10.001
149. Baker D, *et al*. Publication guidelines for refereeing and reporting on animal use in experimental autoimmune encephalomyelitis. *J Neuroimmunol*. Jan 18 2012;242(1-2):78-83. doi:10.1016/j.jneuroim.2011.11.003
150. Baker D, *et al*. Critical appraisal of animal models of multiple sclerosis. *Mult Scler*. Jun 2011;17(6):647-57. doi:10.1177/1352458511398885
151. Ramagopalan SV, *et al*. Multiple sclerosis: risk factors, prodromes, and potential causal pathways. *Lancet Neurol*. Jul 2010;9(7):727-39. doi:10.1016/S1474-4422(10)70094-6
152. Ascherio A, *et al*. Environmental risk factors for multiple sclerosis. Part I: the role of infection. *Ann Neurol*. Apr 2007;61(4):288-99. doi:10.1002/ana.21117
153. Levin LI, *et al*. Temporal relationship between elevation of epstein-barr virus antibody titers and initial onset of neurological symptoms in multiple sclerosis. *Jama*. May 25 2005;293(20):2496-500. doi:10.1001/jama.293.20.2496
154. Nielsen TR, *et al*. Multiple sclerosis after infectious mononucleosis. *Arch Neurol*. Jan 2007;64(1):72-5. doi:10.1001/archneur.64.1.72
155. Ascherio A, *et al*. EBV and Autoimmunity. *Curr Top Microbiol Immunol*. 2015;390(Pt 1):365-85. doi:10.1007/978-3-319-22822-8_15
156. Burns DM, *et al*. Memory B-cell reconstitution following allogeneic hematopoietic stem cell transplantation is an EBV-associated transformation event. *Blood*. Dec 17 2015;126(25):2665-2675. doi:10.1182/blood-2015-08-665000
157. Fernandez-Menendez S, *et al*. Epstein-Barr virus and multiple sclerosis. From evidence to therapeutic strategies. *J Neurol Sci*. Feb 15 2016;361:213-9. doi:10.1016/j.jns.2016.01.013
158. Kakalacheva K, *et al*. Infectious Mononucleosis Triggers Generation of IgG Auto-Antibodies against Native Myelin Oligodendrocyte Glycoprotein. *Viruses*. Feb 12 2016;8(2)doi:10.3390/v8020051
159. Bsibsi M, *et al*. Demyelination during multiple sclerosis is associated with combined activation of microglia/macrophages by IFN-γ and alpha B-crystallin. *Acta Neuropathol*. 2014;128(2):215-229.
160. Bajramović JJ, *et al*. Presentation of αB-crystallin to T cells in active multiple sclerosis lesions: an early event following inflammatory demyelination. *The Journal of Immunology*. 2000;164(8):4359-4366.
161. Acheson E, *et al*. Some comments on the relationship of the distribution of multiple sclerosis to latitude, solar radiation, and other variables. *Acta Psychiatrica Scandinavica*. 1960;35(S147):132-147.
162. Kampman MT, *et al*. Vitamin D: a candidate for the environmental effect in multiple sclerosis–observations from Norway. *Neuroepidemiology*. 2008;30(3):140-146.
163. Munger KL, *et al*. Serum 25-hydroxyvitamin

D levels and risk of multiple sclerosis. *Jama*. Dec 20 2006;296(23):2832-8. doi:10.1001/jama.296.23.2832
164. Ebers GC, *et al*. Parent-of-origin effect in multiple sclerosis: observations in half-siblings. *Lancet*. May 29 2004;363(9423):1773-4. doi:10.1016/S0140-6736(04)16304-6
165. Willer CJ, *et al*. Twin concordance and sibling recurrence rates in multiple sclerosis. *Proc Natl Acad Sci U S A*. Oct 28 2003;100(22):12877-82. doi:10.1073/pnas.1932604100
166. Jersild C, *et al*. Histocompatibility determinants in multiple sclerosis, with special reference to clinical course. *Lancet*. Dec 1 1973;2(7840):1221-5. doi:10.1016/s0140-6736(73)90970-7
167. Dyment DA, *et al*. Complex interactions among MHC haplotypes in multiple sclerosis: susceptibility and resistance. *Hum Mol Genet*. Jul 15 2005;14(14):2019-26. doi:10.1093/hmg/ddi206
168. Thompson AJ, *et al*. Diagnosis of multiple sclerosis: 2017 revisions of the McDonald criteria. *Lancet Neurol*. Feb 2018;17(2):162-173. doi:10.1016/S1474-4422(17)30470-2
169. van der Valk P, *et al*. Staging of multiple sclerosis (MS) lesions: pathology of the time frame of MS. *Neuropathol Appl Neurobiol*. Feb 2000;26(1):2-10. doi:10.1046/j.1365-2990.2000.00217.x
170. Duncan ID, *et al*. Thin myelin sheaths as the hallmark of remyelination persist over time and preserve axon function. *Proc Natl Acad Sci U S A*. Nov 7 2017;114(45):E9685-E9691. doi:10.1073/pnas.1714183114
171. Calabrese M, *et al*. Grey matter lesions in MS: from histology to clinical implications. *Prion*. Jan-Feb 2013;7(1):20-7. doi:10.4161/pri.22580
172. Popescu BF, *et al*. Meningeal and cortical grey matter pathology in multiple sclerosis. *BMC Neurol*. Mar 7 2012;12(1):11. doi:10.1186/1471-2377-12-11
173. Mitchell JD, *et al*. Amyotrophic lateral sclerosis. *The Lancet*. 2007;369(9578):2031-2041.
174. Morello G, *et al*. Neuroinflammation and ALS: Transcriptomic Insights into Molecular Disease Mechanisms and Therapeutic Targets. *Mediators Inflamm*. 2017/09/07 2017;2017:7070469. doi:10.1155/2017/7070469
175. Gorter RP, *et al*. Rapidly progressive amyotrophic lateral sclerosis is associated with microglial reactivity and small heat shock protein expression in reactive astrocytes. *Neuropathol Appl Neurobiol*. Aug 2019;45(5):459-475. doi:10.1111/nan.12525
176. O'Rourke JG, *et al*. C9orf72 is required for proper macrophage and microglial function in mice. *Science*. Mar 18 2016;351(6279):1324-1329. doi:10.1126/science.aaf1064
177. Kampinga HH, *et al*. HSPBs: small proteins with big implications in human disease. *Int J Biochem Cell Biol*. Oct 2012;44(10):1706-10. doi:10.1016/j.biocel.2012.06.005
178. Van Weehaeghe D, *et al*. TSPO Versus P2X7 as a Target for Neuroinflammation: An In Vitro and In Vivo Study. *J Nucl Med*. Apr 2020;61(4):604-607. doi:10.2967/jnumed.119.231985
179. Zurcher NR, *et al*. Increased in vivo glial activation in patients with amyotrophic lateral sclerosis: assessed with [(11)C]-PBR28. *Neuroimage Clin*. 2015;7:409-14. doi:10.1016/j.nicl.2015.01.009
180. Venneti S, *et al*. The positron emission tomography ligand DAA1106 binds with high affinity to activated microglia in human neurological disorders. *J Neuropathol Exp Neurol*. Oct 2008;67(10):1001-10. doi:10.1097/NEN.0b013e318188b204
181. Heneka MT, *et al*. Neuroinflammation in Alzheimer's disease. *Lancet Neurol*. Apr 2015;14(4):388-405. doi:10.1016/S1474-4422(15)70016-5
182. Mawuenyega KG, *et al*. Decreased clearance of CNS β-amyloid in Alzheimer's disease. *Science*. 2010;330(6012):1774-1774.
183. Wyss-Coray T, *et al*. Adult mouse astrocytes degrade amyloid-beta in vitro and in situ. *Nat Med*. Apr 2003;9(4):453-7. doi:10.1038/nm838
184. Olabarria M, *et al*. Concomitant astroglial atrophy and astrogliosis in a triple transgenic animal model of Alzheimer's disease. *Glia*. 2010;58(7):831-838.
185. Hamelin L, *et al*. Early and protective microglial activation in Alzheimer's disease: a prospective study using 18 F-DPA-714 PET imaging. *Brain*. 2016;139(4):1252-1264.
186. Versijpt JJ, *et al*. Assessment of neuroinflammation and microglial activation in Alzheimer's disease with radiolabelled PK11195 and single photon emission computed tomography. *European neurology*. 2003;50(1):39-47.
187. Kreisl WC, *et al*. 11C-PBR28 binding to translocator protein increases with progression of Alzheimer's disease. *Neurobiology of aging*. 2016;44:53-61.
188. Kreisl WC, *et al*. In vivo radioligand binding to translocator protein correlates with severity of Alzheimer's disease. *Brain*. 2013;136(7):2228-2238.
189. Lyoo CH, *et al*. Cerebellum Can Serve As a Pseudo-Reference Region in Alzheimer Disease to Detect Neuroinflammation Measured with PET Radioligand Binding to Translocator Protein. *Journal of Nuclear Medicine*. May 1 2015;56(5):701-706. doi:10.2967/jnumed.114.146027
190. Fan Z, *et al*. Influence of microglial activation on neuronal function in Alzheimer's and Parkinson's disease dementia. *Alzheimers Dement*. Jun 2015;11(6):608-21 e7. doi:10.1016/j.jalz.2014.06.016
191. Gui Y, *et al*. Characterization of the 18 kDa translocator protein (TSPO) expression in post-mortem normal and Alzheimer's disease brains. *Brain Pathol*. Jan 2020;30(1):151-164. doi:10.1111/bpa.12763
192. Constantinescu CS, *et al*. Experimental autoimmune encephalomyelitis (EAE) as a model

for multiple sclerosis (MS). *Br J Pharmacol*. Oct 2011;164(4):1079-106. doi:10.1111/j.1476-5381.2011.01302.x

193. Rosen DR*, et al*. Mutations in Cu/Zn superoxide dismutase gene are associated with familial amyotrophic lateral sclerosis. *Nature*. 1993;362(6415):59-62.
194. Dawson TM*, et al*. Animal models of neurodegenerative diseases. *Nat Neurosci*. 2018/10/01 2018;21(10):1370-1379. doi:10.1038/s41593-018-0236-8
195. Coda AR*, et al*. In vivo imaging of CNS microglial activation/macrophage infiltration with combined [(18)F]DPA-714-PET and SPIO-MRI in a mouse model of relapsing remitting experimental autoimmune encephalomyelitis. *Eur J Nucl Med Mol Imaging*. Jan 2021;48(1):40-52. doi:10.1007/s00259-020-04842-7
196. Belloli S*, et al*. (18)F-VC701-PET and MRI in the in vivo neuroinflammation assessment of a mouse model of multiple sclerosis. *J Neuroinflammation*. Feb 5 2018;15(1):33. doi:10.1186/s12974-017-1044-x
197. Gargiulo S*, et al*. Imaging of brain TSPO expression in a mouse model of amyotrophic lateral sclerosis with (18)F-DPA-714 and micro-PET/CT. *Eur J Nucl Med Mol Imaging*. Jul 2016;43(7):1348-59. doi:10.1007/s00259-016-3311-y

PART I

Visualising Microglia in Neurodegeneration

A quantitative neuropathological assessment of translocator protein expression in multiple sclerosis

Erik Nutma, Jodie A. Stephenson, Rianne P. Gorter, Joy de Bruin, Deirdre M. Boucherie, Cornelius K. Donat, Marjolein Breur, Paul van der Valk, Paul M. Matthews, David R. Owen, Sandra Amor

Brain 2019; 142(11):3440-3455

Abstract

The 18kDa translocator protein (TSPO) is increasingly used to study brain and spinal cord inflammation in degenerative diseases of the CNS such as multiple sclerosis. The enhanced TSPO PET signal that arises during disease is widely-considered to reflect activated pathogenic microglia, although quantitative neuropathological data to support this interpretation has not been available. With the increasing interest in the role of chronic microglial activation in multiple sclerosis, characterising the cellular neuropathology associated with TSPO expression is of clear importance for understanding the cellular and pathological processes on which TSPO PET imaging is reporting.

Here we have studied the cellular expression of TSPO and specific binding of two TSPO targeting radioligands ([^{3}H]PK11195 and [^{3}H]PBR28) in tissue sections from 42 multiple sclerosis cases and 12 age-matched controls. Markers of homeostatic and reactive microglia, astrocytes, and lymphocytes were used to investigate the phenotypes of cells expressing TSPO. There was an approximate 20-fold increase in cells double positive for TSPO and human leukocyte antigen -DR in active lesions and in the rim of chronic active lesion, relative to normal appearing white matter. TSPO was uniformly expressed across myeloid cells irrespective of their phenotype, rather than being preferentially associated with pro-inflammatory microglia or macrophages. TSPO$^+$ astrocytes were increased up to 7-fold compared to normal appearing white matter across all lesion sub-types and accounted for 25% of the TSPO+ cells in these lesions. To relate TSPO protein expression to ligand binding, specific binding of the TSPO ligands [^{3}H] PK11195 and [^{3}H]PBR28 was determined in the same lesions. TSPO radioligand binding was increased up to seven times for [^{3}H]PBR28 and up to two times for [^{3}H]PK11195 in active lesions and the centre of chronic active lesions and a strong correlation was found between the radioligand binding signal for both tracers and the number of TSPO$^+$ cells across all of the tissues examined.

In summary, in multiple sclerosis, TSPO expression arises from microglia of different phenotypes, rather than being restricted to microglia which express classical pro-inflammatory markers. While the majority of cells expressing TSPO in active lesions or chronic active rims are microglia/macrophages, our findings also emphasise the significant contribution of activated astrocytes, as well as smaller contributions from endothelial cells. These observations establish a quantitative framework for interpretation of TSPO in multiple sclerosis and highlight the need for neuropathological characterisation of TSPO expression for the interpretation of TSPO PET in other neurodegenerative disorders.

Introduction

The 18 kDa translocator protein (TSPO) is an outer mitochondrial membrane protein that has attracted increasing interest for its use as a PET imaging target to visualise inflammation in the brain. TSPO is expressed in many tissues, including the brain, and has been suggested to be involved in mitochondrial "household" functions, although its exact functions are unknown[1]. TSPO PET signal is markedly upregulated in neurodegenerative and neuroinflammatory diseases including multiple sclerosis[2-6], Alzheimer's disease[7,8], Parkinson's disease[9], viral encephalitis[10,11], amyotrophic lateral sclerosis[12], Huntington's disease[13] and frontotemporal dementia[14] and thus has become recognised as a marker of *in vivo* neuroinflammation[15-17]. A limitation of these applications has been uncertainty regarding the interpretation of increased signal; many of the studies have widely assumed that increased signal reflects activated microglia, while ignoring the potential contributions of astrocytes and other cell types [2,11,12,15,18-30]. Although recent studies using animal models of neurodegenerative diseases have shown astrocytic TSPO[31-44], only a few have examined astrocytic expression of TSPO in the human CNS[45], and these descriptions have been qualitative rather than quantitative[46-48].

In experimental autoimmune encephalomyelitis, and in cuprizone, two animal models of multiple sclerosis, increased TSPO expression has been described in astrocytes and microglia[44,49]. Increased microglial TSPO expression is associated with pro-inflammatory markers in rodents[50]. Based on animal model studies, TSPO has been suggested as a therapeutic target for modulation of the pathogenic microglial phenotypes[44,51]. However, in humans, TSPO is not upregulated in either pro-inflammatory macrophages[52] or primary microglia[53]. These *in vitro* data are consistent with the finding that monocytes isolated from people with multiple sclerosis show lower TSPO expression compared to healthy controls[54]. Additionally, microglia/macrophages in multiple sclerosis lesions adopt an intermediate phenotype, and the classical M1 (pro-inflammatory) and M2 (anti-inflammatory) phenotypes probably represent extreme states only found *in vitro*[55]. Thus, in contrast to the pattern of TSPO expression in rodent models, it may not be so specifically associated with pro-inflammatory microglia in multiple sclerosis[56]. For interpretation of TSPO PET studies of brain inflammation in multiple sclerosis and for exploration of potential therapeutic targeting of TSPO, it is thus crucial to determine whether specific microglial markers are associated with TSPO expression and to what extent these cells contribute to the TSPO PET signal in neuroinflammatory diseases *in vivo*.

Here we have performed a quantitative neuropathological study in a large cohort of multiple sclerosis brain and spinal cord tissues to characterise the cell types and identify the phenotypes of microglia expressing TSPO in lesions in the white and grey matter. We report three important findings. First, we confirm previous data showing that TSPO expression is increased in active and chronic active lesions, and that HLA-DR$^+$ microglia are the cell type responsible for the majority of the signal. However, astrocytes expressing TSPO in the centre of chronic active and in inactive lesions also are important contributors to the total number of TSPO$^+$ cells. Second, we show that, in humans, TSPO reports on microglia density rather than relative microglial activation and polarization. Finally, we confirm a strong, direct relationship between TSPO expression and TSPO radioligand binding in brain tissue *ex vivo*. Therefore, we show that whilst expression of TSPO reflects activated microglia, it is misleading to characterise TSPO as a marker restricted to pro-inflammatory microglia.

Materials and methods

Human brain tissue

Human brain tissue was obtained at autopsy from 42 people with multiple sclerosis and 12 age-matched cases with no neurological disorders or peripheral inflammation. Biopsy material from MRI tumour-like lesions was taken from 4 patients with suspected multiple sclerosis. Patient data and clinical details are summarized in Table 1. The rapid autopsy regimen of the Netherlands Brain Bank in Amsterdam (coordinator Dr. I. Huitinga) was used to acquire the samples, with the approval of the Medical Ethical Committee of the Amsterdam UMC. All participants or next of kin had given informed consent for autopsy and use of their tissues for research purposes. Tissue samples from multiple sclerosis cases were selected from regions of interest after *ex vivo* MRI[57,58]. Brain samples were cut in half and fixed in 10% formalin and embedded in paraffin or snap-frozen and stored in liquid nitrogen. The cases and lesions were selected from a large cohort of multiple sclerosis cases based on the size and lesion type for quantitative analysis. Lesion stages were based on immunohistochemical detection for myelin proteolipid protein (PLP) to detect areas of myelin loss and expression of human leukocyte antigen DR (HLA-DR)[59,60]. Briefly, active lesions were characterised by a focal area of myelin loss filled with myelin-laden 'foamy' macrophages; chronic active lesions were identified by a rim of activated microglia/macrophages surrounding a hypocellular centre, and inactive white matter lesions as a demyelinated area with few or no HLA-DR$^+$ cells. The normal appearing white and grey matter in the same tissue blocks from multiple sclerosis cases and control white and grey matter from age-matched controls were analysed as reference samples for the expression of cell markers.

Immunohistochemistry

Paraffin sections were de-paraffinized using xylene, rehydrated through descending alcohol solutions and washed in phosphate buffered saline. Frozen sections were air-dried and fixed in 2% paraformaldehyde for 10 mins at room temperature and washed in phosphate buffered saline. Endogenous peroxidase activity was blocked using 0.3% (w/v) H_2O_2. Following washing, paraffin sections underwent antigen retrieval in citrate or TRIS/EDTA buffer in a water bath at 95°C for 30 mins. After cooling, sections were washed and incubated in primary antibodies overnight in antibody diluent (Immunologic, Duiven, The Netherlands). After washing, sections were incubated in the appropriate secondary antibodies. Horseradish peroxidase labelled secondary antibodies were developed using 3,3'-diaminobenzidine (1:50, DAB, DAKO, CA) for 10 min after which sections were washed in tris buffered saline. Liquid permanent red (1:100, DAKO) was used to visualise alkaline phosphatase labelled antibodies. Sections were washed with tris buffered saline, counterstained with haematoxylin, washed and mounted in Aquatex (Merck, Darmstadt, Germany). For immunofluorescence, sections were incubated with Alexa Fluor labelled secondary antibodies in antibody diluent for 90 mins and nuclei were stained with 4',6-diamidino-2-phenylindole. Appropriate negative controls were used by omitting the primary antibodies.

Table 1. Clinical details of multiple sclerosis and control cases

Case	Age	Gender	Genotype*	Diagnosis	Duration	PM delay hrs:mins	Cause of death
Multiple sclerosis							
1	69	F		PPMS/SPMS	53	7:30	Respiratory failure
2	70	F		PPMS/SPMS	40	6:55	Urine tract infection
3	50	M		PPMS/SPMS	15	5:25	Pneumonia
4	66	F		SPMS	11	6:00	Pneumonia
5	75	F		PPMS/SPMS	24	5:00	Heart failure
6	49	M		SPMS	25	8:00	Pneumonia
7	66	M		SPMS	26	7:30	Ileus
8	64	F	Low	SPMS	31	10:10	Urinary tract infection
9	61	M	High	SPMS	18	9:15	Euthanasia
10	77	F		PPMS	24	10:00	Euthanasia
11	67	F	Mixed	SPMS	25	9:15	Palliative sedation
12	45	M		PPMS	10	7:45	Pulmonary embolism
13	59	F		SPMS	24	4:45	Euthanasia
14	58	F		SPMS	36	10:40	Euthanasia
15	44	M		PPMS	21	10:15	End stage of MS
16	51	M		SPMS	19	11:00	Unknown
17	57	F	Low	RRMS	26	8:40	Urosepsis
18	57	F	High	PPMS	29	11:00	Euthanasia
19	73	M	Mixed	RRMS	26	8:00	Urosepsis
20	76	F	High	SPMS	25	7:55	Euthanasia
21	56	M	Mixed	PPMS	14	9:50	Cachexia
22	74	M	Mixed	PPMS	15	10:15	Heart failure
23	60	F	Mixed	SPMS	7	10:40	Euthanasia
24	54	M	Low	PPMS	12	8:15	Euthanasia
25	75	M	Mixed	PPMS	46	10:10	Pneumonia
26	50	F	Mixed	SPMS	17	7:35	Euthanasia
27	53	M		SPMS	24	10:00	Euthanasia
28	66	F		PPMS	13	9:35	Euthanasia
29	56	M	Mixed	SPMS	14	10:10	Suicide
30	66	F		SPMS	16	10:45	Pulmonary hypertension
31	81	F		SPMS	31	4:35	Pneumonia
32	63	M		SPMS	25	8:15	Pneumonia
33	75	F	High	SPMS	Unknown	9:45	Subdural hematoma
34	61	F	High	Unknown	Unknown	10:00	Euthanasia
35	50	M	Low	SPMS	21	10:50	Unknown
36	49	F		Unknown	Unknown	8:30	Unknown
37	50	F		SPMS	18	09:05	Euthanasia
38	57	M		PPMS	24	10:15	Sepsis
39	35	F		SPMS	10	10:20	Euthanasia
40	54	F		Unknown	27	09:25	Respiratory failure
41	67	M		SPMS	38	11:00	Sudden death
42	54	M		SPMS	29	06:40	Euthanasia
Biopsy							
1	51	M	Demyelinating disease, suspected MS				
2	Unknown		Demyelinating disease, suspected MS				
3	27	M	Demyelinating disease, suspected MS				
4	31	F	Demyelinating disease, suspected MS				
Control							
1	61	F		control	N/A	6:50	Euthanasia
2	73	F		control	N/A	4:00	Lung fibrosis
3	67	M		control	N/A	4:30	Cardiac shock
4	81	M		control	N/A	5:30	Prostate carcinoma
5	67	M		control	N/A	18:35	Myocardial infarction
6	84	F		control	N/A	4:45	Respiratory failure
7	91	F		control	N/A	7:45	Decompensatio cordis
8	56	M	Mixed	control	N/A	14:00	Heart failure
9	92	F		control	N/A	7:00	Acute death
10	62	M	Mixed	control	N/A	7:20	Unknown
11	49	M	Mixed	control	N/A	6:15	Euthanasia
12	51	M		control	N/A	7:30	Euthanasia

*cases selected for autoradiography, F = female, M = male, MS = multiple sclerosis, N/A = not applicable, PM = post mortem, PP = primary progressive, RR = relapsing remitting, SP = secondary progressive.

Table 2. Antibodies for immunohistochemistry

Antigen	Source	Antibody #	Species	Dilution
TSPO (PBR)	Abcam	AB109497	Rabbit	1:750
PLP	Bio-Rad	MCA839G	Mouse	1:3000
HLA-DR (LN3)	Biolegend	327011	Mouse	1:1000
Vimentin	Homemade	N/A	Mouse	1:6000
GFAP	Millipore	AB5541	Chicken	1:1000
Olig2	Millipore	AB9610	Rabbit	1:500
CD3	Agilent	A0452	Rabbit	1:1500
CD20	Agilent	M0755	Mouse	1:100
TMEM119	Merck	HPA051870	Rabbit	1:250
P2RY12	ANASPEC	AS55042A	Rabbit	1:200
CD40	Bio-Rad	MCA1590	Mouse	1:50
CD206	BD Biosciences	555953	Mouse	1:50
S100β	Merck	S2532	Mouse	1:200
GLUT-1	Merck	AB1783	Guinea pig	1:100

TSPO = translocator protein, PLP = proteolipid protein, HLA-DR = human leukocyte antigen - DR, CD = Cluster of differentiation, GFAP = Glia fibrillary acidic protein, TMEM119 = transmembrane protein 119, P2RY12 = purinergic receptor P2Y12, GLUT-1 = glucose transporter

Image and statistical analyses

Images of each lesion type and randomly sampled areas of normal appearing white (NAWM) and grey matter (NAGM), and white and grey matter from controls were collected with a Leica DC500 microscope (Leica Microsystems, Heidelberg, Germany) at 200 x magnification. Fluorescent images were taken with a Leica TCS SP8 STED 3X confocal microscope. Pictures were analysed using ImageJ software and nuclei and positive cells were manually counted with the cell counter plugin (de Vos, University of Sheffield, UK). All nuclei except those within blood vessels were counted to determine the number of cells per field. Expression levels were analysed using TSPO+ pixels with a threshold of signal intensity that represented all DAB^+ pixels per field. Inter-observer consistency shown with a correlation coefficient of 0.98. Data was analysed using GraphPad Prism 7.02. All data was tested for normality distribution with the Shapiro-Wilk normality test. Differences between lesion types were analysed using ANOVA or Kruskal-Wallis analyses. When positive, Dunnett's *post hoc* analysis was performed to test the different groups to their respective NAWM or NAGM and control, corrected for multiple comparisons. Accordingly, white and grey matter from control cases were compared to NAWM and NAGM of multiple sclerosis tissue, respectively. Data was considered significant when $P<0.05$.

Genotyping

DNA extraction and genotyping were performed on snap frozen brain samples (LGC Group Ltd, Hoddesdon, UK). In brief, following DNA extraction, the SNP-specific KASPTM Assay mix and the universal KASPTM Master mix were added to the DNA samples and placed in a thermal cycler for a minimum of 35 cycles, producing an allele-specific fluorescent signal in accordance with primers specific to rs6971 and rs6972. Each allele-specific primer produces a unique tail sequence which is associated with a fluorescent resonant energy transfer cassette, labelled with a FAMTM dye, or HEXTM dye. Plates were read on a BMG PHERAStar plate reader (BMG Labtech GmbH, Germany). In-house Kraken software was used to automatically identify genotypes, which were verified by staff at the LGC facility.

Autoradiography

Brain sections were prepared from frozen tissue blocks corresponding to the paraffin-embedded tissue blocks described above, allowing direct comparison of the same lesion for pathology and autoradiography. Sections were cut at 10 µm and thaw-mounted on standard glass microscope slides (VWR International Ltd, PA). Slides were dried for 30-60 mins at room temperature and stored at -80˚C. At the time of use, tissue had been stored for a maximum of 36 days. Prior to autoradiography, sections were thawed at room temperature for 15 mins, washed for 20 mins in assay buffer (50mM Tris-HCl, pH 7.4 and incubated for 1 h in assay buffer containing the radioligand [^{3}H]-PK11195 1-(2-chlorophenyl)-N-methyl-N-(1-methylpropyl)-3-isoquinolinecarboxamide (Perkin Elmer, specific activity 82.7 Ci/mmol) and [^{3}H]-PBR28 (N-[2-(methyloxy)phenyl]methyl-N-[4-(pheyloxy)-3-pyridinyl] acetamide (Tritec, UK, specific activity 81 Ci/mmol). The concentrations were 1 nMol/L for [^{3}H]-PK11195 and 0.5 nMol/L for [^{3}H]-PBR28 as measured by liquid scintillation counting (Beckman LS 6500, UK). Adjacent sections were incubated with the radioligand and 10 µMol/L PK11195 (Tocris, UK) to determine non-specific binding. Following incubation, sections were washed twice for 2 mins each in washing buffer (50 mM Tris-HCl, pH 7.4/4°C) on ice followed by 30 sec in ice-cold ultra-pure water. All slides were air dried for 15-20 mins and dehydrated for a minimum of 24 h in a sealed container in the presence of phosphorous pentoxide. Slides were then exposed to BAS-TR2040 imaging plates (Fuji Film, Japan) alongside [^{3}H]-standards (American Radiolabelled Chemicals, USA) for 19 days. Imaging plates were scanned using a Typhoon FLA 7000 (GE, UK) and analysed using QuantityOne (BioRad, USA).

Autoradiography and genotyping analysis

Regions of interest were drawn around lesions, normal appearing white matter (NAWM), and normal appearing grey matter (NAGM) on total binding images using immunohistochemical staining of adjacent sections as a reference. Corresponding regions of interest were drawn on the non-specific binding images for white and grey matter separately to determine the individual nonspecific binding. A global background reading was obtained from a free area on the plate and subtracted from all other measurements. Radioligand signal from each area of non-specific binding was also subtracted from the corresponding ligand-bound section to eliminate non-specific signal. Radioactive concentrations were calculated from optical densities using a linear regression derived from the radioactive standards. Final values are expressed as fmol/mg tissue equivalent (TE). rs6971 causes a single amino acid substitution at position 147 of the TSPO, which has a substantial impact on the affinity with which PBR28 binds TSPO. The binding affinity of PBR28 for TSPO is reduced by a factor of approximately 50 in subjects with threonine at position 147 (termed “low affinity binders”) relative to subjects with alanine at position 147 (termed “high affinity binders”). Heterozygotes (termed “mixed affinity binders”) express both copies of TSPO (147Alanine and 147Threonine) and hence present both the high affinity and low affinity binding sites in roughly equal proportion. Therefore, for a given expression level of the TSPO protein detected by immunohistochemistry, the [^{3}H]-PBR28 radioligand binding signal will be genotype dependent, showing rank order high affinity binders > mixed affinity binders > low affinity binders. Including all 3 genotypes in a correlation of the [^{3}H]PBR28 signal with immunohistochemistry would therefore artificially weaken the correlation, and hence for this analysis, only high affinity binders were used. This phenomenon is not relevant for [^{3}H]PK11195 as the affinity of this radioligand for TSPO is insensitive to the 147Threonine/Alanine substitution.

Results

Heterogeneity of TSPO$^+$ cells in multiple sclerosis lesions

Expression and localisation of TSPO$^+$ cells were investigated in NAWM and in active, chronic active and inactive white matter lesions from brains and spinal cord of people with multiple sclerosis and in control tissue from people who died of non-neurological diseases (Fig. 1A-F). TSPO immunostaining had a punctate appearance across the cytoplasm of cells in both the controls and in cells from multiple sclerosis tissue, as is expected with a mitochondrial protein. The density of TSPO$^+$ cells per mm^2 was a five-fold greater in active white matter lesions (P<0.0001) and four-fold greater in rims of chronic active brain lesions (P=0.0001) compared to control white matter. Compared to NAWM, the density of TSPO$^+$ cells was a mean of two-fold higher for active lesions (P=0.004) and chronic active lesions (P=0.0170, Fig. 1G). We next investigated the characteristics of the TSPO$^+$ cells. HLA-DR$^+$ cells expressing TSPO were 11- to 14-fold more abundant in active lesions and chronic active lesion rims compared to the control white matter (active: P=0.0220, CA rim: P=0.0022; Fig. 1H) and 16- to 21-fold greater than NAWM (active: P=0.0196, CA rim: P=0.0019, Fig. 1H). TSPO$^+$HLA-DR$^-$ cells with an astrocytic morphology expressing GFAP were found in all lesion sub-types (Fig. 1I-N). Between 15- to 20-fold more TSPO$^+$GFAP$^+$ cells were observed in all lesion sub-types

relative to control white matter (P<0.0001, Fig. 1O). The relative number of TSPO$^+$GFAP$^+$ cells in lesions was five to seven-fold greater than in the NAWM (P<0.0001, Fig. 1O). HLA-DR$^+$ microglia/macrophages expressing TSPO accounted for a mean of 40% of total TSPO$^+$ cells in active lesions and in the rims of chronic active lesion (Fig. 1P) and GFAP$^+$ astrocytes constituted about 25% of TSPO$^+$ cells in active lesions and in the rims of chronic active lesions. However, in the centre of chronic active and in inactive lesions TSPO$^+$GFAP$^+$ astrocytes represented as many as 65% of the TSPO$^+$ cells although it must be emphasised that the center of these lesions are hypocellular relative to the chronic lesion rims or the NAWM. In active lesion areas, a few cells were found co-expressing TSPO and Olig2, an oligodendrocyte marker (Fig. 1P, insert). TSPO$^+$ astrocytes did not only colocalise with GFAP but also with vimentin, glut-1 and S100β (Fig. 1Q-T). Most of the remaining fraction of TSPO$^+$ cells that did not express HLA-DR or GFAP had microglial or macrophage morphology but were not further characterised. To examine if the same is true of lesions in early multiple sclerosis we used biopsy material from rapidly expanding active white matter lesions from 4 cases of multiple sclerosis. All samples also showed strong expression of TSPO in HLA-DR$^+$ macrophages and microglia (Fig. 1U), as well as in scattered GFAP$^+$ astrocytes (Fig. 1V).

Together, microglia and to a lesser extent astrocytes in multiple sclerosis lesions appeared to account for most of the TSPO$^+$ cells in lesions and NAWM in the multiple sclerosis brains. TSPO$^+$ vascular endothelial cells also were identified commonly but made up less than 5% of the TSPO$^+$ cells. Vascular TSPO expression patterns in multiple sclerosis lesions were not different from their expression in blood vessels of the NAWM and in control tissue.

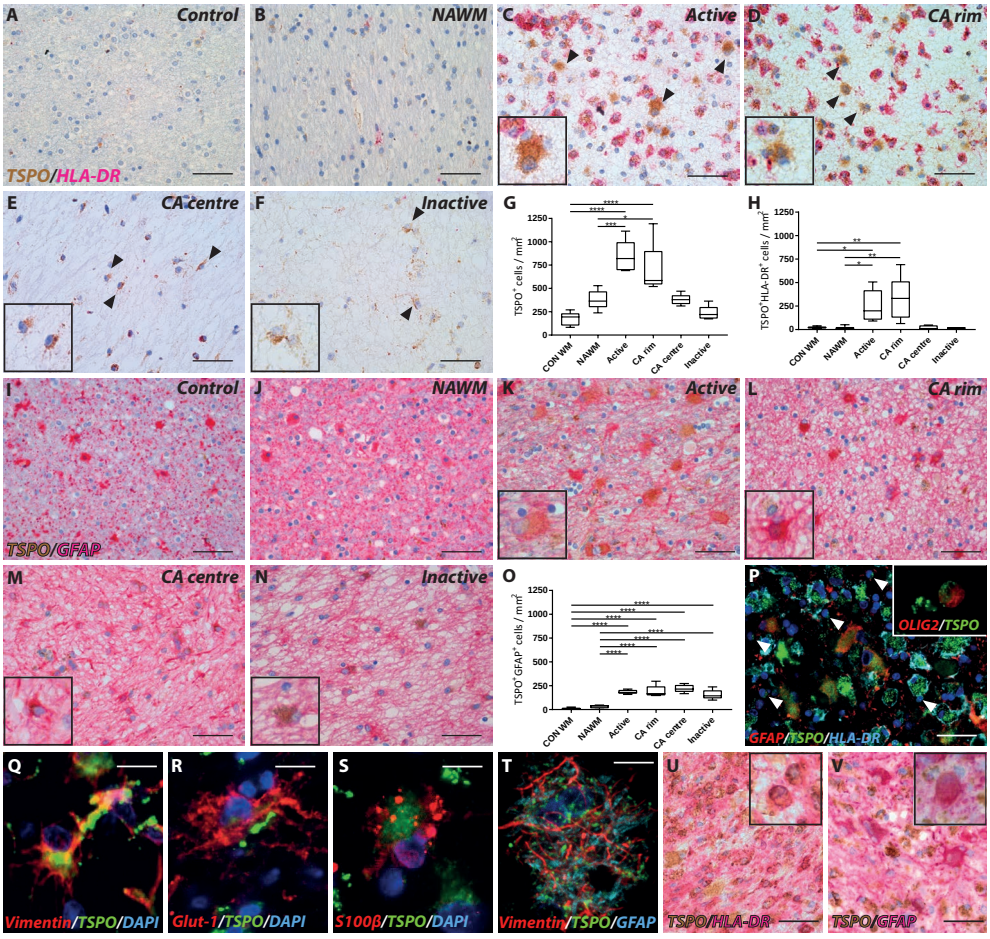

Figure 1. Astrocyte and microglial expression of TSPO in white matter lesions. Representative images of TSPO expression in control (A, I) and multiple sclerosis lesions (B-F, J-N); NAWM (B, J), active (C, K), CA rim (D, L) and centre (E, M), and inactive (F, N) lesions. Expression of TSPO in HLA-DR$^-$ cells (black arrowheads; inserts C-F). Quantitative analysis of number of TSPO$^+$ cells showed a significant increase up to five times in active and in the rim of chronic active lesions compared to control and NAWM (G). An 11- to 14-fold increase in TSPO$^+$HLA-DR$^+$ cells was found in active and the rim of chronic active lesions compared to control and NAWM (H). A five-fold increase in TSPO$^+$GFAP$^+$ cells was found throughout all lesion stages compared to control and NAWM contributing up to 25% of the TSPO$^+$ cells (I-O, inserts). An overview of cellular TSPO signal of astrocytes and activated microglia macrophages (P) and oligodendrocytes (P, white arrowheads, insert). Representative images of astrocytic markers with TSPO expression in one multiple sclerosis lesion (Q-T). Biopsy material showing high TSPO expression in HLA-DR$^+$ and GFAP$^+$ cells (U,V, insert). *=P<0.05; **=P<0.01; ***=P<0.001; ****=P<0.0001. Scale bars (A-F, I-N, P, U, V) = 50 µm, (Q-T) = 12.5 µm. Inserts are digitally zoomed in to 800x., NAWM = normal appearing white matter, A =active, CA = chronic active, IA = inactive.

TSPO expression in microglial phenotypes

To investigate further whether TSPO expression in microglial cells defined a functionally specific phenotype, we tested for co-expression with more specific markers for microglia and their polarisation. TMEM119 is reported to differentiate activated microglia from myeloid-derived macrophages and has been used to identify CNS-resident microglia. P2RY12 is a marker that identifies homeostatic microglia in normal white matter. Markers for pro-

inflammatory (CD40) and anti-inflammatory (mannose receptor, CD206) activated microglia and macrophages also were used[61,62]. Microglia/macrophages that express both CD40 and CD206 are described as having an intermediate phenotype. No significant differences were found in proportions of TMEM119$^+$ microglia expressing TSPO across the lesion sub-types (Fig. 2A-D). As reported previously[56], P2RY12$^+$ cells expressing TSPO were substantially reduced in active lesions (Fig. 2E-H). Numbers of macrophages and microglia showing an intermediate phenotype, and expressing TSPO were very low in control cases and were not detected in the NAWM in multiple sclerosis (Fig. 2I,J). The density of microglia/macrophages with the intermediate phenotype represented 18% of the total TSPO$^+$ cell population, in active lesions and in the rims of chronic active lesions (Fig. 2J). By contrast, few TSPO$^+$ microglia/macrophages with the intermediate phenotype were present in the centres of chronic active lesions or in inactive lesions, (Fig. 2J). Cells that were solely expressing the pro-inflammatory marker CD40 or the anti-inflammatory mannose receptor CD206 always expressed TSPO, but were present in very low numbers in multiple sclerosis lesions (<1% of total TSPO+ cells, data not shown). Thus, TSPO expression was not specifically associated with either solely pro- or anti-inflammatory microglia/macrophage phenotype based on these markers.

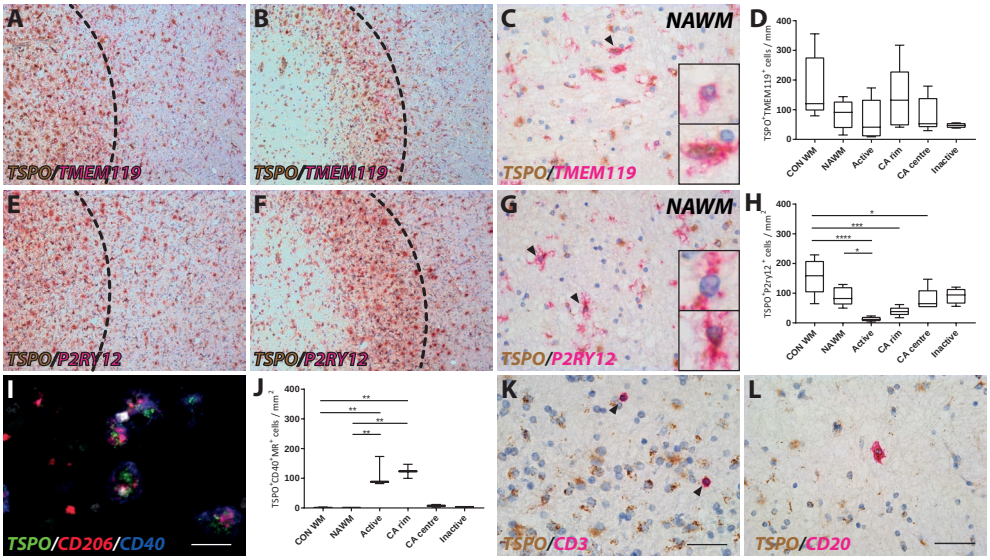

Figure 2. TSPO expression in microglial phenotypes and lymphocytes. Resident microglia expressing TSPO in an active and chronic active lesion and the periplaque white matter (A,B) as well as in NAWM (C). Resident microglia did not show any significant difference in TSPO expression compared to control or NAWM (D). Overview of expression of the homeostatic marker P2RY12 with TSPO in an active and chronic active lesion and the periplaque white matter (E,F), as well as in NAWM (G). A loss in homeostatic microglia expressing TSPO was found in active and chronic active lesions stages (H). Both TSPO$^+$ and TSPO$^-$ microglia were found expressing TMEM119 or P2RY12 in multiple sclerosis lesions (black arrowheads; inserts; C,G). In contrast, active and chronic active lesions showed an increase in CD206$^+$CD40$^+$ cells expressing TSPO (I,J). T-cells (CD3) showed low expression of TSPO in multiple sclerosis lesions (K) in contrast to B-cells (CD20) which showed strong localisation with TSPO (L). *=P<0.05; **=P<0.01; ***=P<0.001; ****=P<0.0001. Scale bars (A,B,E,F) 200 µm, (C,G,K,L) = 50 µm, (I) = 25 µm. Inserts are digitally zoomed in to 800x., NAWM = normal appearing white matter, A =active, CA = chronic active, IA = inactive.

TSPO expression in lymphocytes

Expression of TSPO in adaptive immune cells was investigated by double staining CD20$^+$ B-cells and CD3$^+$ T-cells in white matter lesions in multiple sclerosis (Fig. 2K,L). The density of TSPO expression in CD3$^+$ T-cells was very low in all lesion types (Fig. 2K) compared to expression by microglia. CD20$^+$ B-cells showed relatively stronger expression of TSPO in active (Fig. 2L), chronic active and inactive lesion types. However, in the cases studied in this study T and B-cell numbers were low in multiple sclerosis lesions and in the NAWM, and did not contribute significantly to the total number of TSPO$^+$ cells (<1% of total TSPO$^+$ cells).

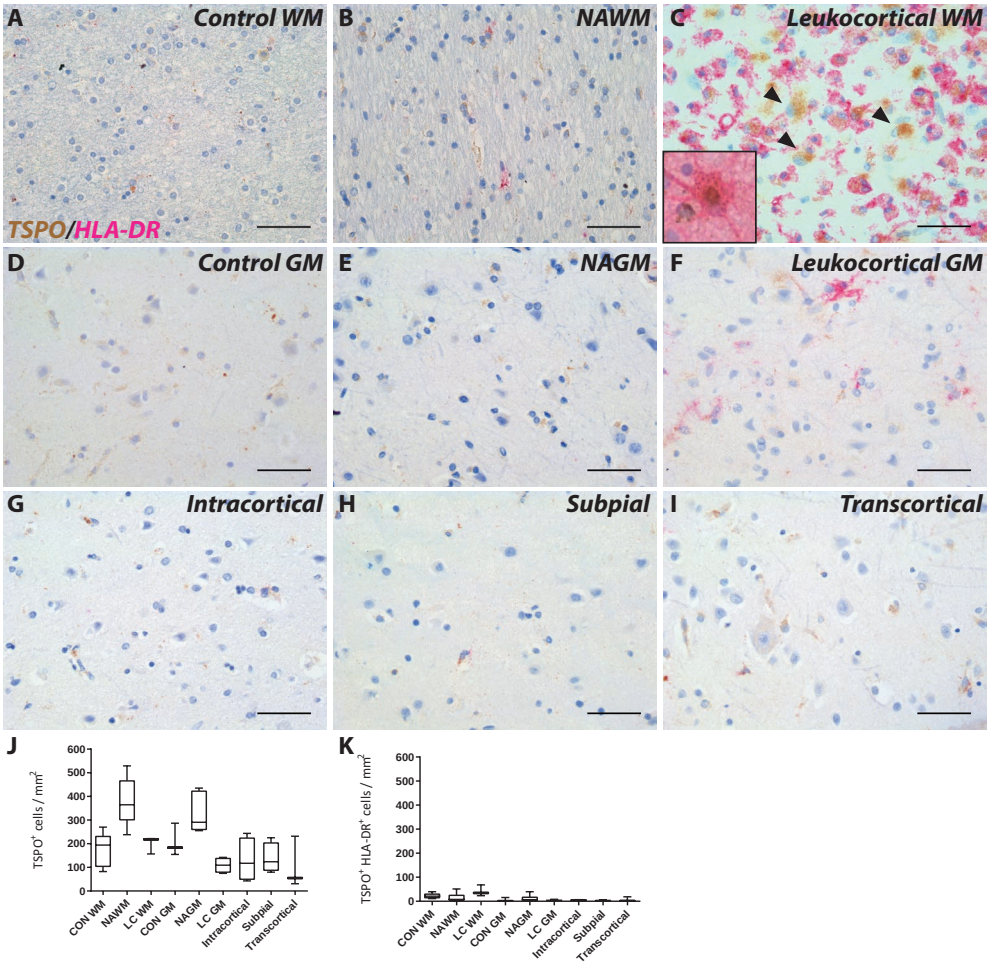

Figure 3. TSPO expression in grey matter lesions. Representative images of TSPO expression in control (A,D) and multiple sclerosis (B,C,E-I) in grey matter lesions; NAWM (B), and NAGM (E); leukocortical white matter (C), and grey matter (F); intracortical (G), subpial (H), and transcortical (I) lesions. Similar to WM lesions leukocortical WM lesions showed large TSPO$^+$HLA-DR$^-$ cells (black arrowheads; C) which were GFAP$^+$ astrocytes (C, insert). No differences were found in TSPO$^+$ cells in grey matter lesions (J). No significant increase in TSPO$^+$HLA-DR$^+$ cells were found in grey matter lesions compared to control (K). Data is expressed as mean ±. Scale bars (A-I) = 50 µm. Inserts are digitally zoomed in to 800x., LC = leukocortical, WM = white matter, GM = grey matter, NAWM = normal appearing white matter, NAGM = normal appearing grey matter.

TSPO expression in multiple sclerosis lesions in the cortical grey matter and spinal cord

Expression and localisation of TSPO in the grey matter of multiple sclerosis brain was investigated in leukocortical, intracortical, subpial and transcortical lesions (Fig. 3A-I)[63]. No significant differences were found in the number of cells that express TSPO in grey matter lesions compared to NAGM or to control grey matter (Fig. 3J). HLA-DR$^+$ cells expressing TSPO were not significantly more abundant in the white and grey matter of leukocortical lesions than in the normal appearing white and grey matter or to control tissue (Fig. 3K) and the density of TSPO$^+$HLA-DR$^+$ microglia was low compared to white matter lesions. We observed scattered GFAP$^+$ astrocytes expressing TSPO only in the white matter of leukocortical lesions, similar to those found in purely white matter lesions (Fig. 3C, insert). The density of TSPO$^+$ cells in the NAWM of the spinal cord was no greater than in control spinal cord white matter and neither was the TSPO$^+$ cell density greater in white matter lesions in the spinal cord compared to NAWM or control white matter (Fig. 4A-F). However, the density of TSPO$^+$HLA-DR$^+$ cells in active white matter lesions was approximately doubled relative to control white matter (P=0.0324; Fig. 4G). Active and chronic active lesions in the spinal cord also showed GFAP+ astrocytes expressing TSPO similar to the brain (Fig. 4C, D, insert; black arrowheads).

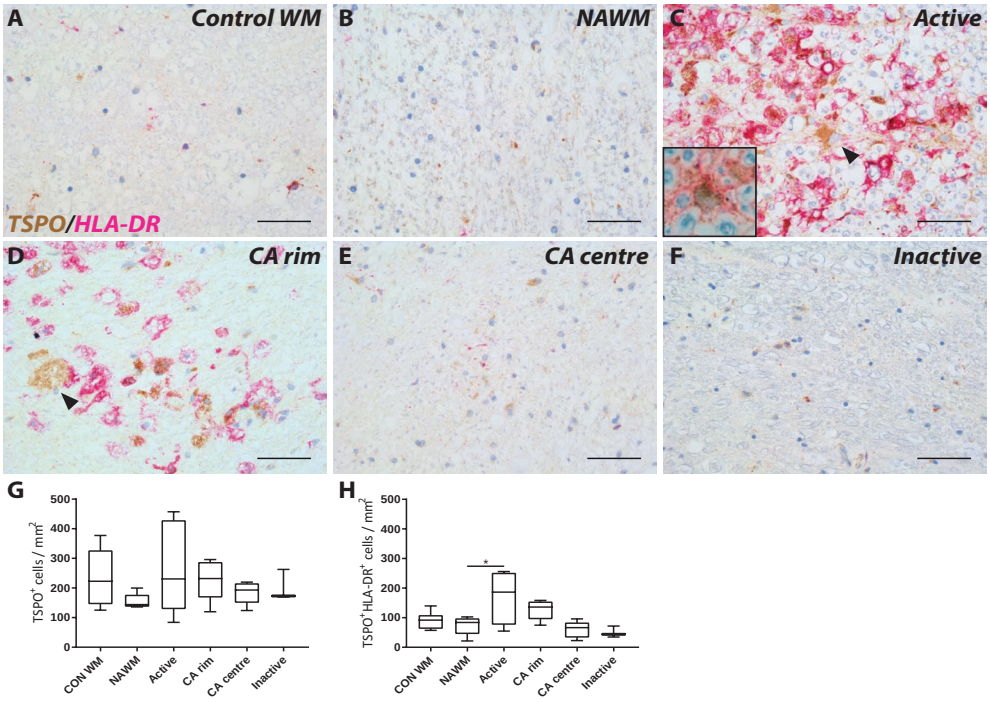

Figure 4. TSPO expression in white matter lesions in spinal cord. Representative images of TSPO expression in control (A) and multiple sclerosis lesions (B-F); NAWM (B), active (C), CA rim (D) and centre (E), and inactive (F) lesions. Expression of TSPO was found in HLA-DR$^-$ cells (black arrowheads; C,D). GFAP$^+$ astrocytes expressing TSPO were also found in the spinal cord (C, insert). Quantitative analysis of the number of TSPO$^+$ cells did not show significant differences between lesion types compared to control or NAWM (G,H). Increased expression of TSPO in HLA-DR$^+$ cells was found in active lesions compared to NAWM (I). *p<0.05. Scale bars (A-F) = 50 µm. Inserts are digitally zoomed in to 800x. CON = control, NAWM = normal appearing white matter, A =active, CA = chronic active, IA = inactive.

TSPO pixels and radioligand binding are increased in active lesions

To investigate the relationship between TSPO expression and radioligand binding of [^{3}H] PBR28 or [^{3}H]PK11195, results from a pixel-based analysis of immunochemically-defined TSPO were integrated with TSPO radioligand autoradiography of white and grey matter lesions from sections in the same tissue blocks from multiple sclerosis and control brains (Fig. 5). In white matter lesions, the number of TSPO$^+$ pixels were increased by five-fold compared to control white matter (active: P<0.0001; CA rim: P=0.0003) and by nine-fold compared to NAWM (active: P<0.0001; CA rim: P<0.0001; Fig. 6A). Endothelial TSPO expression contributed minimally (up to 8% in inactive lesions) to the amount of TSPO$^+$ pixels in the white matter (Supplementary Fig. 1A). TSPO$^+$ pixels were found to be increased markedly in the white matter component of leukocortical lesions relative to NAWM (P<0.0001, Fig. 6D) and to control white matter (P<0.0001). A smaller increase in TSPO$^+$ pixels was found in the grey matter (P=0.0096) of leukocortical lesions relative to NAGM. However, no significant increase in TSPO$^+$ pixels was found in other sub-types of grey matter lesions. Endothelial TSPO expression was decreased in grey matter lesions compared to the NAGM (P<0.005) and control grey matter (P<0.05, Supplementary Fig. 1B). Furthermore, endothelial TSPO expression was up to a fourfold higher in the NAGM and control grey matter compared to NAWM (P<0.0001) and control white matter (P=0.0033) in the brains of people with multiple sclerosis (Supplementary Fig. 1B).

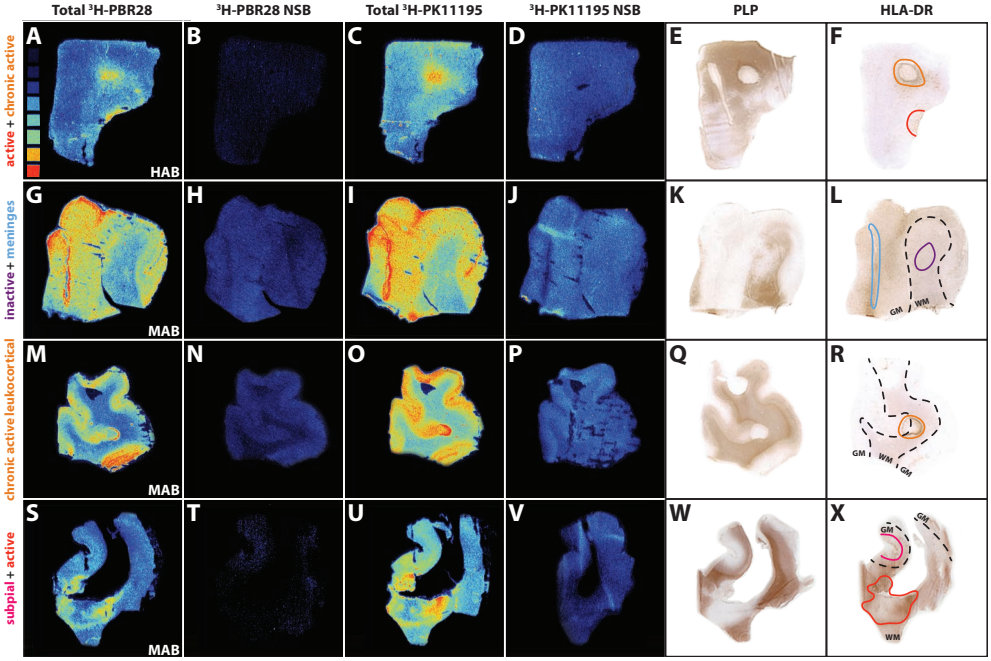

Figure 5. Overview of [^{3}H]PBR28 and [^{3}H]PK11195 autoradiography of multiple sclerosis lesions. Scale bar (A) ranges from low radioactivity to high radioactivity (0.42 TE nCi/mg to 16.23 TE nCi/mg). Total binding of [^{3}H]PBR28 (A,G, M & S), non-specific binding of [^{3}H]PBR28 (B, H, N & T), total binding of [^{3}H]PK11195 (C, I, O & U), non-specific binding of [^{3}H]PK11195 (D, J, P & V), PLP (E, K, Q & W) and HLA-DR (F, L, R & X) images. LN3 staining denotes areas for active (red), chronic active (orange), inactive (purple) and subpial (pink) lesions, meninges (blue) and the grey and white matter border (dashed lines).

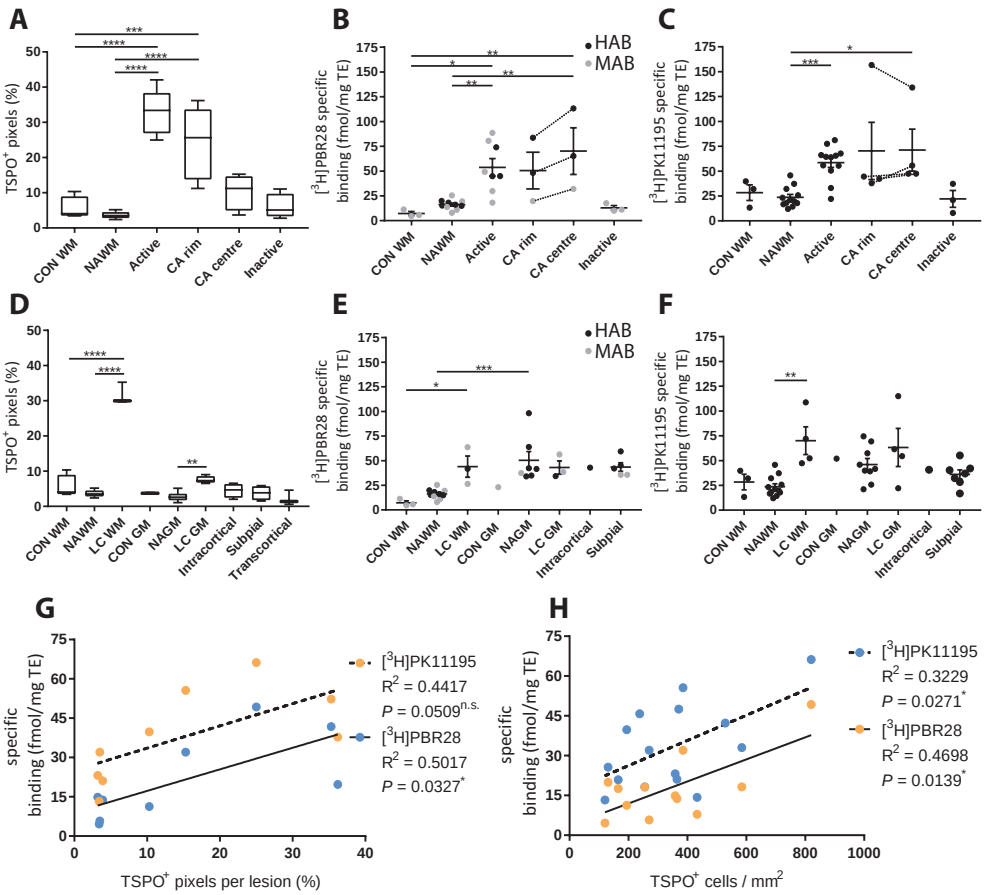

Figure 6. [³H]PBR28 and [³H]PK11195 autoradiography of multiple sclerosis lesions. An increase in TSPO⁺ pixels was found in active and chronic active lesions compared to control and NAWM (A). [³H]PBR28 and [³H]PK11195 binding was increased in active white matter lesions and the centre of chronic active lesions (B, C). For grey matter lesions an increase was found in TSPO⁺ pixels in leukocortical lesion WM and GM compared to their respective normal appearing tissue (D). Similar to white matter lesions [³H]PBR28 and [³H]PK11195 binding was increased in leukocortical lesion white matter areas (E, F). An increase in specific binding in NAGM relative to NAWM was found for [³H]PBR28. Mixed affinity binders (MAB) are depicted in grey while high affinity binders are depicted in black (HAB). Correlations were found for specific binding of [³H]PBR28 and [³H]PK11195 for both TSPO⁺ pixels per lesion and TSPO⁺ cells per mm2 (G, H). CON WM = control white matter, NAWM = normal appearing white matter, CON GM = control grey matter, NAGM = normal appearing grey matter, CA = chronic active, LC = leukocortical lesion.

Specific tracer binding was calculated from [³H]PBR28 and [³H]PK11195 autoradiography in lesional and non-lesional areas of white and grey matter in the multiple sclerosis brains and in control tissue (Fig. 5). No specific binding was found in four brains with low affinity binding genotypes for [³H]PBR28, identified by the rs6971 polymorphism. In all other cases, control white matter, NAWM and inactive lesions all showed relatively low binding of both ligands compared to active and chronic active lesions (Fig. 6B, C). [³H]PBR28 binding was seven times greater in active lesions compared to control white matter (*P*=0.0228) and three times greater than NAWM (*P*=0.0064). Similarly, greater binding was found in the centres of chronic active lesions compared to NAWM (*P*=0.0046) or control white matter (*P*=0.0084, Fig. 6B). [³H]PK11195 binding was approximately doubled in the active (*P*=0.0006) and tripled in

the chronic active centre (P=0.0392) compared to NAWM (Fig. 6C). In grey matter lesions (Fig. 6E, F), binding was not greater for either [^{3}H]PBR28 or [^{3}H]PK11195 than in NAGM. An increased signal was found in the white matter of leukocortical lesions compared to control (P=0.0414) for [^{3}H]PBR28 or compared to NAWM (P=0.0019) for [^{3}H]PK11195. Specific binding in NAGM was more than tripled relative to NAWM for [^{3}H]PBR28 (P=0.0009). A strong positive correlation between the pixel-based analysis of TSPO expression and specific binding of the ligand [^{3}H]PBR28 was found (R^2=0.5017, P=0.0327), while only a trend was found for [^{3}H]PK11195 (R^2=0.4417, P=0.0509, Fig. 6G). Strong correlations were also found between the relative number of TSPO$^+$ cells and specific binding for [^{3}H]PBR28 (R^2=0.4698, P=0.0139) and [^{3}H]PK11195 (R^2=0.3229, P=0.0271, Fig. 6H).

Discussion

TSPO is a marker of inflammation commonly attributed to microglial activation in neuroinflammatory and neurodegenerative diseases[64]. Surprisingly, there has been very little data on which to base precise interpretations to date[65]. Knowledge of the cellular and phenotypic correlates of the TSPO PET signal is important to better understand the clinical meaningfulness of the heterogeneity of TSPO PET radioligand uptake in T2-hyperintense lesions in multiple sclerosis before and after initiation of disease modifying therapies[66].

Here we have examined the expression and localisation of TSPO in a large cohort of *post mortem* multiple sclerosis in white and grey matter lesions of the brain and spinal cord. Similar to previous studies, TSPO expression was found in microglia in active and chronic active lesions[36,45,46,67,68]. Similar to a recent study combining quantitative susceptibility mapping and immunohistochemistry[45], our studies revealed non trivial expression of TSPO in astrocytes in all sub-types of lesions examined. The astrocytic TSPO accounted for approximately 25% of the TSPO$^+$ cells in active lesions or chronic active lesion rims and for 65% of the TSPO$^+$ cells in the centres of chronic active and inactive lesions. Autoradiography using [^{3}H]PBR28 and [^{3}H]PK11195 revealed a strong correlation between TSPO$^+$ cells and radioligand binding across all cell sub-types. This suggests that TSPO PET signal arises from astrocytes as well as microglia, which is consistent with reports that newer generation ligands for TSPO bind to reactive astrocytes[32,45]. Interpretation of the signal therefore needs to be context dependent. This finding is of clear importance for use of TSPO PET as an outcome measure in studies of modulation of these inflammatory processes.

While some studies have found reduced TSPO binding after anti-inflammatory treatments[69,70], it has also been suggested that current disease modifying therapy may have a limited impact on microglial activity[66,71]. However, as centres of chronic active and inactive lesions show increased expression of TSPO in reactive astrocytes, observations of TSPO expression alone are more ambiguous; treatment may reduce microglial density or activation without a reduction in TSPO PET signal, if astrocytic numbers increase simultaneously. The astrocytic contribution of the TSPO signal could also complicate differentiation of multiple sclerosis from leukodystrophies that have significant astrocytic but not microglial involvement[72].

While percentages of microglia in the grey matter have been reported to be significantly higher in white versus grey matter[73] an increase of radioligand binding in the NAGM compared to the NAWM was observed. This may be attributed to the increased contribution of TSPO$^+$ endothelial cells due to the reported increased vascularity of grey verses white matter[74]. That TSPO protein expression does not correlate with the PBR28 findings in the grey matter

likely reflects the fundamentally different measurements of antibody binding (pixel counts) and autoradiography (ligand binding); the antibody detects the C terminus of the TSPO and autoradiography the binding of the ligand in the active site of the TSPO. Autoradiography has greater sensitivity because each molecule of radioligand contributes to the signal, whereas for immunohistochemistry a pixel is only $TSPO^{+}$ if a threshold is reached. Hence when the levels of TSPO are low, and thus the signal of DAB positivity is very low, differences between autoradiography and the pixels counts may arise.

Increased TSPO expression was also observed in leukocortical lesions in multiple sclerosis but not in other grey matter lesions[75]. This may well reflect the greater microglia and astrocyte activity in the white matter; pure cortical lesions in *post mortem* tissues show little or no inflammation[57,76,77], although early lesions have been associated with prominent microglial activation[78]. Leukocortical lesions, which can have a white matter inflammatory component, may show differences in behaviour with inflammatory processes diffusing into the cortical grey matter. Similar considerations may hold with active leptomeningeal inflammation[79,80]. The spatial resolution of PET is low relative to cortical thickness, making confident assignment of TSPO PET signal to cortex (rather than adjacent white matter or meninges) problematic. While populations of patients undoubtedly show heterogeneity of grey matter pathology, our observations here raise questions about the interpretation of widespread TSPO PET signal in the cortical region as arising from cortical lesions[81], as opposed to meningeal[79] or leukocortical inflammation. Highly localised relative increases in TSPO signal in the cortex[82], may represent a more rare, relatively acute cortical lesion, rather than what is more typically defined *post mortem*.

Increased TSPO expression also has commonly been attributed to activated microglia/macrophages and there is often an implication that the activation is pro-inflammatory[64]. Recently, we have shown *in vitro* that, although TSPO gene and protein expression and TSPO radioligand binding increases in rodent microglia and macrophages with inflammatory stimulation, relative TSPO gene expression in human microglia and TSPO ligand binding in human monocyte derived macrophages are reduced with pro-inflammatory activation[53]. Here, we show that the increased TSPO expression in multiple sclerosis lesions primarily represents an intermediate activation state in which cells expressed both CD40 and CD206[55,62]; microglia solely expressing the pro-inflammatory marker CD40 or the anti-inflammatory marker mannose receptor CD206 were sparsely represented. This new observation thus confirms *in vitro* data suggesting that TSPO expression signal does not distinguish between microglial phenotypes in human tissue[53]. To the extent that increased TSPO PET signal can be used as a marker of microglia, it thus should be interpreted as reflecting increased microglial density rather than a change in activation state.

In principle, chronic active lesions showing a high expression of TSPO in the rims and a lower expression in the core could be distinguished from either active lesions that show high expression of TSPO throughout their volume or from inactive lesions with low cell density and low TSPO expression. Those chronic active lesions with increased rim TSPO expression might identify those that will expand slowly over time. The neuropathological active lesions with homogeneously high TSPO expression may define those most likely to decrease in volume over time[83,84]. However, in practice, this discrimination could be confounded by the limited signal resolution of PET (typically 3-5 mm linearly) and consequent local signal averaging across commonly encountered lesions. This question deserves further investigations, e.g., by

combining longitudinal MRI monitoring of the evolution of individual lesions with TSPO PET.

In the present study, TSPO expression in cells of the adaptive immune system was also investigated across the different lesion sub-types. A previous study has highlighted TSPO expression in several T-cell populations in blood[54], but our study did not find a strong expression of TSPO in T-cells in the brain. On the other hand, we did see strong expression of TSPO in B-cells in active, chronic active, and inactive lesions. However, lymphocyte numbers are low, so these contribute only a negligible amount to the total TSPO$^+$ cells and thus will not influence the TSPO PET signal significantly.

TSPO expression in vascular endothelial cells in all blood vessels contributes to the diffuse TSPO PET signal in the healthy human brain[85]. Moreover, the endothelial component of TSPO PET, which is dependent on the vascular density in the brain, differs between regions, and may change with ageing and pathology[85-87]. We therefore investigated TSPO expression in endothelial cells by pixel count. In the white matter, endothelial TSPO expression did not contribute significantly to the total amount of TSPO expression (on average 5% of total TSPO pixels). However, as expected, we found an increase in endothelial contribution to TSPO expression relative to white matter as well as relative to grey matter lesions, which is consistent with the reported greater vascularity of grey verses white matter[74] and the hypo-cellularity of grey matter lesions[63].

The abundance of TSPO expression in astrocytes in the centres of chronic active lesions may suggest a more important role for TSPO in the pathophysiology of multiple sclerosis than previous data suggested[46]. The human GFAP-driven conditional knockout of TSPO in mice resulted in significantly reduced severity of experimental autoimmune encephalomyelitis [88]. In humans, activated microglia are capable of producing neurotoxic, reactive astrocytes in multiple sclerosis lesions[89]. The apparent effects of TSPO ligands to reduce pathology in animal disease models could be mediated through effects on astrocytes[90,91]. Similar to TSPO expression after cessation of lesion activity in multiple sclerosis, TSPO was found to be expressed long after recovery from experimental autoimmune encephalomyelitis and in cuprizone-mediated demyelination[92,93], implicating a role of TSPO in regenerative processes such as remyelinating lesions, possibly through production of neurotrophic factors such as pregnenolone and progesterone[94]. These activities may be mediated by activated astrocytes.

There are limitations to our study suggesting future work. HLA-DR, Iba1 and CD68 are often used as markers for microglia interchangeably. Although these markers may be co-expressed, some Iba1$^+$ and CD68$^+$ cells do not express HLA-DR[95]. This likely accounts for the TSPO$^+$ cells with microglial morphology that did not express HLA-DR. These appear to constitute a fraction of up to 35% of the active lesions and the chronic active lesion rims, but confirmation of this is warranted. A more general problem is that characterisation of the complexity of microglial/macrophage activation phenotypes well ideally demands use of more than one or two markers. Future work employing cytokine expression assays and cell receptor markers simultaneously (e.g., using imaging mass cytometry) would add to their characterisation.

In summary, our studies confirm that TSPO PET imaging provides a general marker of glial activation in multiple sclerosis, but emphasise that precise interpretations depend on the specific pathological context. With a single MRI scan, active, chronic active and inactive lesions cannot be distinguished well, leaving uncertainties regarding the interpretation of a paired TSPO PET scan. With other pathologies e.g., in Alzheimer's disease[96], the

interpretation of increased TSPO PET signal also may reflect differences in relative abundance of microglia and astrocytes. Based on this and our previous work, we raise the possibility that a successful therapeutic intervention, which modulates the microglia from pro-inflammatory to neuroprotective or homeostatic phenotypes, might potentially have no effect on the TSPO PET signal, although interventions that reduce the density of activated glial cells may. Understanding the cellular neuropathology of TSPO expression quantitatively is a fundamental step in the evaluation of TSPO as a potential therapeutic target.

Acknowledgements

The authors thank the UK MS society for financial support (grant number: C008-16.1). PMM acknowledges generous support from Edmond J Safra Foundation and Lily Safra, the NIHR Investigator programme and the UK Dementia Research Institute. PMM and DRJO thank the Imperial College Healthcare Trust-NIHR Biomedical Research Centre for infrastructure support and the Medical Research Council for support of TSPO studies.

References

1. Bonsack F, *et al*. TSPO: An Evolutionarily Conserved Protein with Elusive Functions. *Int J Mol Sci*. Jun 7 2018;19(6)doi:10.3390/ijms19061694
2. Vowinckel E, *et al*. PK11195 binding to the peripheral benzodiazepine receptor as a marker of microglia activation in multiple sclerosis and experimental autoimmune encephalomyelitis. *Journal of Neuroscience Research*. Oct 15 1997;50(2):345-353. doi:Doi 10.1002/(Sici)1097-4547(19971015)50:2<345::Aid-Jnr22>3.0.Co;2-5
3. Versijpt J, *et al*. Microglial imaging with positron emission tomography and atrophy measurements with magnetic resonance imaging in multiple sclerosis: a correlative study. *Mult Scler*. Apr 2005;11(2):127-34. doi:10.1191/1352458505ms1140oa
4. Oh U, *et al*. Translocator protein PET imaging for glial activation in multiple sclerosis. *J Neuroimmune Pharmacol*. Sep 2011;6(3):354-61. doi:10.1007/s11481-010-9243-6
5. Rissanen E, *et al*. In Vivo Detection of Diffuse Inflammation in Secondary Progressive Multiple Sclerosis Using PET Imaging and the Radioligand (1)(1)C-PK11195. *J Nucl Med*. Jun 2014;55(6):939-44. doi:10.2967/jnumed.113.131698
6. Datta G, *et al*. Translocator positron-emission tomography and magnetic resonance spectroscopic imaging of brain glial cell activation in multiple sclerosis. *Mult Scler*. Oct 2017;23(11):1469-1478. doi:10.1177/1352458516681504
7. Edison P, *et al*. Microglia, amyloid, and cognition in Alzheimer's disease: An [11C](R)PK11195-PET and [11C]PIB-PET study. *Neurobiol Dis*. Dec 2008;32(3):412-9. doi:10.1016/j.nbd.2008.08.001
8. Yasuno F, *et al*. Increased binding of peripheral benzodiazepine receptor in Alzheimer's disease measured by positron emission tomography with [11C]DAA1106. *Biol Psychiatry*. Nov 15 2008;64(10):835-41. doi:10.1016/j.biopsych.2008.04.021
9. Ouchi Y, *et al*. Microglial activation and dopamine terminal loss in early Parkinson's disease. *Ann Neurol*. Feb 2005;57(2):168-75. doi:10.1002/ana.20338
10. Banati RB, *et al*. [11C](R)-PK11195 positron emission tomography imaging of activated microglia in vivo in Rasmussen's encephalitis. *Neurology*. Dec 10 1999;53(9):2199-203. doi:10.1212/wnl.53.9.2199
11. Cagnin A, *et al*. In vivo visualization of activated glia by [11C] (R)-PK11195-PET following herpes encephalitis reveals projected neuronal damage beyond the primary focal lesion. *Brain*. Oct 2001;124(Pt 10):2014-27. doi:10.1093/brain/124.10.2014
12. Turner MR, *et al*. Evidence of widespread cerebral microglial activation in amyotrophic lateral sclerosis: an [11C](R)-PK11195 positron emission tomography study. *Neurobiol Dis*. Apr 2004;15(3):601-9. doi:10.1016/j.nbd.2003.12.012
13. Messmer K, *et al*. Increased peripheral benzodiazepine binding sites in the brain of patients with Huntington's disease. *Neurosci Lett*. Jan 23 1998;241(1):53-6. doi:10.1016/s0304-3940(97)00967-1
14. Cagnin A, *et al*. In vivo detection of microglial activation in frontotemporal dementia. *Ann Neurol*. Dec 2004;56(6):894-7. doi:10.1002/ana.20332
15. Banati RB, *et al*. The peripheral benzodiazepine binding site in the brain in multiple sclerosis: quantitative in vivo imaging of microglia as a measure of disease activity. *Brain*. Nov 2000;123 (Pt 11)(11):2321-37. doi:10.1093/brain/123.11.2321
16. Colasanti A, *et al*. In Vivo Assessment of Brain White Matter Inflammation in Multiple Sclerosis with (18)F-PBR111 PET. *J Nucl Med*. Jul 2014;55(7):1112-8. doi:10.2967/jnumed.113.135129
17. Venneti S, *et al*. The peripheral benzodiazepine receptor (Translocator protein 18kDa) in microglia: from pathology to imaging. *Prog Neurobiol*. Dec 2006;80(6):308-22. doi:10.1016/j.pneurobio.2006.10.002
18. Debruyne JC, *et al*. PET visualization of microglia in multiple sclerosis patients using [11C]PK11195. *Eur J Neurol*. May 2003;10(3):257-64. doi:10.1046/j.1468-1331.2003.00571.x
19. Gerhard A, *et al*. [11C](R)-PK11195 PET imaging of microglial activation in multiple system atrophy. *Neurology*. Sep 9 2003;61(5):686-9. doi:10.1212/01.wnl.0000078192.95645.e6
20. Gerhard A, *et al*. In vivo imaging of microglial activation with [11C](R)-PK11195 PET in idiopathic Parkinson's disease. *Neurobiol Dis*. Feb 2006;21(2):404-12. doi:10.1016/j.nbd.2005.08.002
21. Gerhard A, *et al*. In vivo imaging of microglial activation with [11C](R)-PK11195 PET in progressive supranuclear palsy. *Mov Disord*. Jan 2006;21(1):89-93. doi:10.1002/mds.20668
22. Gerhard A, *et al*. In vivo imaging of microglial activation with [11C](R)-PK11195 PET in corticobasal degeneration. *Mov Disord*. Oct 2004;19(10):1221-6. doi:10.1002/mds.20162
23. Ghadery C, *et al*. Microglial activation in Parkinson's disease using [(18)F]-FEPPA. *J Neuroinflammation*. Jan 11 2017;14(1):8. doi:10.1186/s12974-016-0778-1
24. Groom GN, *et al*. PET of peripheral benzodiazepine binding sites in the microgliosis of Alzheimer's disease. *J Nucl Med*. Dec 1995;36(12):2207-10.
25. Henkel K, *et al*. Imaging of activated microglia with PET and [11C]PK 11195 in corticobasal degeneration. *Mov Disord*. Jul 2004;19(7):817-821. doi:10.1002/mds.20040
26. Politis M, *et al*. Increased central microglial activation associated with peripheral cytokine

levels in premanifest Huntington's disease gene carriers. *Neurobiol Dis*. Nov 2015;83:115-21. doi:10.1016/j.nbd.2015.08.011
27. Tai YF, *et al*. Imaging microglial activation in Huntington's disease. *Brain Res Bull*. Apr 30 2007;72(2-3):148-51. doi:10.1016/j.brainresbull.2006.10.029
28. Tomasi G, *et al*. Novel reference region model reveals increased microglial and reduced vascular binding of 11C-(R)-PK11195 in patients with Alzheimer's disease. *J Nucl Med*. Aug 2008;49(8):1249-56. doi:10.2967/jnumed.108.050583
29. Venneti S, *et al*. PK11195 labels activated microglia in Alzheimer's disease and in vivo in a mouse model using PET. *Neurobiol Aging*. Aug 2009;30(8):1217-26. doi:10.1016/j.neurobiolaging.2007.11.005
30. Yankam Njiwa J, *et al*. Quantitative longitudinal imaging of activated microglia as a marker of inflammation in the pilocarpine rat model of epilepsy using [(11)C]-(R)-PK11195 PET and MRI. *J Cereb Blood Flow Metab*. Apr 2017;37(4):1251-1263. doi:10.1177/0271678X16653615
31. Arlicot N, *et al*. Evaluation of CLINDE as potent translocator protein (18 kDa) SPECT radiotracer reflecting the degree of neuroinflammation in a rat model of microglial activation. *Eur J Nucl Med Mol Imaging*. Dec 2008;35(12):2203-11. doi:10.1007/s00259-008-0834-x
32. Dickens AM, *et al*. Detection of microglial activation in an acute model of neuroinflammation using PET and radiotracers 11C-(R)-PK11195 and 18F-GE-180. *J Nucl Med*. Mar 2014;55(3):466-72. doi:10.2967/jnumed.113.125625
33. Domene A, *et al*. Expression of Phenotypic Astrocyte Marker Is Increased in a Transgenic Mouse Model of Alzheimer's Disease versus Age-Matched Controls: A Presymptomatic Stage Study. *Int J Alzheimers Dis*. 2016;2016:5696241. doi:10.1155/2016/5696241
34. Israel I, *et al*. Combined [(18)F]DPA-714 micro-positron emission tomography and autoradiography imaging of microglia activation after closed head injury in mice. journal article. *J Neuroinflammation*. Jun 7 2016;13(1):140. doi:10.1186/s12974-016-0604-9
35. Ji B, *et al*. Imaging of peripheral benzodiazepine receptor expression as biomarkers of detrimental versus beneficial glial responses in mouse models of Alzheimer's and other CNS pathologies. *J Neurosci*. Nov 19 2008;28(47):12255-67. doi:10.1523/JNEUROSCI.2312-08.2008
36. Lavisse S, *et al*. Reactive astrocytes overexpress TSPO and are detected by TSPO positron emission tomography imaging. *J Neurosci*. Aug 8 2012;32(32):10809-18. doi:10.1523/JNEUROSCI.1487-12.2012
37. Lavisse S, *et al*. [18F]DPA-714 PET imaging of translocator protein TSPO (18 kDa) in the normal and excitotoxically-lesioned nonhuman primate brain. *Eur J Nucl Med Mol Imaging*. Mar 2015;42(3):478-94. doi:10.1007/s00259-014-2962-9
38. Maeda J, *et al*. Phase-dependent roles of reactive microglia and astrocytes in nervous system injury as delineated by imaging of peripheral benzodiazepine receptor. *Brain Res*. Jul 9 2007;1157:100-11. doi:10.1016/j.brainres.2007.04.054
39. Mattner F, *et al*. Evaluation of [(1)(2)(3)I]-CLINDE as a potent SPECT radiotracer to assess the degree of astroglia activation in cuprizone-induced neuroinflammation. *Eur J Nucl Med Mol Imaging*. Aug 2011;38(8):1516-28. doi:10.1007/s00259-011-1784-2
40. Nguyen DL, *et al*. Longitudinal positron emission tomography imaging of glial cell activation in a mouse model of mesial temporal lobe epilepsy: Toward identification of optimal treatment windows. *Epilepsia*. Jun 2018;59(6):1234-1244. doi:10.1111/epi.14083
41. Rojas S, *et al*. Imaging brain inflammation with [(11)C]PK11195 by PET and induction of the peripheral-type benzodiazepine receptor after transient focal ischemia in rats. *J Cereb Blood Flow Metab*. Dec 2007;27(12):1975-86. doi:10.1038/sj.jcbfm.9600500
42. Serriere S, *et al*. Amyloid load and translocator protein 18 kDa in APPswePS1-dE9 mice: a longitudinal study. *Neurobiol Aging*. Apr 2015;36(4):1639-1652. doi:10.1016/j.neurobiolaging.2014.11.023
43. Wang Y, *et al*. PET imaging of neuroinflammation in a rat traumatic brain injury model with radiolabeled TSPO ligand DPA-714. *Eur J Nucl Med Mol Imaging*. Jul 2014;41(7):1440-9. doi:10.1007/s00259-014-2727-5
44. Daugherty DJ, *et al*. A TSPO ligand is protective in a mouse model of multiple sclerosis. *EMBO Mol Med*. Jun 2013;5(6):891-903. doi:10.1002/emmm.201202124
45. Kaunzner UW, *et al*. Quantitative susceptibility mapping identifies inflammation in a subset of chronic multiple sclerosis lesions. *Brain*. Jan 1 2019;142(1):133-145. doi:10.1093/brain/awy296
46. Cosenza-Nashat M, *et al*. Expression of the translocator protein of 18 kDa by microglia, macrophages and astrocytes based on immunohistochemical localization in abnormal human brain. *Neuropathol Appl Neurobiol*. Jun 2009;35(3):306-28. doi:10.1111/j.1365-2990.2008.01006.x
47. Liu B, *et al*. In Vivo Detection of Age- and Disease-Related Increases in Neuroinflammation by 18F-GE180 TSPO MicroPET Imaging in Wild-Type and Alzheimer's Transgenic Mice. *J Neurosci*. Nov 25 2015;35(47):15716-30. doi:10.1523/JNEUROSCI.0996-15.2015
48. Maeda J, *et al*. In vivo positron emission tomographic imaging of glial responses to amyloid-beta and tau pathologies in mouse models

of Alzheimer's disease and related disorders. *J Neurosci*. Mar 23 2011;31(12):4720-30. doi:10.1523/JNEUROSCI.3076-10.2011
49. Nack A, *et al*. Expression of Translocator Protein and [18F]-GE180 Ligand Uptake in Multiple Sclerosis Animal Models. *Cells*. Jan 28 2019;8(2)doi:10.3390/cells8020094
50. Beckers L, *et al*. Increased Expression of Translocator Protein (TSPO) Marks Pro-inflammatory Microglia but Does Not Predict Neurodegeneration. *Mol Imaging Biol*. Feb 2018;20(1):94-102. doi:10.1007/s11307-017-1099-1
51. Ravikumar B, *et al*. Differential efficacy of the TSPO ligands etifoxine and XBD-173 in two rodent models of Multiple Sclerosis. *Neuropharmacology*. Sep 2016;108:229-37. doi:10.1016/j.neuropharm.2016.03.053
52. Narayan N, *et al*. The macrophage marker translocator protein (TSPO) is down-regulated on pro-inflammatory 'M1' human macrophages. *PLOS ONE*. 2017;12(10):e0185767. doi:10.1371/journal.pone.0185767
53. Owen DR, *et al*. Pro-inflammatory activation of primary microglia and macrophages increases 18 kDa translocator protein expression in rodents but not humans. *J Cereb Blood Flow Metab*. Aug 2017;37(8):2679-2690. doi:10.1177/0271678X17710182
54. Harberts E, *et al*. Translocator protein 18 kDa (TSPO) expression in multiple sclerosis patients. *J Neuroimmune Pharmacol*. Mar 2013;8(1):51-7. doi:10.1007/s11481-012-9397-5
55. Peferoen LA, *et al*. Activation status of human microglia is dependent on lesion formation stage and remyelination in multiple sclerosis. *J Neuropathol Exp Neurol*. Jan 2015;74(1):48-63. doi:10.1097/NEN.0000000000000149
56. Zrzavy T, *et al*. Loss of 'homeostatic' microglia and patterns of their activation in active multiple sclerosis. *Brain*. Jul 1 2017;140(7):1900-1913. doi:10.1093/brain/awx113
57. Bo L, *et al*. Magnetic resonance imaging as a tool to examine the neuropathology of multiple sclerosis. *Neuropathol Appl Neurobiol*. Apr 2004;30(2):106-17. doi:10.1111/j.1365-2990.2003.00521.x
58. De Groot CJ, *et al*. Post-mortem MRI-guided sampling of multiple sclerosis brain lesions: increased yield of active demyelinating and (p) reactive lesions. *Brain*. Aug 2001;124(Pt 8):1635-45. doi:10.1093/brain/124.8.1635
59. Kipp M, *et al*. Pathology of multiple sclerosis. *CNS Neurol Disord Drug Targets*. Aug 2012;11(5):506-17. doi:10.2174/187152712801661248
60. van der Valk P, *et al*. Staging of multiple sclerosis (MS) lesions: pathology of the time frame of MS. *Neuropathol Appl Neurobiol*. Feb 2000;26(1):2-10. doi:10.1046/j.1365-2990.2000.00217.x
61. Giles DA, *et al*. Myeloid cell plasticity in the evolution of central nervous system autoimmunity. *Ann Neurol*. Jan 2018;83(1):131-141. doi:10.1002/ana.25128
62. Vogel DY, *et al*. Macrophages in inflammatory multiple sclerosis lesions have an intermediate activation status. *J Neuroinflammation*. Mar 4 2013;10:35. doi:10.1186/1742-2094-10-35
63. Bo L. The histopathology of grey matter demyelination in multiple sclerosis. *Acta Neurol Scand Suppl*. 2009;120(189):51-7. doi:10.1111/j.1600-0404.2009.01216.x
64. Guilarte TR. TSPO in diverse CNS pathologies and psychiatric disease: A critical review and a way forward. *Pharmacol Ther*. Feb 2019;194:44-58. doi:10.1016/j.pharmthera.2018.09.003
65. Matthews PM, *et al*. Positron-emission tomography molecular imaging of glia and myelin in drug discovery for multiple sclerosis. *Expert Opin Drug Discov*. May 2015;10(5):557-70. doi:10.1517/17460441.2015.1032240
66. Datta G, *et al*. (11)C-PBR28 and (18)F-PBR111 Detect White Matter Inflammatory Heterogeneity in Multiple Sclerosis. *J Nucl Med*. Sep 2017;58(9):1477-1482. doi:10.2967/jnumed.116.187161
67. Loth MK, *et al*. TSPO in a murine model of Sandhoff disease: presymptomatic marker of neurodegeneration and disease pathophysiology. *Neurobiol Dis*. Jan 2016;85:174-186. doi:10.1016/j.nbd.2015.11.001
68. Martin A, *et al*. Evaluation of the PBR/TSPO radioligand [(18)F]DPA-714 in a rat model of focal cerebral ischemia. *J Cereb Blood Flow Metab*. Jan 2010;30(1):230-41. doi:10.1038/jcbfm.2009.205
69. Ratchford JN, *et al*. Decreased microglial activation in MS patients treated with glatiramer acetate. *J Neurol*. Jun 2012;259(6):1199-205. doi:10.1007/s00415-011-6337-x
70. Sucksdorff M, *et al*. Evaluation of the Effect of Fingolimod Treatment on Microglial Activation Using Serial PET Imaging in Multiple Sclerosis. *J Nucl Med*. Oct 2017;58(10):1646-1651. doi:10.2967/jnumed.116.183020
71. Bunai T, *et al*. Neuroinflammation following disease modifying therapy in multiple sclerosis: A pilot positron emission tomography study. *J Neurol Sci*. Feb 15 2018;385:30-33. doi:10.1016/j.jns.2017.12.004
72. van der Knaap MS, *et al*. Leukodystrophies: a proposed classification system based on pathological changes and pathogenetic mechanisms. *Acta Neuropathol*. Sep 2017;134(3):351-382. doi:10.1007/s00401-017-1739-1
73. Mittelbronn M, *et al*. Local distribution of microglia in the normal adult human central nervous system differs by up to one order of magnitude. *Acta Neuropathol*. Mar 2001;101(3):249-55. doi:10.1007/s004010000284
74. Hase Y, *et al*. White matter capillaries in vascular and neurodegenerative dementias. *Acta Neuropathol Commun*. Feb 7 2019;7(1):16. doi:10.1186/s40478-

019-0666-x
75. Bo L, *et al*. Subpial demyelination in the cerebral cortex of multiple sclerosis patients. *J Neuropathol Exp Neurol*. Jul 2003;62(7):723-32. doi:10.1093/jnen/62.7.723
76. Brink BP, *et al*. The pathology of multiple sclerosis is location-dependent: no significant complement activation is detected in purely cortical lesions. *J Neuropathol Exp Neurol*. Feb 2005;64(2):147-55. doi:10.1093/jnen/64.2.147
77. van Horssen J, *et al*. The blood-brain barrier in cortical multiple sclerosis lesions. *J Neuropathol Exp Neurol*. Apr 2007;66(4):321-8. doi:10.1097/nen.0b013e318040b2de
78. Lucchinetti CF, *et al*. Inflammatory cortical demyelination in early multiple sclerosis. *N Engl J Med*. Dec 8 2011;365(23):2188-97. doi:10.1056/NEJMoa1100648
79. Howell OW, *et al*. Meningeal inflammation is widespread and linked to cortical pathology in multiple sclerosis. *Brain*. Sep 2011;134(Pt 9):2755-71. doi:10.1093/brain/awr182
80. Absinta M, *et al*. Gadolinium-based MRI characterization of leptomeningeal inflammation in multiple sclerosis. *Neurology*. Jul 7 2015;85(1):18-28. doi:10.1212/WNL.0000000000001587
81. Politis M, *et al*. Increased PK11195 PET binding in the cortex of patients with MS correlates with disability. *Neurology*. Aug 7 2012;79(6):523-30. doi:10.1212/WNL.0b013e3182635645
82. Herranz E, *et al*. Neuroinflammatory component of gray matter pathology in multiple sclerosis. *Ann Neurol*. Nov 2016;80(5):776-790. doi:10.1002/ana.24791
83. Sethi V, *et al*. Slowly eroding lesions in multiple sclerosis. *Mult Scler*. Mar 2017;23(3):464-472. doi:10.1177/1352458516655403
84. Elliott C, *et al*. Slowly expanding/evolving lesions as a magnetic resonance imaging marker of chronic active multiple sclerosis lesions. *Mult Scler*. Dec 2019;25(14):1915-1925. doi:10.1177/1352458518814117
85. Veronese M, *et al*. Kinetic modelling of [(11)C] PBR28 for 18 kDa translocator protein PET data: A validation study of vascular modelling in the brain using XBD173 and tissue analysis. *J Cereb Blood Flow Metab*. Jul 2018;38(7):1227-1242. doi:10.1177/0271678X17712388
86. Mann DM, *et al*. Quantitative changes in cerebral cortical microvasculature in ageing and dementia. *Neurobiol Aging*. Sep-Oct 1986;7(5):321-30. doi:10.1016/0197-4580(86)90158-2
87. Wimberley C, *et al*. Impact of Endothelial 18-kDa Translocator Protein on the Quantification of (18) F-DPA-714. *J Nucl Med*. Feb 2018;59(2):307-314. doi:10.2967/jnumed.117.195396
88. Daugherty DJ, *et al*. The hGFAP-driven conditional TSPO knockout is protective in a mouse model of multiple sclerosis. *Sci Rep*. Mar 1 2016;6:22556. doi:10.1038/srep22556
89. Liddelow SA, *et al*. Neurotoxic reactive astrocytes are induced by activated microglia. *Nature*. Jan 26 2017;541(7638):481-487. doi:10.1038/nature21029
90. Ryu JK, *et al*. Peripheral benzodiazepine receptor ligand PK11195 reduces microglial activation and neuronal death in quinolinic acid-injected rat striatum. *Neurobiol Dis*. Nov 2005;20(2):550-61. doi:10.1016/j.nbd.2005.04.010
91. Veiga S, *et al*. Ro5-4864, a peripheral benzodiazepine receptor ligand, reduces reactive gliosis and protects hippocampal hilar neurons from kainic acid excitotoxicity. *J Neurosci Res*. Apr 1 2005;80(1):129-37. doi:10.1002/jnr.20430
92. Agnello D, *et al*. Increased peripheral benzodiazepine binding sites and pentraxin 3 expression in the spinal cord during EAE: relation to inflammatory cytokines and modulation by dexamethasone and rolipram. *J Neuroimmunol*. Sep 22 2000;109(2):105-11. doi:10.1016/s0165-5728(00)00279-4
93. Chen MK, *et al*. Imaging the peripheral benzodiazepine receptor response in central nervous system demyelination and remyelination. *Toxicol Sci*. Jun 2006;91(2):532-9. doi:10.1093/toxsci/kfj172
94. Le Goascogne C, *et al*. Neurosteroid progesterone is up-regulated in the brain of jimpy and shiverer mice. *Glia*. Jan 1 2000;29(1):14-24. doi:10.1002/(sici)1098-1136(20000101)29:1<14::aid-glia2>3.3.co;2-e
95. Hendrickx DAE, *et al*. Staining of HLA-DR, Iba1 and CD68 in human microglia reveals partially overlapping expression depending on cellular morphology and pathology. *J Neuroimmunol*. Aug 15 2017;309:12-22. doi:10.1016/j.jneuroim.2017.04.007
96. Okello A, *et al*. Microglial activation and amyloid deposition in mild cognitive impairment: a PET study. *Neurology*. Jan 6 2009;72(1):56-62. doi:10.1212/01.wnl.0000338622.27876.0d

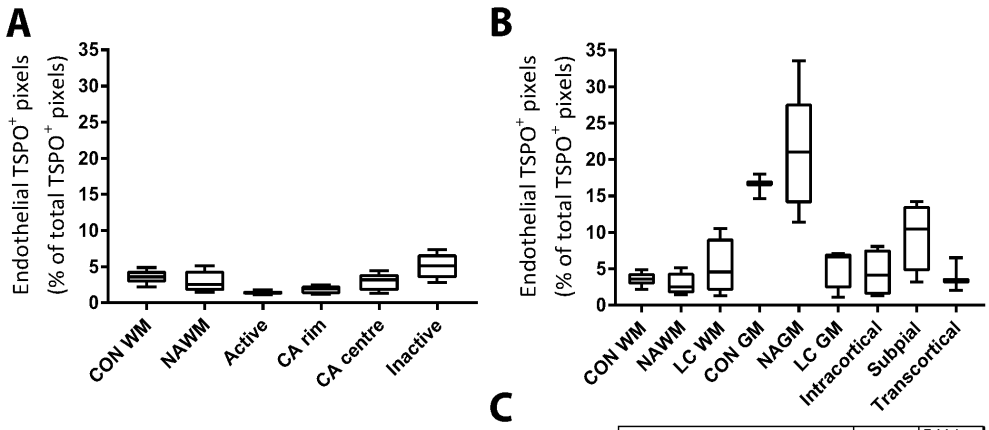

C

Sidak's multiple comparisons test		*P* Value
CON GM vs. Type 1 GM	*	0.0225
CON GM vs. Type 2	*	0.0104
CON GM vs. Type 4	*	0.0144
NAGM vs. Type 1 GM	****	<0.0001
NAGM vs. Type 2	****	<0.0001
NAGM vs. Type 3	**	0.0023
NAGM vs. Type 4	****	<0.0001
CON WM vs. CON GM	**	0.0033
NAWM vs. NAGM	****	<0.0001

Supplementary Figure 1. TSPO expression in endothelial cells in white and grey matter lesions. Endothelial TSPO expression shown as a percentage of total TSPO expression. Endothelial TSPO expression contributes for a small part to total TSPO expression in the white matter (A). Endothelial contribution to the TSPO signal is increased in control grey matter and NAGM compared to the white matter and the NAWM, as well as compared to grey matter lesions (B). P-values see table. CON WM= control white matter, NAWM= normal appearing white matter, CON GM= control grey matter, NAGM= normal appearing grey matter, CA= chronic active, LC = leukocortical lesion.

Activated microglia do not increase 18kDa Translocator Protein (TSPO) expression in the multiple sclerosis brain

Erik Nutma, Emeline Gebro, Manuel C. Marzin, Paul van der Valk, Paul M Matthews, David R. Owen, Sandra Amor

Glia 2021; 69(10):2447-2458

Abstract

To monitor innate immune responses in the CNS, the 18kDa Translocator protein (TSPO) is a frequently used target for PET imaging. The frequent assumption that increased TSPO expression in the human CNS reflects pro-inflammatory activation of microglia has been extrapolated from rodent studies. However, TSPO expression does not increase in activated human microglia *in vitro*. Studies of multiple sclerosis (MS) lesions reveal that TSPO is not restricted to pro-inflammatory microglia/macrophages, but also present in homeostatic or reparative microglia. Here, we investigated quantitative relationships between TSPO expression and microglia/macrophage phenotypes in white matter and lesions of brains with MS pathology. In white matter from brains with no disease pathology, normal appearing white matter (NAWM), active MS lesions and chronic active lesion rims, over 95% of TSPO+ cells are microglia/macrophages. Homeostatic microglial markers in NAWM and control tissue are lost/reduced in active lesions and chronic active lesion rims, reflecting cell activation. Nevertheless, pixel analysis of TSPO+ cells (n=12,225) revealed that TSPO expression per cell is no higher in active lesions and chronic active lesion rims (where myeloid cells are activated) relative to NAWM and control. This data suggests that whilst almost all the TSPO signal in active lesions, chronic active lesion rims, NAWM and control is associated with microglia/macrophages, their TSPO expression predominantly reflects cell density and not activation phenotype. This finding has implications for the interpretation of TSPO PET signal in MS and other CNS diseases, and further demonstrates the limitation of extrapolating TSPO biology from rodents to humans.

Introduction

Multiple sclerosis (MS) is a chronic demyelinating inflammatory disease of the central nervous system (CNS). While current anti-inflammatory strategies targeting the adaptive immune response effectively reduce the frequency of relapses, they fail to limit the neurodegeneration driving disease progression and irreversible accumulation of disability. One potential explanation for this is that innate immune responses, particularly microglia activation linked to ageing of the CNS and the immune system, may be a major contributing factor in neurodegeneration and irreversible disease progression[1].

The 18kDa Translocator Protein (TSPO) is widely used to monitor innate immune responses in the CNS in neuroinflammatory diseases using PET imaging *in vivo*[2-4]. While such expression is commonly considered to reflect activated pathogenic microglia, the early assumption that TSPO expression increases in human microglia as they become activated was inferred from animal studies using rodents[5-9]. However, we recently demonstrated that TSPO expression in primary human macrophages and microglia does not increase with classical pro-inflammatory or anti-inflammatory activation *in vitro*[8]. Similarly, TSPO mRNA was reported to be equal among all different microglia clusters in Alzheimer's disease[10]. We subsequently showed that TSPO expression in microglia co-localizes with *both* classical pro-inflammatory and anti-inflammatory phenotypic markers in brains from people with MS[11]. These studies also revealed expression of TSPO in a substantial number of brain glial cells which were negative for HLA-DR, a classical marker for activated microglia. In inactive MS lesions and in the centre of chronic active lesions, these TSPO+ cells were mainly astrocytes. However, in other regions, the identity of these TSPO+, HLA-DR negative cells was not determined.

Here, we substantially extended the characterisation of TSPO+ cells in the MS brain *post mortem* using a range of microglia and macrophage cell markers (IBA-1, CD68, HLA-DR) to test the hypothesis that the TSPO+, HLA-DR negative cells were primarily HLA-DR negative microglia. We also investigated quantitatively the relationship between TSPO expression and microglia/macrophage phenotypes across the MS brain. We show that previously unidentified TSPO+ cells are microglia and macrophages and that in control tissue and, in brains of people with MS, in normal appearing white matter (NAWM), active lesions and the rim of chronic active lesions nearly all TSPO+ cells (approximately 95%) are microglia and macrophages. As expected, the phenotype of these cells differs across regions. In control brain tissue and NAWM in MS, microglia and macrophages predominantly express IBA-1 and CD68, while in active MS lesions HLA-DR expression appears in addition. As previously documented, P2ry12 and TMEM119 are expressed in control tissue and NAWM microglia, but expression is lost or reduced in active lesions and in the rims of chronic active lesions. Nevertheless, despite the phenotypic change in microglial cells in control and NAWM relative to active and rim of chronic active lesions, the TSPO pixel count per cell is similar across regions. We conclude that the increased TSPO expression in the MS brain can be attributed to an increase in microglia and macrophage cell density predominantly and not due to activation of these cells. This is unlike the rodent brain, where both factors can contribute substantially in inflammatory pathology.

Materials and methods

Human Brain Tissue

Human brain tissues were obtained from 19 MS patients diagnosed by the McDonald criteria[12] and 6 age-matched controls with non-neurological conditions (Table 1). Controls were selected from a larger cohort based on the clinical and pathological profile and were excluded if they were recorded as having neurological disorders, cancer or other inflammatory CNS diseases. The rapid autopsy regime of the Netherlands Brain Bank in Amsterdam (coordinator, Dr I. Huitinga) was followed to obtain donor tissues. Participants or next of kin had given informed consent for brain autopsy and for use of their tissue for research purposes. Tissues were fixed in 4% paraformaldehyde, processed, and embedded in paraffin. Tissues were selected and classified based on the size and type of lesion for quantitative analyses. Identification of the lesions was acquired by immunohistochemistry for myelin proteolipid protein (PLP) to detect myelin loss and HLA-DR to detect microglia and macrophage activation[13].

Table 1. Clinical details of multiple sclerosis and control cases

Case	Age	Sex	Diagnosis	Duration years	PM delay h:min	Cause of death
Multiple sclerosis						
1	50	F	SPMS	17	7:35	Euthanasia
2	66	F	PPMS	13	9:35	Euthanasia
3	77	F	PPMS	24	10:00	Euthanasia
4	54	F	Unknown	27	9:25	Respiratory failure
5	63	F	Unknown	Unknown	10:50	Unknown
6	70	M	SPMS	38	9:25	Euthanasia
7	61	M	SPMS	18	9:15	Euthanasia
8	60	F	SPMS	10	10:40	Euthanasia
9	64	F	SPMS	31	10:10	Urinary tract infection by MS
10	56	M	SPMS	14	10:10	Unknown
11	71	M	Unknown	Unknown	7:15	Pneumonia
12	70	M	SPMS	38	9:25	Euthanasia
13	45	M	PPMS	10	7:45	Pulmonary embolism
14	63	M	Unknown	Unknown	10:00	Pneumonia / Sepsis
15	63	M	Unknown	Unknown	11:00	Pneumonia / Sepsis
16	67	M	SPMS	38	11:00	Pneumonia
17	77	F	Unknown	Unknown	9:45	Aspiration pneumonia
18	35	F	SPMS	10	10:20	Euthanasia
19	66	F	Unknown	Unknown	09:30	Euthanasia
Controls						
1	49	M	Control	N/A	6:15	Euthanasia
2	56	M	Control	N/A	14:00	Heart failure
3	81	M	Control	N/A	5:30	Prostate carcinoma
4	92	F	Control	N/A	7:00	Pulmonary embolism
5	62	M	Control	N/A	7:20	Unknown
6	71	M	Control	N/A	8:55	Pancreatic / rectal carcinoma

F = female; M = male; MS = multiple sclerosis; N/A = not applicable; PM = post-mortem; PP = primary progressive; SP = secondary progressive.

Immunofluorescence

Paraffin sections were immersed in xylene for 5 min for de-paraffinization and rehydrated in descending concentrations of ethanol and washed in phosphate buffered saline (PBS). To reduce autofluorescence sections were incubated in 0.1% glycine for 10 min. Antigen retrieval was performed with citrate or TRIS buffer in the microwave (10 min, 180 Watt). Sections then were incubated with primary antibodies diluted in antibody diluent (Sigma, U3510) overnight, washed and afterwards incubated with Alexa Fluor®-labelled secondary

Table 2. Antibodies for immunohistochemistry

Antigen	Host	Source	Antibody	Dilution
CD68	Mouse	DAKO	M0814	1:500
CD68	Rabbit	Atlas Antibody	HPA048982	1:4000
HLA-DP,-DQ,-DR	Mouse	DAKO	M0775	1:400
HLA-DR (LN3)	Mouse	Biolegend	327011	1:750
IBA-1	Rabbit	Wako	1919741	1:10.000
TSPO (PBR)	Goat	Novus Biologicals	NB100-41398	1:750
P2RY12	Rabbit	ANASPEC	AS55042A	1:200
TMEM119	Rabbit	Merck	HPA051870	1:250
CD68	Mouse	DAKO	M0814	1:500
CD68	Rabbit	Atlas Antibody	HPA048982	1:4000

antibodies for 1 h at room temperature (Table 2). Autofluorescent background signal was reduced with Sudan black (0.1% in 70% EtOH) for 10 min after which sections were thoroughly rinsed. Nuclei were stained with 4,6-diami-dino-2-phenylindole (DAPI) and mounted with Fluormount (Invitrogen; #00-4959-52). For all fluorescent staining procedures negative controls in which either the primary or secondary antibodies were omitted were used to control the presence of background signal.

Imaging and quantitative analyses

Images of each lesion type were collected using a Leica DM6000 microscope (Leica Microsystems, Heidelberg, Germany) for fluorescent images. Images were obtained randomly in the white matter of controls, and from MS in normal appearing white matter (NAWM) and white matter lesions. Pictures were analysed using ImageJ software and stained cells were counted manually using the cell counter plugin (de Vos, University of Sheffield, UK). Cells were counted as single, double, or triple positive based, and co-localisation of markers was based on observation of overlapping fluorescent signal. To justify the accuracy of the counting, 18 pictures were manually counted by 3 independent observers (EN, EG, MM). The inter-observer consistency was evaluated, resulting in a correlation coefficient of > 0.90. For the Sholl analysis, microglia were manually traced using ImageJ software. Afterwards, the traced microglial masks were analysed using the Sholl Analysis Plugin[14]. Data was analysed using GraphPad Prism 8.2.1 software. All data was tested for normal distribution, using the Shapiro-Wilk normality test[15]. Significant differences between the lesions were tested using the one-way analysis of variance test (ANOVA)[16], or the Kruskal-Wallis test, in case of non-normally distributed data. When positive, Dunnett's post-hoc analysis was performed to analyse which groups differ significantly from their respective control or NAWM in MS tissue[17]. Data was considered significant when $P < 0.05$.

Results

Expression of microglia and macrophage markers in multiple sclerosis lesions

The LN3 antibody (Table 2) was used to denote the expression of HLA-DR in human tissues[18]. To investigate whether the lack of expression of HLA-DR by some microglia or macrophages is due to the antibody specificity we used another antibody (CR3/43) targeting HLA-DR, DP and DQ. We compared expression in the white matter of controls (Fig. 1A) with non-neurological diseases, and in NAWM, active (Fig. 1B), chronic active (Fig. 1C), and inactive (Fig. 1D) MS lesions in post mortem tissue. Immunostaining of HLA-DR, DP, DQ and HLA-DR showed a

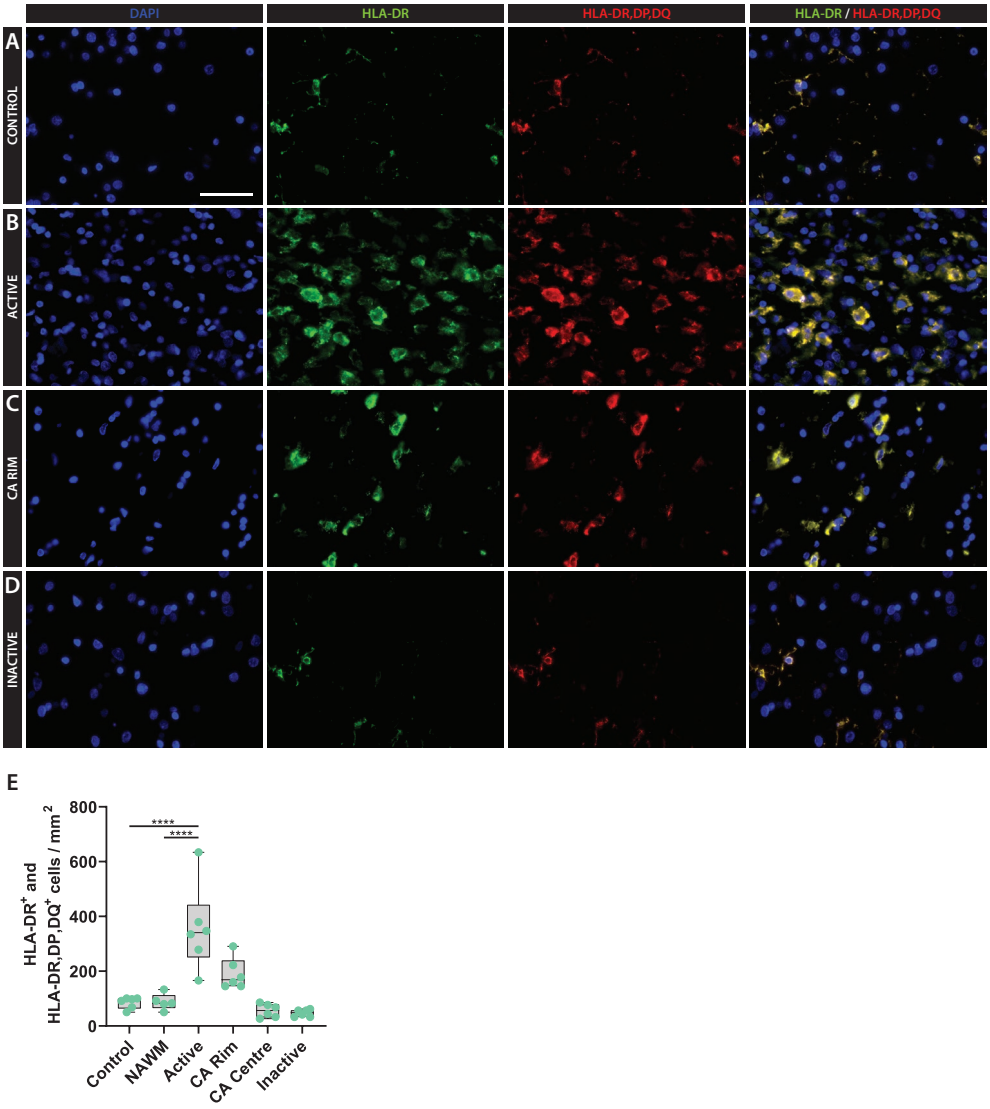

Figure 1. Expression of HLA-DR/DP/DQ in white matter lesions in MS. Representative images of HLA-DR/DP/DQ expression in control (a) and multiple sclerosis lesions (b-d); Active (b), chronic active (CA) rim (c) and inactive (d) lesions. (e) Quantitative analysis of the number of HLA-DR and HLA-DR/DP/DQ positive cells showed an increase in active lesions compared to control and NAWM tissues. (f) HLA-DR positive cells and HLA-DP/DQ/DR positive cells from single immunostainings show an overlap in the number of positive stained cells. ****P<0.0001. Scale bar = 50 µm. NAWM = normal appearing white matter, CA = chronic active.

complete overlap with HLA-DR in all MS and control. The number of cells positive for both HLA-DR and HLA-DR, DP, DQ was increased four-fold in active lesions compared to control ($P < 0.0001$) or NAWM ($P < 0.0001$, Fig. 1E).

To characterise the distribution of the markers IBA-1, CD68 and HLA-DR, a triple staining was performed in control (Fig. 2A), and in NAWM, active (Fig. 2B), chronic active (Fig. 2C), and inactive (Fig. 2D) MS lesions. In control and NAWM, most microglia and macrophages

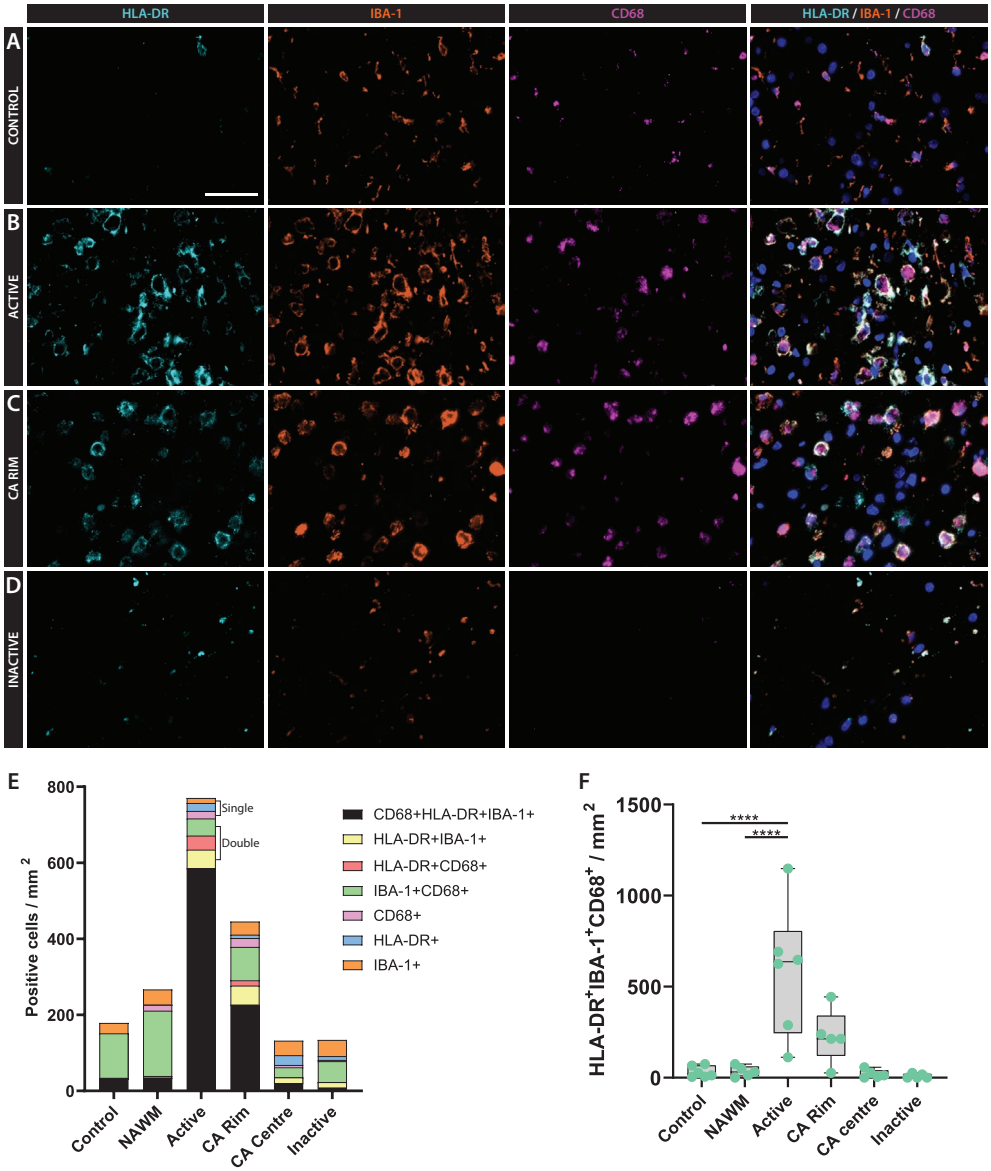

Figure 2. Expression of microglia/macrophage markers in white matter lesions in MS. Representative images of HLA-DR, IBA-1 and CD68 expression in control (a) and multiple sclerosis lesions (b-d); Active (b), chronic active (CA) rim (c) and inactive (d) lesions. (e) Quantitative analysis of the number of positive cells for the three microglia/macrophage markers showing an increase in microglia/macrophage cell density in the active lesion areas (f). ****P<0.0001. Scale bar = 50 µm. NAWM = normal appearing white matter, CA = chronic active.

(64%, SEM 6%) were positive for IBA-1 and CD68 but negative for HLA-DR (Fig. 2E). The few remaining cells were triple positive. However, in active white matter lesions and the rim of chronic active lesions, most microglia and macrophages (76%, SEM 19%) were triple positive, and the few remaining cells were double (either IBA-1/CD68, IBA-1/HLA-DR, or HLA-DR/CD68) or single positive (Fig. 2E).

The number of microglia and macrophages expressing all three markers was approximately 18-fold greater in active lesions compared to control (P<0.0001) or to NAWM (P<0.0001) (Fig. 2F). This large increase is a combination of 1) an increase in the percentage of microglia and macrophages which are triple positive, as described above, and 2) an increase in microglia and macrophage density in active lesions of approximately 4-fold. In inactive lesions, the microglia and macrophage population was substantially smaller than in control and NAWM regions, and the percentage of triple positive cells was

lower, too, contributing only approximately 15% of the microglia and macrophage population. In summary, most microglia and macrophages express IBA-1 and CD68 in control and NAWM, while in active MS lesions, many microglia and macrophages also express HLA-DR.

Identity of TSPO+ cells in MS lesions

As we reported previously[11] TSPO+HLA- cells were observed in control, NAWM and lesional white matter (Fig. 3A). TSPO+HLA- cells are most abundant in the centres of chronic active lesions and in inactive lesions. We have previously shown that the TSPO+HLA- cells are astrocytes in these regions[11].

In other regions, the TSPO+HLA- population is approximately 30% lower, but, and the identity of these cells has not been made clear. Morphologically these TSPO+HLA- cells resemble microglia or macrophages. To test the hypothesis that these are indeed macrophages and/or microglia, we performed triple-immunostaining for TSPO and different pairs of three microglial and macrophage markers; TSPO/HLA-DR/IBA (Fig. 3B), TSPO/HLA-DR/CD68 (Fig. 3C), and TSPO/IBA-1/CD68 (Fig. 3D). All three triple stains (Fig. 3E-G) showed an increase of triple positive cells in active lesion areas compared to control and NAWM. The triple stain for TSPO, IBA-1 and CD68 (Fig. 3J) showed that in control and NAWM and in the rims of chronic active lesions, almost all TSPO+ cells were microglia and macrophages. In control tissue, every TSPO+ cell was also double positive for IBA-1 and CD68 (n=36 cells / mm2) (Fig. 1S). In NAWM, every TSPO+ cell (n=35 cells / mm2) expressed at least one of IBA-1 or CD68, and most (88%) were double positive (Fig. 3J). In the rim of chronic active lesions, 98% of TSPO+ cells were double positive for IBA-1 and CD68. In active lesions, only 88% of TSPO+ cells expressed at least one of IBA-1 or CD68. However, the majority of the remaining 12% of cells which were IBA-1 and CD68 negative are likely to be microglia/macrophages, because the triple stains which included HLA-DR, instead of CD68, showed that only 6% of TSPO+ cells were HLA-DR and IBA-1 negative (Fig. 3H,I). As expected, the percentage of TSPO+ cells which were negative for microglia/macrophage markers was high in inactive lesions (75%) and in the centre of chronic active lesions (25%). These percentages are consistent with our previous work which identified these cells as astrocytes[11].

In summary, almost all TSPO+ cells in control, NAWM, active lesions, and the rims of chronic active lesions are microglia and/or macrophages, although, in the centres of chronic active lesions and inactive lesions, there is a substantial proportion of TSPO+ cells which are astrocytes.

Figure 3. Co-localisation of TSPO with microglia/macrophage markers in white matter lesions in MS. Images of TSPO+HLA-DR- cells in active lesions in MS (a), and images showing colocalisation between TSPO and HLA-DR/IBA-1 (b), HLA-DR/CD68 (c), IBA-1/CD68 (d). Microglia markers are increased in active lesions (e-g). Percentages showing that nearly all TSPO+ cells in white matter MS lesions colocalise microglia/macrophage markers (h-j). **P<0.01, ***P<0.001, ****P<0.0001. Scale bar = 50 µm. NAWM = normal appearing white matter, CA = chronic active.

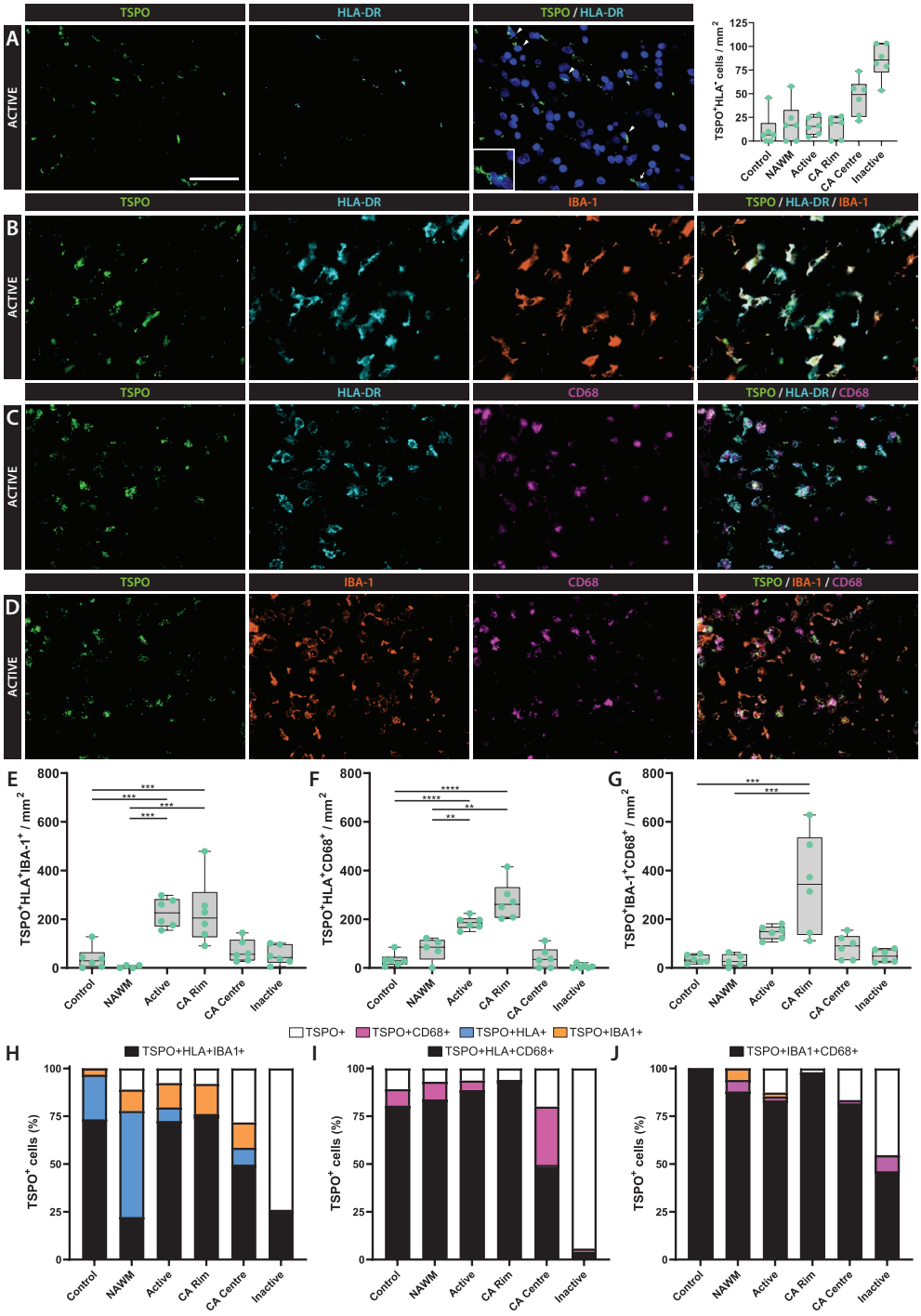
A
ACTIVE
TSPO
HLA-DR
TSPO / HLA-DR
TSPO+HLA+ cells / mm2
Control
NAWM
Active
CA Rim
CA Centre
Inactive
B
ACTIVE
TSPO
HLA-DR
IBA-1
TSPO / HLA-DR / IBA-1
C
ACTIVE
TSPO
HLA-DR
CD68
TSPO / HLA-DR / CD68
D
ACTIVE
TSPO
IBA-1
CD68
TSPO / IBA-1 / CD68
E
TSPO+HLA+IBA-1+ / mm2
F
TSPO+HLA+CD68+ / mm2
G
TSPO+IBA-1+CD68+ / mm2
TSPO+
TSPO+CD68+
TSPO+HLA+
TSPO+IBA1+
H
TSPO+HLA+IBA1+
I
TSPO+HLA+CD68+
J
TSPO+IBA1+CD68+
TSPO+ cells (%)

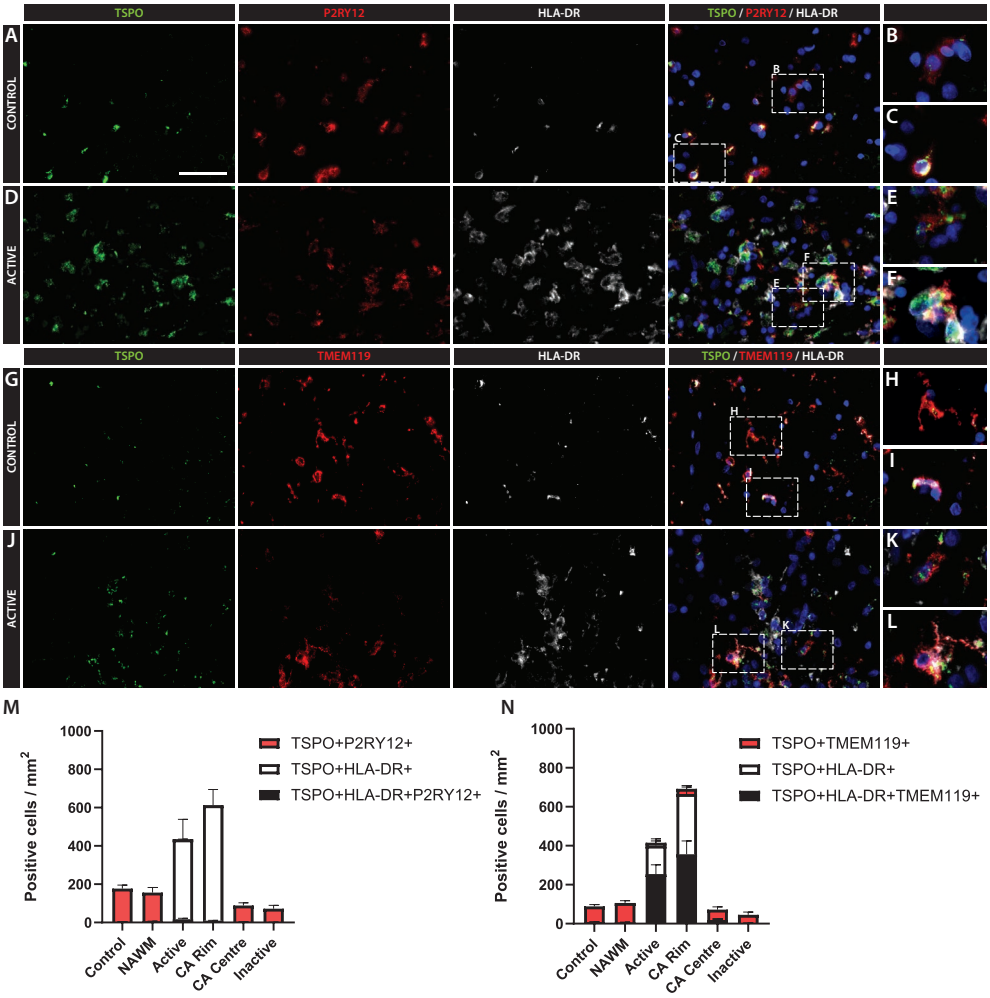

Figure 4. Microglia show a phenotypic shift in active lesions. Representative images of TSPO, P2ry12 and HLA-DR (a-f) in control white matter (a-c) and an active MS white matter lesion (d-f) showing both TSPO+P2ry12+HLA-DR- cells (b,e) as well as TSPO+P2ry12+HLA-DR+ cells (c,f). Representative images of TSPO, TMEM119 and HLA-DR (g-l) in control white matter (g-i) and an active white matter lesion (j-l) showing both TSPO+TMEM119+HLA-DR- cells (h,k) as well as TSPO+TMEM119+HLA-DR+ cells (i,l). Quantitative analysis showed a phenotypic shift and subsequent loss of P2ry12 expression in active lesion areas (m), as well as an increase in the cell density of microglia but a reduction in the percentage of TMEM119+ microglia/macrophages (n). Scale bar = 50 µm. NAWM = normal appearing white matter, CA = chronic active.

Expression of homeostatic markers TMEM119 and P2ry12 by TSPO+HLA+ cells

Expression of the homeostatic markers TMEM119 and P2ry12 is reported to be mostly limited to NAWM and inactive lesions[19,20]. To further characterise the relationship between TSPO expression and phenotypic markers, we performed triple staining of P2ry12 or TMEM119 in combination with HLA-DR and TSPO to identify whether TSPO+ cells expressed markers of both activated (HLA-DR) and homeostatic (TMEM119 and P2ry12) microglial cells. The triple stains showed that in control (Fig. 4A,G), NAWM, active (Fig. 4D,J), chronic active and inactive

lesions P2ry12+TSPO+ cells as well as TMEM119+TSPO+ cells are found with (Fig. 4C,F,I,L) and without (Fig. 4B,E,H,K) HLA-DR expression. As expected, all TSPO+ cells in control and NAWM, which we demonstrated above are microglia or macrophages, express both P2ry12 and TMEM119. Also as expected, TSPO+ cells in active lesions and the rim of chronic active lesions, which again we have demonstrated above are microglia and macrophages, showed evidence of altered phenotype compared to control and NAWM. In these lesion areas, P2ry12 expression is lost in almost all cells (Fig. 4M), TMEM119 expression is lost in approximately 50% of cells, and HLA-DR expression increases so that it appears in almost all cells (Fig. 4N).

TSPO pixels per cell do not change across regions with different microglial phenotypes and morphology

We have shown that almost all TSPO+ cells in control, NAWM, active lesions and rim of chronic active lesions are microglia and macrophages. We have also shown that, as expected, microglia and macrophages in the active lesions and rim of chronic active lesions express activation markers. Therefore, the TSPO expression per cell was compared across the different regions of white matter to determine whether it is increased when the microglial cells are activated compared to when the cells are homeostatic. To do this, the number of TSPO+ pixels across 12,225 TSPO+ cells were analysed (Fig. 5A-C). The percentages of pixels that were TSPO+ were similar across all of the regions of the white matter (control, 0.036% (±0.015), NAWM, 0.033% (±0.008), Active lesions; 0.041% (±0.014), CA rim; 0.038% (±0.014)) and were not statistically significant (Fig. 5A). Furthermore, nearly all the cells in white matter lesions that express a microglia/macrophage marker are positive for TSPO (Fig. 5B). To further investigate the amount of TSPO expression in microglia/macrophages on a per cell basis, the morphology

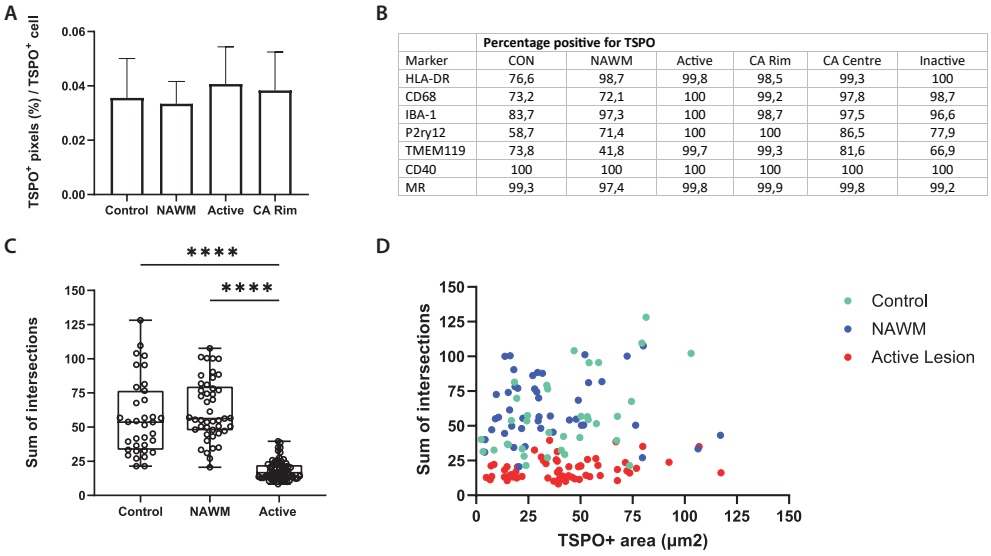

	Percentage positive for TSPO					
Marker	CON	NAWM	Active	CA Rim	CA Centre	Inactive
HLA-DR	76,6	98,7	99,8	98,5	99,3	100
CD68	73,2	72,1	100	99,2	97,8	98,7
IBA-1	83,7	97,3	100	98,7	97,5	96,6
P2ry12	58,7	71,4	100	100	86,5	77,9
TMEM119	73,8	41,8	99,7	99,3	81,6	66,9
CD40	100	100	100	100	100	100
MR	99,3	97,4	99,8	99,9	99,8	99,2

Figure 5. TSPO pixel count does not change across regions with different microglial morphology. The overall TSPO+ pixels per TSPO+ cell did not change in active lesion areas compared to control white matter and NAWM p>0.05 (a). A table showing the percentages of microglia/macrophages that were positive for TSPO subdivided by lesion type (b). Microglia lose their complex morphology in active lesions, shown by a loss of intersections (c). No correlation was observed between the amount of TSPO+ area and the morphology of microglia in control, NAWM or active lesions (d). MR = mannose receptor, NAWM = normal appearing white matter, CA = chronic active.

was investigated using the Sholl analysis. Using this approach we found no correlation between the complex morphological changes that microglia/macrophages undertake, as shown by a loss in intersections of microglia/macrophages in active lesions (Fig. 5C), and the amount of TSPO expression per cell (R^2 = 0.006278, P = 0.3521) (Fig. 5D) when transitioning from an homeostatic to activated state.

In summary, although the microglia and macrophages in active and rim of chronic active lesions express activation markers, the expression of TSPO at protein level in these cells is no different to the microglia in control and NAWM regions, which express homeostatic microglia/macrophage markers.

Discussion

TSPO is used widely as a target for PET imaging in studies of CNS inflammation. Many of these studies are interpreted assuming that TSPO is upregulated in activated glial cells such as microglia, macrophages and astrocytes with neuroinflammation[21]. This interpretation is based on studies of cellular expression of TSPO performed in rodents[5-9]. However, recent investigations have shown that TSPO expression does not increase in human microglia and macrophages *in vitro* after classical pro-inflammatory stimulation[8], and that in the TSPO expression in microglia in the MS brain *post mortem* co-localizes with *both* classical pro-inflammatory and anti-inflammatory phenotypic markers[11]. Furthermore, an earlier study found that transformation of microglia to ameboid phagocytes is not necessary for maximal PK11195 binding[22].

In the current study, the expression of macrophage/microglia markers was examined in *post mortem* MS tissue to characterize the phenotype of cells expressing TSPO. We initially examined a large population of TSPO+ but HLA-DR- cells, presumed to be microglia based on morphology and the lack of GFAP expression[11]. Examination of IBA-1 and CD68 staining established that almost all cells were IBA-1+ or CD68+, and hence this population must be microglia/macrophages.

To further characterize TSPO expression in microglia and macrophages, MS lesions were stained for combinations of microglia/macrophage markers with TSPO. Cells expressing TSPO and microglia/macrophage markers were most abundant in active lesion areas, as expected from PET data showing increased TSPO signal in lesions[3,23-26]. In control tissue, NAWM, active lesions and the rim of chronic active lesions very few TSPO+ cells were negative for the markers IBA-1, CD68 or HLA-DR indicating that the majority of the TSPO+ cells in these areas are likely to be microglia. In the centre of chronic active lesions and in inactive lesion areas there were substantial numbers of TSPO+ cells that lacked expression of any microglial or macrophage marker. Indeed, up to 70% of TSPO+ cells do not colocalise with IBA-1, CD68 or HLA-DR in inactive lesions. This is consistent with our previous findings, showing that approximately 65% of the total population of TSPO+ cells in inactive lesions are astrocytes[11,27,28]. Although TSPO is also expressed in endothelial cells an can be found at low levels in oligodendrocytes and neurons, our data suggests that in the MS brain the largest proportion of TSPO PET signal in the white matter originates from microglia, except in the proportionally smaller volumes of inactive lesions, in which most of the signal must originate from astrocytes[11,29-32].

Microglia adopt intricate and complicated phenotypes that cannot be well defined by single markers[19,33,34]. As expected, using a range of markers, our data revealed evidence of a phenotypic

shift across lesion type. In active MS lesions microglia and macrophages predominantly express all three commonly used markers CD68, IBA-1 and HLA-DR suggesting that these cells have the capacity to scavenge, present antigens as well as phagocytose debris from their environment[35-38]. In control and NAWM tissue, microglia and macrophages predominantly expressed IBA-1 and CD68 but not HLA-DR, indicating that HLA-DR expression arises during activation of microglia in active MS lesions, corroborating previous studies[19]. Recently, P2ry12 and TMEM119 have been identified as markers of homeostatic microglia[20,39,40], some of which express TSPO[11]. Microglia expressing TMEM119 also express CD68 in control tissue as well as in early MS lesions[19] indicating that resident microglia (expressing P2ry12 and TMEM119) express activation markers the balance of which is likely regulated by inflammatory cytokines in their environment[41]. As expected, we show that TMEM119 and P2ry12 expression is constitutive in regions where microglia are homeostatic (control, NAWM) and lost in areas where microglia are activated (active lesions and the rim of chronic active lesions). We also show the colocalization of P2ry12 and HLA-DR, suggesting that these cells are either transitioning from their homeostatic status towards a more inflammatory profile or *vice versa,* from active to homeostatic cells.

That almost all TSPO+ cells across a range of white matter regions were microglia, and that – as expected - the phenotype in control and NAWM was homeostatic, and the phenotype in active lesions and the rim of chronic active lesions was activated, allowed for examination of the relationship between activation and TSPO expression. We analysed the percentage of TSPO+ pixels in TSPO+ cells (n=12,225 cells) and compared regions containing homeostatic microglia with regions containing activated microglia. There was no difference in pixel count per cell between these regions. This implies that although TSPO+ cells in active lesion areas are activated microglia/macrophages, their TSPO expression does ***not*** increase on a per cell basis relative to microglia/macrophages from homeostatic regions. Additionally, there was no correlation between the morphology and the amount of TSPO expression in microglia and macrophages. These findings are consistent with previous reports from our own group and others showing a lack of increase in TSPO expression in activated myeloid cells[8,42], and co-localisation of TSPO with markers of both pro-inflammatory and reparative phenotypes in the MS brain[11]. In support of our studies, a recent study showed that single cell RNA-seq of microglia in Alzheimer's disease reported comparable TSPO mRNA levels across all microglial sub-types suggesting TSPO PET to be a good proxy for total microglia count[10]. Taken together, these findings support generalisation of the hypothesis that when human myeloid cells adopt a pro-inflammatory phenotype, TSPO expression itself does not increase, and any change in signal likely reflects an increase in myeloid cell density rather than a phenotypic shift. The data also highlights the limitations of extrapolating from rodents to humans when examining TSPO biology.

References

1. Labzin LI, *et al*. Innate Immunity and Neurodegeneration. *Annu Rev Med*. Jan 29 2018;69:437-449. doi:10.1146/annurev-med-050715-104343
2. Banati RB, *et al*. The peripheral benzodiazepine binding site in the brain in multiple sclerosis: quantitative in vivo imaging of microglia as a measure of disease activity. *Brain*. Nov 2000;123 (Pt 11)(11):2321-37. doi:10.1093/brain/123.11.2321
3. Colasanti A, *et al*. In Vivo Assessment of Brain White Matter Inflammation in Multiple Sclerosis with (18) F-PBR111 PET. *J Nucl Med*. Jul 2014;55(7):1112-8. doi:10.2967/jnumed.113.135129
4. Venneti S, *et al*. The peripheral benzodiazepine receptor (Translocator protein 18kDa) in microglia: from pathology to imaging. *Prog Neurobiol*. Dec 2006;80(6):308-22. doi:10.1016/j.pneurobio.2006.10.002
5. Bae KR, *et al*. Translocator protein 18 kDa negatively regulates inflammation in microglia. *J Neuroimmune Pharmacol*. Jun 2014;9(3):424-37. doi:10.1007/s11481-014-9540-6
6. Gottfried-Blackmore A, *et al*. Brain microglia express steroid-converting enzymes in the mouse. *J Steroid Biochem Mol Biol*. Mar 2008;109(1-2):96-107. doi:10.1016/j.jsbmb.2007.12.013
7. Karlstetter M, *et al*. Translocator protein (18 kDa) (TSPO) is expressed in reactive retinal microglia and modulates microglial inflammation and phagocytosis. *J Neuroinflammation*. Jan 8 2014;11:3. doi:10.1186/1742-2094-11-3
8. Owen DR, *et al*. Pro-inflammatory activation of primary microglia and macrophages increases 18 kDa translocator protein expression in rodents but not humans. *Journal of Cerebral Blood Flow & Metabolism*. 2017;37(8):2679-2690.
9. Wang M, *et al*. Macroglia-microglia interactions via TSPO signaling regulates microglial activation in the mouse retina. *J Neurosci*. Mar 5 2014;34(10):3793-806. doi:10.1523/JNEUROSCI.3153-13.2014
10. Olah M, *et al*. Single cell RNA sequencing of human microglia uncovers a subset associated with Alzheimer's disease. *Nat Commun*. Nov 30 2020;11(1):6129. doi:10.1038/s41467-020-19737-2
11. Nutma E, *et al*. A quantitative neuropathological assessment of translocator protein expression in multiple sclerosis. *Brain*. Nov 1 2019;142(11):3440-3455. doi:10.1093/brain/awz287
12. Polman CH, *et al*. Diagnostic criteria for multiple sclerosis: 2005 revisions to the "McDonald Criteria". *Ann Neurol*. Dec 2005;58(6):840-6. doi:10.1002/ana.20703
13. van der Valk P, *et al*. Staging of multiple sclerosis (MS) lesions: pathology of the time frame of MS. *Neuropathol Appl Neurobiol*. Feb 2000;26(1):2-10. doi:10.1046/j.1365-2990.2000.00217.x
14. Ferreira TA, *et al*. Neuronal morphometry directly from bitmap images. *Nat Methods*. Oct 2014;11(10):982-4. doi:10.1038/nmeth.3125
15. Ghasemi A, *et al*. Normality tests for statistical analysis: a guide for non-statisticians. *Int J Endocrinol Metab*. Spring 2012;10(2):486-9. doi:10.5812/ijem.3505
16. Kim TK. Understanding one-way ANOVA using conceptual figures. *Korean J Anesthesiol*. Feb 2017;70(1):22-26. doi:10.4097/kjae.2017.70.1.22
17. Lee S, *et al*. What is the proper way to apply the multiple comparison test? *Korean J Anesthesiol*. Oct 2018;71(5):353-360. doi:10.4097/kja.d.18.00242
18. Peferoen LA, *et al*. Activation status of human microglia is dependent on lesion formation stage and remyelination in multiple sclerosis. *J Neuropathol Exp Neurol*. Jan 2015;74(1):48-63. doi:10.1097/NEN.0000000000000149
19. Zrzavy T, *et al*. Loss of 'homeostatic' microglia and patterns of their activation in active multiple sclerosis. *Brain*. Jul 1 2017;140(7):1900-1913. doi:10.1093/brain/awx113
20. Satoh J, *et al*. TMEM119 marks a subset of microglia in the human brain. *Neuropathology*. Feb 2016;36(1):39-49. doi:10.1111/neup.12235
21. Beckers L, *et al*. Increased Expression of Translocator Protein (TSPO) Marks Pro-inflammatory Microglia but Does Not Predict Neurodegeneration. *Mol Imaging Biol*. Feb 2018;20(1):94-102. doi:10.1007/s11307-017-1099-1
22. Banati RB, *et al*. PK ('peripheral benzodiazepine')--binding sites in the CNS indicate early and discrete brain lesions: microautoradiographic detection of [3H]PK11195 binding to activated microglia. *J Neurocytol*. Feb 1997;26(2):77-82. doi:10.1023/a:1018567510105
23. Debruyne JC, *et al*. PET visualization of microglia in multiple sclerosis patients using [11C]PK11195. *Eur J Neurol*. May 2003;10(3):257-64. doi:10.1046/j.1468-1331.2003.00571.x
24. Datta G, *et al*. (11)C-PBR28 and (18)F-PBR111 Detect White Matter Inflammatory Heterogeneity in Multiple Sclerosis. *J Nucl Med*. Sep 2017;58(9):1477-1482. doi:10.2967/jnumed.116.187161
25. Unterrainer M, *et al*. TSPO PET with [(18)F]GE-180 sensitively detects focal neuroinflammation in patients with relapsing-remitting multiple sclerosis. *Eur J Nucl Med Mol Imaging*. Jul 2018;45(8):1423-1431. doi:10.1007/s00259-018-3974-7
26. Vomacka L, *et al*. TSPO imaging using the novel PET ligand [(18)F]GE-180: quantification approaches in patients with multiple sclerosis. *EJNMMI Res*. Oct 26 2017;7(1):89. doi:10.1186/s13550-017-0340-x
27. Kaunzner UW, *et al*. Quantitative susceptibility mapping identifies inflammation in a subset of chronic multiple sclerosis lesions. *Brain*. Jan 1 2019;142(1):133-145. doi:10.1093/brain/awy296

28. Dickens AM, *et al*. Detection of microglial activation in an acute model of neuroinflammation using PET and radiotracers 11C-(R)-PK11195 and 18F-GE-180. *J Nucl Med*. Mar 2014;55(3):466-72. doi:10.2967/jnumed.113.125625
29. Veronese M, *et al*. Kinetic modelling of [(11)C] PBR28 for 18 kDa translocator protein PET data: A validation study of vascular modelling in the brain using XBD173 and tissue analysis. *J Cereb Blood Flow Metab*. Jul 2018;38(7):1227-1242. doi:10.1177/0271678X17712388
30. Wimberley C, *et al*. Impact of Endothelial 18-kDa Translocator Protein on the Quantification of (18) F-DPA-714. *J Nucl Med*. Feb 2018;59(2):307-314. doi:10.2967/jnumed.117.195396
31. Banati RB. Neuropathological imaging: in vivo detection of glial activation as a measure of disease and adaptive change in the brain. *Br Med Bull*. 2003;65(1):121-31. doi:10.1093/bmb/65.1.121
32. Cosenza-Nashat M, *et al*. Expression of the translocator protein of 18 kDa by microglia, macrophages and astrocytes based on immunohistochemical localization in abnormal human brain. *Neuropathol Appl Neurobiol*. Jun 2009;35(3):306-28. doi:10.1111/j.1365-2990.2008.01006.x
33. Vogel DY, *et al*. Human macrophage polarization in vitro: maturation and activation methods compared. *Immunobiology*. Sep 2014;219(9):695-703. doi:10.1016/j.imbio.2014.05.002
34. Holtman IR, *et al*. Transcriptional control of microglia phenotypes in health and disease. *J Clin Invest*. Sep 1 2017;127(9):3220-3229. doi:10.1172/JCI90604
35. Hendrickx DAE, *et al*. Staining of HLA-DR, Iba1 and CD68 in human microglia reveals partially overlapping expression depending on cellular morphology and pathology. *J Neuroimmunol*. Aug 15 2017;309:12-22. doi:10.1016/j.jneuroim.2017.04.007
36. Sasaki Y, *et al*. Iba1 is an actin-cross-linking protein in macrophages/microglia. *Biochem Biophys Res Commun*. Aug 17 2001;286(2):292-7. doi:10.1006/bbrc.2001.5388
37. Ito D, *et al*. Microglia-specific localisation of a novel calcium binding protein, Iba1. *Brain Res Mol Brain Res*. Jun 1 1998;57(1):1-9. doi:10.1016/s0169-328x(98)00040-0
38. Ohsawa K, *et al*. Microglia/macrophage-specific protein Iba1 binds to fimbrin and enhances its actin-bundling activity. *J Neurochem*. Feb 2004;88(4):844-56. doi:10.1046/j.1471-4159.2003.02213.x
39. Butovsky O, *et al*. Identification of a unique TGF-beta-dependent molecular and functional signature in microglia. *Nat Neurosci*. Jan 2014;17(1):131-43. doi:10.1038/nn.3599
40. Bennett ML, *et al*. New tools for studying microglia in the mouse and human CNS. *Proc Natl Acad Sci U S A*. Mar 22 2016;113(12):E1738-46. doi:10.1073/pnas.1525528113
41. van Wageningen TA, *et al*. Regulation of microglial TMEM119 and P2RY12 immunoreactivity in multiple sclerosis white and grey matter lesions is dependent on their inflammatory environment. *Acta Neuropathol Commun*. Dec 11 2019;7(1):206. doi:10.1186/s40478-019-0850-z
42. Harberts E, *et al*. Translocator protein 18 kDa (TSPO) expression in multiple sclerosis patients. *J Neuroimmune Pharmacol*. Mar 2013;8(1):51-7. doi:10.1007/s11481-012-9397-5

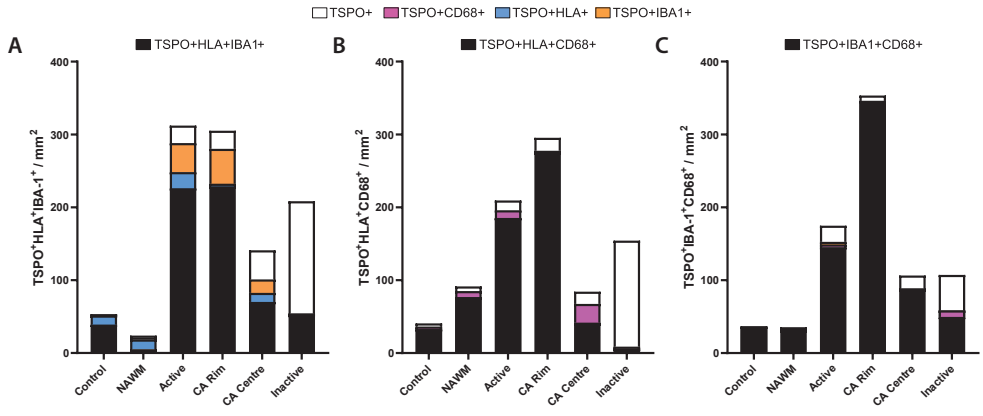

Figure S1. Number of microglia/macrophage markers in white matter lesions in MS. Numbers of positive cells per mm2 showing that nearly all TSPO+ cells in white matter MS lesions co-localize with at least one or two microglia/macrophage markers (a–c). Scale bar = 50µm. NAWM = normal appearing white matter, CA = chronic active.

Translocator protein is a marker of activated microglia in rodent models but not human neurodegenerative diseases

Erik Nutma[+], Nurun Fancy[+], Maria Weinert[+], Manuel C. Marzin, Stergios Tsartsalis, Robert C.J. Muirhead, Irene Falk, Joy de Bruin, David Hollaus, Robin Pieterman, Jasper Anink, David Story, Siddharthan Chandran, Jiabin Tang, Maria C. Trolese, Takashi Saito, Takaomi C. Saido, Katie Wiltshire, Paula Beltran-Lobo, Alexandra Philips, Jack Antel, Luke Healy, Craig S. Moore, Caterina Bendotti, Eleonora Aronica, Carola I. Radulescu, Samuel J. Barnes, David W. Hampton, Paul van der Valk, Steven Jacobson, Paul M. Matthews, Sandra Amor[*], David R. Owen[*]

[+]shared first author

[*]shared senior author

Manuscript submitted

Abstract

Microglial activation plays central roles in neuro-inflammatory and neurodegenerative diseases. Positron emission tomography (PET) targeting 18kDa Translocator Protein (TSPO) is widely used for localising inflammation *in vivo*, but its quantitative interpretation remains uncertain. We show that TSPO expression increases in activated microglia in mouse brain disease models but does not change in a non-human primate disease model or in common neurodegenerative and neuroinflammatory human diseases. We describe genetic divergence in the TSPO gene promoter, consistent with the hypothesis that the increase in TSPO expression in activated myeloid cells is unique to a subset of species within the *Muroidea* superfamily of rodents. We show that TSPO is mechanistically linked to classical pro-inflammatory myeloid cell function in rodents but not humans. These data emphasise that TSPO expression in human myeloid cells is related to different phenomena than in mice, and that TSPO PET reflects density of inflammatory cells rather than activation state.

Introduction

Neuronal-microglial signalling limits microglial inflammatory responses under homeostatic conditions[1]. The loss of this cross talk in central nervous system (CNS) pathology partly explains why microglia adopt an activated phenotype in many neurodegenerative diseases[2,3]. Genomic, *ex vivo* and preclinical data imply that microglial activation also may contribute to neurodegeneration[4], for example, by releasing inflammatory molecules in response to infectious or damage-related triggers[5]. These lead to both neuronal injury and, more directly, pathological phagocytosis of synapses[5,6]. Development of tools which can reliably detect and quantify microglial activation in the living human brain has been an important goal. By enabling improved stratification and providing early pharmacodynamic readouts, these would accelerate experimental medicine studies probing disease mechanisms and early therapeutics.

Detection of 18kDa Translocator Protein (TSPO) with positron emission tomography (PET) has been widely used to quantify microglial activation *in vivo*[7]. In the last 5 years alone, there have been ~300 clinical studies using TSPO PET to quantify microglial responses in the human brain, making it the most commonly used research imaging technique for this purpose.

The TSPO signal is not specific to microglia, and the contribution from other cell types (particularly astrocytes and endothelial cells) is increasingly acknowledged[8]. The justification for quantifying TSPO as a marker of microglial activation is based on the assumption that when microglia become activated, they adopt a classical pro-inflammatory phenotype and TSPO expression is substantially increased[7,9,10]. This has been demonstrated repeatedly in mice, both *in vitro* and *in vivo*[11-14]. We have shown, however, that classical proinflammatory stimulation of human microglia and macrophages *in vitro* with the TLR4 ligand lipopolysaccharide (LPS) does not induce expression of TSPO[15]. Furthermore, in multiple sclerosis (MS), TSPO does not appear to be increased in microglia with activated morphology [16]. These data appear inconsistent with the assumption that TSPO is a marker of activated microglia in humans.

To address this issue, we performed a meta-analysis of publicly available expression array data and found that across a range of pro-inflammatory activation stimuli, TSPO expression is consistently and substantially increased in mouse, but not human macrophages and microglia *in vitro*. We then performed a comparative analysis of the TSPO promoter region in a range of mammalian species and found that the binding site for AP1 (a transcription factor which regulates macrophage activation in rodents[17]) is present in and unique to a subset of species within the *Muroidea* superfamily of rodents. Consistent with the hypothesis that this binding site is required for the increase in TSPO expression that accompanies pro-inflammatory stimulation, we show that TSPO is inducible by LPS in the rat (another *Muroidea* species with the AP1 binding site in the TSPO core promoter) but not in other mammals. Because neuronal interactions modulate microglial phenotype, we then compared microglial TSPO expression in neurodegenerative diseases affecting the brain and spinal cord (Alzheimer's Disease (AD) and amyotrophic lateral sclerosis (ALS), respectively) as well as the classical neuroinflammatory brain disease MS which features highly activated microglia. We compared each human disease to its respective commonly used mouse models (amyloid precursor protein ($App^{NL\text{-}G\text{-}F}$)[18], tau ($Tau^{P301S}$)[19], superoxide dismutase 1 ($SOD1^{G93A}$)[20], and experimental autoimmune encephalomyelitis (EAE) in young and aged animals[21]. We also studied TSPO expression with EAE in the marmoset in conjunction with frequent MRI scanning that allowed for identification of the acute lesions which contain pro-inflammatory microglia. Consistent

with the *in vitro* data, we show that in AD, ALS and MS, and in marmoset EAE, TSPO protein expression does not increase in CNS myeloid cells that express a pro-inflammatory phenotype, while expression is markedly increased in activated myeloid cells in all mouse models of these diseases. With exploration of the relative expression of TSPO in publicly available CNS single cell RNA sequencing (scRNAseq) data from brains of the human diseases and rodent models, we again show an increase in microglial TSPO gene expression in mice with proinflammatory stimuli, but not humans. Finally, using functional studies and examination of transcriptomic co-expression networks, we find that TSPO is mechanistically linked to classical pro-inflammatory myeloid cell function in rodents but not humans.

These data suggest that the commonly held assumption that TSPO PET is sensitive to microglial *activation* is true only for a subset of species within the *Muroidea* superfamily of rodents. In contrast, in humans and other mammals, it simply reflects the local density of inflammatory cells irrespective of the disease context. The clinical interpretation of the TSPO PET signal therefore needs to be revised.

Methods

Meta-analysis of TSPO gene expression

Datasets were searched using the search terms "Macrophage/Monocyte/Microglia" and filtered for '*Homo sapiens'* and '*Mus musculus'*. Datasets with accessible raw data and at least three biological replicates per treatment group were used. To avoid microarray platform-based differences only datasets with Affymetrix chip were used. Raw microarray datasets were downloaded from ArrayExpress (https://www.ebi.ac.uk/arrayexpress/) and RMA normalisation was used. The 'Limma v.3.42.2' R package was used to compute differentially expressed genes, and the resulting *P*-values are adjusted for multiple testing with Benjamini and Hochberg's method to control the false discovery rate[22]. Meta-analysis was performed using R package 'meta v.5.1.1'. A meta *P*-value was calculated using the random-effect model.

ChIP-seq data processing and visualisation

ChIP-seq datasets were downloaded from GSE66594[23] (human) and GSE38377[24] (mouse). Raw fastq sequences were aligned with Bowtie2 v.2.2.9[25] to the human reference genome hg19 or to mouse reference genome mm9, annotated SAM files are converted to tag directories using HOMER v.4.11.1[26] using the makeTagDirectory module. These directories are further used for peak calling using-style histone parameter or converted to the bigWig format normalized to 10^6 total tag counts with HOMER using the makeUCSCfile module with-fsize parameter set at 2e9. For the analysis of histone ChIP-seq data input samples were utilized as control files during peak detection, whereas IgG control files were used during peak correction of the PU.1 ChIP-seq data. Peaks were visualised using UCSC genome browser[27]

Multiple sequence alignment and phylogenetic tree construction

We have retrieved the TSPO promoter region starting from 1 Kbp upstream and 500 bp downstream of the putative transcription start site (TSS) of 34 rodent and non-rodent mammals from ENSEMBL genome database (http://www.ensembl.org/index.htmls). The full list can be found in Supplementary File 2. The multiple sequence alignment was performed using the T-Coffee (v13.45.0.4846264) multiple sequencing tool with the parameter-mode=procoffee which is specifically designed to align the promoter region[28,29]. The sequence alignment and the phylogenetic tree were visualised using Jalview (v 2.11.1.6)[30]. Phylogenetic tree

was constructed using MEGA11 using Maximum Parsimony method with 1000 bootstrap replication. The MP tree was obtained using the Tree-Bisection-Regrafting (TBR) algorithm[31].

Motif finding and motif enrichment

We have used SEA (Simple Enrichment Analysis) from the MEME-suite (v 5.4.1) to calculate the relative motif enrichment between Muroidea family species and non-Muroidea mammals[32,33]. We set the TSPO promoter sequences for the three Muroidea species (Mouse, Rat, Chinese Hamster) as the input sequence and the rest of species as the control sequence. We set the E-value ≤ 10 for calculating significance. We used the motifs for AP1, ETS and SP1 from JASPAR motif database (https://jaspar.genereg.net/).

Multi-species TSPO expression in macrophage and microglia

Datasets were searched using the search terms "Macrophage/Monocyte", "Microglia" and "LPS". Dataset featuring stimulation less than 3 hours were excluded. Datasets with accessible raw data and at least three biological replicates were used. Microarray datasets were analysed as the same way described in section "Meta-analysis of TSPO gene expression". Raw gene count data for the RNAseq datasets were downloaded from either ArrayExpress or GEO (https://www.ncbi.nlm.nih.gov/geo/) and differential expression was performed using DESeq2 v.1.26.0[34]. For S1a, the mouse *Tspo* expression (GEO ID: GSE38371) fold change was directly used from the respective study since biological replicates were not publicly accessible[35].

Human and mouse scRNAseq analysis of microglia

We assessed alterations in gene expression of *TSPO* in human and mouse activated microglia in publicly available scRNAseq datasets. *Postmortem* human brain samples are predominantly studied using single *nucleus* RNA sequencing (snRNAseq) rather than single *cell* RNAseq (sc) RNAseq because the latter requires intact cells which cannot be recovered from frozen brain tissue samples. However, *TSPO* is detected in a very low percentage of nuclei from snRNAseq experiments which prevents accurate assessment of differential expression of *TSPO* across disease or microglial states[36]. For this reason, we searched MEDLINE for human scRNAseq experiments involving AD, MS and ALS donors and mouse brain scRNAseq datasets derived from the respective mouse models, as well as of pro-inflammatory activation with LPS treatment. We found three human studies involving donors with AD[37] and MS[38,39]. Where microglia from CSF samples were analysed with scRNAseq. We found no studies with ALS donors. We found three mouse studies: an LPS activated model[40] an AD model[41] and acute EAE[42]. A fourth mouse scRNAseq dataset was identified from LPS-treated mice[43], however, due to its small size (less than 400 microglial cells were sequenced), this dataset was discarded from further analysis. Raw count matrices were downloaded from the Gene Expression Omnibus (GEO) with the following accession numbers: GSE130119[42], GSE115571[40], GSE98969[41], GSE138266[38] and GSE134578[37]. Data were processed with Seurat (v3)[44] or nf-core/scflow[45]. Quality control, sample integration, dimension reduction and clustering were performed using default parameters as previously described[36,46]. Microglial cells (mouse datasets) and microglia-like cells were identified using previously described cell markers. Differential gene expression analysis was performed using MAST[47] implemented in Seurat to perform zero-inflated regression analysis by fitting a fixed-effects model. Disease vs control group comparisons were performed for all datasets, except for the Keren-Shaul dataset where the AD-associated microglia phenotype was compared to the rest of the microglial population in 5XFAD mice. In all cases, we assessed expression of activated microglial markers. Gene

expression alterations were considered significant when the adjusted p value was equal to or lower than 0.05.

Bulk RNA-seq data preparation and WGCNA network analysis

RAW RNA-seq fastq files for publicly available datasets were downloaded from SRA. Four public human dataset accession are: GSE100382, GSE55536, EMTAB7572, GSE57494 and mouse dataset accession are: GSE103958, GSE62641, GSE82043, GSE58318, E_ERAD_165. The GEO accession ID for the in-house human RNA-seq data is awaiting. Both human and mouse RNA-seq analysis was then performed using nf-core/rnaseq v.1.4.2 pipeline[48]. Human RNA-seq data was aligned to Homo sapiens genome GRCh38 and Mus musculus genome mm10 respectively. Raw count data was first transformed using variance stabilizing transformation (VST) from R package 'DESeq2 v. 1.26.0'. Genes with an expression value of 1 count in at least 50% of the samples were included in the analysis. Batch correction across datasets were then performed on VST-transformed data using removeBatchEffect function from R package 'Limma v. 3.42.2' using the dataset ID as the batch. Batch-corrected normalised data was then used for co-expression network analysis using the R package 'WGCNA v. 1.69'[49]. The power parameter ranging from 1-20 was screened out using the 'pickSoftThreshold' function. A suitable soft threshold of 6 was selected, as it met the degree of independence of 0.85 with the minimum power value. We generated a signed-hybrid network using Pearson correlation with a minimum module size of 30. Subsequently, modules were constructed, and following dynamic branch cutting with a cut height of 0.95. Functional enrichment analysis of the gene modules was performed using the R package 'WebGestaltR v. 0.4.3'[50] using default parameters and 'genome_protein-coding' as the background geneset.

Human Brain Tissue

The rapid autopsy regimen of the Netherlands Brain Bank in Amsterdam (coordinator Prof I. Huitinga) was used to acquire the samples. Human tissue was obtained at autopsy from the spinal cord (cervical, thoracic, lumbar levels) from 12 ALS patients, 7 with short disease duration (SDD; <18 months survival; mean survival 11.1 ± 3.4 months) and 4 with medium disease duration (MDD; >24 months survival; mean survival 71.5 ± 31.5 months). Tissues for controls were collected from 10 age-matched cases with no neurological disorders or peripheral inflammation (Table S1). The hippocampal region was collected from 5 AD patients with Braak stage 6, and 5 aged-matched controls that had no cognitive impairments prior to death (Table S2). Active MS lesions were obtained from 5 MS cases as well as white matter from age-matched controls (Table S3). All tissue was collected with the approval of the Medical Ethical Committee of the Amsterdam UMC. All participants or next of kin had given informed consent for autopsy and use of their tissue for research purposes.

Generation and details of mouse and marmoset models

Mouse EAE

Spinal cord tissue from mice with EAE was obtained from Biozzi ABH mice housed at Queen Mary University of London, UK (originally obtained from Harlan UK Ltd, Bicester, UK). The mice were raised under pathogen-free conditions and showed a uniform health status throughout the studies. EAE was induced via injection of mouse spinal cord homogenate in complete Freund's adjuvant (CFA) into mice of 8-12 weeks or 12 months of age as described previously[51,52]. Immediately, and 24 h after injection mice were given 200ng *Bordetella pertussis* toxin (PT). Age-matched control groups were immunized with CFA and PT. Table

S4 gives an overview of the EAE mice used in this study, including a score of neurological signs (0 = normal, 1 = flaccid tail, 2 = impaired righting reflex, 3 = partial hindlimb paresis, 4 = complete hindlimb paresis, 5 = moribund). Spinal cord was collected from acute (aEAE)[51] in the young mice, and progressive EAE (PEAE) in the 12 month old mice. Animal procedures complied with national and institutional guidelines (UK Animals Scientific Procedures Act 1986) and adhered to the 3R guidelines[53].

Marmoset EAE

EAE was induced by subcutaneous immunization with 0.2 g of white matter homogenate emulsified in CFA in 3 adult common marmosets (*Callithrix jacchus*) at 4 dorsal sites adjacent to inguinal and axillary lymph nodes. Animals were monitored daily for clinical symptoms of EAE progression and assigned clinical EAE scores weekly based on extent of disability. Neurological exams were performed by a neurologist prior to each MRI scan. All animals discussed in this study are shown in Table S5. Animal #8 was treated with prednisolone for 5 days as part of a concurrent study (primary results not yet published). These animals were the first within their twin pair that showed three or more brain lesions by *in vivo* MRI and received corticosteroid treatment with the goal to reduce the severity of inflammation and potentially allow longer-term evaluation of the lesions. MRI analyses were performed according to previously published marmoset imaging protocols using T1, T2, T2*, and PD-weighted sequences on a Bruker 7T animal magnet[54]. Marmosets were scanned biweekly over the course of the EAE study. Following the completion of EAE studies, the brains, spinal cords, and optic nerves excised from euthanized animals were scanned by MRI for *postmortem* characterization of brain lesions and previously uncharacterized spinal lesions and optic nerve lesions. Animal procedures complied with national and institutional guidelines (NIH, Bethesda, USA)

SOD1^{G93A}

Female hemizygous transgenic SOD1^{G93A} mice on 129SvHsd genetic background (n=10) and corresponding non transgenic littermates (n=9) were used. This mouse line was raised at the Mario Negri Institute for Pharmacological Research-IRCCS, Milan, Italy, derived from the line (B6SJL-TgSOD1^{G93A}-1Gur, originally purchased from Jackson Laboratories, USA) and maintained on a 129S2/SvHsd background[55]. The thoracic segments of spinal cord were collected from 10- and 16-week-old mice and processed as previously described[56]. Briefly, anaesthetised mice were transcardially perfused with 0.1M PBS followed by 4% PFA. The spinal cord was quickly dissected out and left PFA overnight at 4°C, rinsed, and stored 24 h in 10% sucrose with 0.1% sodium azide in 0.1 M PBS at 4°C for cryoprotection, before mounting in optimal cutting temperature compound (OCT) and stored at-80°C.

Procedures involving animals and their care were conducted in conformity with the following laws, regulations, and policies governing the care and use of laboratory animals: Italian Governing Law (D.lgs 26/2014; Authorization 19/2008-A issued 6 March, 2008 by Ministry of Health); Mario Negri Institutional Regulations and Policies providing internal authorization for persons conducting animal experiments; the National Institutes of Health's Guide for the Care and Use of Laboratory Animals (2011 edition), and European Union directives and guidelines (EEC Council Directive, 2010/63/UE).

APP^{NL-G-F}

For the *APP^{NL-G-F}* model of AD, male and female brain tissue was obtained from 11 homozygous

(*APP*$^{NL\text{-}G\text{-}F/NL\text{-}G\text{-}F}$) APP knock-in mice and 11 wild type mice. Mice were bred at Charles River Laboratories, UK and sampled at the Imperial College London, UK. Brain tissue samples were collected fresh from 10- and 28 week-old mice that were euthanised with sodium pentobarbital and exsanguinated. Animal procedures complied with national and institutional guidelines (UK Animals Scientific Procedures Act 1986) and adhered to 3R guidelines. Hippocampal areas were used as region of interest for characterization.

Tau^{P301S}

Male brain tissue was obtained from 10 homozygous P301S knock-in mice[57-59] and 8 wild-type C57/Bl6-OLA mice (Envigo, UK) from the Centre for Clinical Brain Sciences, Edinburgh, United Kingdom. Brain tissue samples were collected from 8- and 20-week-old mice that were perfused with PBS and 4% paraformaldehyde, with tissues being post-fixed overnight before being cryopreserved in 30% sucrose and frozen embedded in tissue tec (Leica, UK). Sections were cut, 20mm, on a cryostat onto superfrost plus slides and stored in-80 freezer. Animal procedures complied with national and institutional guidelines (UK Animals Scientific Procedures Act 1986 & University of Edinburgh Animal Care Committees) and adhered to 3R guidelines. Hippocampal areas were used as region of interest for characterization.

For all studies mice were housed 4-5 per standard cages in specific pathogen-free and controlled environmental conditions (temperature: 22±2°C; relative humidity: 55±10% and 12 h of light/dark). Food (standard pellets) and water were supplied *ad libitum*.

Immunohistochemistry

Paraffin sections were de-paraffinized by immersion in xylene for 5 min and rehydrated in descending concentrations of ethanol and fixed-frozen sections were dried overnight. After washing in PBS, endogenous peroxidase activity was blocked with 0.3 % H_2O_2 in PBS while for immunofluorescence sections were incubated in 0.1% glycine. Antigen retrieval was performed with citrate or TRIS/EDTA buffer, depending on the antibody, in a microwave for 3 min at 1000W and 10 min at 180W. Sections were cooled down to RT and incubated with primary antibodies (Table S6) diluted in antibody diluent (Sigma, U3510) overnight. Sections were washed with PBS and afterwards incubated with the appropriate secondary antibodies for 1 h at room temperature. HRP labelled antibodies were developed with diluted 3,3'-diaminobenzidine (DAB; 1:50, DAKO) for 10 min and counterstained with haematoxylin. Sections were immersed in ascending ethanol solutions and xylene for dehydration and mounted with Quick-D. For immunofluorescence, sections were incubated with Alexa Fluor®-labelled secondary antibodies. Autofluorescent background signal was reduced by incubating sections in Sudan black (0.1% in 70% EtOH) for 10 min. Nuclei were stained with 4,6-diami-dino-2-phenylindole (DAPI) and slides were mounted onto glass coverslips with Fluoromount™ (Merck).

Imaging mass cytometry

Antibody conjugation was performed using the Maxpar X8 protocol (Fluidgm). 51 slides of paraffin-embedded tissue from the Medial Temporal Gyrus (MTG) and 48 slides of paraffin-embedded tissue from the Somatosensory Cortex (SSC) underwent IMC staining and ablation. Each slide was within 5-10µm in thickness. The slides underwent routine dewaxing and rehydration before undergoing antigen retrieval, in a pH8 Ethylenediaminetetraacetic acid (EDTA) buffer. The slides were blocked in 10% normal horse serum (Vector Laboratories) before incubation with a conjugated-antibody cocktail (Table S6) at 4^{o}C overnight. Slides

were then treated in 0.02% Triton X-100 (Sigma-Aldrich) before incubation with an Iridium-intercalator (Fluidigm) then washed in dH2O and air-dried. Image acquisition took place using a Hyperion Tissue Imager (Fluidigm) coupled to a Helios mass cytometer. The instrument was tuned using the manufacturer's 3-Element Full Coverage Tuning Slide before the slides were loaded into the device. 4 500x500µm regions of interest within the grey matter were selected and then ablated using a laser at a frequency of 200Hz at a 1µm resolution. The data was stored as .mcd files compatible with MCD Viewer software (Fluidigm) then exported as TIFF files. Post-acquisition image processing using ImageJ (v1.53c) software allowed threshold correction and the despeckle function to reduce background noise. The data was opened with HistoCAT (BodenmillerGroup) to quantify the signal of each Ln-channel and exported as .csv files.

Multiplex immunofluorescence

To immunophenotype microglia/macrophages expressing TSPO in the marmoset CNS, a multi-color multiplex immunofluorescence panel was used to stain for Iba1, PLP, and TSPO. Deparaffinised sections were washed twice in PBS supplemented with 1 mg/ml BSA (PBS/BSA), followed by two washes in distilled water. Antigen retrieval was performed by boiling the slide in 10mM citrate buffer (pH 6) for 10 min in an 800W microwave at maximum power, after which they were allowed to cool for 30 min and washed twice in distilled water. To reduce nonspecific Fc receptor binding, the section was incubated in 250 µl of FcR blocker (Innovex Biosciences, cat. no. NB309) for 15 min at room temperature and washed twice in distilled water. To further reduce background, sections were coated with 250 µl Background Buster (Innovex Biosciences, cat. no. NB306) for 15 min at room temperature and washed twice in distilled water. Sections were incubated for 45 min at room temperature in a primary antibody cocktail containing antibodies diluted in PBS/BSA (Supplemental Table 1), washed in PBS/BSA and three changes of distilled water. They were then incubated for 45 min in a secondary antibody cocktail composed of secondary antibodies diluted in PBS/BSA containing DAPI (Invitrogen, cat. no. D1306, 100 ng/ml) (Supplemental Table 2), then washed once in PBS/BSA and twice in distilled water. To facilitate mounting, the sections were air-dried for 15 min at room temperature, sealed with a coverslip as described previously, and allowed to dry overnight prior to image acquisition.

Imaging and statistical analyses

Brightfield images were collected at 40x magnification using a Leica DC500 microscope (Leica Microsystems, Heidelberg, Germany, Japan), or a Leica DM6000 (Leica Microsystems, Heidelberg, Germany) or a Zeiss AxioImager.Z2 wide field scanning microscope for fluorescent images. For AD, $APP^{NL\text{-}G\text{-}F}$, and TAU^{P301S} tissue images were collected from the hippocampus. For ALS tissue, images of the ventral horn and the lateral column were obtained from cervical, thoracic, and lumbar spinal cord levels. For mouse EAE and $SOD1^{G93A}$ mice, images of grey and white matter of the spinal cord were collected per case. ImageJ software was used for picture analyses. Nuclei and stained cells were counted manually using the cell counter plugin (de Vos, University of Sheffield, UK), excluding nuclei at the rim of each picture and within blood vessels. To determine inter-observer variation 18 pictures were manually counted by 3 independent observers with a correlation coefficient of > 0.9. To determine single cell TSPO expression, IBA+ or GFAP+ cells were outlined manually using the imageJ using the ROI manager. Afterwards TSPO+ pixels were measured within IBA+ and GFAP+ ROIs per cell. Data were analyzed using GraphPad Prism 9.1.0 software. All data were tested for normal

distribution, using the Shapiro-Wilk normality test. Significant differences were detected using an unpaired t-test or one-way analysis of variance test. Dunnett's post-hoc test was performed to analyze which groups differ significantly. Number of mice were calculated by power analysis and as a maximum 6-8 mice were used per group based on previous studies[52]. Data was considered significant when $P < 0.05$.

BV2 and primary mouse macrophage culture

All cells were kept at 37°C, 5% CO_2 and 95% humidity. Mouse BV2 cells (a kind gift from Federico Roncaroli, Manchester) were cultured in RPMI-1640 containing 2mM GlutaMAX and 10% heat inactivated FBS (all Gibco). For experiments BV2 were seeded at 1x10^4 cells per well of a 96-well plate the day before treatment. Primary mouse bone marrow-derived macrophages (BMDMs) were obtained from bone marrow of adult C57BL/6 mice and cultured in DMEM containing 10% FBS, penicillin/streptomycin, and glutamine supplemented with M-CSF (10ng/mL; Peprotech) as previously described (Ying et al. 2013). All animal procedures were approved by the Memorial University Animal Care Committee in accordance with the guidelines set by the Canadian Council in Animal Care.

Primary human macrophage culture

All donors gave informed consent under a REC approved protocol (12/LO/0538). Human monocyte derived macrophages (MDMs) were obtained from fresh blood of male and female, healthy donors between 20 and 60 years after CD14-affinity purification. In brief, whole blood was diluted 1:1 with DPBS (Sigma), layered onto Ficoll (Sigma) and spun for 20 min at 800xg with minimal acceleration/deceleration. Peripheral mononuclear cells were collected, washed, and labelled with CD14-affinity beads (Miltenyi) according to the manufacturers protocol. CD14 monocytes were eluted and cultured at 5x10^5 cells/ml in RPMI-1640 containing 2mM GlutaMAX, 10% heat inactivated FBS, and 25ng/ml M-CSF (all Gibco) with medium change after 3 days. MDMs were used after 7 days in-vitro culture. For monocytes, M-CSF was omitted from the medium and cells were used immediately ex-vivo.

Human TSPO genotyping

Genotyping at rs6971 was performed by LGC. Where not specified, studies were performed with homozygous A carriers due to the high affinity for XBD-173 (high-affinity binders; HAB). Homozygous T carriers were grouped as low affinity binders (LAB). Heterozygous rs6971 carriers were omitted from this study.

iPSC culture and microglia-like cell differentiation

The human induced pluripotent stem cell (iPSC) line SFC841-03-01 (https://hpscreg.eu/cell-line/STBCi044-A), previously derived from a healthy donor[60], Oxford Parkinson's Disease Centre/StemBANCC) was obtained under MTA from the James Martin Stem Cell Facility, University of Oxford and cultured in feeder-free, fully defined conditions. In brief, iPSCs were maintained in E8 medium on Geltrex (both Gibco) and fed every day until 80% confluent. For cell cluster propagation, iPSCs were lifted with 0.5 mM EDTA (Thermo) in DPBS and upon visible dissociation, EDTA was removed, and iPSC were diluted 4-6 times in E8 for culture maintenance. iPSCs were screened genotypically for chromosomal abnormalities using single nucleotide polymorphism analysis and phenotypically using Nanog (Cell Signalling) and Tra-1-60 (BioLegend) immune positivity. Mycoplasma infection was excluded based on LookOut test (Sigma) according to manufacturer's protocol. Microglia-like cells were differentiated

according to Haenseler et al 2017[61]. In short, on day 0 iPSCs were dissociated with TrypLE Express (Gibco) and 4x10^6 iPSCs were added to one well of 24-well AggreWell™ 800 (Stem Cell Technology) according to the manufacturer's protocol in 2ml EB medium (E8, SCF (20ng/ml, Miltenyi), BMP4 (50ng/ml; Gibco), VEGF (50ng/ml, PeproTech)) with 10uM ROCK inhibitor (Y-27632, Abcam). From day 1 to 6, 75% medium was exchanged with fresh EB. On day 7 embryoid bodies were transferred to 2x T175 flasks containing factory medium (XVIVO-15 (Lonza), 2mM GlutaMAX, 50uM 2-Mercaptoethanol, 25ng/ml IL-3, and 100ng/ml M-CSF (all Gibco)) and fed weekly with factory medium. Starting from week 4 after transfer, medium was removed and tested for the presence of primitive macrophages using CD45 (immunotools), CD14 (immunotools) and CD11b (Biolegend) immunopositivity by flow cytometry (FACSCalibur, BD Biosciences). Primitive macrophages were transferred to microglia medium (SILAC Adv DMEM/F12 (Gibco), 10 mM glucose (Sigma), 2 mM GlutaMAX, 0.5 mM L-lysine (Sigma), 0.5 mM L-arginine (Sigma), 0.00075% phenol red (Sigma), 100ng/ml IL-34 (PeproTech), 10gn/ml GM-CSF (Gibco)), fed every 3-4 days and used for experiments after 7 days.

Drug treatments and cell activation

Cells were treated with XBD-173 at the indicated concentrations for 1h prior to LPS activation or for 20h prior to phagocytosis. Pro-inflammatory activation was induced with lipopolysaccharide (100ng/ml; Sigma) for 24h. For live-cell phagocytosis assays, pHrodo®-labelled zymosan A bioparticles (Thermo) were added to the culture medium and incubated for 2h at 37°C with 5% CO_2. pHrodo®-fluorescence intensity was acquired in a plate reader (Cytation5, BioTek) or by Flow cytometry (FACSCalibur, BD Biosciences).

Cytokine analysis

Cytokines were assessed from cell-free cell culture supernatant using enzyme-linked immunosorbent assay (ELISA) according to the manufacturers' protocols. The following assays were used: mouse-TNFα and mouse-IL-6 ELISA (R&D Systems), huma-TNFα and human-IL-6 (BD Biosciences). Absorbance was measured in a Spark plate reader (Tecan).

RNA sequencing

RNA was extracted from control and LPS treated (100ng/mL, 24 hours) primary human macrophages using the RNeasy Mini Kit. cDNA libraries (Total RNA with rRNA depletion) were prepared and sequenced using a HiSeq4000. Lanes were run as 75 bases Paired End. Sequencing depth was minimum 40 million reads per sample.

LC-MSMS analysis of supernatant for XBD173 concentration

Supernatant samples were stored at -20°C or lower until analysis. Samples (25 µL) were prepared for analysis by protein precipitation with acetonitrile containing internal standard (tolbutamide) (200 µL) followed by mixing (150 rpm, 15 min) and centrifugation (3000 rpm, 15 min). The supernatant (50) µL was diluted with water (100 µL) and mixed (100 rpm, 15min). Samples were analysed by LC-MSMS (Shimadzu Nexera X2 UHPLC/Shimadzu LCMS 8060) with Phenomenex Kinetex Biphenyl (50 x 2.1)mm, 1.7 µm column and mobile phase components water/0.1% formic acid (A) and acetonitrile/0.1% formic acid (B). Mobile phase gradient was 0 to 0.3 min 2% B; 0.3 to 1.1 min increase to 95% B; 1.1 to 1.75 min 95% B, 1.75 to 1.8 min decrease to 2% B; 1.8 to 2.5 min 2% B. Flow rate was 0.4 mL/min. Injection volume was 1 µL. Calibration standards were prepared by spiking XDB173 into control supernatant

over the range 2-10000 ng/mL, then preparing and analysing as for the study samples. Lower limit of detection was 2 ng/mL.

Results

TSPO expression and epigenetic regulation in primary macrophages

To investigate *TSPO* gene expression changes in human and mouse a meta-analysis was performed using publicly available macrophage and microglia transcriptomic datasets upon pro-inflammatory stimulation (Fig. 1). We found 10 datasets (Fig. 1a) derived from mouse macrophages and microglia in samples from 68 mice and with inflammatory stimuli including activation with LPS, Type 1 interferon (IFN), IFNγ, and LPS plus IFNγ. We performed a meta-analysis and found that *Tspo* was upregulated under pro-inflammatory conditions (Fig. 1a). In the individual datasets, *Tspo* was significantly upregulated in 9 of the 10 experiments. We then interrogated 42 datasets from primary human macrophages and microglia involving samples from 312 participants, with stimuli including inflammatory activation with LPS, IFNγ, IL1, IL6, Poly I:C, viruses, and bacteria (Fig. 1b).

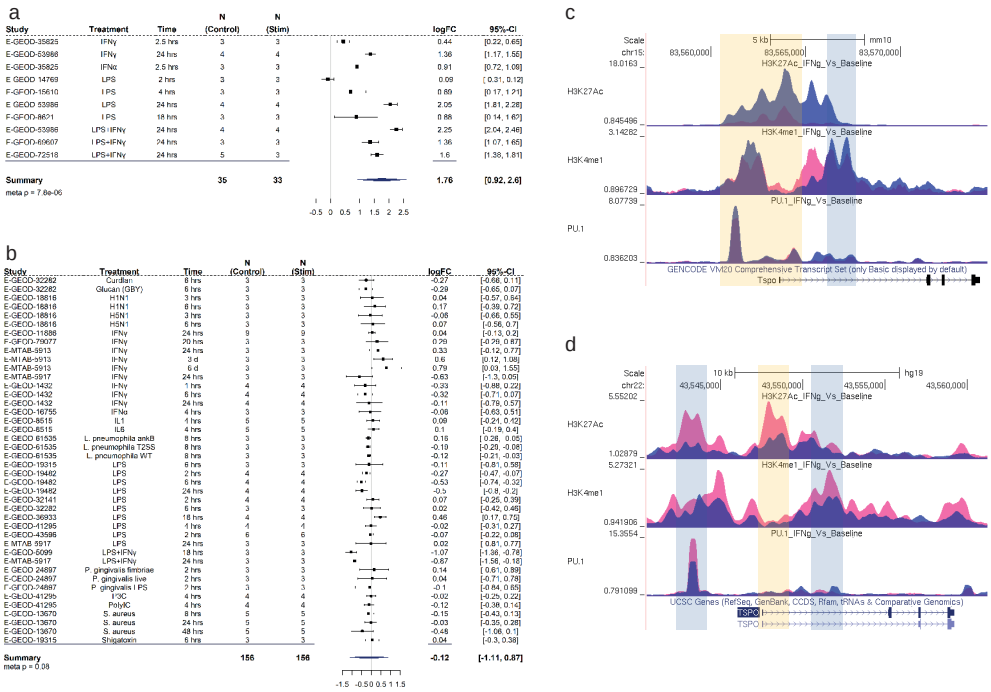

Figure 1. *TSPO* gene expression and epigenetic profile in human and mouse macrophages. **a,b** Forest plot of the meta-analysis for TSPO expression in **a** mouse and **b** human myeloid cells treated with a pro-inflammatory stimulus. The random-effect model was applied when combining the gene expression. The black squares represent the logFC value of each dataset. The horizontal lines indicate the 95% confidence intervals of each study. The diamond represents the pooled logFC. **c,d** ChIP-seq data, generated from **c** mouse and **d** human myeloid cells treated with IFNγ, visualisation of histone modification peaks (H3K27Ac, H3K4me3, H3K4me1) and PU.1 binding peaks at TSPO loci in IFNγ-treated (pink) and baseline (blue) conditions. Yellow vertical shading corresponds to the TSS along with promoter and light blue shading corresponds to the enhancer region of the loci.

In the meta-analysis, there was a non-significant trend towards a *reduction* in human *TSPO* expression under pro-inflammatory conditions (Fig. 1b). In the individual datasets, *TSPO* was unchanged in 33/42 (79%) of the datasets, significantly downregulated in 8/42 (19%) and significantly upregulated in 1/42 (2%). In contrast to the findings in mice, our analysis thus suggests that TSPO expression is not upregulated in human microglia and macrophages after pro-inflammatory stimulation *in vitro*.

To test whether TSPO gene expression changes are regulated at an epigenetic level, we analysed publicly available ChIP-seq datasets for histone modification in mouse and human macrophages before and after treatment with IFNγ[23 35] (Fig. 1c-f). Levels of H3K27Ac and H3K4me1 histone marks in the enhancer regions are associated with increased gene expression[23,62]. While both histone modifications were increased after IFNγ treatment in TSPO promoter regions in macrophages from mouse, they were decreased in humans (Fig. 1c,d). Consistent with this epigenetic regulation, *Tspo* gene expression was upregulated in mouse macrophages after IFNγ but not in human macrophages in RNAseq data from the same set of samples (Fig. S1a).

The PU.1 transcription factor is a master regulator of macrophage proliferation and macrophage differentiation[63,64]. Because PU.1 increases *Tspo* gene expression in the immortalised C57/BL6 mouse microglia BV-2 cell line[65], we next investigated whether *TSPO* expression in macrophages is regulated by PU.1 binding in human in publicly available ChIP-seq datasets. An increase in PU.1 binding in the mouse *Tspo* promoter after IFNγ treatment was observed (Fig. 1c). However, PU.1 binding to the human *TSPO* promoter was decreased after IFNγ treatment (Fig. 1d). To test whether the reduced PU.1 binding at the human *TSPO* promoter was due to reduced PU.1 expression, we analysed RNAseq data from the same set of samples. Expression of SPI-1, the gene that codes for PU.1, was not altered in human macrophages after IFNγ treatment (Fig. S1b), suggesting that the reduced binding of PU.1 to the human *TSPO* promoter region was unlikely to be due to reduced PU.1 levels. This suggests that repressive chromatin remodelling in the human cells leads to decreased PU.1 binding, a consequence of which could be the downregulation of *TSPO* transcript expression. This is consistent with the meta-analysis (Fig. 1a,b); although *TSPO* expression with inflammatory stimuli did not significantly change in most studies, in 8/9 (89%) of studies where TSPO did significantly change, it was downregulated (Fig. 1b). Together this data shows that *in vitro*, pro-inflammatory stimulation of mouse myeloid cells increases TSPO expression, histone marks in the enhancer regions and PU.1 binding. These changes are not found following pro-inflammatory stimulation of human myeloid cells.

The presence of the AP1 binding site in the TSPO promoter and LPS inducible TSPO expression is unique to the *Muroidea* superfamily of rodents

To understand why TSPO expression is inducible by pro-inflammatory stimuli in mouse but not human myeloid cells, we performed multiple sequence alignment of the *TSPO* promoter region of 15 species including primates, rodents, and other mammals (Fig. 2). We found that an AP1 binding site is present uniquely in a subset of species within the *Muroidea* superfamily of rodents including mouse, rat and chinese hamster (Fig. 2a). These binding sites were not present in other rodents (squirrel, guinea pig), nor in other non-rodent mammals (Fig. 2a). We generated a phylogenetic tree which shows a clear branching in the *TSPO* promoter of

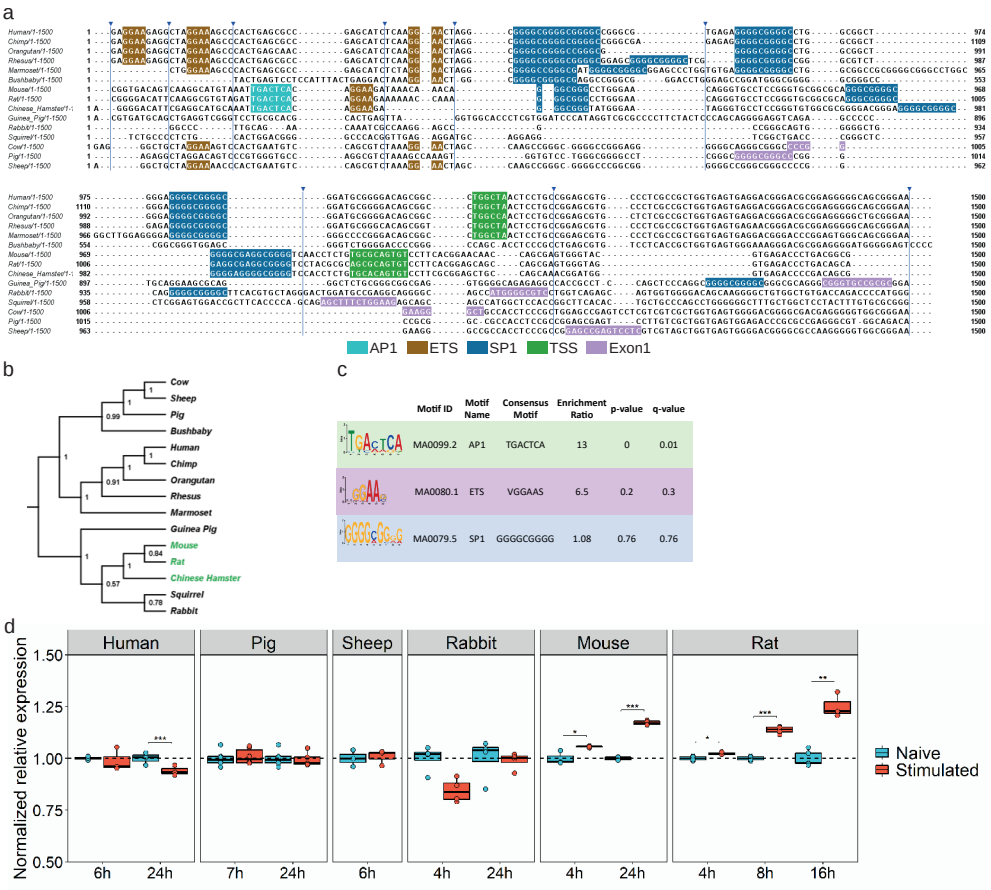

Figure 2. AP1 binding site in the TSPO promoter and LPS inducible TSPO expression is unique to the Muroidea superfamily of rodents. a Multiple sequence alignment of TSPO promoter region of 15 species from primate, rodent, non-primate mammals. AP1 (cyan) and an adjacent ETS (brown) site is present in only a sub-group of rodent family which includes mouse, rat and Chinese hamster. The ETS site which binds transcription factor PU.1 is present across species. SP1 (blue) site is found in the core promoter close to the TSS (green). For species where the TSS is not known Exon1 (pink) location is shown. Blue arrowhead indicates sequence without any motif hidden for visualization. **b** Phylogenetic tree is showing a clear branching of rat, mouse and Chinese hamster TSPO promoter from the rest of the species from rodents. Primates including marmoset forms a separate clade while sheep, cow and pig are part for the same branch. Green highlights represent species that contain the AP1 site in TSPO promoter. Phylogenetic tree was generated using the Maximum Parsimony method in MEGA11. The most parsimonious tree with length = 4279 is shown. The consistency index (CI) is 0.760458 (0.697014) and the retention index is 0.656386 (RI) (0.656386) for all sites and parsimony-informative sites (in parentheses). The percentage of replicate trees in which the associated taxa clustered together in the bootstrap test (1000 replicates) are shown next to the branches. **c** Differential motif enrichment analysis between rodent vs non-rodent TSPO promoter region by SEA tools from MEME-suite confirms the significant enrichment of AP1 site in rodent promoter whereas SP1 site does not show any differential enrichment. TSS; Transcription start site. **d** TSPO gene expression in macrophages or microglia isolated from multiple species after LPS stimulation. In line with the multiple sequence alignment of the TSPO promoter, species (mouse, rat) that contains an adjacent AP1 and ETS motif shows an upregulation of TSPO gene after LPS stimulation. Species lacking (human, pig, sheep, rabbit) those sites show a downregulation or no change in expression after stimulation.

rat, mouse and chinese hamster from the other rodents and non-rodent mammals (Fig. 2b). Differential motif enrichment analysis of the *TSPO* promotor region between *Muroidea* vs non-*Muroidea* species confirmed a significant enrichment of the AP1 binding site in the

Muroidea promoter (Fig. 2c). We expanded this motif search and *TSPO* promoter sequence divergence analysis to a wider range of 24 rodent species from the *Muroidea* superfamily and other non-*Muroidea* rodents. Again, we found that the AP1 site is confined only to a subset of the superfamily *Muroidea* (Fig. S2).

Silencing AP1 impairs LPS induced TSPO expression in the immortalized mouse BV2 cell line[65]. We therefore tested the hypothesis that LPS inducible TSPO expression occurs only in species with the AP1 binding site in the promoter region. In species that lack the AP1 binding site (human, pig, sheep, rabbit), TSPO expression was not induced by LPS (Fig. 2d). However, in the rat, where the AP1 binding site is present, TSPO was increased under these conditions (Fig. 2d).

Microglial TSPO expression is unchanged in the AD hippocampus, but is increased in amyloid mouse models

Microglia-neuronal interactions, which modulate microglia inflammatory phenotype[1], are lost in monocultures *in vitro*. We therefore examined TSPO expression within inflammatory microglia *in situ* with quantitative neuropathology using *postmortem* samples from AD (Table S1). We compared data from human *postmortem* AD brain to the $App^{NL\text{-}G\text{-}F}$ and TAU^{P301S} mouse models.

We examined the hippocampal region, one of the most severely affected regions in AD[66,67], comparing it to non-neurological disease controls (Fig. 3a-c). No increases were observed in the number of IBA1+ microglia (Fig. 3d), HLA-DR+ microglia (Fig. 3e) or astrocytes (Fig. 3f) and the density of TSPO+ cells in AD did not differ compared to controls (Fig. 3g). Additionally, there was no increase in TSPO+ microglia (Fig. 3h,i) and astrocytes (Fig. 3j). We then quantified TSPO+ area (μm^2) in microglia and astrocytes as an index of individual cellular expression (see methods). There was no difference in individual cellular TSPO expression in microglia (Fig. 3k) or astrocytes (Fig. 3k) in AD relative to controls.

We next conducted multiplexed proteomics with imaging mass cytometry (IMC) for further characterisation of cellular phenotype. As with the IHC, we did not see an increase in microglial density, as defined by the number of IBA1+ cells per mm^2, (Fig. S3a) nor in the density of astrocytes (Fig. S3b). Furthermore, again in agreement with the IHC, we did not see an increase in the number of microglia and astrocytes expressing TSPO (Fig. S3c,d). However, IMC did reveal an increase in CD68+ microglia cells (Fig S3e) in AD compared to control, providing evidence, consistent with the literature[68,69], that microglia are activated in AD. However, despite microglial activation, we did not find an increase in individual cellular TSPO expression, defined here as mean cellular TSPO signal, in either microglia (Fig. S3f) or astrocytes (Fig. S3g) in AD donors relative to control. Because proximity to amyloid plaques is associated with activation of microglia[68], we next tested whether cellular TSPO expression was higher in plaque microglia relative to (more distant) non-plaque microglia in the same tissue sections from the AD brains only. We saw no differences in cellular TSPO expression between the plaque and non-plaque microglia (Fig. S3h).

We next compared the human AD data to that from mouse $App^{NL\text{-}G\text{-}F}$ (Fig. 4a,b) and TAU^{P301S} (Fig. 4,i,j). The $App^{NL\text{-}G\text{-}F}$ model avoids artefacts introduced by APP overexpression by utilising a knock-in strategy to express human APP at wild-type levels and with appropriate cell-type and temporal specificity[18]. In this model, APP is not overexpressed. Instead, amyloid plaque

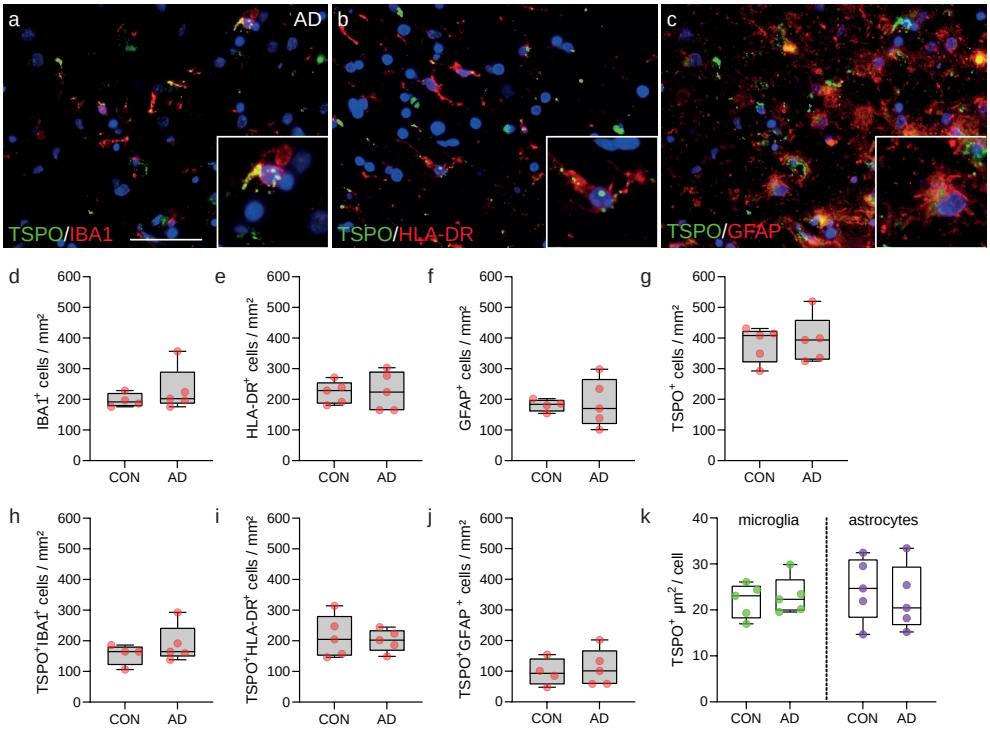

Figure 3. TSPO expression is not altered in the AD hippocampus. a-c Representative images of TSPO expression in microglia and astrocytes in AD hippocampus. **d-g** No increases were observed in microglia (P=0.5159, U=7, ranks=17, 28), activated microglia (P = 0.8997, t=0.1301, df=8) astrocytes (P = 0.8599, t=0.1831, df=7) or TSPO+ cells (P = 0.7329, t=0.3534, df=8) in the AD hippocampus. **h-j** Concurrently no increases were observed in the number of TSPO+IBA1+ microglia (P = 0.3573, t=0.9854, df=7), TSPO+HLA-DR+ microglia (P = 0.7239, t=0.3659, df=8) and astrocytes (P = 0.7181, t=0.3760, df=7). **k** Even though microglia in the AD brain show signs of activation microglia do not upregulate TSPO expression in the hippocampus (P = 0.6717, t=0.4398, df=8), nor do astrocytes (P = 0.6475, t=0.4750, df=8). Statistical significance in **d-k** was determined by a two-tailed unpaired *t*-test or Mann-Whitney U-test when not normally distributed. Box and whiskers mark the 25th to 75th percentiles and min to max values, respectively, with the median indicated. Scale bar = 50µm, inserts are digitally zoomed in (200%).

Density is elevated due to the combined effects of three mutations associated with familial AD (NL; Swedish, G: Arctic, F: Iberian). The *App*$^{NL-G-F}$ line is characterised by formation of amyloid plaques, microgliosis and astrocytosis[18]. We also investigated TSPO expression in a model of tauopathy, TAU^{P301S} mice, which develop tangle-like inclusions in the brain parenchyma associated with microgliosis and astrocytosis[19]. The use of these two models allows differentiation of effects of the amyloid plaques and neurofibrillary tangles on the expression of TSPO in the mouse hippocampus. In *App*$^{NL-G-F}$ mice, an increase in the density of microglia was observed at 28-weeks (Fig. 4c), but not in the density of astrocytes (Fig. 4d). An increase in TSPO+ cells was also observed (Fig. 4e), due to an increase in numbers of TSPO+ microglia and macrophages (Fig. 4f). No differences were observed in the density of TSPO+ astrocytes in *App*$^{NL-G-F}$ at 10 weeks, although a small (relative to that with microglia) increase was observed at 28 weeks (Fig. 4g). Finally, we then quantified TSPO+ area in microglia and astrocytes as an index of TSPO expression in individual cells. In contrast to the human data, expression of TSPO in individual cells was increased by 3-fold in microglia in the *App*$^{NL-G-F}$ mice at 28 weeks (Fig. 4h). It was unchanged in astrocytes. In the TAU^{P301S} mice, no differenceswere

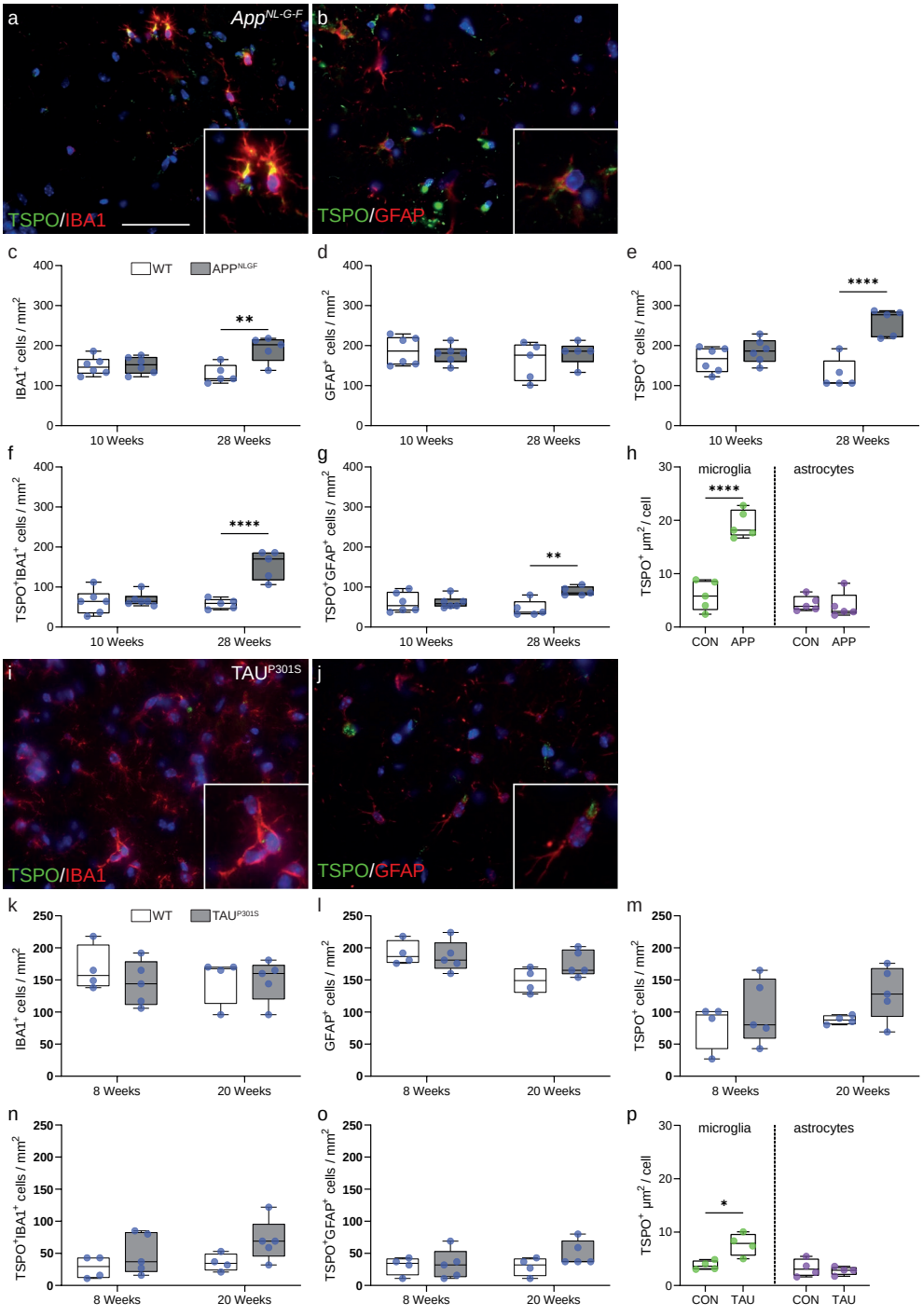
a
App^NL-G-F
TSPO/IBA1
b
TSPO/GFAP
c
WT
APP^NLGF
IBA1+ cells / mm2
10 Weeks
28 Weeks
d
GFAP+ cells / mm2
e
TSPO+ cells / mm2
f
TSPO+IBA1+ cells / mm2
g
TSPO+GFAP+ cells / mm2
h
microglia
astrocytes
TSPO+ µm2 / cell
CON
APP
i
TAU^P301S
j
k
TAU^P301S
8 Weeks
20 Weeks
l
m
n
o
p
TAU

Figure 4. Microglia in the *App*$^{NL\text{-}G\text{-}F}$ and TAU^{P301S} model increase TSPO expression. a,b Representative images of TSPO expression in microglia and astrocytes in *App*$^{NL\text{-}G\text{-}F}$ hippocampus. **c** An increase was observed in IBA1+ microglia at 28 weeks (P = 0.0078, t=3.522, df=8) but not 10 weeks (P = 0.8788, t=0.1565, df=10) in *App*$^{NL\text{-}G\text{-}F}$ hippocampus compared to control. **d** No increase in astrocytes was observed (10 weeks: P = 0.6266, t=0.5019, df=10; 28 weeks: P = 0.4425, t=0.8080, df=8). **e** TSPO+ cells were increased at 28 weeks (P = 0.0079, U=0, ranks=15, 40) but not at 10 weeks (P = 0.2375, t=1.257, df=10) in the *App*$^{NL\text{-}G\text{-}F}$ mice. **f,g** Both TSPO+ microglia (P = 0.0005, t=5.658, df=8) and astrocytes (P = 0.0030, t=4.207, df=8) were increased at 28 weeks in the hippocampus of *App*$^{NL\text{-}G\text{-}F}$ mice but not at 10 weeks (microglia: P = 0.7213, t=0.3670, df=10; astrocytes: P = 0.9561, t=0.056, df=10) . **h** Activated microglia (P < 0.0001, t=7.925, df=8), but not astrocytes (P = 0.3095, U=7, ranks=33, 22), in the *App*$^{NL\text{-}G\text{-}F}$ model have increased TSPO expression. **i,j** Representative images of TSPO expression in microglia and astrocytes in TAU^{P301S} hippocampus. **k-m** No increases in microglia (8 weeks: P = 0.3687, t=0.9608, df=7; 20 weeks; P = 0.9647, t=0.04580, df=7), astrocytes (8 weeks: P = 0.7353, t=0.3519, df=7; 20 weeks; P = 0.0870, t=1.989, df=7) or TSPO+ cells (8 weeks: P = 0.8492, U=9, ranks=19, 26; 20 weeks; P = 0.0876, t=1.985, df=7) were observed in the hippocampus of TAU^{P301S} mice. **n,o** No increase was observed in the number of TSPO+ microglia (8 weeks: P = 0.2787, t=1.174, df=7; 20 weeks; P = 0.0907, t=1.961, df=7) or astrocytes (8 weeks: P = 0.8684, t=0.1718, df=7; 20 weeks; P = 0.1984, U=4.5, ranks=14.5, 30.5). **p** Microglia in the TAU^{P301S} increase TSPO expression (P = 0.0133, t=3.471, df=6) whereas astrocytes do not (P = 0.5800, t=0.5849, df=6). Statistical significance in **c-h** and **k-p** was determined by a two-tailed unpaired *t*-test or Mann-Whitney U-test when not normally distributed. Box and whiskers mark the 25th to 75th percentiles and min to max values, respectively, with the median indicated. Scale bar = 50µm, inserts are digitally zoomed in (200%).

observed in microglia (Fig. 4k) or astrocyte (Fig. 4l) densities, in TSPO+ cell density (Fig. 4m), or in the density of TSPO+ microglia (Fig. 4n) or of TSPO+ astrocytes (Fig. 4o) in the hippocampus at either 8 or 20 weeks (Fig. 4) However, as with the *App*$^{NL\text{-}G\text{-}F}$ mouse (and in contrast to the human), a 2-fold increase in individual cellular TSPO expression was observed within microglia in TAU^{P301S} mice (Fig 4p). Again, as with the *App*$^{NL\text{-}G\text{-}F}$ mouse, individual cellular TSPO expression within astrocytes was unchanged.

In summary, we showed that TSPO cellular expression is increased within microglia from *App*$^{NL\text{-}G\text{-}F}$ and TAU^{P301S} mice, but not in microglia from AD tissue. TSPO was also unchanged in astrocytes from both mouse models and the human disease.

Microglial TSPO is upregulated in SOD1^{G93A} mice but not in ALS

Spinal cord and brain microglia differ with respect to development, phenotype and function[70]. We therefore next investigated ALS (Table S2), that primarily affects the spinal cord rather than the brain. We compared this data to that from the commonly used SOD1^{G93A} mouse model of ALS. TSPO expression was investigated in the ventral horn and lateral columns of the spinal cord in cervical, thoracic, and lumbar regions (Fig. 5a-c). An increase in microglia (Fig. 5d), HLA-DR+ microglia (Fig. 5e) and astrocytes (Fig. 5f) was observed in human ALS spinal cord. The density of TSPO+ cells was increased by 2.5-fold in ALS spinal cords across all regions when compared to controls (Fig. 5g). No additional changes were found when stratifying the cohort based on disease duration or spinal cord regions, white or grey matter, or spinal cord levels. In comparison to the controls, ALS samples exhibited a 3-fold increase in the density of TSPO+ microglia (TSPO+IBA1+ cells, Fig. 5h) and a 3-fold increase in TSPO+ activated microglia/macrophages (TSPO+HLA-DR+ cells, Fig. 5i). A 2.5-fold increase in the density of TSPO+ astrocytes (TSPO+GFAP+ cells) was observed in ALS compared to control (Fig. 5j). We then quantified TSPO+ area in microglia and astrocytes as an index of individual cellular TSPO expression (Fig. 5k). No increase in TSPO+ area (µm^2) was found in microglia or astrocytes in ALS when compared to control (Fig. 5k), implying that TSPO expression does not increase in microglia or astrocytes with ALS.

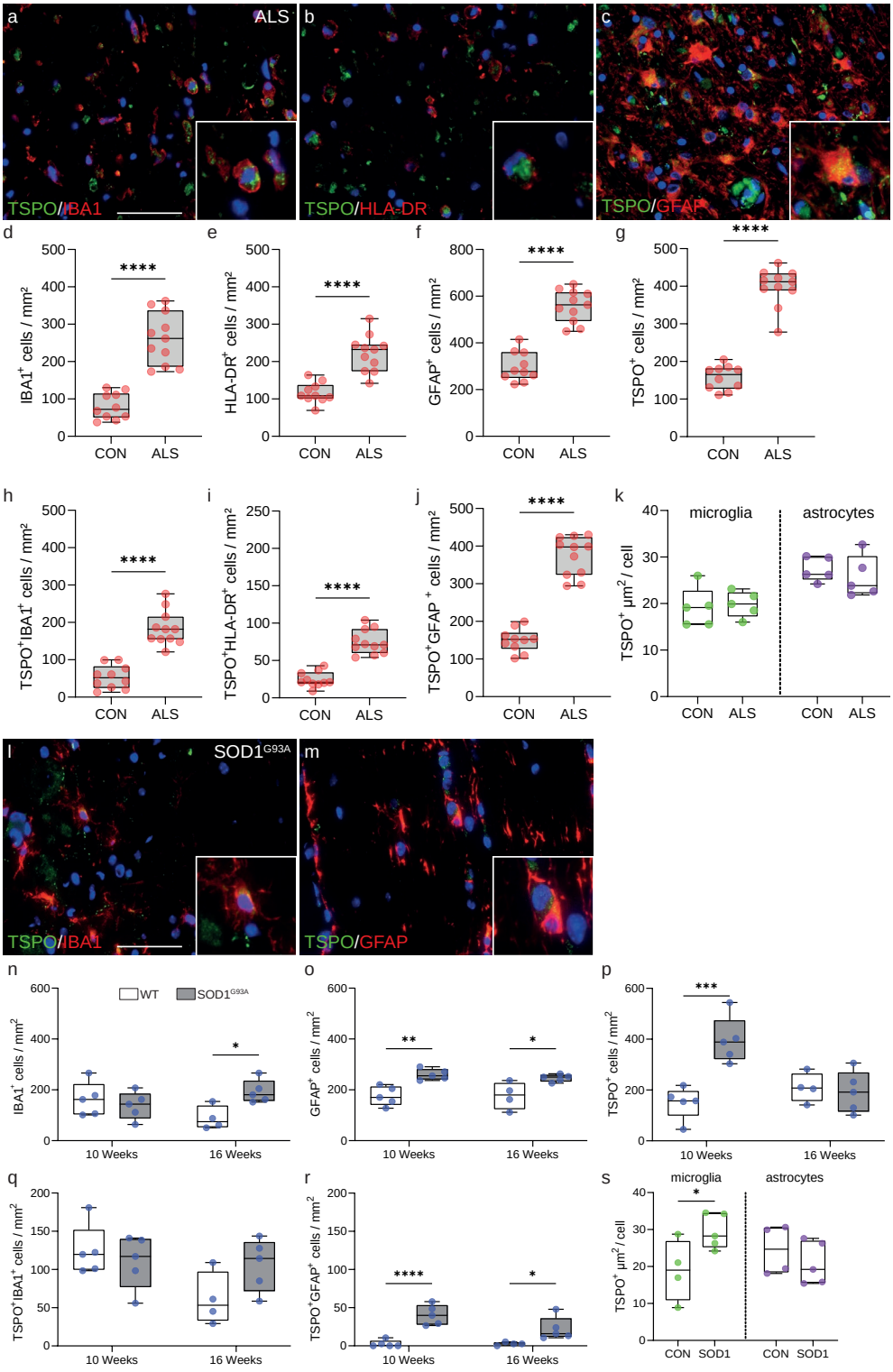
a
ALS
TSPO/IBA1
b
TSPO/HLA-DR
c
TSPO/GFAP
d
IBA1+ cells / mm2
e
HLA-DR+ cells / mm2
f
GFAP+ cells / mm2
g
TSPO+ cells / mm2
CON
ALS
****
h
TSPO+IBA1+ cells / mm2
i
TSPO+HLA-DR+ cells / mm2
j
TSPO+GFAP+ cells / mm2
k
microglia
astrocytes
TSPO+ µm2 / cell
l
SOD1G93A
TSPO/IBA1
m
TSPO/GFAP
n
WT
SOD1G93A
IBA1+ cells / mm2
10 Weeks
16 Weeks
o
GFAP+ cells / mm2
p
TSPO+ cells / mm2
q
TSPO+IBA1+ cells / mm2
r
TSPO+GFAP+ cells / mm2
s
microglia
astrocytes
TSPO+ µm2 / cell
CON
SOD1

Figure 5. TSPO is increased in microglia in SOD1^{G93A} mice but not in ALS spinal cord. a-c Representative images of TSPO expression in microglia and astrocytes in ALS spinal cord. **d-f** An increase was observed in microglia (P < 0.0001, t=7.445, df=19), HLA-DR+ microglia (P < 0.0001, t=6.007, df=19), and astrocytes (P < 0.0001, t=9.024, df=19) in ALS spinal cord when compared to controls. **g** A 2.5-fold increase of TSPO+ cells (P < 0.0001, t=12.88, df=19) was observed in the ALS spinal cord. **h,i** Up to a 3.4-fold increase in the density of TSPO+ microglia (TSPO+IBA1+ cell, P < 0.0001, t=7.541, df=19) (TSPO+HLA-DR+ cells, P < 0.0001, t=3.368, df=19) was observed. **j** TSPO+ astrocytes were significantly increased (P < 0.0001, t=11.77, df=19) in the spinal cord of ALS patients. **k** The increase in activated microglia and astrocytes was not associated with an increase in TSPO expression in microglia (P = 0.7684, t=0.3046, df=8) or in astrocytes (P = 0.5047, t=0.6985, df=8). **l,m** Representative images of TSPO expression in microglia and astrocytes in SOD1^{G93A} spinal cord. **n** An increase was observed in microglia in SOD1^{G93A} spinal cord when compared to controls at 16 weeks (P=0.0115, t=3.395, df=7) but not at 10 weeks (P = 0.5334, t=0.6509, df=8). **o** An increase for astrocytes was observed for both 10 weeks (P = 0.0024, t=4.362, df=8) and 16 weeks (P = 0.0248, t=2.848, df=7) **p** An increase in TSPO+ cells was observed at 10 weeks (P = 0.0011, t=4.931, df=8) but not 16 weeks (P = 0.7299, t=0.3594, df=7). **q** No increase in the number of TSPO+ microglia was observed (10 weeks: P = 0.5244, t=0.6656, df=8; 16 weeks, P = 0.0930, t=1.944, df=7). **r** TSPO+ astrocytes were increased up to 15-fold in the spinal cord of SOD1^{G93A} mice (10 weeks: P = 0.0003, t=6.085, df=8; 16 weeks: P = 0.382, t=2.548, df=7). **s** Despite no increase in the number of TSPO+ microglia, an increase in the amount of TSPO per cell was observed in microglia (P = 0.0451, t=2.435, df=7), but not astrocytes (P = 0.4052, t=0.8856, df=7). Statistical significance in **d-k**, and **o-s** was determined by a two-tailed unpaired *t*-test. Box and whiskers mark the 25th to 75th percentiles and min to max values, respectively, with the median indicated. Scale bar = 50μm, inserts are digitally zoomed in (200%).

SOD1^{G93A} mice express high levels of mutant SOD1 that initiates adult-onset neurodegeneration of spinal cord motor neurons leading to paralysis, and as such these mice have been used as a preclinical model for ALS[20]. To determine the extent to which TSPO+ cells were present in SOD1^{G93A} mice TSPO+ microglia and astrocytes were quantified with immunohistochemistry in the white and grey matter of the spinal cord (Fig. 5l,m). An increase was observed in the total number of microglia (Fig. 5n) and astrocytes (Fig. 5o) in 16-week old SOD1^{G93A} mice but not in 10 week old animals (Fig. 6c,d). The density of TSPO+ cells was increased 2- to 3-fold in presymptomatic disease (10 weeks) compared to non-transgenic littermate control mice in both white and grey matter (Fig. 5p). Increases in the density of TSPO+IBA+ cells were not observed in SOD1^{G93A} mice compared to control animals (Fig. 5q). However, a significant 8- to 15-fold increase in the density of TSPO+GFAP+ astrocytes was observed in 10- and 16-week old SOD1^{G93A} mice compared to 10- and 16-week old wild-type mice (Fig. 5r). Finally, we then quantified TSPO+ area in microglia and astrocytes as an index of individual cellular TSPO expression. In contrast to the human data, where there was no change in disease samples relative to controls, expression of TSPO in individual cells was increased by 1.5-fold in microglia in the rodent model. As with the *App^{NL-G-F}* and TAU^{P301S} mice above, TSPO expression within astrocytes was unchanged (Fig. 5s).

In summary, consistent with the data from AD and relevant mouse models, we have shown that TSPO expression is increased within microglia from SOD1^{G93A} mice, but not increased in microglia from human ALS tissue. TSPO also was unchanged in astrocytes from the SOD1^{G93A} mice and the human disease relatively to those in the healthy control tissues.

Increased myeloid cell TSPO expression is found in mouse EAE, but not in MS or marmoset EAE

Having found no evidence of increased TSPO expression in activated microglia in human neurodegenerative diseases affecting the brain or spinal cord, we next examined MS as an example of a classical neuroinflammatory disease characterised by microglia with a highly activated pro-inflammatory phenotype. We compared data from human *postmortem* MS brain (Table S3) to mice with EAE (Table S4). We also examined brain tissue from marmoset

EAE (Table S5), as *antemortem* MRI assessments in these animals allow for identification of acute lesions which are highly inflammatory.

We previously defined TSPO cellular expression in MS[16,71]. HLA-DR+ microglia expressing TSPO were increased up to 14-fold in active lesions compared to control[71], and these microglia colocalised with CD68 and had lost homeostatic markers P2RY12 and TMEM119, indicating an activated microglial state[16]. Here we quantified individual cellular TSPO expression in both microglia and astrocytes by comparing cells in active white matter lesions to white matter from control subjects. Consistent with the human data from AD and ALS, there was no difference in TSPO expression in individual microglia or astrocytes in MS compared to control tissue (Fig. 6a-c).

We next investigated the relative levels of TSPO expression (Fig. 6d-l) in microglia and astrocytes in acute EAE (aEAE), a commonly used experimental mouse model of MS[21,52]. Neurodegenerative diseases typically occur in old age, whereas aEAE and the AD and ALS relevant rodent models described above are induced in young mice. As age might affect TSPO regulation[72], we also investigated TSPO expression in progressive EAE (PEAE), a model where the pathology is induced in aged mice (12 months).

Increases in numbers of both microglia and astrocytes were observed in aEAE as well as in PEAE mice compared to their respective young and old control groups (Fig. 6f,g). Similarly, increases were observed in the number of TSPO+ microglia and TSPO+ astrocytes in both aEAE and PEAE relative to their respective controls (Fig. 6h-j). When comparing the young control mice (aEAE controls) with the old control mice (PEAE controls), no differences were observed in microglial and TSPO+ microglial density (Fig. 6f,i). Similarly, there was no difference in density of astrocytes or TSPO+ astrocytes between these two control groups (Fig. 6g,j).

To investigate individual cellular TSPO expression, TSPO+ area was measured in microglia and astrocytes. Individual microglia expressed 3-fold greater TSPO and 2-fold greater TSPO in aEAE and PEAE respectively, relative to their control groups. The individual cellular TSPO expression was not higher in microglia from young mice relative to old mice. Again, as with the $SOD1^{G93A}$, $App^{NL\text{-}G\text{-}F}$, and TAU^{P301S} mice, individual cellular TSPO expression within astrocytes was unchanged.

Finally, we investigated TSPO expression in EAE induced in the common marmoset (Callithus jacchus) (Fig. S4, Fig. 6m-o), a non-human primate which, like humans, lacks the AP1 binding site in the core promoter region of TSPO. Both the neural architecture and the immune system of the marmoset are more similar to humans than are those of the mouse[73-75]. Marmoset EAE therefore has features of the human disease which are not seen in mouse EAE, such as perivenular white matter lesions identifiable by MRI, B cell infiltration and CD8+ T cell involvement. Marmosets were scanned with MRI biweekly, which allowed the ages of lesions to be determined and the identification of acute lesions including pro-inflammatory microglia. In acute and subacute lesions, there was an increase of up to 27-fold in the density of TSPO+ microglia relative to control (Fig. S4a-c) and these microglia bore the hallmarks of pro-inflammatory activation. However, TSPO expression in individual microglia, here defined as the percentage of $TSPO^{+}$ pixels using immunofluorescence, was not increased in acute or subacute lesions relative to control (Fig. 6o).

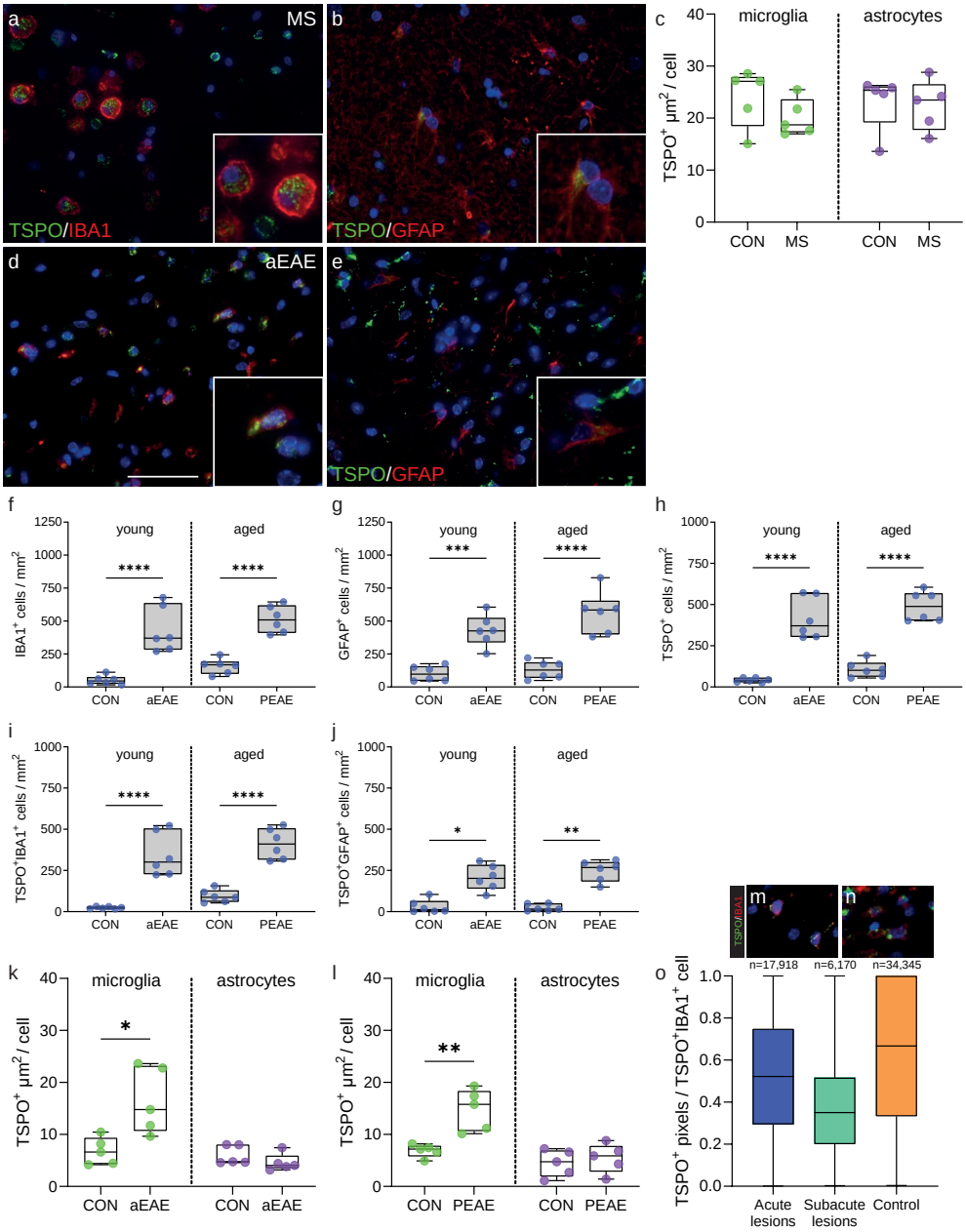

Figure 6. Microglia in mouse aEAE and PEAE, and marmoset EAE, but not MS, increase TSPO expression. a,b Representative images of TSPO+ microglia and astrocytes in MS. **c** TSPO+ microglia ($P = 0.2278$, $t=1.306$, $df=8$) and astrocytes ($P = 0.5476$, $U=9$, ranks=31, 24) do not increase TSPO expression in MS. **d,e** Representative images of TSPO expression in microglia and astrocytes in EAE mice. **f-h** microglia ($P < 0.0001$, $F_{(3,20)}=25.68$), astrocyte ($P < 0.0001$, $F_{(3,20)}=25.51$), and TSPO+ cell numbers ($P < 0.0001$, $F_{(3,20)}=44.53$), are increased during disease in aEAE mice and PEAE. **i,j** An increase in both TSPO+ microglia ($P < 0.0001$, $F_{(3,20)}=30.93$) and TSPO+ astrocytes ($P = 0.0005$, K-W=17.72) is observed during disease. **k,l** TSPO+ microglia increase TSPO expression in aEAE mice ($P = 0.0136$, $t=3.152$, $df=8$), and in PEAE mice ($P = 0.0028$, $t=4.248$, $df=8$). Astrocytes do not increase TSPO expression in aEAE ($P = 0.0556$, $U=3$, ranks=37, 18), and PEAE ($P = 0.5918$, $t=0.5584$, $df=8$). **m,n** Representative images of TSPO+ microglia in marmoset

EAE. **o** TSPO+ pixels are not increased in acute and subacute lesions in marmoset EAE relative to control. Statistical significance in **f-j,o** was determined by a one way ANOVA or Kruskal-Wallis test when not normally distributed, and by a two-tailed unpaired *t*-test or Mann-Whitney U-test when not normally distributed in **c,k** and **l**. Holm-Sidak's and Dunn's multiple comparisons were performed. Box and whiskers mark the 25th to 75th percentiles and min to max values, respectively, with the median indicated. Scale bar = 50μm, inserts are digitally zoomed in (200%).

In summary, and consistent with the AD and ALS data, we have shown that individual cellular TSPO expression is increased in microglia in EAE in both young and aged mouse models, but it is not increased in microglia from MS lesions nor marmoset EAE acute lesions. Again, consistent with previous data, astrocytes did not show an increase in TSPO expression in either MS or EAE.

Single cell RNAseq shows *TSPO* gene expression is upregulated in activated mouse microglia, but not in activated human microglia

Methods for protein quantification by immunohistochemistry in *postmortem* brain are semiquantitative and therefore we also assessed *ex vivo* species-specific TSPO gene expression of microglial under pro-inflammatory conditions to add further confidence to our findings. We employed publicly available human and mouse scRNAseq datasets[37-42]. We first examined evidence for a pro-inflammatory microglial phenotype by quantifying the differential expression of homeostatic and/or activation markers. We then quantified the differential expression of TSPO in pro-inflammatory activated microglia using MAST[47].

In a model of LPS exposure in the mouse[40], scRNAseq yielded 2019 microglial cells that showed evidence of pro-inflammatory activation including a downregulation of the homeostatic marker *P2ry12* and an upregulation of activation markers *Fth1* and *Cd74* (Fig. 7a). In this population, *TSPO* was significantly upregulated. In a mouse model of acute EAE[42], scRNAseq yielded 8470 pro-inflammatory activated microglial cells that showed significant downregulation of *P2ry12*, and a significant upregulation of *Fth1* and *Cd74* (Fig. 7b). *TSPO* was significantly upregulated. Finally, in the 5XFAD mouse model of AD[41], scRNAseq yielded over 6203 microglial cells. Among them, 223 showed enrichment in disease-associated microglia (DAM) markers[41], including increased expression of *Apoe*, *Trem2*, *Tyrobp* and *Cst7* (Fig. 7c). Compared to non-DAM cells, DAM cells showed a significant upregulation of *TSPO*.

In cerebrospinal fluid (CSF)-derived cells isolated from people with AD[37], microglia-like cells (n=522) had an activated phenotype with a significant upregulation of *APOE*, *FTH1* and *SPI1* relative to controls. However, *TSPO* was not differentially expressed (Fig. 7d). In CSF isolated from people with MS[38], microglia-like cells (n=1650) showed evidence of activation: *TREM2, C1QA, C1QB, SPI1, and HLA-DQA1* all were significantly upregulated[38]. However, TSPO was not differentially expressed in these cells (Fig. 7e). In a similarly designed study also using CSF-derived cells, microglia showing upregulation of *HLA-DRB1, HLA-DRB5* and *SPI1* also downregulated TSPO[39] (Fig. 7f).

These experiments are consistent at the gene expression level with our own data at the protein expression level showing that the *TSPO* gene is not increased in microglia in AD or EAE, but is increased in their respective commonly used mouse models.

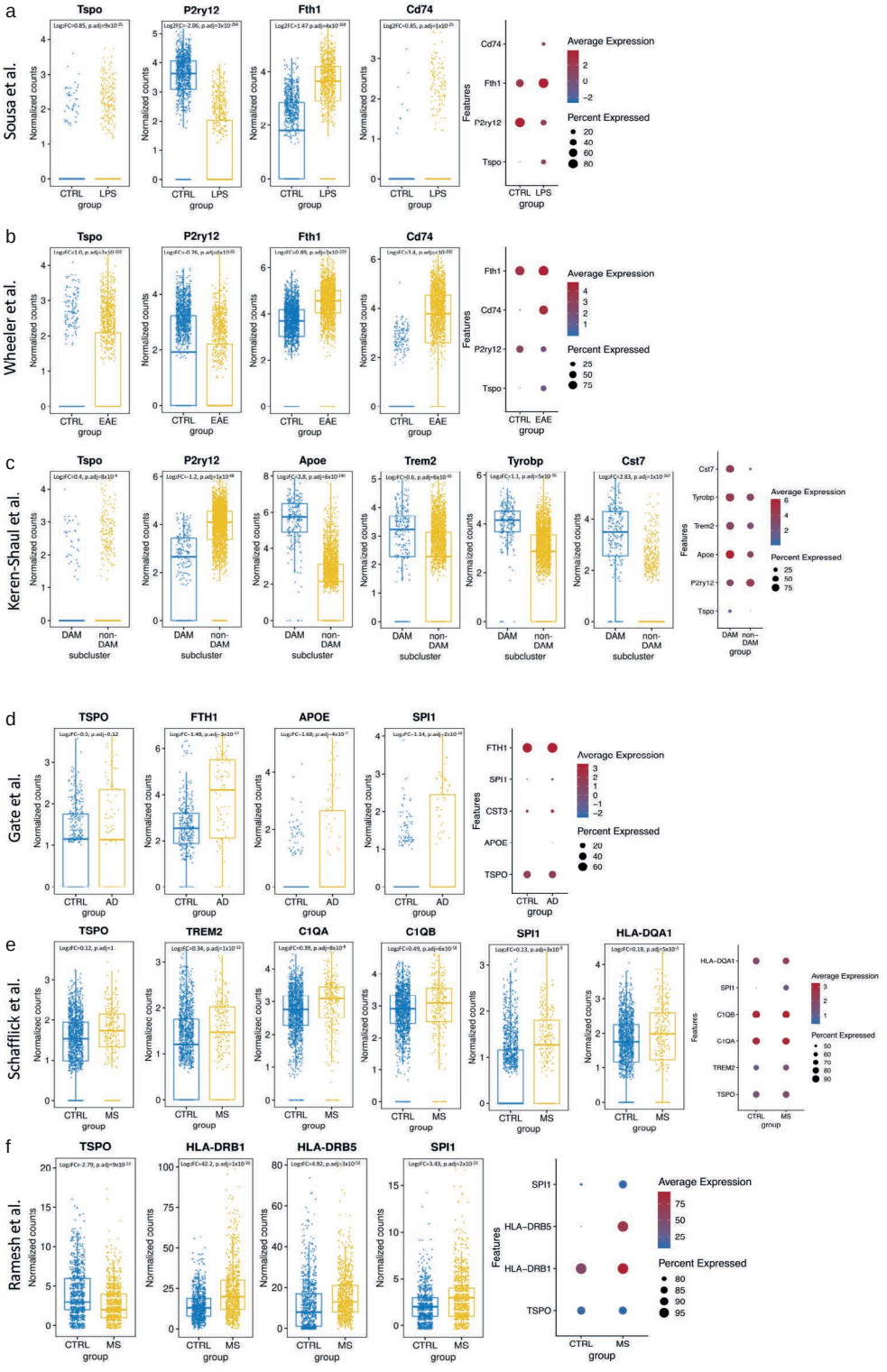
a
Sousa et al.
Tspo
P2ry12
Fth1
Cd74
Normalized counts
CTRL
LPS
group
Features
Average Expression
Percent Expressed
b
Wheeler et al.
CTRL
EAE
c
Keren-Shaul et al.
Apoe
Trem2
Tyrobp
Cst7
DAM
non-DAM
subcluster
d
Gate et al.
TSPO
FTH1
APOE
SPI1
AD
e
Schafflick et al.
TREM2
C1QA
C1QB
HLA-DQA1
MS
f
Ramesh et al.
HLA-DRB1
HLA-DRB5

Figure 7. TSPO is increased in mouse but not human pro-inflammatory activated and disease-associated microglia. **a-c** Boxplots and dotplots showing the significantly elevated expression of *Tspo* in mouse models of pro-inflammatory activation using LPS (GSE115571), of acute EAE (GSE130119) and of AD (GSE98969). The percentage of cells that express *Tspo* in mouse microglia is relatively low, but it is considerably increased after LPS treatment, in the EAE model and in the DAM cells. **d-f** TSPO is not significantly upregulated in microglia-like cells from the CSF of AD (GSE134578) and MS (GSE138266) patients. The percentage of cells that express a given gene corresponds to the size of the dot, whereas the average expression corresponds to the fill colour of the dot.

TSPO is mechanistically linked to classical pro-inflammatory myeloid cell function in mice but not humans.

Having demonstrated species-specific differences in TSPO expression and regulation, we then sought to examine TSPO function in mouse and human myeloid cells. We first examined the effect of pharmacological modulation of the classical microglial pro-inflammatory phenotype using the high affinity TSPO ligand, XBD173. Consistent with the literature[11-13], we found that in primary mouse macrophages and the BV2 mouse microglial cell line, XBD173 reduced LPS induced release of proinflammatory cytokines (Fig. 8a,b,c). However, in primary human macrophages and in human induced pluripotent stem cell (hIPSC) derived microglia, XBD173 had no impact on the release of these cytokines, even at high concentrations associated with 98% TSPO binding site occupancy (Fig. 8d,e,f,g). We found similar results for zymosan phagocytosis. Primary mouse microglia demonstrated a dose dependant increase in phagocytosis upon exposure to XBD173 (Fig. 8h). However, we saw no increase in phagocytosis in primary human macrophages upon XBD173 exposure (Fig. 8i).

XBD173 is metabolised by CYP3A4, which is expressed in myeloid cells. We therefore used LC-MSMS to quantify XBD173 in the supernatant in order to test the hypothesis that the lack of drug effect on human myeloid cells was due to depletion of XBD173. The measured concentration of XBD173 in the supernatant at the end of the assay was no different to the planned concentration (Fig. S5), excluding the possibility that XBD173 metabolism explained the lack of effect.

To understand if TSPO is associated with divergent functional modules in mouse and human we then used weighted gene co-expression network analysis to examine the genes whose expression are correlated with *TSPO* in mouse and human myeloid cells. To construct the gene co-expression networks, we used four publicly available and one in-house RNA-seq data from human (n = 47) and five publicly available mouse (n = 35) datasets of myeloid cells treated with LPS or LPS and IFNγ. In mouse myeloid cells, the gene ontology biological processes associated with the TSPO network related to classical pro-inflammatory functions such as responses to type 1 and 2 interferons, viruses and regulation of cytokine production (Fig. 8j, Supplementary File 1). However, in human myeloid cells, the processes associated with the TSPO co-expression network related to bioenergetic functions such as ATP hydrolysis, respiratory chain complex assembly, and proton transport (Fig. 8k, Supplementary File 1). In mouse myeloid cells there was no overlap in the genes that TSPO is co-expressed with, relative to human (Fig. 8l).

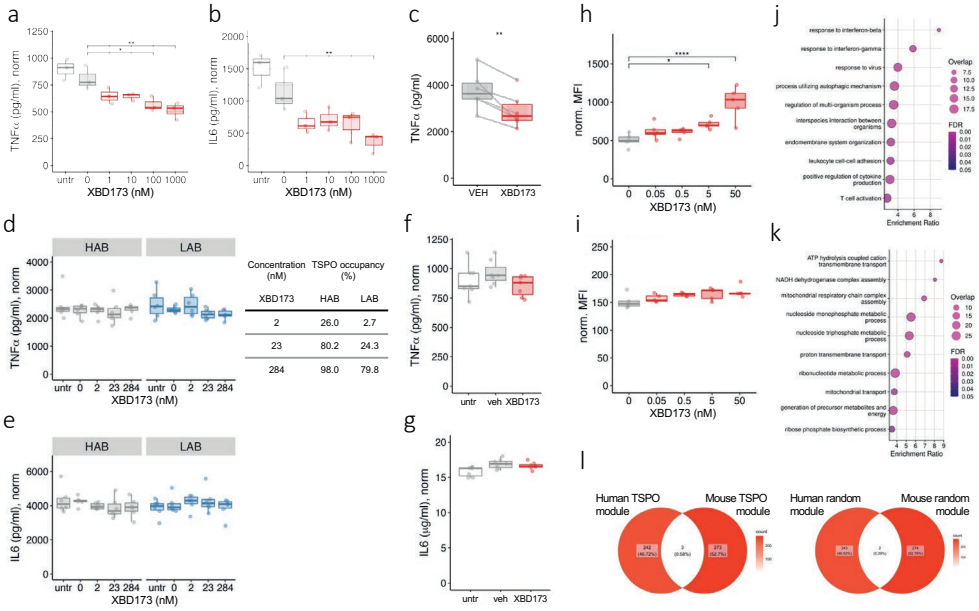

Figure 8. TSPO ligand XBD-173 modulates classical pro-inflammatory myeloid cell function in mouse but not human myeloid cells. a-c The specific TSPO ligand XBD-173 reduces LPS-induced cytokine secretion in mouse BV2 microglia (**a,b**) and primary bone-marrow derived macrophages (**c**; BMDM, XBD = 10nM). (**a** P = 0.0007, F = 9.646, df = 5, n = 3, padj(100) = 0.014, padj(1000) = 0.003; **b** P = 0.0008, F = 9.282, df = 5, n = 3, padj(1000) = 0.006; **c** P = 0.005, n = 6). **d-g** XBD-173 does not reduce LPS-induced cytokine secretion by human primary monocyte-derived macrophages derived from rs6971 AA individuals (high affinity binders, HAB), rs6971 TT individuals (low affinity binders, LAB) (**d,e**) or by hiPSC derived microglia-like cells (**f,g**) (**d** HAB: P = 0.8333, K-W = 1.4624, df = 4, n = 6; LAB: P = 0.141, K-W = 5.8624, df = 4, n = 6; **e** HAB: P = 0.09999, K-W = 7.7796, df = 4, n = 6, LAB: P = 0.2097, F = 0.68, df = 4, n = 6; **f** P = 0.057, n = 7, XBD = 200nM; g P = 0.423, n = 7, XBD = 200nM). **h,i** XBD-173 enhances phagocytosis in mouse BMDM (**h**) but not human monocytes (**i**) (**h** P < 0.0001, F = 12.07, df = 4, n = 5; **i** P = 0.1728, K-W = 6.376, df = 4, n = 5). **j-k** TSPO gene co-expression modules from naïve and pro-inflammatory primary macrophages in mouse and human. Gene ontology biological processes for the mouse TSPO module is enriched in classical proinflammatory pathways (**j**) and the human TSPO module is enriched for bioenergetic pathways (**k**). 3 genes overlap between mouse and human TSPO modules (**l**, left panel), compared to 2 genes overlapping between human and mouse random modules of the same size (**l**, right panel). Statistical significance in **a,b,d,e** and **i,j** was determined by one way ANOVA or Kruskal-Wallis test when not normally distributed and by a two-tailed unpaired t-test or Mann-Whitney U-test when not normally distributed in **c,f** and **g**. Box and whiskers mark the 25th to 75th percentiles and min to max values, respectively, with the median indicated.

Discussion

Microglial activation accompanies and is a major contributor to neurodegenerative and neuroinflammatory diseases[1,4-6,76]. A better understanding of microglial activation in combination with a technique that could reliably quantify activated microglia in the human brain would have broad utility to monitor disease progression as well as response to therapy. TSPO PET has been applied by many with this objective[9,10]. Here we have tested the widely held assumption that *TSPO* cellular expression increases upon microglial activation. We examined *in vitro* data from isolated myeloid cells across 6 species, multiple sequence alignment of the TSPO promoter region across 34 species, and *ex vivo* neuropathological and scRNAseq data from human neuroinflammatory and neurodegenerative diseases, with relevant marmoset and young and aged mouse models. We show that TSPO expression increases in mouse and rat microglia when they are activated by a range of stimuli, but that this phenomenon is

unique to microglia from a subset of species from the *Muroidea* superfamily of rodents. The increase in TSPO expression is likely dependant on the AP1 binding site in the core promoter region of TSPO. Finally, we showed that TSPO is mechanistically linked to classical pro-inflammatory myeloid cell function in mice but not humans.

This finding fundamentally alters the way in which the TSPO PET signal is interpreted, because it implies that the microglial component of the TSPO PET signal reflects density only, rather than a composite of density and activation phenotype. For example, in Parkinson's Disease (PD) there is evidence of activated microglia in the *postmortem* brain but minimal change in microglial density[77]. Three well designed studies using modern TSPO radiotracers found no difference in TSPO signal between PD and controls groups[78-80]. The lack of increase in the TSPO PET signal is consistent with the data presented here, and should therefore not be interpreted as evidence for lack of microglial activation in PD.

Our study has several limitations. First, we have only examined microglia under certain pro-inflammatory conditions and cannot exclude the possibility that other stimulation paradigms would increase TSPO in human myeloid cells. However, the *in vitro* stimuli which were examined included a broad range of pro-inflammatory triggers, and the three human diseases are diverse with respect to the mechanisms underlying the activation of microglia. Second, the measurements of cellular TSPO expression we used in brain tissue are semi-quantitative. However, the same IHC quantification methods were used in all human and mouse comparisons, and these methods consistently detected cellular TSPO increases in mouse microglia despite not detecting analogous changes in human microglia. Furthermore, where IMC and immunofluorescence were used, the quantitative data were consistent with IHC. The neuropathology protein quantification was also consistent with gene expression measured by scRNAseq. Third, for RNAseq analysis, we were restricted to single cell rather than single nucleus experiments. This is because *TSPO* is detected in only 5-12% of microglial nuclei[36,81-83] but ~80% of microglial cells[37-42]. Fourth, the *in vitro* assay which most closely mimics *in vivo* PET data is radioligand binding, which quantifies the binding of the radioligand to the binding site itself. Here, we quantified expression of the TSPO gene or protein rather than radioligand binding site density. However, we have previously shown that for TSPO, gene expression, protein expression and radioligand binding site data closely correlate[15]. Finally, whilst we present data correlating inducible TSPO expression with the presence of the AP1 binding site in the TSPO core promoter region, to demonstrate causation the AP1 binding site would need to be knocked out from the mouse or rat, and knocked in to a non-*Muroidea* rodent. Furthermore, although we were able to find array expression data for a range of non-rodent mammals that show TSPO is not induced upon myeloid cell activation, we were unable to find array expression data for those rodents that lack the AP1 binding site, such as squirrel or naked mole rat.

In summary, we present *in vitro* expression and sequence alignment data from a range of species, as well as *ex vivo* data from neurodegenerative and neuroinflammatory diseases and associated animal models. We show that inflammation-induced increases in cellular TSPO expression are restricted to microglia from a subset of species within the *Muroidea* superfamily of rodents, and that TSPO is mechanistically linked to classical pro-inflammatory myeloid cell function in mice, but not humans. This challenges the commonly held view that TSPO provides a readout of microglial activation in the human brain and shows that the TSPO PET signal likely reflects the local density of inflammatory cells irrespective of phenotype. The interpretation of TSPO PET data therefore requires revision.

References

1. Cunningham C. Microglia and neurodegeneration: the role of systemic inflammation. *Glia*. Jan 2013;61(1):71-90. doi:10.1002/glia.22350
2. Heneka MT*, et al*. Locus ceruleus controls Alzheimer's disease pathology by modulating microglial functions through norepinephrine. *Proc Natl Acad Sci U S A*. Mar 30 2010;107(13):6058-63. doi:10.1073/pnas.0909586107
3. O'Sullivan JB*, et al*. Noradrenaline reuptake inhibitors limit neuroinflammation in rat cortex following a systemic inflammatory challenge: implications for depression and neurodegeneration. *Int J Neuropsychopharmacol*. Jun 2009;12(5):687-99. doi:10.1017/S146114570800967X
4. Brown GC*, et al*. How microglia kill neurons. *Brain Res*. Dec 2 2015;1628(Pt B):288-297. doi:10.1016/j.brainres.2015.08.031
5. Brown GC*, et al*. Inflammatory neurodegeneration and mechanisms of microglial killing of neurons. *Mol Neurobiol*. Jun 2010;41(2-3):242-7. doi:10.1007/s12035-010-8105-9
6. Brown GC*, et al*. Microglial phagocytosis of live neurons. *Nat Rev Neurosci*. Apr 2014;15(4):209-16. doi:10.1038/nrn3710
7. Guilarte TR. TSPO in diverse CNS pathologies and psychiatric disease: A critical review and a way forward. *Pharmacol Ther*. Feb 2019;194:44-58. doi:10.1016/j.pharmthera.2018.09.003
8. Guilarte TR*, et al*. Imaging neuroinflammation with TSPO: A new perspective on the cellular sources and subcellular localization. *Pharmacol Ther*. Nov 27 2021:108048. doi:10.1016/j.pharmthera.2021.108048
9. Pascoal TA*, et al*. Microglial activation and tau propagate jointly across Braak stages. *Nat Med*. Sep 2021;27(9):1592-1599. doi:10.1038/s41591-021-01456-w
10. Jucaite A*, et al*. Effect of the myeloperoxidase inhibitor AZD3241 on microglia: a PET study in Parkinson's disease. *Brain*. Sep 2015;138(Pt 9):2687-700. doi:10.1093/brain/awv184
11. Bae KR*, et al*. Translocator protein 18 kDa negatively regulates inflammation in microglia. *J Neuroimmune Pharmacol*. Jun 2014;9(3):424-37. doi:10.1007/s11481-014-9540-6
12. Wang M*, et al*. Macroglia-microglia interactions via TSPO signaling regulates microglial activation in the mouse retina. *J Neurosci*. Mar 5 2014;34(10):3793-806. doi:10.1523/JNEUROSCI.3153-13.2014
13. Karlstetter M*, et al*. Translocator protein (18 kDa) (TSPO) is expressed in reactive retinal microglia and modulates microglial inflammation and phagocytosis. *J Neuroinflammation*. Jan 8 2014;11:3. doi:10.1186/1742-2094-11-3
14. Gottfried-Blackmore A*, et al*. Brain microglia express steroid-converting enzymes in the mouse. *J Steroid Biochem Mol Biol*. Mar 2008;109(1-2):96-107. doi:10.1016/j.jsbmb.2007.12.013
15. Owen DR*, et al*. Pro-inflammatory activation of primary microglia and macrophages increases 18 kDa translocator protein expression in rodents but not humans. *J Cereb Blood Flow Metab*. Aug 2017;37(8):2679-2690. doi:10.1177/0271678X17710182
16. Nutma E*, et al*. Activated microglia do not increase 18 kDa translocator protein (TSPO) expression in the multiple sclerosis brain. *Glia*. Oct 2021;69(10):2447-2458. doi:10.1002/glia.24052
17. Srivastava PK*, et al*. JunD/AP1 regulatory network analysis during macrophage activation in a rat model of crescentic glomerulonephritis. *BMC systems biology*. Sep 22 2013;7:93. doi:10.1186/1752-0509-7-93
18. Saito T*, et al*. Single App knock-in mouse models of Alzheimer's disease. *Nat Neurosci*. May 2014;17(5):661-3. doi:10.1038/nn.3697
19. Yoshiyama Y*, et al*. Synapse loss and microglial activation precede tangles in a P301S tauopathy mouse model. *Neuron*. Feb 1 2007;53(3):337-51. doi:10.1016/j.neuron.2007.01.010
20. Gurney ME*, et al*. Motor neuron degeneration in mice that express a human Cu,Zn superoxide dismutase mutation. *Science*. Jun 17 1994;264(5166):1772-5. doi:10.1126/science.8209258
21. Baker D*, et al*. Induction of chronic relapsing experimental allergic encephalomyelitis in Biozzi mice. *J Neuroimmunol*. Aug 1990;28(3):261-70. doi:10.1016/0165-5728(90)90019-j
22. Benjamini Y*, et al*. Controlling the False Discovery Rate- a Practical and Powerful Approach to Multiple Testing. *Journal of the Royal Statistical Society Series B-Statistical Methodology*. 1995;57(1):289-300. doi:DOI 10.1111/j.2517-6161.1995.tb02031.x
23. Schmidt SV*, et al*. The transcriptional regulator network of human inflammatory macrophages is defined by open chromatin. *Cell Res*. Feb 2016;26(2):151-70. doi:10.1038/cr.2016.1
24. Felton JM*, et al*. Epigenetic Analysis of the Chromatin Landscape Identifies a Repertoire of Murine Eosinophil-Specific PU.1-Bound Enhancers. *J Immunol*. Aug 15 2021;207(4):1044-1054. doi:10.4049/jimmunol.2000207
25. Langmead B*, et al*. Ultrafast and memory-efficient alignment of short DNA sequences to the human genome. *Genome Biol*. 2009/03/04 2009;10(3):R25. doi:10.1186/gb-2009-10-3-r25
26. Heinz S*, et al*. Simple combinations of lineage-determining transcription factors prime cis-regulatory elements required for macrophage and B cell identities. *Mol Cell*. May 28 2010;38(4):576-89. doi:10.1016/j.molcel.2010.05.004
27. Kent WJ*, et al*. The human genome browser at UCSC. *Genome Res*. Jun 2002;12(6):996-1006. doi:10.1101/gr.229102

28. Notredame C, *et al*. T-Coffee: A novel method for fast and accurate multiple sequence alignment. *J Mol Biol*. Sep 8 2000;302(1):205-17. doi:10.1006/jmbi.2000.4042
29. Erb I, *et al*. Use of ChIP-Seq data for the design of a multiple promoter-alignment method. *Nucleic Acids Res*. Apr 2012;40(7):e52. doi:10.1093/nar/gkr1292
30. Waterhouse AM, *et al*. Jalview Version 2--a multiple sequence alignment editor and analysis workbench. *Bioinformatics*. May 1 2009;25(9):1189-91. doi:10.1093/bioinformatics/btp033
31. Tamura K, *et al*. MEGA11: Molecular Evolutionary Genetics Analysis Version 11. *Mol Biol Evol*. Jun 25 2021;38(7):3022-3027. doi:10.1093/molbev/msab120
32. Bailey TL, *et al*. The MEME Suite. *Nucleic Acids Res*. Jul 1 2015;43(W1):W39-49. doi:10.1093/nar/gkv416
33. Bailey TL, *et al*. SEA: Simple Enrichment Analysis of motifs. *bioRxiv*. 2021;
34. Love MI, *et al*. Moderated estimation of fold change and dispersion for RNA-seq data with DESeq2. *Genome Biol*. 2014;15(12):550. doi:10.1186/s13059-014-0550-8
35. Ostuni R, *et al*. Latent enhancers activated by stimulation in differentiated cells. *Cell*. Jan 17 2013;152(1-2):157-71. doi:10.1016/j.cell.2012.12.018
36. Smith AM, *et al*. Diverse human astrocyte and microglial transcriptional responses to Alzheimer's pathology. *Acta Neuropathol*. Jan 2022;143(1):75-91. doi:10.1007/s00401-021-02372-6
37. Gate D, *et al*. Clonally expanded CD8 T cells patrol the cerebrospinal fluid in Alzheimer's disease. *Nature*. Jan 2020;577(7790):399-404. doi:10.1038/s41586-019-1895-7
38. Schafflick D, *et al*. Integrated single cell analysis of blood and cerebrospinal fluid leukocytes in multiple sclerosis. *Nat Commun*. Jan 14 2020;11(1):247. doi:10.1038/s41467-019-14118-w
39. Ramesh A, *et al*. A pathogenic and clonally expanded B cell transcriptome in active multiple sclerosis. *Proc Natl Acad Sci U S A*. Sep 15 2020;117(37):22932-22943. doi:10.1073/pnas.2008523117
40. Sousa C, *et al*. Single-cell transcriptomics reveals distinct inflammation-induced microglia signatures. *EMBO Rep*. Nov 2018;19(11):e46171. doi:10.15252/embr.201846171
41. Keren-Shaul H, *et al*. A Unique Microglia Type Associated with Restricting Development of Alzheimer's Disease. *Cell*. Jun 15 2017;169(7):1276-1290 e17. doi:10.1016/j.cell.2017.05.018
42. Wheeler MA, *et al*. MAFG-driven astrocytes promote CNS inflammation. *Nature*. Feb 2020;578(7796):593-599. doi:10.1038/s41586-020-1999-0
43. Duan L, *et al*. PDGFRbeta Cells Rapidly Relay Inflammatory Signal from the Circulatory System to Neurons via Chemokine CCL2. *Neuron*. Oct 10 2018;100(1):183-200 e8. doi:10.1016/j.neuron.2018.08.030
44. Stuart T, *et al*. Comprehensive Integration of Single-Cell Data. *Cell*. Jun 13 2019;177(7):1888-1902 e21. doi:10.1016/j.cell.2019.05.031
45. Khozoie C, *et al*. scFlow: A Scalable and Reproducible Analysis Pipeline for Single-Cell RNA Sequencing Data. Authorea Preprints; 2021.
46. Tsartsalis S, *et al*. Single nuclear transcriptional signatures of dysfunctional brain vascular homeostasis in Alzheimer's disease. 2021;
47. Finak G, *et al*. MAST: a flexible statistical framework for assessing transcriptional changes and characterizing heterogeneity in single-cell RNA sequencing data. *Genome Biol*. Dec 10 2015;16(1):278. doi:10.1186/s13059-015-0844-5
48. Ewels PA, *et al*. The nf-core framework for community-curated bioinformatics pipelines. *Nat Biotechnol*. Mar 2020;38(3):276-278. doi:10.1038/s41587-020-0439-x
49. Langfelder P, *et al*. WGCNA: an R package for weighted correlation network analysis. *BMC Bioinformatics*. Dec 29 2008;9(1):559. doi:10.1186/1471-2105-9-559
50. Zhang B, *et al*. WebGestalt: an integrated system for exploring gene sets in various biological contexts. *Nucleic Acids Res*. Jul 1 2005;33(Web Server issue):W741-8. doi:10.1093/nar/gki475
51. Al-Izki S, *et al*. Practical guide to the induction of relapsing progressive experimental autoimmune encephalomyelitis in the Biozzi ABH mouse. *Mult Scler Relat Disord*. Jan 2012;1(1):29-38. doi:10.1016/j.msard.2011.09.001
52. Peferoen LA, *et al*. Ageing and recurrent episodes of neuroinflammation promote progressive experimental autoimmune encephalomyelitis in Biozzi ABH mice. *Immunology*. Oct 2016;149(2):146-56. doi:10.1111/imm.12644
53. Baker D, *et al*. Publication guidelines for refereeing and reporting on animal use in experimental autoimmune encephalomyelitis. *J Neuroimmunol*. Jan 18 2012;242(1-2):78-83. doi:10.1016/j.jneuroim.2011.11.003
54. Maggi P, *et al*. Magnetic resonance imaging of experimental autoimmune encephalomyelitis in the common marmoset. *J Neuroimmunol*. Mar 15 2017;304:86-92. doi:10.1016/j.jneuroim.2016.09.016
55. Nardo G, *et al*. Transcriptomic indices of fast and slow disease progression in two mouse models of amyotrophic lateral sclerosis. *Brain*. Nov 2013;136(Pt 11):3305-32. doi:10.1093/brain/awt250
56. Nardo G, *et al*. Immune response in peripheral axons delays disease progression in SOD1(G93A) mice. *J Neuroinflammation*. Oct 7 2016;13(1):261. doi:10.1186/s12974-016-0732-2
57. Hampton DW, *et al*. HspB5 Activates a Neuropro-

tective Glial Cell Response in Experimental Tauopathy. *Front Neurosci*. 2020;14:574. doi:10.3389/fnins.2020.00574
58. Hampton DW*, et al*. Cell-mediated neuroprotection in a mouse model of human tauopathy. *J Neurosci*. Jul 28 2010;30(30):9973-83. doi:10.1523/JNEUROSCI.0834-10.2010
59. Torvell M*, et al*. A single systemic inflammatory insult causes acute motor deficits and accelerates disease progression in a mouse model of human tauopathy. *Alzheimers Dement (N Y)*. 2019/01/01/ 2019;5:579-591. doi:10.1016/j.trci.2019.09.001
60. Haenseler W*, et al*. Excess alpha-synuclein compromises phagocytosis in iPSC-derived macrophages. *Sci Rep*. Aug 21 2017;7(1):9003. doi:10.1038/s41598-017-09362-3
61. Haenseler W*, et al*. A Highly Efficient Human Pluripotent Stem Cell Microglia Model Displays a Neuronal-Co-culture-Specific Expression Profile and Inflammatory Response. *Stem Cell Reports*. Jun 6 2017;8(6):1727-1742. doi:10.1016/j.stemcr.2017.05.017
62. Shlyueva D*, et al*. Transcriptional enhancers: from properties to genome-wide predictions. *Nat Rev Genet*. Apr 2014;15(4):272-86. doi:10.1038/nrg3682
63. Celada A*, et al*. The transcription factor PU.1 is involved in macrophage proliferation. *J Exp Med*. Jul 1 1996;184(1):61-9. doi:10.1084/jem.184.1.61
64. Ghisletti S*, et al*. Identification and characterization of enhancers controlling the inflammatory gene expression program in macrophages. *Immunity*. Mar 26 2010;32(3):317-28. doi:10.1016/j.immuni.2010.02.008
65. Rashid K*, et al*. Transcriptional regulation of Translocator protein (18kDa) (TSPO) in microglia requires Pu.1, Ap1 and Sp factors. *Biochim Biophys Acta Gene Regul Mech*. Dec 2018;1861(12):1119-1133. doi:10.1016/j.bbagrm.2018.10.018
66. Lane CA*, et al*. Alzheimer's disease. *Eur J Neurol*. Jan 2018;25(1):59-70. doi:10.1111/ene.13439
67. Tiwari S*, et al*. Alzheimer's disease: pathogenesis, diagnostics, and therapeutics. *Int J Nanomedicine*. 2019;14:5541-5554. doi:10.2147/IJN.S200490
68. Kellner A*, et al*. Autoantibodies against beta-amyloid are common in Alzheimer's disease and help control plaque burden. *Ann Neurol*. Jan 2009;65(1):24-31. doi:10.1002/ana.21475
69. Hansen DV*, et al*. Microglia in Alzheimer's disease. *J Cell Biol*. Feb 5 2018;217(2):459-472. doi:10.1083/jcb.201709069
70. Xuan FL*, et al*. Differences of Microglia in the Brain and the Spinal Cord. *Front Cell Neurosci*. 2019;13:504. doi:10.3389/fncel.2019.00504
71. Nutma E*, et al*. A quantitative neuropathological assessment of translocator protein expression in multiple sclerosis. *Brain*. Nov 1 2019;142(11):3440-3455. doi:10.1093/brain/awz287
72. Tuisku J*, et al*. Effects of age, BMI and sex on the glial cell marker TSPO - a multicentre [(11)C]PBR28 HRRT PET study. *Eur J Nucl Med Mol Imaging*. Oct 2019;46(11):2329-2338. doi:10.1007/s00259-019-04403-7
73. Gaitan MI*, et al*. Perivenular brain lesions in a primate multiple sclerosis model at 7-tesla magnetic resonance imaging. *Mult Scler*. Jan 2014;20(1):64-71. doi:10.1177/1352458513492244
74. t Hart BA*, et al*. Non-invasive measurement of brain damage in a primate model of multiple sclerosis. *Trends Mol Med*. Feb 2004;10(2):85-91. doi:10.1016/j.molmed.2003.12.008
75. Lefeuvre JA*, et al*. The spectrum of spinal cord lesions in a primate model of multiple sclerosis. *Mult Scler*. Mar 2020;26(3):284-293. doi:10.1177/1352458518822408
76. Stephenson J*, et al*. Inflammation in CNS neurodegenerative diseases. *Immunology*. Jun 2018;154(2):204-219. doi:10.1111/imm.12922
77. Doorn KJ*, et al*. Microglial phenotypes and toll-like receptor 2 in the substantia nigra and hippocampus of incidental Lewy body disease cases and Parkinson's disease patients. *Acta Neuropathol Commun*. Aug 7 2014;2:90. doi:10.1186/s40478-014-0090-1
78. Ghadery C*, et al*. Microglial activation in Parkinson's disease using [(18)F]-FEPPA. *J Neuroinflammation*. Jan 11 2017;14(1):8. doi:10.1186/s12974-016-0778-1
79. Koshimori Y*, et al*. Imaging Striatal Microglial Activation in Patients with Parkinson's Disease. *PLOS ONE*. 2015;10(9):e0138721. doi:10.1371/journal.pone.0138721
80. Varnäs K*, et al*. PET imaging of [11C] PBR28 in Parkinson's disease patients does not indicate increased binding to TSPO despite reduced dopamine transporter binding. *Eur J Nucl Med Mol Imaging*. 2019;46(2):367-375.
81. Mathys H*, et al*. Author Correction: Single-cell transcriptomic analysis of Alzheimer's disease. *Nature*. Jul 2019;571(7763):E1. doi:10.1038/s41586-019-1329-6
82. Grubman A*, et al*. A single-cell atlas of entorhinal cortex from individuals with Alzheimer's disease reveals cell-type-specific gene expression regulation. *Nat Neurosci*. Dec 2019;22(12):2087-2097. doi:10.1038/s41593-019-0539-4
83. Zhou Y*, et al*. Human and mouse single-nucleus transcriptomics reveal TREM2-dependent and TREM2-independent cellular responses in Alzheimer's disease. *Nat Med*. Jan 2020;26(1):131-142. doi:10.1038/s41591-019-0695-9

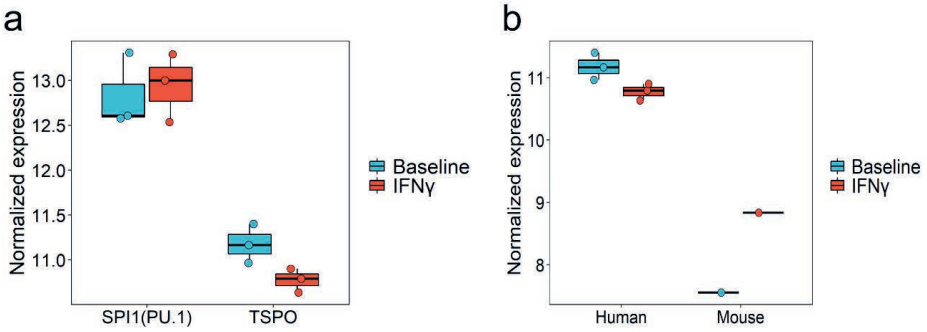

Figure S1. a Boxplot showing TSPO fold change in human and mouse macrophages in baseline and IFNγ treated samples. **b** Boxplot showing PU.1 (SPI1) transcription factor and TSPO gene expression change in IFNγ treated macrophage compared to baseline condition.

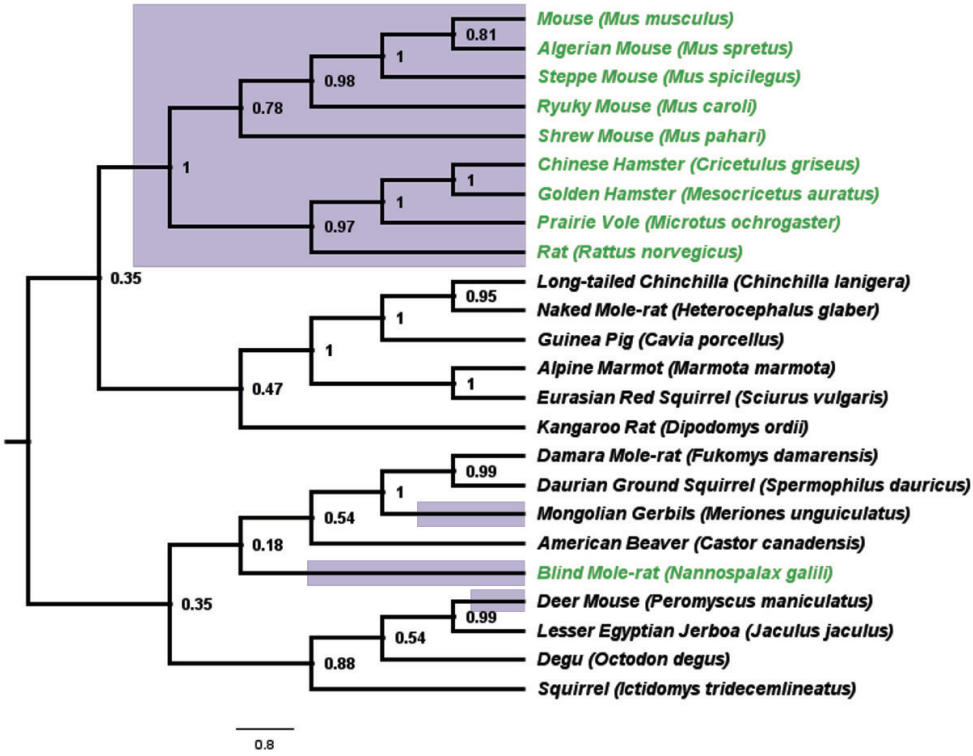

Figure S2. Of the 24 rodent species examined here, 12/24 are from the Muroidea superfamily (purple branches). 10 of these 12 Muroidea species contain the AP1 binding site in the TSPO promoter (green highlight). We did not find any rodent species outside the Muroidea superfamily that contain the AP1 binding site in the TSPO promoter. The phylogenetic analysis shows that majority of the species (9/12) from Muroidea superfamily forms a single clade. Phylogenetic tree was generated using the Maximum Parsimony method in MEGA11. The consistency index (CI) is 0.623399 (0.553120) and the retention index (RI) is 0.525671 (0.525671) for all sites and parsimony-informative sites (in parentheses). The percentage of replicate trees in which the associated taxa clustered together in the bootstrap test (1000 replicates) are shown next to the branches.

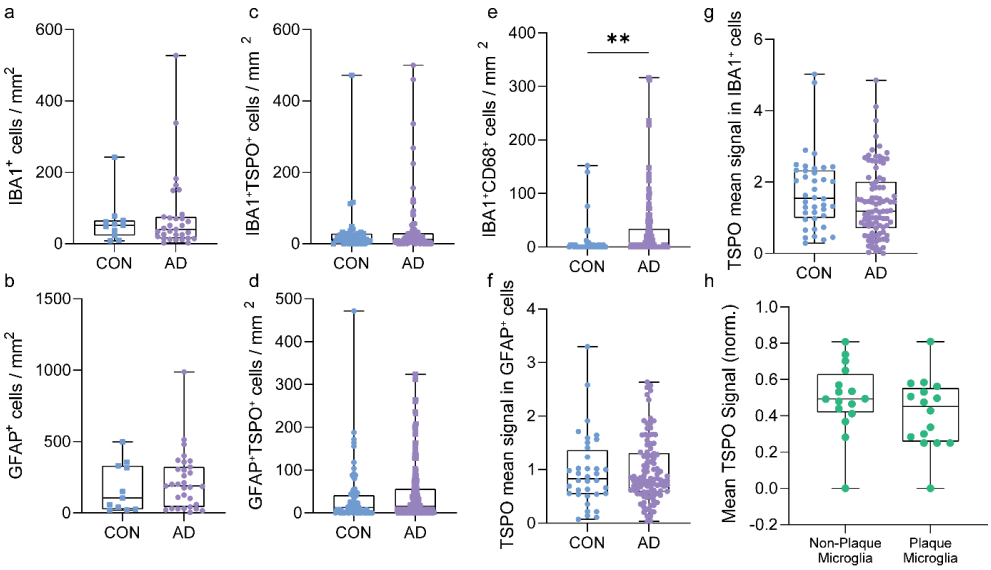

Figure S3. a-d No increase in total or TSPO+ microglia and astrocytes are observed in control versus AD. **e** An increase in CD68+IBA1+ cells is observed in AD. **f,g** No increases in mean TSPO signal in microglia and astrocytes is observed in AD relative to control. **h** No differences are observed in mean TSPO signal in microglia associated with plaques compared to mean TSPO signal in microglia that are distant from plaques.

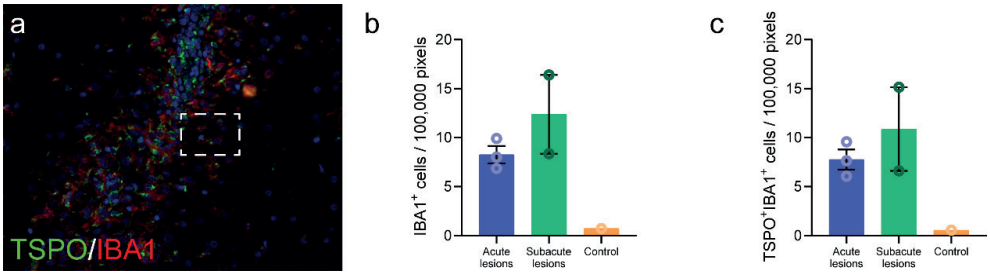

Figure S4. a Representative image of an acute lesion in marmoset EAE. **b,c** IBA1+ and TSPO+IBA1+ cells are increased in acute and subacute lesions compared to white matter in control marmoset.

Planned Concentration (nM)	Measured Concentration (nM)
XDB173	XDB173
Cell supernatant 1.78nM XBD	2.0
Cell supernatant 1.78nM XBD	1.9
Cell supernatant 22.5nM XBD	21.8
Cell supernatant 22.5nM XBD	20.6
Cell supernatant 284nM XBD	290.6
Cell supernatant 284nM XBD	318.8

Figure S5. Planned and measured concentrations of XBD173 in medium for experiments described in Figures 8d and 8e.

Table S1. Clinical details of AD and control cases

Case	Age/sex	Diagnosis	Region	Braak stage	PMD, h:min
AD cases					
1	81/F	AD	HC (anterior)	6	05:30
2	88/F	AD	HC (anterior)	6	06:19
3	62/M	AD	HC (anterior)	6	06:15
4	64/F	AD	HC (anterior)	6	06:30
5	76/M	AD	HC (anterior)	6	04:40
Controls					
1	65/F	NDC	HC	2	07:10
2	90/F	NDC	HC	3	06:10
3	81/F	NDC	HC	3	05:30
4	77/M	NDC	HC (anterior)	2	04:30
5	81/F	Ischemic changes	HC (anterior)	4	05:50

Abbreviations: F – female; HC – hippocampus; M – male; NDC – non-demented control; PMD – postmortem delay.

Table S2. Clinical details of ALS and control cases

Case	Age/ sex	Diagnosis	DD, months	Cause of death	PMD, h	Primary onset	SPC levels
ALS short disease duration							
1	70/F	sALS	6	respiratory failure	< 12	leg	C/T/L
2	63/M	sALS	7	respiratory failure	< 12	leg	C/T/L
3	61/F	sALS	12	euthanasia	< 12	arm	C/T/L
4	60/M	sALS	12	euthanasia	< 12	arm	C/T/L
5	81/M	sALS	12	respiratory failure	< 12	respiratory	T/L
6	84/F	sALS	13	euthanasia	< 12	bulbar	C/T
7	56/F	sALS	16	euthanasia	< 12	leg	C/T/L
ALS medium disease duration							
8	43/M	sALS	36	unknown	< 12	arm	C/T/L
9	64/F	fALS	57	pneumonia	< 12	leg	C/T/L
10	68/M	sALS	87	euthanasia	< 12	arm	C/T/L
11	79/M	sALS (C9orf72)	107	pneumonia	< 12	arm	C/T/L
Controls							
12	60/M	bricker-bladder	N/A	lung embolism	< 24	N/A	C/T/L
13	63/M	kidney carcinoma	N/A	lung embolism	< 24	N/A	C/T/L
14	81/F	heart ischemia	N/A	endocarditis	< 24	N/A	C/T/L
15	63/F	adeno-carcinoma	N/A	paralytic ileus	< 24	N/A	C/T/L
16	69/M	oesophagus carcinoma	N/A	multi-organ failure	< 24	N/A	C/T/L
17	78/F	cholangio-carcinoma	N/A	multi-organ failure	< 24	N/A	T
18	75/M	COPD, pneumonia	N/A	respiratory failure	< 12	N/A	C/T
19	59/F	pleuritis carcinomatosa	N/A	respiratory failure	< 24	N/A	C/T/L
20	47/F	pancreas carcinoma	N/A	abdominal bleeding	< 24	N/A	C/T/L
21	54/F	gallbladder carcinoma	N/A	heart failure	< 48	N/A	C/T/L

Abbreviations: C – cervical; COPD – chronic obstructive pulmonary disease; DD – disease duration; F – female; fALS – familial ALS; L – lumbar; M – male; PMD – postmortem delay; S – sacral; sALS – sporadic ALS; SPC – spinal cord; T – thoracic.

Table S3. Clinical details of MS and control cases

Case	Age/sex	Diagnosis	Disease duration, years	Cause of death	PMD, h:min
MS cases					
1	35/F	SPMS	10	Euthanasia	10:20
2	54/F	SPMS	27	Respiratory failure	9:25
3	50/F	SPMS	18	Euthanasia	9:05
4	50/M	SPMS	21	Unknown	10:50
5	63/F	Unknown	Unknown	Unknown	10:50
Controls					
1	84/M	NNC	N/A	Heart failure	5:35
2	89/F	NNC	N/A	Pneumonia	3:52
3	79/M	NNC	N/A	Heart failure	6:20
4	73/F	NNC	N/A	Mamma carcinoma	7:45
5	87/F	NNC	N/A	Pneumonia	7:00

Abbreviations: F – female; M – male; N/A – not applicable; NNC – non-neurological control; PMD – postmortem delay; SPMS – secondary progressive multiple sclerosis.

Table S4. Clinical history of mice with EAE

Mouse number	Sampling day (EAE score)	Age (weeks)
Acute young (aEAE)		
1	14 (4)	10-15
2	12 (4)	10-15
3	15 (4.5)	10-15
4	15 (4)	10-15
5	13 (4.5)	10-15
6	20 (4.5)	10-15
Acute old (PEAE)		
1	15 (4.5)	> 50
2	13 (5)	> 50
3	13 (4.5)	> 50
4	16 (4.5)	> 50
5	15 (5)	> 50
6	17 (4.5)	> 50

EAE mice were immunized with SCH in CFA and monitored (sampling day refers to the day of euthanasia after immunization). Indicated clinical scores are the maximal scores during neurological episodes of EAE. Abbreviations: CFA – complete Freund's adjuvant; EAE – experimental autoimmune encephalomyelitis; aEAE – acute EAE, PEAE – progressive EAE; SCH – spinal cord homogenate.

Table S5. Clinical history of marmosets

Animal ID	Sex	Disease Status	Age at EAE induction (years)	Disease duration (days)	Age (years)
1	M	Control	N/A	N/A	3
4	F	EAE	2.0	32	2.1
5	F	EAE	1.6	105	1.9
8	F	EAE	1.6	123	1.9

Abbreviations: EAE – experimental autoimmune encephalitis; F – female; M – male; N/A – not applicable.

Table S6. Antibodies for immunohistochemistry and imaging mass cytometry

Antigen	Species (isotype)	Clonality	Dilution	Antigen Retrieval	Product Number	Supplier
TSPO	goat	pAb	1:750	Citrate	NB100-41398	Novus Biologicals
TSPO	rabbit	mAb	1:750	Citrate	AB109497	Abcam
IBA1	rabbit	pAb	1:10000	Tris-EDTA	019-19741	Wako
IBA1	goat	pAb	1:1000	Tris-EDTA	AB48004	Abcam
IBA1	guinea pig	pAb	1:100	Citrate	234004	Synaptic Systems
GFAP	chicken	pAb	1:500	Citrate	AB5541	Millipore
HLA-DR	mouse (IgG2B)	mAb	1:750	Citrate	14-9956-82	Invitrogen
Aβ IC16	mouse (IgG2A)	mAb	1:400	Citrate	N/A	in-house[a]
P-Tau AT8	mouse (IgG1)	mAb	1:400	Citrate	AB_223647	Invitrogen
PLP	mouse (IgG2A)	mAb	1:200	Citrate	MCA839G	Bio-Rad
IMC	**Ln-Isotope**					
CD68	159Tb		1:800	EDTA	3159035D	Fluidigm
GFAP	162Dy		1:600	EDTA	Ab218309	Abcam
HLA-DR	174Yb		1:400	EDTA	3174025D	Fluidigm
IBA1	169Tm		1:3000	EDTA	019-197471	Wako
TSPO	149Sm		1:400	EDTA	Ab213654	Abcam

[a]With permission from Carsten Korth, Heinrich Heine University, Düsseldorf, Germany. Abbreviations: CD – cluster of differentiation; GFAP – glial fibrillary acidic protein; IBA1 – ionized calcium-binding adaptor molecule 1; mAb – monoclonal antibody; pAb – polyclonal antibody; P-Tau – phosphorylated Tau (Ser202, Thr205).

Cellular sources of TSPO expression in healthy and diseased brain

Erik Nutma, Kelly Ceyzériat, Sandra Amor, Stergios Tsartsalis, Philippe Millet, David R. Owen, Vassilios Papadopoulos & Benjamin B. Tournier

European Journal of Nuclear Medicine and Molecular Imaging 2021; 49(1):146-143

Abstract

The 18 kDa translocator protein (TSPO) is a highly conserved protein located in the outer mitochondrial membrane. TSPO binding, as measured with positron emission tomography (PET), is considered an in vivo marker of neuroinflammation. Indeed, TSPO expression is altered in neurodegenerative, neuroinflammatory and neuropsychiatric diseases. In PET studies, the TSPO signal is often viewed as a marker of microglial cell activity. However, there is little evidence in support of a microglia-specific TSPO expression. This review describes the cellular sources and functions of TSPO in animal models of disease and human studies, in health and in central nervous system diseases. A discussion of methods of analysis and of quantification of TSPO is also presented. Overall, it appears that the alterations of TSPO binding, their cellular underpinnings and the functional significance of such alterations depend on many factors, notably the pathology or the animal model under study, the disease stage and the involved brain regions. Thus, further studies are needed to fully determine how changes in TSPO binding occur at the cellular level with the ultimate goal of revealing potential therapeutic pathways.

Introduction

The 18 kDa translocator protein (TSPO) is increasingly used as a marker for *in vivo* neuroinflammation with positron emission tomography (PET) in a wide variety of CNS diseases. Many of these studies reveal that TSPO PET signal is altered in neurodegenerative, neuroinflammatory and neuropsychiatric diseases when compared to healthy individuals[1]. Historically, TSPO has been viewed as a marker of microglial cell activity. Indeed, the first studies showing a correlation between the binding of one of the TSPO tracers and microglia speculated that TSPO is a marker for pathogenic microglial cells[1,2]. This idea is no longer maintained. Indeed, the presence of TSPO in other cell types, notably astrocytes and endothelial cells, has been demonstrated[3-6].

TSPO is not the only molecular target for PET imaging of neuroinflammation. Several other receptors that are expressed in brain cells and are potentially upregulated in neuroinflammation have been identified and specific radiotracers are developed to label them *in vivo*. For instance, radiotracers binding the cannabinoid receptor 2 (CB_2) receptor[7,8] and cyclooxygenase-2 (COX-2)[9,10] have been validated in preclinical models of brain disease and generally showed a robust increase in binding associated with neuroinflammation, while the first results from human PET studies are encouraging[11,12]. In addition, radiotracers binding the purinergic receptor subtype 7 (P2X7)[13-15], the sphingosine-1-phosphate receptor 1 (S1PR1)[16], reactive oxygen species[17], and the colony stimulating factor 1 receptor (CSF1R)[18] are at initial stages of preclinical validation. In light of these results, it is clear that TSPO is the most extensively studied molecular target for *in vivo* PET imaging of neuroinflammation to date.

Here we review the cellular sources and functions of TSPO in animal models and humans in health and in CNS diseases. This will contribute to a better understanding of the function of TSPO, the physiology of TSPO expression, and its functional consequences in the human body and the CNS. Furthermore, knowledge about the expression of TSPO in CNS diseases provides insight into expression patterns and its predictive potential in diagnosing CNS diseases and disease progression with TSPO PET.

TSPO functions in health

TSPO participates in many essential mitochondria-based physiological processes, including metabolism and cellular bioenergetics, mitochondrial respiration, cholesterol transport and steroidogenesis, immunomodulation, porphyrin transport, and heme biosynthesis[19-23]. It has also been suggested that TSPO may play critical roles in cell proliferation, tumorigenesis, and apoptosis[23-25]. In order to discern and evaluate the function of any protein, particularly one like TSPO that seems to be multifunctional, one must consider specific characteristics that could provide clues to the possible roles it may play. The characteristics that need to be investigated should include its: (i) tissue, cellular, and subcellular localization, (ii) characteristics and effects of endogenous and exogenous ligands, (iii) molecular structure and cellular functions, (iv) genetics and genetic models, and (v) evolution.

Tissue, cellular and subcellular localization

TSPO was first characterized for its ability to bind with specificity and high affinity various classes of chemicals such as benzodiazepines, isoquinoline carboxamides, indole acetamides, pyrazolopyrimidines, and aryloxyanilides, as well as endogenous ligands including porphyrins, the endozepine diazepam binding inhibitor[19-23,26-32]. Radioligand binding and later on

immunodetection studies revealed that the distribution pattern of TSPO between rodents and humans is similar; secretory and glandular tissues were particularly rich in TSPO. These studies also indicated that although TSPO is present in most tissues in most species at various levels of expression, it is most abundant in steroid-synthesizing adrenal and gonadal tissues. The heart and kidney express intermediate levels of TSPO, while lower levels are found in the liver and brain. Interestingly, when considering the mitochondrial content of each tissue, there is not always a clear correlation between TSPO levels and mitochondrial content. This finding suggests that tissue- and cell-specific factors regulating *TSPO* gene expression are driving TSPO content rather than factors driving mitochondria formation.

Steady-state mRNA profiling shows that *TSPO* mRNA is present in all tissues, and correlates well with reported protein expression levels[24]. Moreover, the expression patterns of mouse TSPO, were found to be well-correlated and similar to that reported for human *TSPO*[33,34].

TSPO levels were found to be elevated in cancer cell lines and numerous cancers suggesting a role for TSPO in cell proliferation and carcinogenesis[23,24,28,35-37]. Increased TSPO levels in cancer are due to gene amplification; Sp1, Sp3, and Sp4 transcription factor regulation of constitutive TSPO expression; and epigenetic modifications of the proximal promoter and first intron[24,38,39].

TSPO is an integral outer mitochondrial membrane protein spanning the membrane through its 5 α-helical domains[40-53]. While TSPO is a nuclear encoded protein, unlike most mitochondrial proteins, TSPO does not possess a mitochondrial targeting sequence, although it contains information on the C-terminus that is essential for its mitochondrial import[54]. After integration into the OMM, TSPO forms dimers and sometimes polymers[19,55,56] at the outer and inner mitochondrial membrane contact sites where it becomes part of a larger protein complex[57]. This complex includes the OMM voltage-dependent anion channel 1 (VDAC1); ATPase family AAA domain-containing protein 3 (ATAD3), a protein that spans across the mitochondrial membranes, and in steroidogenic cells; and the inner mitochondrial membrane cytochrome P450 side-chain cleavage enzyme (CYP11A1), among others[57,58]. In addition, cytosolic, endoplasmic reticulum and Golgi proteins have been shown to associate with TSPO to form functional complexes[58-60]. When assembled together, these proteins function as a signal transduction complex, or "transduceosome" mediating the transmission of information to mitochondrial TSPO.

Although 95 % of TSPO is found in the mitochondria, the protein can be found in intracellular locations other than mitochondria, such as the (peri)nuclear region and plasma membrane, likely playing different functions. Nevertheless, non-mitochondrial TSPO[42,61] has received little attention so far.

Characteristics and effects of endogenous and exogenous ligands

TSPO is involved primarily in the mitochondria of steroid synthesizing cells. Steroidogenesis in the mitochondria begins with the transport of substrate cholesterol from intracellular stores into the mitochondria. Therefore, the role or roles of TSPO in mitochondrial steroidogenesis and cholesterol transport, in particular, were investigated.

With the availability of high-affinity TSPO ligands, the function of TSPO in various tissues was explored, aiming to assess whether these ligands could affect mitochondrial function, including steroid production. Several TSPO ligands were found to affect mitochondrial

respiration[62], increase oxygen consumption[63] and ATP synthesis[64]. At the same time, detailed studies demonstrated the ability of these ligands to induce cholesterol transport into mitochondria and steroid formation in all steroidogenic cells in vitro and in vivo[55,65,66]. These studies were later extended to neurosteroid synthesizing glia cells in the brain[67-70]. TSPO ligands were also shown to affect intracellular cholesterol trafficking and lipid droplet accumulation, a function that may not be related to steroidogenesis[71,72].

However, there are ligand-specific differences as well as off-target effects. These differences may be explained by the tissue and cell-specific microenvironment and the presence of endogenous ligands, e.g. porphyrins and endozepines, in specific tissues/cells that may compete with the exogenous ligand. Moreover, the fact that TSPO exists within large protein complexes suggests that TSPO ligand selectivity may be governed by the protein-complex composition and not only by the interaction with TSPO alone[73]. In addition, it was recently shown that TSPO ligands have different occupancy times for TSPO and this affects their ability to induce steroid formation[74,75]. Concerning the off-target effects, most of the time these are linked to the use of high concentrations of TSPO ligands, thousands of time higher than the affinity of these compounds for TSPO. Indeed, lipophilic TSPO ligands used at high concentrations are likely to interact with membranes or other not yet identified targets resulting in off-target effects[65,76]. In addition, TSPO ligands were found to exert cell-type specific effects raising again the question of the role of the microenvironment, ligand residence time, and the presence of endogenous ligands[77,78].

Over the years, the effects of TSPO drug ligands with various mitochondrial activities/functions have also been shown, including changes in VDAC1, F-ATP synthase and ANT activities, modulation of reactive oxygen species (ROS) production, and calcium levels and effects on mitochondrial membrane potential and permeability transition pore (MPTP)[50,51,58,79-84]. These effects were found to be tissue- and cell-specific and sometimes ligand-specific or observed only in cell lines. However, in some cases, the effects were observed in the presence of micromolar concentrations of TSPO ligands, far beyond the affinity of the protein for the compounds. The complex formed by the mitochondrial TSPO in association with VDAC1 has been suggested to have a role in apoptosis, possibly through MPTP opening, and cholesterol transport. TSPO drug ligands have been found to exert both proliferative and anti-apoptotic effects, as well as anti-proliferative properties, acting in a biphasic manner[23,24,28,35-37,85].

Molecular structure and cellular functions

The drug ligand binding domains of TSPO have been mapped[86] and it was subsequently shown that TSPO is a high-affinity cholesterol binding protein containing a conserved cholesterol recognition amino acid consensus domain in the C-terminus[87,88]. The drug and cholesterol binding domains were found to be in distinct domains of the protein results confirmed by NMR[86,87,89]. Moreover, these findings were further confirmed in structural studies by NMR and crystallography studies that reported the atomic structure of TSPO[90-95]. These studies also proposed that the functional TSPO is a dimer, that ligand binding to TSPO can promote cholesterol movement, and that cholesterol is an allosteric regulator of TSPO[90,92,93,96].

The ability of TSPO to bind drug ligands and cholesterol is its two major intrinsic properties and mostly likely the ones determining its function. We summarized above the reported effects of TSPO ligands on mitochondrial function. Although in steroidogenic and liver cells the role of a cholesterol binding protein segregating the steroidogenic pool of cholesterol

from structural cholesterol and facilitating its import into the mitochondria for steroid and formation is obvious, for other cells it is not so clear. However, cholesterol transfer in the inner mitochondrial membrane is needed for biogenesis of mitochondrial membranes during cell proliferation and/or repair. TSPO may also function as a sink for cholesterol which when free could be toxic for the cells. It is also possible that TSPO may be facilitating the movement of free cholesterol from the mitochondria to other organelles, as shown in astrocytes[71], fibroblasts[71], macrophages[97], retinal cells[98] and the steroidogenic Leydig cells[72]. Moreover, TSPO-mediated accumulation of free cholesterol in the mitochondria may affect mitochondrial membrane fluidity/permeability, fission/fusion processes, membrane protein/transporter function(s), and/or membrane potential[71,82,99-101].

TSPO was also shown to regulate mitophagy[58,102]. TSPO, by binding to VDAC1, reduces mitochondrial coupling and promotes an overproduction of ROS that counteracts parkin-mediated ubiquitination of proteins. These data suggested TSPO as an element in the regulation of mitochondrial quality control by autophagy. Further studies showed that TSPO deregulates mitochondrial Ca^{2+} signalling, leading to a parallel increase in the cytosolic Ca^{2+} pools that activate the Ca^{2+}-dependent NADPH oxidase, thereby increasing ROS[103]. The inhibition of mitochondrial Ca^{2+} uptake by TSPO is a consequence of the phosphorylation of VDAC1 by PKA, which is recruited to the mitochondria by ACBD3, VDAC1, ACBD3, PKA, and all transduceosome components recruited at TSPO. This is proposed as a novel OMM-based pathway to control intracellular Ca^{2+} dynamics and redox transients in cytotoxicity[103].

Genetics and genetic models

A series of articles came out in the last 15 years assessing the direct role of TSPO in various cellular pathways. First, the role of TSPO in opening the MPTP in liver mitochondrial function was investigated in an animal model depleted of liver TSPO[104]. The data obtained showed that the absence of TSPO does not affect liver MPTP function. Then, studies in rodents with genetic depletion of *TSPO* led to conflicting results including no effect on steroid synthesis[105-107], reduced steroid output, inhibition of corticosteroid response to adrenocorticotropic hormone, changes in lipid homeostasis in Leydig cells and reduction of circulating testosterone levels, and suppression of neurosteroid formation[108-111]. In addition, discordant data was reported on MA-10 mouse Leydig cells. Knockdown of *TSPO* expression using antisense oligonucleotides or antisense RNA reduces the ability of the cells to form steroids, while CRISPR/Cas9-guided *TSPO* deletion has either no effect or abolishes steroid synthesis[112-115]. These differences have been discussed in detail in other reviews[65,66].

Among all these studies, it seems that there is consistency between laboratories on the role of TSPO in neurosteroid formation where genetic deletion of TSPO led to reduced neurosteroid synthesis[109,111]. These results suggest that the role of TSPO in steroid formation may be primary and rate-determining in cells where steroid formation is independent on hormonal control, e.g. brain, compared to the classical peripheral steroid forming gonads and adrenal where pituitary hormones control the massive steroid production. In peripheral steroidogenic organs, TSPO may play a secondary role or play a role in cases where the cells do not respond to pituitary hormones, as in male hypogonadism where TSPO ligands can recover the drug- or age-induced reduction in androgen formation[65].

Numerous biochemical, pharmacological, and clinical data in the field of photodynamic therapy in oncology have demonstrated the role of ability of TSPO to bind porphyrins and its

role in porphyrin and heme transport and synthesis[116-118]. Using the same mice as before[106] the same group failed to show a role for TSPO in porphyrin and heme biosynthesis or transport[119].

TSPO deficiency decreased the oxygen consumption rate and mitochondrial membrane potential in mouse fibroblasts[119], MA-10 mouse Leydig cells[115] and C20 human microglia cells where it also reduced respiratory function[120]. Mitochondrial membrane potential depends on the flux of respiratory substrates adenosine triphosphate, adenosine diphosphate, and Pi through VDAC. Adenine nucleotide translocator also plays a role in maintenance of the membrane potential[115]. Therefore, TSPO likely controls cellular and mitochondrial metabolism via regulation of the mitochondrial membrane potential and affects OMM permeability and/or outer and inner membrane contacts/fusion.

Interestingly, lack of TSPO was shown to affect mitochondrial respiration and increase oxygen consumption in some cell and animal *Tspo* KO models, but not in others[62,64,78,106,107,119,120]. More recent studies also failed to show a direct link of TSPO to F-ATP synthase, which was shown to form the MPTP[121].

The differences underlying the disparate results from these genetic animal and cell models are not well understood. However, they clearly indicate differences between the pharmacology of TSPO and its intrinsic cellular functions. It is also likely that species differences, the presence of external or intrinsic stimuli, as well as differences in age, sex, and metabolic status of the species used may control the expression of TSPO. Considering that TSPO is one of the evolutionarily oldest proteins (see below), we proposed that it serves as the basis for fundamental functions and, thus, in case of its absence, compensatory mechanisms may have evolved. Moreover, even if its absence may not always affect animal phenotype, its presence, concentrated at the OMM, plays a regulatory role in mitochondrial function and associated tissue-specific phenotypes. Moreover, its presence provides us with a molecular target able to modulate mitochondrial and cell functions.

TSPO genetics in humans provide some of the most important information on the function of this protein. No humans have been identified lacking TSPO. In humans, the presence of a number of polymorphisms have been identified in the *TSPO* gene, including rs6971[122]. This polymorphism causes a non-conservative amino acid substitution, Ala147Thr, resulting in altered binding affinity of TSPO for specific ligands[122]. The presence of this *TSPO* polymorphism has been linked to the function of the hypothalamic-pituitary-adrenal axis, predisposing carriers to psychiatric disorders[123-126], and potentially impairing the response of patients to anxiolytic TSPO drug ligands[127,128]. The presence of this *TSPO* polymorphism was linked to reduced pregnenolone[129] and adrenocorticotropic hormone (ACTH)-induced corticosteroid levels[109] and shown to be associated with dysregulated cortisol rhythms and consequent clinical exacerbations in bipolar disorders[130]. This finding provides clear evidence of the link between TSPO, cholesterol binding, and steroid formation under normal and stress conditions.

Evolution

TSPO is an evolutionary conserved 3.5-billion-year-old protein[131]. Structural and functional evolution of the translocator protein (18 kDa. TSPO, named for its high tryptophan content and apparent role in the regulation of the transition between photosynthesis and respiration, is the mammalian TSPO orthologue in the photosynthetic bacterium *Rhodobacter*[132] a close

living relative of mitochondria[56]. Detailed evolutionary studies indicated that the *Tspo* gene family has been expanded by gene duplications from a bacterial environmental sensor or signal transducer to a functional bioregulator adapted to organism-, tissue-, cell-, and organelle-specific needs. Interestingly, the mammalian protein is able to rescue the phenotypes of bacterial *TspO* KO suggesting a conserved function[133] and that one compensates for the loss of oxygen sensing function that occurs when the other is depleted.

An additional Tspo family member, Tspo2, has been characterized[134]. Comparative analysis of Tspo1, the first family member to be identified, and Tspo2 structure and function indicates that TSPO2 was characterized by the loss of diagnostic drug ligand binding, but retention of cholesterol binding properties, and is involved in cholesterol redistribution during erythropoiesis[134]. Whether there are additional family members in mammals or humans remains to be determined. However, the highly conserved sequence would seem to indicate that such expansion in members was not needed to support the rich expansion of cellular functions.

Pharmacological and structural evidence supports TSPO functioning in tetrapyrrole biosynthesis, porphyrin transport, heme metabolism, cholesterol transport/trafficking, steroid formation, control of ROS levels, and the protection of mitochondria from free radical damage. All evolutionarily conserved functions are linked to mitochondria and affected by changes in mitochondrial membrane potential, a function dependent on the presence of TSPO. Few years ago, we proposed that the central role of TSPO throughout evolution is in oxygen-mediated metabolism. This central function has diversified roles in tissue- and cell-specific signalling, metabolism, cholesterol trafficking, immunological responses, apoptosis, steroid synthesis, and host-defence response to disease and injury, all oxygen-mediated pathways[21,131].

Summary

TSPO is a multifunctional protein involved in a wide array of cellular functions that are essential for human health. Its central location in the mitochondria, a multifunctional organelle itself, underscores its importance at the crossroads of critical homeostatic pathways. Its evolutionarily conserved sequence also supports its cellular significance. As we continue to elucidate the intricacies of the role of TSPO in health and disease, we will have the opportunity to identify new therapeutic and diagnostic targets that will have significant impact in the near and long term.

TSPO cell origin in wild-type and preclinical models of neurological disease

Wild-type

The density and cell origin of TSPO were assessed in the mouse brain. The specificity of TSPO staining was confirmed using a TSPO-deficient strain[135]. Two major findings were reported: TSPO is not homogeneously expressed in the various brain regions and the cell origin also varies across brain regions. The cerebellum shows high levels of TSPO staining as does the choroid plexus and the ependyma of the ventricular system. In addition, TSPO expression in the white matter is generally higher than in the grey matter. Regarding the cell origin of TSPO, in the cortex, astrocytes and microglia lack the constitutive TSPO expression observed in white matter. In contrast, in the hippocampus, TSPO is predominantly present in the

Table 1. TSPO cell origin in preclinical models of neurological diseases.

Human use	Preclinical model	Microglia	Astrocytes	Endothelial	Reference
Acute inflammation	LV-CNTF	x	x		136
	AAV-TNF	x	x	x	137
Ischemia	MCAO	x	x		138-140
Multiple sclerosis	EAE	x			141,142
	EAE in TSPOko		x		143
	CPZ	x	x		144,145
Alzheimer's disease	APP23		x		146
	PS19	x			146
	$APP_{swe}/PSEN1_{\Delta E9}$	x	x		147,148
	APP^{NL-G-F}	x			149
	3xTg-AD	x	x		150
	5xFAD	x			148,151
Schizophrenia	MIA	x	x	x	152

Abbreviations: LV-CNTF = Lentivirus encoding ciliary neurotrophic factor, AAV-TNF = Adeno-associated virus encoding tumour necrosis factor, MCAO = Middle cerebral artery occlusion, EAE = Experimental autoimmune encephalomyelitis, TSPOko = 18kDa translocator protein knock-out, CPZ = Cuprizone, APP = Amyloid precursor protein, PSEN = Presenilin, 3xTg = Triple transgenic model, 5xFAD = Five AD-linked mutation model, MIA = Maternal immune activation model.

subgranular layer and partially colocalizes with astrocytes but not with microglia. In the cerebellum, Purkinje cells are responsible for the expression of TSPO. Endothelial cells and pericytes of blood vessels also express TSPO. Furthermore, TSPO-positive NG2 cells were found in the spinal cord of mice[142]. Finally, TSPO seems to be absent from neurons and oligodendrocytes in all brain regions. However, a recent study shows a strong colocalization between TSPO and tyrosine hydroxylase (the limiting enzyme of dopamine synthesis) in the substantia nigra[153]. The authors concluded of that study that TSPO is present in the neurons of the dopaminergic system.

CNTF and TNF

Numerous studies have sought to highlight the alterations in its expression in response to either inflammatory stimuli. A first study evaluated the response to the over-expression of the ciliary neurotrophic factor (CNTF)[136]. The authors administered a lentivirus coding for the CNTF (containing an export sequence to be released outside the cell) via an intracerebral injection to focally induce an artificial expression of the CNTF in the brain. Two to six months after the injection, a significant increase in TSPO binding was observed on the ipsilateral side in PET imaging, which was confirmed *ex vivo* by western blotting and mRNA quantification. In order to characterize the cells that accounted for this upregulation, double immunofluorescence was performed for TSPO, IBA1 (a marker of microglia), and GFAP (a marker of astrocytes). In the contralateral (vehicle-treated) side, TSPO was found in microglial cells but not in astrocytes. Conversely, on the ipsilateral side, TSPO was localized in microglia as well as astrocytes indicating that CNTF induced TSPO in astrocytes. In contrast, in microglia, it is difficult to conclude whether a modification of the TSPO has taken place or not, in the absence of quantification. Indeed, although the TSPO is present on both sides of the brain (treated and control), it is possible that its level is increased in response to the chronic CNTF exposure. In a second study using a similar approach, an adenovirus encoding the sequence of the tumour necrosis factor (TNF) gene was injected into the mouse brain and analyses were performed at 3 or 5 days post injection[154]. Colocalization studies demonstrated the presence of TSPO in astrocytes and microglia. In addition, compared to the non-injected side, there was an increase in the number of double-positive cells for TSPO with GFAP, CD11b (a

microglial marker), as well as CD31 (an endothelial marker), as revealed by flow cytometry.

Ischemia

One of the most popular animal models of ischemia is achieved by a unilateral occlusion of the middle cerebral artery (MCAO)[155]. This intervention induces a progressive inflammatory reaction that is associated with an increase in TSPO at the mRNA and protein levels[138,139]. To determine the cellular origin of TSPO in this experimental model, 1 week after a 60-min intraluminal occlusion of MCA, $TSPO^+$ labelling was reported in microglial cells (as shown by lectin immunoreactivity) at the site of the core of the ischemia[139]. At the periphery of the ischemic core, some of the $GFAP^+$ cells were also $TSPO^+$, compared with the contralateral side. Using a similar protocol but with an occlusion time of 90 min, there was a strong $TSPO^+CD11b^+$ colocalization indicative of a microglial origin of TSPO[138]. However, these data are qualitative and an assessment of the colocalization between TSPO and other cell-type markers was not performed. A third study showed an increase in the number of $TSPO^+$ cells in response to the occlusion of MCA as demonstrated by cytometry[140]. More precisely, the $TSPO^+$ cells expressed microglial markers ($Cd11b^+CD45^{int}$ or $IBA1^+$). Interestingly, pretreatment with the TSPO agonist etifoxine helped to contain the size of ischemia, decreased neurological symptoms, and reduced cytokine release in response to the MCAO. These effects were abolished in a model of ischemia combined with a chemical inactivation of microglia[140]. Thus, it is probable that TSPO from microglia plays a role in inflammation in MCAO models. However, the search for TSPO in other cell types is not constant and will therefore require further investigations to better define, for example, the role of TSPO of astrocytic origin.

Multiple sclerosis

Experimental autoimmune encephalomyelitis (EAE) and cuprizone (CPZ) intoxication models induce demyelination and proliferation of microglial and astrocytic cells and are thus useful animal models of multiple sclerosis (MS)[156,157]. An increase in TSPO density has been reported in such animal models, using TSPO radioligands ($[^3H]$(R)-PK11195,$[^{18}F]$DPA-714,$[^{18}F]$GE180)[141,144,145]. By assessing the colocalization between TSPO and IBA1 or GFAP after exposure to CPZ (administered *per os* in the animals' food) for 1, 3 or 5 weeks, virtually all $IBA1^+$ cells expressed TSPO in both control and CPZ-treated animal. In contrast, only a small portion of $GFAP^+$ were $TSPO^+$ positive in control animals, whereas about 35% of $GFAP^+$ cells become $TSPO^+$ after 5 weeks of treatment. These changes were mainly localized in the *corpus callosum* and, to a lesser extent, in the grey matter cortex[144]. The CPZ models make it possible to investigate the expression of TSPO during the demyelinating phase (during CPZ treatment), as well as during the remyelination phase (after CPZ treatment). Thus, Zinnhardt et al. (2019) used a 4- and a 6-week CPZ treatment to explore both phases of the CPZ treatment[145]. They observed increases in TSPO binding in both states compared with the controls. TSPO levels in the demyelination phase are higher than during the remyelination phase. TSPO expression was mainly microglial during the demyelination phase and both microglial and astrocytic during the remyelination phase. These results were based on the colocalization of $TSPO^+IBA1^+$ and $TSPO^+GFAP^+$, a qualitative finding, without precise quantitative information regarding the relative contribution of these two glial cell types in the alterations in TSPO binding. In a mouse EAE model, photoemulsion of the *in vitro* binding of$[^3H]$(R)-PK11195 on brain sections[141] showed that the TSPO radioligand binding was colocalized with OX-42 (a marker of microglia). The authors reported no co-staining between$[^3H]$(R)-PK11195 and GFAP. However, in a mouse model of specific TSPO deficiency in astrocytes (hGFAP-driven conditional TSPO

knockout mice), the astrocytic proliferation and the behavioural signs, both associated with EAE, were milder, compared to wild-type animals[143]. Importantly, treatment with the TSPO ligand etifoxine decreases the severity and increases the symptomatic recovery in a EAE mouse model of MS[142]. These findings suggest that the microglial and astrocytic TSPO differentially contribute to animal models of MS.

Alzheimer's disease

Alzheimer's disease (AD) is characterized by the accumulation of amyloid deposits mainly formed by the beta amyloid peptide (Aβ) and by the presence of neurofibrillary tangles formed from abnormal forms of the Tau protein. Animal genetic models of the disease are produced by the induction of Aβ overexpression (by adding transgenes encoding human forms of APP or PS1) or overexpression of abnormal forms of Tau (by adding transgenes coding for human Tau forms)[147]. In all AD models, an overexpression of TSPO is observed[2,5,146,148-151,158-160]. However, there is no consensus on the cellular origin of TSPO[161]. Indeed, in the APP23 transgenic (Tg) mice model, astrocytes represent the cellular source of TSPO expression in the vicinity of extracellular amyloid deposits[146]. In contrast to this model, the PS19 Tg mice show microglia TSPO expression[146]. The presence of a significant spatial correlation between[^{3}H](R)-PK11195 binding and IBA1 staining that is not present in the case of GFAP staining, suggests that the origin of TSPO is predominantly microglial in the APP_{SWE}/$PSEN1_{\Delta E9}$ mice model[2]. However, double-immunofluorescence revealed that the cellular origin of TSPO may mainly be microglial although $TSPO^+GFAP^+$ cells were also present[148]. The predominance of a microglial origin to the TSPO binding is also observed in the 3xTgAD model (APP_{SWE}/$PS1_{M146V}$/Tau_{P301L}) with the use of IBA1 and GFAP co-staining with TSPO[150]. In a model combining three APP mutations and two PS1 mutations (5XFAD), colocalization of TSPO with GFAP or S100β for astrocytes is absent while $TSPO^+IBA1^+$ cells are observed. Interestingly, Liu et al. (2005) also reported that subtypes of microglial cells are differentially contributing to the expression of TSPO. Indeed, TSPO strongly colocalizes with the CD68 microglial pro-inflammatory marker. In addition, TSPO is also present in microglia positive for the CD206 anti-inflammatory marker when these cells are in the vicinity of the amyloid deposits[148]. Thus, the complexity of glial cell types and the differential expression of TSPO by the various subclasses of glial cells add another level of complexity that needs to be further studied.

Schizophrenia

In contrast to the aforementioned pathologies, the density of TSPO is decreased in schizophrenia (see details in the next chapter). Using the maternal immune activation (MIA) animal model of schizophrenia, a decrease in the TSPO levels was reported[162]. The authors observed a decrease in colocalization of TSPO with IBA1, GFAP, and Glut1 (a marker of the brain vasculature)[162], suggesting the involvement of multiple different cell types.

General considerations

Overall, it is important to discuss several critical issues. First, the assessment of TSPO in other cell types than microglia has not been examined systematically, e.g. in astrocytes and even less in endothelial cells. Secondly, many studies use IBA1 as a marker of microglia, but it represents a ubiquitous labelling of this cell type and not of any specific activated forms or phenotypes. Without a more in-depth analysis of the $TSPO^+IBA1^+$ cells, it cannot be completely affirmed that it is indeed active microglia and even if it is, the pathophysiological significance of a particular phenotype of activated microglia or indeed other cells of the

monocyte family that also express IBA1. In this context, several reports using mouse primary glial cell cultures demonstrate that TSPO is more likely to be modified in activated (by pro-inflammatory stimuli) forms of microglia and astrocytes[154,163,164]. Finally, studies of the number of cells expressing TSPO based on immunofluorescence do not determine if a change in the number of TSPO binding sites per cell is present. Finally, although evidence is scarce, a direct implication of TSPO on the pathophysiology of the various neuropsychiatric conditions may not be ruled out.

TSPO expression in human CNS in health, ageing, and neurological disease

Health and Ageing

Little is known of the distribution and expression of TSPO during development, healthy aging, and how such expression differs in regions of the CNS in humans. Consideration of these features, as well as the mode of analysis, e.g. PET, autoradiography, quantitative assays, or pathology of post-mortem (PM) brain, is of key importance to explain TSPO expression in PET imaging.

Much of what is known about TSPO expression in humans comes from PET imaging where differential expression may be due to the different affinity patterns for TSPO ligands. PET studies report an increased expression of TSPO with aging in healthy subjects in several cortical and subcortical areas[165-167]. However, little is known about the levels and cellular expression of TSPO during (early) development or in healthy elderly subjects as determined in post-mortem control tissues. Quantitative immunoblotting approaches reveal that TSPO protein levels are 2- to 70-fold higher than those reported by *in vitro* binding assays and expression is widely distributed in the CNS in grey and white matter at all ages[165]. At birth TSPO protein levels are highest in the frontal cortex possibly reflecting expression in neuronal precursor cells although pathology studies have not yet supported this hypothesis. Levels of TSPO decline in the first 3 months after birth and subsequently increase modestly during adulthood/senescence[165]. The relatively high binding and protein expression reported in aging may reflect subtle changes due to senescence or, alternatively, due to changes in the morphology or phenotype of aging cells in the CNS parenchyma. Pathology studies on PM tissues of normal human brains reported that a variety of cell types express TSPO, the levels and extent of expression depending on the TSPO antibody used[168]. Endothelial cells, arachnoid cells, cells within the choroid plexus as well as astrocytes, microglia, and to a lesser degree oligodendrocytes and immune cells within blood vessels revealed a punctate expression typical for mitochondrial expression markers[168] However, these studies were limited to tissues from aged donors and it is difficult to conclude, based on the available pathology studies, that the cellular expression of TSPO in the normal brain is due to normal aging.

Neuroinflammation

TSPO PET imaging is widely used to monitor inflammation in MS, a chronic inflammatory demyelinating and neurodegenerative disease with onset in young adults[169]. The PET signal in MS is frequently assumed to represent pathogenic microglia yet pathology studies have detailed a more widespread cellular expression. Compared to normal appearing white matter in MS tissues where TSPO is expressed in scattered HLA+ cells throughout the CNS, the expression is approximately 20-fold higher in active MS lesions and the rim of chronic active lesions[170]. In addition to microglia, this study revealed that expression is also observed

Table 2. TSPO cell origin in human neurological diseases.

Human disease		Microglia	Astrocytes	Neurons	Endothelial	VSMCs	Refs
Neuroinflammation	MS	x	x				6,171
Neurodegenerative	AD	x	x		x	x	175,176
	LBD	x					176
Infections	HIV	x	x	x	x		168
	Creutzfeldt-Jakob	x					177
Neuropsychiatric	MDD	x					178-180
Stroke		x	x				168
Epilepsy		x	x	x			181

Abbreviations: AD = Alzheimer's disease, HIV = Human immunodeficiency virus, LBD = Lewy-body dementia, MDD = Major depressive disorder, MS = Multiple sclerosis, VSMCs = vascular smooth muscle cells

in astrocytes, predominantly in chronic active and inactive lesions, and that the astrocyte signal contributes significantly to the active lesions and rim of chronic active lesions. In addition, this study highlights that TSPO is expressed in some but not all M1 (pathogenic) and M2 (immune-regulatory) phenotypes as well as intermediate microglia/macrophages[171,172]. Furthermore, a percentage of both TMEM119$^+$ and P2RY12$^+$ cells, markers that represent homeostatic microglia, express TSPO in MS lesions indicating that TSPO PET is not merely a reflection of pathogenic microglia, although the trigger of TSPO upregulation in MS CNS is still unclear. In addition, in MS, TSPO is also expressed by T and B cells in the CNS and thus such cellular expression during disease must be considered in TSPO PET imaging.

Neurodegenerative Diseases

An association between microglia activation, astrogliosis, and neuronal damage has been reported for several neurodegenerative diseases, e.g. AD, Parkinson's disease, and Amyotrophic lateral Sclerosis (ALS; motor neuron disease)[173]. As with MS, TSPO PET imaging is widely-considered to reflect the pathogenic microglia in neurodegenerative diseases *in vivo*. Using post-mortem brain tissues, several studies have used autoradiography to determine TSPO density in human brain tissues but few have examined the cellular distribution in detail (reviewed by [174]). Recently, a study using immunohistochemistry on AD human brain tissues revealed TSPO expression by microglia, astrocytes, endothelial cells, and vascular smooth muscle cells[175]. TSPO expression was not quantified by cell counts but rather by the amount of TSPO immunoreactivity. Although the authors reported a slight increase of TSPO immunoreactivity in the grey matter compared to healthy subjects, such expression was not associated with Braak stage, Aβ plaques or neurofibrillary tangles or cortical thickness. While these authors showed TSPO expression by CD68 and IBA1$^+$ microglia/macrophages, they did not examine expression in specific microglia phenotypes. Receptor density was not found to be increased in post-mortem AD brain or in dementia with Lewy-bodies (DLB) as investigated with quantitative autoradiography[176]. Interestingly, a significant decrease in receptor density or receptor binding was found in the *substantia nigra* of AD and DLB. No studies have been conducted to investigate the TSPO expression at the cellular level in other neurodegenerative diseases such as ALS, Huntington's disease, or spinocerebellar atrophy.

Infections

TSPO expression in the CNS of a few cases with HIV was reported to be similar to healthy human brain[168]. TSPO is reported in metabolic glia, a form of reactive astrocyte, and microglial cells. Tissues from HIV encephalitis (HIVE) cases revealed an increased expression of TSPO in

lesioned areas. In cases where the origin of the infection was more unclear, there was a general increase of TSPO expression in activated microglia. HIVE brains showed perivascular $TSPO^+$ infiltrates as well as $TSPO^+$ microglial nodules and multinucleated giant cells. Studies to determine TSPO expression in infections of the central nervous systems have utilised PET imaging as reported for ZIKA[182], and herpes encephalitis animal models[183-185], as well as Creutzfeldt-Jakob disease patients[177] but have not yet investigated expression in post-mortem tissues from humans.

Neuropsychiatric disorders

Several PET studies of TSPO as a marker of inflammation in psychiatric disorders have been performed but with differing outcomes. For example, PET studies in schizophrenia show different outcomes, either an increase, decrease, or no change compared to controls[186]. A recent review combining several meta-analyses[187-189] showed that overall patients with schizophrenia have lowered TSPO concentrations compared to healthy individuals[190]. On the other hand, in depression, TSPO seems to be upregulated mostly in the anterior cingulate and prefrontal cortex[178-180]. TSPO was overall lower in depression patients receiving SSRI medication compared to unmedicated patients[190]. For bipolar disorder, an increase of TSPO mRNA and protein together with inflammasome activation was found in peripheral blood monocytes[191]. However, while an increasing number of studies show TSPO changes in neuropsychiatric disorders with TSPO PET, there is a paucity of data using human CNS tissues to determine the cellular expression of TSPO in neuropsychiatric disorders to substantiate findings of TSPO PET.

Stroke

TSPO PET in brain trauma could aid in monitoring regenerative processes after stroke. Depending on the region and severity of the infarct, TSPO is expressed to differing degrees by surrounding microglia and hypertrophic astrocytes. In a subacute infarct in the cerebellar cortex, $TSPO^+$ microglia were found to be surrounding/ encapsulating Purkinje cells[168].

Epilepsy

PET studies show increased binding of TSPO ligand in both ipsilateral and contralateral regions in temporal lobe epilepsy (TLE) suggesting inflammation distant to the seizure foci. Examination of brain tissue surgically resected revealed high TSPO expression in microglia and neurons and low expression in astrocytes[181].

FACS-RTT: A new technique to access the cellular origin of TSPO

To measure TSPO overexpression, some studies have used histological staining[135,150]. However, even if this technique presents the advantage of an intact cellular architecture of the tissue, there is not enough quantitative precision to determine the contribution of each cell population of the brain in TSPO signal. Similarly, histological approaches do not allow to assess an important parameter: does an alteration of TSPO in the tissue result from the modulation of the number of cells expressing TSPO? Or does each cell produce more TSPO?

To assess if the overexpression of TSPO is due to a cellular proliferation or an increased expression of TSPO in the cell, an innovative approach was recently developed[192]. This methodology combined the fluorescence-activated cell sorting (FACS) to isolate astrocytes,

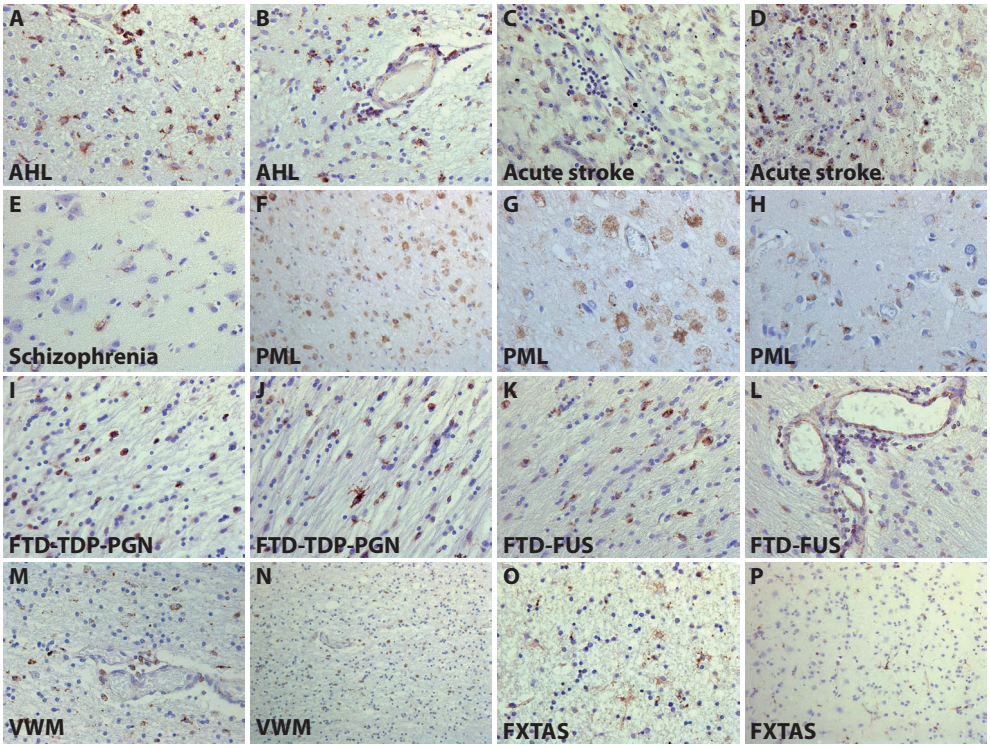

Figure 1. Cellular sources of TSPO expression in the CNS. Multiple cell origin of TSPO in the pathological human brain. Astrocytes and perivascular macrophages are positive for TSPO in acute hemorrhagic leukoencephalopathy (A, B). At the site of injury, acute stroke cells express TSPO in two separate cases (C, D). A schizophrenia patient with TSPO+ microglia and endothelial cells in the anterior cingulate cortex (E). Lesions in progressive multifocal leukoencephalopathy are abundant with TSPO in microglia, macrophages, and astrocytes in the white and gray matter (F, G, H). Patients with frontotemporal dementia with mutations for TDP, proganulin, and FUS have a macrophage-like cells expressing TSPO in the white matter and in perivascular spaces (I, J, K, L). Macrophages in vanishing white matter express TSPO throughout the white matter areas in the brain parenchyma (M, N). Fragile X-associated tremor/ataxia syndrome has TSPO+ astrocytes in the white matter and microglia in both white and gray matter (O, P).

microglia, neurons, and endothelial cells and the radioligand-mediated labelling of TSPO (RTT, radioligand-treated tissues).

TSPO overexpression was studied in response to acute unilateral injection of lipopolysaccharide (LPS) or of ciliary neurotrophic factor (CNTF), in a rat model of AD and in the AD brain[192,193]. In all these pathological contexts, TSPO is overexpressed. However, the cellular origin of TSPO overexpression is context-dependent and cellular mechanisms leading to this increase are heterogeneous (proliferation of the cell population and/or changes in TSPO expression by each single cell).

Furthermore, the involvement of endothelial TSPO binding in the overall TSPO signal is at the centre of *in vivo* imaging interrogations. In the case of these models of inflammation, endothelial cells contributed to basal TSPO signal but not to its increase[192,193]. These results potentially answer a fundamental question in the domain of *in vivo* imaging of neuroinflammation, i.e. regarding the necessity to take the endothelial TSPO signal into account when quantifying TSPO *in vivo* using PET. Still, it is important to keep in mind that

endothelial cells may contribute to TSPO signal in other conditions. Overall, these results confirm the complexity of TSPO and show the necessity to validate their cellular origin in each pathological context before quantifying and interpreting the *in vivo* imaging signal.

Conclusion

Since its identification, TSPO has been widely studied for its different roles in the periphery and more recently within the CNS itself. Its cellular origin demonstrated in the brain in microglia, although it is clear that other cell types also express TSPO and its presence in astrocytes and endothelial cells is now well accepted (Fig. 1). The cellular origin of TSPO alterations likely not only depends on the pathology but also on the developmental stage and mode of cell activation. Monitoring of TSPO levels is now widely used as a marker of inflammation, but research still needs to better characterize the means and cells involved. In this sense, it has recently been reported that the expression of TSPO concerns not only the pro-inflammatory types of microglia but also the anti-inflammatory subtypes. Future studies should also reveal the therapeutic potential of a change in its levels.

Acknowledgements

Authors thank the MS society of Great Britain and Northern Ireland. Authors K.C. and B.B.T. are supported by the Velux foundation (project n. 1123). Author S.T. received support from the Swiss National Science Foundation (Early PostDoc.Mobility Scholarship, no. P2GEP3_191446), the Prof Dr Max Cloëtta Foundation (Clinical Medicine Plus scholarship) and the Jean and Madeleine Vachoux Foundation. Author D.R.O. is supported by the MRC (MR/N008219/1). Author V.P. was supported by the John Stauffer Dean's Chair in Pharmaceutical Sciences (University of Southern California). This work was supported by the Swiss National Science Foundation (no. 320030-184713).

References

1. Guilarte TR. TSPO in diverse CNS pathologies and psychiatric disease: A critical review and a way forward. *Pharmacol Ther*. Feb 2019;194:44-58. doi:10.1016/j.pharmthera.2018.09.003
2. Venneti S*, et al*. PK11195 labels activated microglia in Alzheimer's disease and in vivo in a mouse model using PET. *Neurobiol Aging*. Aug 2009;30(8):1217-26. doi:10.1016/j.neurobiolaging.2007.11.005
3. Gui Y*, et al*. Characterization of the 18 kDa translocator protein (TSPO) expression in post-mortem normal and Alzheimer's disease brains. *Brain Pathol*. Jan 2020;30(1):151-164. doi:10.1111/bpa.12763
4. Kaunzner UW*, et al*. Quantitative susceptibility mapping identifies inflammation in a subset of chronic multiple sclerosis lesions. *Brain*. Jan 1 2019;142(1):133-145. doi:10.1093/brain/awy296
5. Maeda J*, et al*. In vivo positron emission tomographic imaging of glial responses to amyloid-beta and tau pathologies in mouse models of Alzheimer's disease and related disorders. *J Neurosci*. Mar 23 2011;31(12):4720-30. doi:10.1523/JNEUROSCI.3076-10.2011
6. Nutma E*, et al*. A quantitative neuropathological assessment of translocator protein expression in multiple sclerosis. *Brain*. Nov 1 2019;142(11):3440-3455. doi:10.1093/brain/awz287
7. Ahmad R*, et al*. Whole-body biodistribution and radiation dosimetry of the cannabinoid type 2 receptor ligand [11C]-NE40 in healthy subjects. *Mol Imaging Biol*. Aug 2013;15(4):384-90. doi:10.1007/s11307-013-0626-y
8. Attili B*, et al*. Preclinical evaluation of [(18) F]MA3: a CB2 receptor agonist radiotracer for PET. *Br J Pharmacol*. May 2019;176(10):1481-1491. doi:10.1111/bph.14564
9. Kumar JSD*, et al*. Radiosynthesis and evaluation of [(18)F]FMTP, a COX-2 PET ligand. *Pharmacol Rep*. Oct 2020;72(5):1433-1440. doi:10.1007/s43440-020-00124-z
10. Shrestha S*, et al*. PET measurement of cyclooxygenase-2 using a novel radioligand: upregulation in primate neuroinflammation and first-in-human study. *J Neuroinflammation*. May 2 2020;17(1):140. doi:10.1186/s12974-020-01804-6
11. Hosoya T*, et al*. In vivo TSPO and cannabinoid receptor type 2 availability early in post-stroke neuroinflammation in rats: a positron emission tomography study. *J Neuroinflammation*. Mar 29 2017;14(1):69. doi:10.1186/s12974-017-0851-4
12. Pottier G*, et al*. PET imaging of cannabinoid type 2 receptors with [(11)C]A-836339 did not evidence changes following neuroinflammation in rats. *J Cereb Blood Flow Metab*. Mar 2017;37(3):1163-1178. doi:10.1177/0271678X16685105
13. Territo PR*, et al*. Characterization of (11) C-GSK1482160 for Targeting the P2X7 Receptor as a Biomarker for Neuroinflammation. *J Nucl Med*. Mar 2017;58(3):458-465. doi:10.2967/jnumed.116.181354
14. Berdyyeva T*, et al*. PET Imaging of the P2X7 Ion Channel with a Novel Tracer [(18)F]JNJ-64413739 in a Rat Model of Neuroinflammation. *Mol Imaging Biol*. Oct 2019;21(5):871-878. doi:10.1007/s11307-018-01313-2
15. Kolb HC*, et al*. Preclinical Evaluation and Nonhuman Primate Receptor Occupancy Study of (18) F-JNJ-64413739, a PET Radioligand for P2X7 Receptors. *J Nucl Med*. Aug 2019;60(8):1154-1159. doi:10.2967/jnumed.118.212696
16. Liu H*, et al*. PET Imaging Study of S1PR1 Expression in a Rat Model of Multiple Sclerosis. *Mol Imaging Biol*. Oct 2016;18(5):724-32. doi:10.1007/s11307-016-0944-y
17. Weng CC*, et al*. Correlation analysis of [(18) F]ROStrace using ex vivo autoradiography and dihydroethidium fluorescent imaging in lipopolysaccharide-treated animals. *Biochem Biophys Res Commun*. Aug 20 2019;516(2):397-401. doi:10.1016/j.bbrc.2019.06.062
18. Horti AG*, et al*. PET imaging of microglia by targeting macrophage colony-stimulating factor 1 receptor (CSF1R). *Proc Natl Acad Sci U S A*. Jan 29 2019;116(5):1686-1691. doi:10.1073/pnas.1812155116
19. Papadopoulos V*, et al*. Translocator protein (18kDa): new nomenclature for the peripheral-type benzodiazepine receptor based on its structure and molecular function. *Trends Pharmacol Sci*. Aug 2006;27(8):402-9. doi:10.1016/j.tips.2006.06.005
20. Rupprecht R*, et al*. Translocator protein (18 kDa) (TSPO) as a therapeutic target for neurological and psychiatric disorders. *Nat Rev Drug Discov*. Dec 2010;9(12):971-88. doi:10.1038/nrd3295
21. Veenman L*, et al*. Channel-like functions of the 18-kDa translocator protein (TSPO): regulation of apoptosis and steroidogenesis as part of the host-defense response. *Curr Pharm Des*. 2007;13(23):2385-405. doi:10.2174/138161207781368710
22. Gavish M*, et al*. Enigma of the peripheral benzodiazepine receptor. *Pharmacol Rev*. Dec 1999;51(4):629-50.
23. Austin CJ*, et al*. The translocator protein (TSPO): a novel target for cancer chemotherapy. *Int J Biochem Cell Biol*. Jul 2013;45(7):1212-6. doi:10.1016/j.biocel.2013.03.004
24. Batarseh A*, et al*. Regulation of translocator protein 18 kDa (TSPO) expression in health and disease states. *Mol Cell Endocrinol*. Oct 7 2010;327(1-2):1-12. doi:10.1016/j.mce.2010.06.013
25. Caballero B*, et al*. Role of mitochondrial translocator protein (18 kDa) on mitochondrial-related cell death processes. *Recent Pat Endocr Metab Immune Drug Discov*. May 2013;7(2):86-

101. doi:10.2174/1872214811307020002
26. Papadopoulos V. Peripheral-type benzodiazepine/diazepam binding inhibitor receptor: biological role in steroidogenic cell function. *Endocr Rev*. Apr 1993;14(2):222-40. doi:10.1210/edrv-14-2-222
27. Veenman L, *et al*. The peripheral-type benzodiazepine receptor and the cardiovascular system. Implications for drug development. *Pharmacol Ther*. Jun 2006;110(3):503-24. doi:10.1016/j.pharmthera.2005.09.007
28. Galiegue S, *et al*. Immunohistochemical assessment of the peripheral benzodiazepine receptor in breast cancer and its relationship with survival. *Clin Cancer Res*. Mar 15 2004;10(6):2058-64. doi:10.1158/1078-0432.ccr-03-0988
29. Tonon MC, *et al*. Endozepines and their receptors: Structure, functions and pathophysiological significance. *Pharmacol Ther*. Apr 2020;208:107386. doi:10.1016/j.pharmthera.2019.06.008
30. Chen MK, *et al*. Translocator protein 18 kDa (TSPO): molecular sensor of brain injury and repair. *Pharmacol Ther*. Apr 2008;118(1):1-17. doi:10.1016/j.pharmthera.2007.12.004
31. Taliani S, *et al*. Translocator protein ligands as promising therapeutic tools for anxiety disorders. *Curr Med Chem*. 2009;16(26):3359-80. doi:10.2174/092986709789057653
32. Liu GJ, *et al*. The 18 kDa translocator protein, microglia and neuroinflammation. *Brain Pathol*. Nov 2014;24(6):631-53. doi:10.1111/bpa.12196
33. Wang HJ, *et al*. Translocator protein (Tspo) gene promoter-driven green fluorescent protein synthesis in transgenic mice: an in vivo model to study Tspo transcription. *Cell Tissue Res*. Nov 2012;350(2):261-75. doi:10.1007/s00441-012-1478-5
34. Bribes E, *et al*. Immunohistochemical assessment of the peripheral benzodiazepine receptor in human tissues. *J Histochem Cytochem*. Jan 2004;52(1):19-28. doi:10.1177/002215540405200103
35. Katz Y, *et al*. Increased density of peripheral benzodiazepine-binding sites in ovarian carcinomas as compared with benign ovarian tumours and normal ovaries. *Clin Sci (Lond)*. Feb 1990;78(2):155-8. doi:10.1042/cs0780155
36. Bhoola NH, *et al*. Translocator Protein (TSPO) as a Potential Biomarker in Human Cancers. *Int J Mol Sci*. Jul 25 2018;19(8)doi:10.3390/ijms19082176
37. Han Z, *et al*. Expression of peripheral benzodiazepine receptor (PBR) in human tumors: relationship to breast, colorectal, and prostate tumor progression. *J Recept Signal Transduct Res*. 2003;23(2-3):225-38. doi:10.1081/rrs-120025210
38. Batarseh A, *et al*. Functional characterization of the human translocator protein (18kDa) gene promoter in human breast cancer cell lines. *Biochim Biophys Acta*. Jan 2012;1819(1):38-56. doi:10.1016/j.bbagrm.2011.09.001
39. Hardwick M, *et al*. Peripheral-type benzodiazepine receptor (PBR) gene amplification in MDA-MB-231 aggressive breast cancer cells. *Cancer Genet Cytogenet*. Nov 2002;139(1):48-51. doi:10.1016/s0165-4608(02)00604-0
40. Anholt RR, *et al*. The peripheral-type benzodiazepine receptor. Localization to the mitochondrial outer membrane. *J Biol Chem*. Jan 15 1986;261(2):576-83.
41. Garnier M, *et al*. Diazepam binding inhibitor is a paracrine/autocrine regulator of Leydig cell proliferation and steroidogenesis: action via peripheral-type benzodiazepine receptor and independent mechanisms. *Endocrinology*. Jan 1993;132(1):444-58. doi:10.1210/endo.132.1.8380386
42. Hardwick M, *et al*. Peripheral-type benzodiazepine receptor (PBR) in human breast cancer: correlation of breast cancer cell aggressive phenotype with PBR expression, nuclear localization, and PBR-mediated cell proliferation and nuclear transport of cholesterol. *Cancer Res*. Feb 15 1999;59(4):831-42.
43. Doble A, *et al*. Photoaffinity labeling of peripheral-type benzodiazepine-binding sites. *Mol Pharmacol*. Jan 1987;31(1):42-9.
44. Antkiewicz-Michaluk L, *et al*. Purification and characterization of a protein associated with peripheral-type benzodiazepine binding sites. *J Biol Chem*. Nov 25 1988;263(33):17317-21.
45. Riond J, *et al*. Characterization of a peripheral-type benzodiazepine-binding site in the mitochondria of Chinese hamster ovary cells. *FEBS Lett*. Mar 13 1989;245(1-2):238-44. doi:10.1016/0014-5793(89)80229-7
46. Sprengel R, *et al*. Molecular cloning and expression of cDNA encoding a peripheral-type benzodiazepine receptor. *J Biol Chem*. Dec 5 1989;264(34):20415-21.
47. Riond J, *et al*. Molecular cloning and chromosomal localization of a human peripheral-type benzodiazepine receptor. *Eur J Biochem*. Jan 30 1991;195(2):305-11. doi:10.1111/j.1432-1033.1991.tb15707.x
48. Chang YJ, *et al*. The human "peripheral-type" benzodiazepine receptor: regional mapping of the gene and characterization of the receptor expressed from cDNA. *DNA Cell Biol*. Jul-Aug 1992;11(6):471-80. doi:10.1089/dna.1992.11.471
49. Parola AL, *et al*. Cloning and expression of a pharmacologically unique bovine peripheral-type benzodiazepine receptor isoquinoline binding protein. *J Biol Chem*. Jul 25 1991;266(21):14082-7.
50. Garnier M, *et al*. In vitro reconstitution of a functional peripheral-type benzodiazepine receptor from mouse Leydig tumor cells. *Mol Pharmacol*. Feb 1994;45(2):201-11.
51. McEnery MW, *et al*. Isolation of the mitochondrial benzodiazepine receptor: association with the voltage-dependent anion channel and the adenine nucleotide carrier. *Proc Natl Acad Sci U S A*. Apr 15

1992;89(8):3170-4. doi:10.1073/pnas.89.8.3170
52. Levitt D. Gramicidin, VDAC, porin and perforin channels. *Curr Opin Cell Biol*. Aug 1990;2(4):689-94. doi:10.1016/0955-0674(90)90112-r
53. Le Fur G, *et al*. Differentiation between two ligands for peripheral benzodiazepine binding sites, [3H] RO5-4864 and [3H]PK 11195, by thermodynamic studies. *Life Sci*. Aug 1 1983;33(5):449-57. doi:10.1016/0024-3205(83)90794-4
54. Rone MB, *et al*. Targeting and insertion of the cholesterol-binding translocator protein into the outer mitochondrial membrane. *Biochemistry*. Jul 28 2009;48(29):6909-20. doi:10.1021/bi900854z
55. Lacapere JJ, *et al*. Peripheral-type benzodiazepine receptor: structure and function of a cholesterol-binding protein in steroid and bile acid biosynthesis. *Steroids*. Sep 2003;68(7-8):569-85. doi:10.1016/s0039-128x(03)00101-6
56. Li F, *et al*. Translocator Protein 18 kDa (TSPO): An Old Protein with New Functions? *Biochemistry*. May 24 2016;55(20):2821-31. doi:10.1021/acs.biochem.6b00142
57. Rone MB, *et al*. Identification of a dynamic mitochondrial protein complex driving cholesterol import, trafficking, and metabolism to steroid hormones. *Mol Endocrinol*. Nov 2012;26(11):1868-82. doi:10.1210/me.2012-1159
58. Gatliff J, *et al*. TSPO interacts with VDAC1 and triggers a ROS-mediated inhibition of mitochondrial quality control. *Autophagy*. 2014;10(12):2279-96. doi:10.4161/15548627.2014.991665
59. Issop L, *et al*. Organelle plasticity and interactions in cholesterol transport and steroid biosynthesis. *Mol Cell Endocrinol*. May 22 2013;371(1-2):34-46. doi:10.1016/j.mce.2012.12.003
60. Aghazadeh Y, *et al*. Pharmacological regulation of the cholesterol transport machinery in steroidogenic cells of the testis. *Vitam Horm*. 2015;98:189-227. doi:10.1016/bs.vh.2014.12.006
61. Oke BO, *et al*. Cell surface localization of the peripheral-type benzodiazepine receptor (PBR) in adrenal cortex. *Mol Cell Endocrinol*. Sep 1992;87(1-3):R1-6. doi:10.1016/0303-7207(92)90248-5
62. Hirsch JD, *et al*. Mitochondrial benzodiazepine receptors mediate inhibition of mitochondrial respiratory control. *Mol Pharmacol*. Jan 1989;35(1):157-63.
63. Larcher JC, *et al*. Effects of peripheral benzodiazepines upon the O2 consumption of neuroblastoma cells. *Eur J Pharmacol*. Feb 28 1989;161(2-3):197-202. doi:10.1016/0014-2999(89)90843-1
64. Lejri I, *et al*. TSPO Ligands Boost Mitochondrial Function and Pregnenolone Synthesis. *J Alzheimers Dis*. 2019;72(4):1045-1058. doi:10.3233/JAD-190127
65. Papadopoulos V, *et al*. Translocator protein-mediated pharmacology of cholesterol transport and steroidogenesis. *Mol Cell Endocrinol*. Jun 15 2015;408:90-8. doi:10.1016/j.mce.2015.03.014
66. Papadopoulos V, *et al*. Translocator protein (18 kDa): an update on its function in steroidogenesis. *J Neuroendocrinol*. Feb 2018;30(2)doi:10.1111/jne.12500
67. Costa E, *et al*. The pharmacology of neurosteroidogenesis. *J Steroid Biochem Mol Biol*. Jun 1994;49(4-6):385-9. doi:10.1016/0960-0760(94)90284-4
68. Papadopoulos V, *et al*. Pregnenolone biosynthesis in C6-2B glioma cell mitochondria: regulation by a mitochondrial diazepam binding inhibitor receptor. *Proc Natl Acad Sci U S A*. Jun 1 1992;89(11):5113-7. doi:10.1073/pnas.89.11.5113
69. Arbo BD, *et al*. Therapeutic actions of translocator protein (18 kDa) ligands in experimental models of psychiatric disorders and neurodegenerative diseases. *J Steroid Biochem Mol Biol*. Nov 2015;154:68-74. doi:10.1016/j.jsbmb.2015.07.007
70. Porcu P, *et al*. Neurosteroidogenesis Today: Novel Targets for Neuroactive Steroid Synthesis and Action and Their Relevance for Translational Research. *J Neuroendocrinol*. Feb 2016;28(2):12351. doi:10.1111/jne.12351
71. Falchi AM, *et al*. Intracellular cholesterol changes induced by translocator protein (18 kDa) TSPO/PBR ligands. *Neuropharmacology*. Aug 2007;53(2):318-29. doi:10.1016/j.neuropharm.2007.05.016
72. Chung JY, *et al*. Cholesterol accumulation, lipid droplet formation, and steroid production in Leydig cells: Role of translocator protein (18-kDa). *Andrology*. May 2020;8(3):719-730. doi:10.1111/andr.12733
73. Lacapere JJ, *et al*. Insight into the Structural Features of TSPO: Implications for Drug Development. *Trends Pharmacol Sci*. Feb 2020;41(2):110-122. doi:10.1016/j.tips.2019.11.005
74. Costa B, *et al*. TSPO ligand residence time: a new parameter to predict compound neurosteroidogenic efficacy. *Sci Rep*. Jan 11 2016;6:18164. doi:10.1038/srep18164
75. Costa B, *et al*. The Anxiolytic Etifoxine Binds to TSPO Ro5-4864 Binding Site with Long Residence Time Showing a High Neurosteroidogenic Activity. *ACS Chem Neurosci*. Jul 19 2017;8(7):1448-1454. doi:10.1021/acschemneuro.7b00027
76. Hatty CR, *et al*. Protein-ligand and membrane-ligand interactions in pharmacology: the case of the translocator protein (TSPO). *Pharmacol Res*. Oct 2015;100:58-63. doi:10.1016/j.phrs.2015.07.029
77. Kletsas D, *et al*. Peripheral-type benzodiazepine receptor (PBR) and PBR drug ligands in fibroblast and fibrosarcoma cell proliferation: role of ERK, c-Jun and ligand-activated PBR-independent pathways. *Biochem Pharmacol*. May 15 2004;67(10):1927-32. doi:10.1016/j.bcp.2004.01.021
78. Bader S, *et al*. Differential effects of TSPO ligands on mitochondrial function in mouse microglia cells. *Psychoneuroendocrinology*. Aug 2019;106:65-76.

doi:10.1016/j.psyneuen.2019.03.029
79. Veenman L, *et al*. VDAC activation by the 18 kDa translocator protein (TSPO), implications for apoptosis. *J Bioenerg Biomembr*. Jun 2008;40(3):199-205. doi:10.1007/s10863-008-9142-1
80. Veenman L, *et al*. Potential involvement of F0F1-ATP(synth)ase and reactive oxygen species in apoptosis induction by the antineoplastic agent erucylphosphohomocholine in glioblastoma cell lines : a mechanism for induction of apoptosis via the 18 kDa mitochondrial translocator protein. *Apoptosis*. Jul 2010;15(7):753-68. doi:10.1007/s10495-010-0460-5
81. Veenman L, *et al*. The role of 18 kDa mitochondrial translocator protein (TSPO) in programmed cell death, and effects of steroids on TSPO expression. *Curr Mol Med*. May 2012;12(4):398-412. doi:10.2174/1566524011207040398
82. Azarashvili T, *et al*. The peripheral-type benzodiazepine receptor is involved in control of Ca2+-induced permeability transition pore opening in rat brain mitochondria. *Cell Calcium*. Jul 2007;42(1):27-39. doi:10.1016/j.ceca.2006.11.004
83. Zulian A, *et al*. The translocator protein (peripheral benzodiazepine receptor) mediates rat-selective activation of the mitochondrial permeability transition by norbormide. *Biochim Biophys Acta*. Dec 2011;1807(12):1600-5. doi:10.1016/j.bbabio.2011.08.007
84. Galiegue S, *et al*. The peripheral benzodiazepine receptor: a promising therapeutic drug target. *Curr Med Chem*. Aug 2003;10(16):1563-72. doi:10.2174/0929867033457223
85. Katz Y, *et al*. Increase in peripheral benzodiazepine binding sites in colonic adenocarcinoma. *Oncology*. 1990;47(2):139-42. doi:10.1159/000226806
86. Lacapere JJ, *et al*. Insight into the Structural Features of TSPO: Implications for Drug Development. *Trends Pharmacol Sci*. Dec 18 2019;doi:10.1016/j.tips.2019.11.005
87. Li H, *et al*. Peripheral-type benzodiazepine receptor function in cholesterol transport. Identification of a putative cholesterol recognition/interaction amino acid sequence and consensus pattern. *Endocrinology*. Dec 1998;139(12):4991-7. doi:10.1210/endo.139.12.6390
88. Li H, *et al*. Cholesterol binding at the cholesterol recognition/ interaction amino acid consensus (CRAC) of the peripheral-type benzodiazepine receptor and inhibition of steroidogenesis by an HIV TAT-CRAC peptide. *Proc Natl Acad Sci U S A*. Jan 30 2001;98(3):1267-72. doi:10.1073/pnas.031461598
89. Jamin N, *et al*. Characterization of the cholesterol recognition amino acid consensus sequence of the peripheral-type benzodiazepine receptor. *Mol Endocrinol*. Mar 2005;19(3):588-94. doi:10.1210/me.2004-0308
90. Jaipuria G, *et al*. Cholesterol-mediated allosteric regulation of the mitochondrial translocator protein structure. *Nat Commun*. Mar 30 2017;8:14893. doi:10.1038/ncomms14893
91. Jaremko L, *et al*. Structure of the mitochondrial translocator protein in complex with a diagnostic ligand. *Science*. Mar 21 2014;343(6177):1363-6. doi:10.1126/science.1248725
92. Li F, *et al*. Protein structure. Crystal structures of translocator protein (TSPO) and mutant mimic of a human polymorphism. *Science*. Jan 30 2015;347(6221):555-8. doi:10.1126/science.1260590
93. Korkhov VM, *et al*. Three-dimensional structure of TspO by electron cryomicroscopy of helical crystals. *Structure*. Jun 9 2010;18(6):677-87. doi:10.1016/j.str.2010.03.001
94. Iatmanen-Harbi S, *et al*. Characterization of the High-Affinity Drug Ligand Binding Site of Mouse Recombinant TSPO. *Int J Mol Sci*. Mar 21 2019;20(6) doi:10.3390/ijms20061444
95. Guo Y, *et al*. Protein structure. Structure and activity of tryptophan-rich TSPO proteins. *Science*. Jan 30 2015;347(6221):551-5. doi:10.1126/science.aaa1534
96. Jaipuria G, *et al*. Insights into Cholesterol/Membrane Protein Interactions Using Paramagnetic Solid-State NMR. *Chemistry*. Nov 27 2018;24(66):17606-17611. doi:10.1002/chem.201804550
97. Taylor JM, *et al*. Targeting mitochondrial 18 kDa translocator protein (TSPO) regulates macrophage cholesterol efflux and lipid phenotype. *Clin Sci (Lond)*. Nov 2014;127(10):603-13. doi:10.1042/CS20140047
98. Biswas L, *et al*. Retinal pigment epithelium cholesterol efflux mediated by the 18 kDa translocator protein, TSPO, a potential target for treating age-related macular degeneration. *Hum Mol Genet*. Nov 15 2017;26(22):4327-4339. doi:10.1093/hmg/ddx319
99. Elustondo P, *et al*. Mitochondrial cholesterol import. *Biochim Biophys Acta Mol Cell Biol Lipids*. Jan 2017;1862(1):90-101. doi:10.1016/j.bbalip.2016.08.012
100. Rone MB, *et al*. Cholesterol transport in steroid biosynthesis: role of protein-protein interactions and implications in disease states. *Biochim Biophys Acta*. Jul 2009;1791(7):646-58. doi:10.1016/j.bbalip.2009.03.001
101. Mari M, *et al*. Mitochondrial glutathione, a key survival antioxidant. *Antioxid Redox Signal*. Nov 2009;11(11):2685-700. doi:10.1089/ARS.2009.2695
102. Gatliff J, *et al*. TSPO is a REDOX regulator of cell mitophagy. *Biochem Soc Trans*. Aug 2015;43(4):543-52. doi:10.1042/BST20150037
103. Gatliff J, *et al*. A role for TSPO in mitochondrial Ca(2+) homeostasis and redox stress signaling. *Cell Death Dis*. Jun 22 2017;8(6):e2896. doi:10.1038/cddis.2017.186

104. Sileikyte J, *et al*. Regulation of the mitochondrial permeability transition pore by the outer membrane does not involve the peripheral benzodiazepine receptor (Translocator Protein of 18 kDa (TSPO)). *J Biol Chem*. May 16 2014;289(20):13769-81. doi:10.1074/jbc.M114.549634
105. Morohaku K, *et al*. Translocator protein/peripheral benzodiazepine receptor is not required for steroid hormone biosynthesis. *Endocrinology*. Jan 2014;155(1):89-97. doi:10.1210/en.2013-1556
106. Tu LN, *et al*. Peripheral benzodiazepine receptor/translocator protein global knock-out mice are viable with no effects on steroid hormone biosynthesis. *J Biol Chem*. Oct 3 2014;289(40):27444-54. doi:10.1074/jbc.M114.578286
107. Banati RB, *et al*. Positron emission tomography and functional characterization of a complete PBR/TSPO knockout. *Nat Commun*. Nov 19 2014;5:5452. doi:10.1038/ncomms6452
108. Fan J, *et al*. Conditional steroidogenic cell-targeted deletion of TSPO unveils a crucial role in viability and hormone-dependent steroid formation. *Proc Natl Acad Sci U S A*. Jun 9 2015;112(23):7261-6. doi:10.1073/pnas.1502670112
109. Owen DR, *et al*. TSPO mutations in rats and a human polymorphism impair the rate of steroid synthesis. *Biochem J*. Nov 21 2017;474(23):3985-3999. doi:10.1042/BCJ20170648
110. Barron AM, *et al*. Steroidogenic abnormalities in translocator protein knockout mice and significance in the aging male. *Biochem J*. Jan 2 2018;475(1):75-85. doi:10.1042/BCJ20170645
111. Barron AM, *et al*. Regulation of Anxiety and Depression by Mitochondrial Translocator Protein-Mediated Steroidogenesis: the Role of Neurons. *Mol Neurobiol*. Feb 2021;58(2):550-563. doi:10.1007/s12035-020-02136-5
112. Hauet T, *et al*. Peripheral-type benzodiazepine receptor-mediated action of steroidogenic acute regulatory protein on cholesterol entry into leydig cell mitochondria. *Mol Endocrinol*. Feb 2005;19(2):540-54. doi:10.1210/me.2004-0307
113. Kelly-Hershkovitz E, *et al*. Effects of peripheral-type benzodiazepine receptor antisense knockout on MA-10 Leydig cell proliferation and steroidogenesis. *J Biol Chem*. Mar 6 1998;273(10):5478-83. doi:10.1074/jbc.273.10.5478
114. Tu LN, *et al*. PK11195 effect on steroidogenesis is not mediated through the translocator protein (TSPO). *Endocrinology*. Mar 2015;156(3):1033-9. doi:10.1210/en.2014-1707
115. Fan J, *et al*. CRISPR/Cas9Mediated Tspo Gene Mutations Lead to Reduced Mitochondrial Membrane Potential and Steroid Formation in MA-10 Mouse Tumor Leydig Cells. *Endocrinology*. Feb 1 2018;159(2):1130-1146. doi:10.1210/en.2017-03065
116. Verma A, *et al*. Photodynamic tumor therapy: mitochondrial benzodiazepine receptors as a therapeutic target. *Mol Med*. Jan 1998;4(1):40-5.
117. Verma A, *et al*. Porphyrins are endogenous ligands for the mitochondrial (peripheral-type) benzodiazepine receptor. *Proc Natl Acad Sci U S A*. Apr 1987;84(8):2256-60. doi:10.1073/pnas.84.8.2256
118. Taketani S, *et al*. Involvement of peripheral-type benzodiazepine receptors in the intracellular transport of heme and porphyrins. *J Biochem*. Apr 1995;117(4):875-80. doi:10.1093/oxfordjournals.jbchem.a124790
119. Zhao AH, *et al*. Mitochondrial Translocator Protein (TSPO) Function Is Not Essential for Heme Biosynthesis. *J Biol Chem*. Jan 22 2016;291(4):1591-1603. doi:10.1074/jbc.M115.686360
120. Milenkovic VM, *et al*. CRISPR-Cas9 Mediated TSPO Gene Knockout alters Respiration and Cellular Metabolism in Human Primary Microglia Cells. *Int J Mol Sci*. Jul 9 2019;20(13)doi:10.3390/ijms20133359
121. Urbani A, *et al*. Purified F-ATP synthase forms a Ca(2+)-dependent high-conductance channel matching the mitochondrial permeability transition pore. *Nat Commun*. Sep 25 2019;10(1):4341. doi:10.1038/s41467-019-12331-1
122. Owen DR, *et al*. An 18-kDa translocator protein (TSPO) polymorphism explains differences in binding affinity of the PET radioligand PBR28. *J Cereb Blood Flow Metab*. Jan 2012;32(1):1-5. doi:10.1038/jcbfm.2011.147
123. Costa B, *et al*. Ala147Thr substitution in translocator protein is associated with adult separation anxiety in patients with depression. *Psychiatr Genet*. Apr 2009;19(2):110-1. doi:10.1097/YPG.0b013e32832080f6
124. Nakamura K, *et al*. Evidence that variation in the peripheral benzodiazepine receptor (PBR) gene influences susceptibility to panic disorder. *Am J Med Genet B Neuropsychiatr Genet*. Apr 5 2006;141B(3):222-6. doi:10.1002/ajmg.b.30211
125. Colasanti A, *et al*. Bipolar Disorder is associated with the rs6971 polymorphism in the gene encoding 18 kDa Translocator Protein (TSPO). *Psychoneuroendocrinology*. Nov 2013;38(11):2826-9. doi:10.1016/j.psyneuen.2013.07.007
126. Da Pozzo E, *et al*. Translocator protein (TSPO) and neurosteroids: implications in psychiatric disorders. *Curr Mol Med*. May 2012;12(4):426-42. doi:10.2174/156652412800163451
127. Rupprecht R, *et al*. Translocator protein (18 kD) as target for anxiolytics without benzodiazepine-like side effects. *Science*. Jul 24 2009;325(5939):490-3. doi:10.1126/science.1175055
128. Owen DR, *et al*. Variation in binding affinity of the novel anxiolytic XBD173 for the 18 kDa translocator protein in human brain. *Synapse*. Mar 2011;65(3):257-9. doi:10.1002/syn.20884
129. Costa B, *et al*. The spontaneous Ala147Thr amino acid substitution within the translocator

protein influences pregnenolone production in lymphomonocytes of healthy individuals. *Endocrinology*. Dec 2009;150(12):5438-45. doi:10.1210/en.2009-0752
130. Prossin AR, *et al*. Functional TSPO polymorphism predicts variance in the diurnal cortisol rhythm in bipolar disorder. *Psychoneuroendocrinology*. Mar 2018;89:194-202. doi:10.1016/j.psyneuen.2018.01.013
131. Fan J, *et al*. Structural and functional evolution of the translocator protein (18 kDa). *Curr Mol Med*. May 2012;12(4):369-86. doi:10.2174/1566524011207040369
132. Yeliseev AA, *et al*. A sensory transducer homologous to the mammalian peripheral-type benzodiazepine receptor regulates photosynthetic membrane complex formation in Rhodobacter sphaeroides 2.4.1. *J Biol Chem*. Sep 8 1995;270(36):21167-75. doi:10.1074/jbc.270.36.21167
133. Yeliseev AA, *et al*. A mammalian mitochondrial drug receptor functions as a bacterial "oxygen" sensor. *Proc Natl Acad Sci U S A*. May 13 1997;94(10):5101-6. doi:10.1073/pnas.94.10.5101
134. Fan J, *et al*. Translocator protein 2 is involved in cholesterol redistribution during erythropoiesis. *J Biol Chem*. Oct 30 2009;284(44):30484-97. doi:10.1074/jbc.M109.029876
135. Betlazar C, *et al*. Cellular Sources and Regional Variations in the Expression of the Neuroinflammatory Marker Translocator Protein (TSPO) in the Normal Brain. *Int J Mol Sci*. Sep 11 2018;19(9)doi:10.3390/ijms19092707
136. Lavisse S, *et al*. Reactive astrocytes overexpress TSPO and are detected by TSPO positron emission tomography imaging. *J Neurosci*. Aug 8 2012;32(32):10809-18. doi:10.1523/JNEUROSCI.1487-12.2012
137. Pannell M, *et al*. Imaging of translocator protein upregulation is selective for pro-inflammatory polarized astrocytes and microglia. *Glia*. Sep 3 2019;doi:10.1002/glia.23716
138. Pulagam KR, *et al*. Evaluation of the novel TSPO radiotracer [(18)F] VUIIS1008 in a preclinical model of cerebral ischemia in rats. *EJNMMI Res*. Nov 25 2017;7(1):93. doi:10.1186/s13550-017-0343-7
139. Rojas S, *et al*. Imaging brain inflammation with [(11)C]PK11195 by PET and induction of the peripheral-type benzodiazepine receptor after transient focal ischemia in rats. *J Cereb Blood Flow Metab*. Dec 2007;27(12):1975-86. doi:10.1038/sj.jcbfm.9600500
140. Li HD, *et al*. A translocator protein 18 kDa agonist protects against cerebral ischemia/reperfusion injury. *J Neuroinflammation*. Jul 28 2017;14(1):151. doi:10.1186/s12974-017-0921-7
141. Banati RB, *et al*. The peripheral benzodiazepine binding site in the brain in multiple sclerosis: quantitative in vivo imaging of microglia as a measure of disease activity. *Brain*. Nov 2000;123 (Pt 11):2321-37. doi:10.1093/brain/123.11.2321
142. Daugherty DJ, *et al*. A TSPO ligand is protective in a mouse model of multiple sclerosis. *EMBO Mol Med*. Jun 2013;5(6):891-903. doi:10.1002/emmm.201202124
143. Daugherty DJ, *et al*. The hGFAP-driven conditional TSPO knockout is protective in a mouse model of multiple sclerosis. *Sci Rep*. Mar 1 2016;6:22556. doi:10.1038/srep22556
144. Nack A, *et al*. Expression of Translocator Protein and [18F]-GE180 Ligand Uptake in Multiple Sclerosis Animal Models. *Cells*. Jan 28 2019;8(2)doi:10.3390/cells8020094
145. Zinnhardt B, *et al*. Molecular Imaging of Immune Cell Dynamics During De- and Remyelination in the Cuprizone Model of Multiple Sclerosis by [(18)F]DPA-714 PET and MRI. *Theranostics*. 2019;9(6):1523-1537. doi:10.7150/thno.32461
146. Ji B, *et al*. Imaging of peripheral benzodiazepine receptor expression as biomarkers of detrimental versus beneficial glial responses in mouse models of Alzheimer's and other CNS pathologies. *J Neurosci*. Nov 19 2008;28(47):12255-67. doi:10.1523/JNEUROSCI.2312-08.2008
147. Esquerda-Canals G, *et al*. Mouse Models of Alzheimer's Disease. *J Alzheimers Dis*. 2017;57(4):1171-1183. doi:10.3233/JAD-170045
148. Liu B, *et al*. In Vivo Detection of Age- and Disease-Related Increases in Neuroinflammation by 18F-GE180 TSPO MicroPET Imaging in Wild-Type and Alzheimer's Transgenic Mice. *J Neurosci*. Nov 25 2015;35(47):15716-30. doi:10.1523/JNEUROSCI.0996-15.2015
149. Sacher C, *et al*. Longitudinal PET Monitoring of Amyloidosis and Microglial Activation in a Second Generation Amyloid-beta Mouse Model. *J Nucl Med*. Jul 13 2019;doi:10.2967/jnumed.119.227322
150. Tournier BB, *et al*. TSPO and amyloid deposits in sub-regions of the hippocampus in the 3xTgAD mouse model of Alzheimer's disease. *Neurobiol Dis*. Jan 2019;121:95-105. doi:10.1016/j.nbd.2018.09.022
151. Mirzaei N, *et al*. In vivo imaging of microglial activation by positron emission tomography with [(11)C]PBR28 in the 5XFAD model of Alzheimer's disease. *Glia*. Jun 2016;64(6):993-1006. doi:10.1002/glia.22978
152. Notter T, *et al*. Translational evaluation of translocator protein as a marker of neuroinflammation in schizophrenia. *Mol Psychiatry*. Jan 17 2017;doi:10.1038/mp.2016.248
153. Gong J, *et al*. Translocator Protein Ligand Protects against Neurodegeneration in the MPTP Mouse Model of Parkinsonism. *J Neurosci*. May 8 2019;39(19):3752-3769. doi:10.1523/JNEUROSCI.2070-18.2019
154. Pannell M, *et al*. Imaging of translocator protein upregulation is selective for pro-inflammatory polarized astrocytes and microglia. *Glia*. Feb 2020;68(2):280-297. doi:10.1002/glia.23716

155. Chiang T, *et al*. Mouse model of middle cerebral artery occlusion. *J Vis Exp*. Feb 13 2011;(48) doi:10.3791/2761
156. Constantinescu CS, *et al*. Experimental autoimmune encephalomyelitis (EAE) as a model for multiple sclerosis (MS). *Br J Pharmacol*. Oct 2011;164(4):1079-106. doi:10.1111/j.1476-5381.2011.01302.x
157. Torkildsen O, *et al*. The cuprizone model for demyelination. *Acta Neurol Scand Suppl*. 2008;188:72-6. doi:10.1111/j.1600-0404.2008.01036.x
158. James ML, *et al*. PET imaging of translocator protein (18 kDa) in a mouse model of Alzheimer's disease using N-(2,5-dimethoxybenzyl)-2-18F-fluoro-N-(2-phenoxyphenyl)acetamide. *J Nucl Med*. Feb 2015;56(2):311-6. doi:10.2967/jnumed.114.141648
159. Rapic S, *et al*. Imaging microglial activation and glucose consumption in a mouse model of Alzheimer's disease. *Neurobiol Aging*. Jan 2013;34(1):351-4. doi:10.1016/j.neurobiolaging.2012.04.016
160. Serriere S, *et al*. Amyloid load and translocator protein 18 kDa in APPswePS1-dE9 mice: a longitudinal study. *Neurobiol Aging*. Apr 2015;36(4):1639-52. doi:10.1016/j.neurobiolaging.2014.11.023
161. Tournier BB, *et al*. In Vivo TSPO Signal and Neuroinflammation in Alzheimer's Disease. *Cells*. Aug 21 2020;9(9)doi:10.3390/cells9091941
162. Notter T, *et al*. Translational evaluation of translocator protein as a marker of neuroinflammation in schizophrenia. *Mol Psychiatry*. Feb 2018;23(2):323-334. doi:10.1038/mp.2016.248
163. Beckers L, *et al*. Increased Expression of Translocator Protein (TSPO) Marks Pro-inflammatory Microglia but Does Not Predict Neurodegeneration. *Mol Imaging Biol*. Feb 2018;20(1):94-102. doi:10.1007/s11307-017-1099-1
164. Owen DR, *et al*. Pro-inflammatory activation of primary microglia and macrophages increases 18 kDa translocator protein expression in rodents but not humans. *J Cereb Blood Flow Metab*. Aug 2017;37(8):2679-2690. doi:10.1177/0271678X17710182
165. Tong J, *et al*. Concentration, distribution, and influence of aging on the 18 kDa translocator protein in human brain: Implications for brain imaging studies. *J Cereb Blood Flow Metab*. May 2020;40(5):1061-1076. doi:10.1177/0271678X19858003
166. Yokokura M, *et al*. Depiction of microglial activation in aging and dementia: Positron emission tomography with [(11)C]DPA713 versus [(11)C](R)PK11195. *J Cereb Blood Flow Metab*. Mar 2017;37(3):877-889. doi:10.1177/0271678X16646788
167. Paul S, *et al*. Building a database for brain 18 kDa translocator protein imaged using [(11)C]PBR28 in healthy subjects. *J Cereb Blood Flow Metab*. Jun 2019;39(6):1138-1147. doi:10.1177/0271678X18771250
168. Cosenza-Nashat M, *et al*. Expression of the translocator protein of 18 kDa by microglia, macrophages and astrocytes based on immunohistochemical localization in abnormal human brain. *Neuropathol Appl Neurobiol*. Jun 2009;35(3):306-28. doi:10.1111/j.1365-2990.2008.01006.x
169. Werry EL, *et al*. Recent Developments in TSPO PET Imaging as A Biomarker of Neuroinflammation in Neurodegenerative Disorders. *Int J Mol Sci*. Jun 28 2019;20(13)doi:10.3390/ijms20133161
170. Nutma E, *et al*. A quantitative neuropathological assessment of translocator protein expression in multiple sclerosis. *Brain*. Oct 3 2019;doi:10.1093/brain/awz287
171. Peferoen LA, *et al*. Activation status of human microglia is dependent on lesion formation stage and remyelination in multiple sclerosis. *J Neuropathol Exp Neurol*. Jan 2015;74(1):48-63. doi:10.1097/NEN.0000000000000149
172. Vogel DY, *et al*. Macrophages in inflammatory multiple sclerosis lesions have an intermediate activation status. *J Neuroinflammation*. Mar 4 2013;10:35. doi:10.1186/1742-2094-10-35
173. Zhang D, *et al*. Astrogliosis in CNS pathologies: is there a role for microglia? *Mol Neurobiol*. Jun 2010;41(2-3):232-41. doi:10.1007/s12035-010-8098-4
174. Guilarte TR. TSPO in diverse CNS pathologies and psychiatric disease: A critical review and a way forward. *Pharmacol Ther*. Sep 4 2018;doi:10.1016/j.pharmthera.2018.09.003
175. Gui Y, *et al*. Characterization of the 18 kDa translocator protein (TSPO) expression in post-mortem normal and Alzheimer's disease brains. *Brain Pathol*. Jul 5 2019;doi:10.1111/bpa.12763
176. Xu J, *et al*. Translocator protein in late stage Alzheimer's disease and Dementia with Lewy bodies brains. *Ann Clin Transl Neurol*. Aug 2019;6(8):1423-1434. doi:10.1002/acn3.50837
177. Iaccarino L, *et al*. An In Vivo (11)C-(R)-PK11195 PET and In Vitro Pathology Study of Microglia Activation in Creutzfeldt-Jakob Disease. *Mol Neurobiol*. Apr 2018;55(4):2856-2868. doi:10.1007/s12035-017-0522-6
178. Holmes SE, *et al*. Elevated Translocator Protein in Anterior Cingulate in Major Depression and a Role for Inflammation in Suicidal Thinking: A Positron Emission Tomography Study. *Biol Psychiatry*. Jan 1 2018;83(1):61-69. doi:10.1016/j.biopsych.2017.08.005
179. Setiawan E, *et al*. Association of translocator protein total distribution volume with duration of untreated major depressive disorder: a cross-sectional study. *Lancet Psychiatry*. Apr 2018;5(4):339-347. doi:10.1016/S2215-0366(18)30048-8

180. Li H, *et al*. Translocator protein (18kDa TSPO) binding, a marker of microglia, is reduced in major depression during cognitive-behavioral therapy. *Prog Neuropsychopharmacol Biol Psychiatry*. Apr 20 2018;83:1-7. doi:10.1016/j.pnpbp.2017.12.011
181. Weidner LD, *et al*. The expression of inflammatory markers and their potential influence on efflux transporters in drug-resistant mesial temporal lobe epilepsy tissue. *Epilepsia*. Aug 2018;59(8):1507-1517. doi:10.1111/epi.14505
182. Kuszpit K, *et al*. [(18)F]DPA-714 PET Imaging Reveals Global Neuroinflammation in Zika Virus-Infected Mice. *Mol Imaging Biol*. Apr 2018;20(2):275-283. doi:10.1007/s11307-017-1118-2
183. Doorduin J, *et al*. [11C]-DPA-713 and [18F]-DPA-714 as new PET tracers for TSPO: a comparison with [11C]-(R)-PK11195 in a rat model of herpes encephalitis. *Mol Imaging Biol*. Nov-Dec 2009;11(6):386-98. doi:10.1007/s11307-009-0211-6
184. Parente A, *et al*. Pharmacokinetic Analysis of 11C-PBR28 in the Rat Model of Herpes Encephalitis: Comparison with (R)-11C-PK11195. *J Nucl Med*. May 2016;57(5):785-91. doi:10.2967/jnumed.115.165019
185. Vallez Garcia D, *et al*. Evaluation of [(11)C]CB184 for imaging and quantification of TSPO overexpression in a rat model of herpes encephalitis. *Eur J Nucl Med Mol Imaging*. Jun 2015;42(7):1106-18. doi:10.1007/s00259-015-3021-x
186. De Picker LJ, *et al*. Microglia and Brain Plasticity in Acute Psychosis and Schizophrenia Illness Course: A Meta-Review. *Front Psychiatry*. 2017;8:238. doi:10.3389/fpsyt.2017.00238
187. Plaven-Sigray P, *et al*. Meta-analysis of the Glial Marker TSPO in Psychosis Revisited: Reconciling Inconclusive Findings of Patient-Control Differences. *Biol Psychiatry*. Feb 1 2021;89(3):e5-e8. doi:10.1016/j.biopsych.2020.05.028
188. Plaven-Sigray P, *et al*. Meta-analytic studies of the glial cell marker TSPO in psychosis - a question of apples and pears? *Psychol Med*. Jul 2019;49(10):1624-1628. doi:10.1017/S003329171800421X
189. Plaven-Sigray P, *et al*. Positron Emission Tomography Studies of the Glial Cell Marker Translocator Protein in Patients With Psychosis: A Meta-analysis Using Individual Participant Data. *Biol Psychiatry*. Sep 15 2018;84(6):433-442. doi:10.1016/j.biopsych.2018.02.1171
190. Meyer JH, *et al*. Neuroinflammation in psychiatric disorders: PET imaging and promising new targets. *Lancet Psychiatry*. Dec 2020;7(12):1064-1074. doi:10.1016/S2215-0366(20)30255-8
191. Scaini G, *et al*. TSPO upregulation in bipolar disorder and concomitant downregulation of mitophagic proteins and NLRP3 inflammasome activation. *Neuropsychopharmacology*. Jun 2019;44(7):1291-1299. doi:10.1038/s41386-018-0293-4
192. Tournier BB, *et al*. Fluorescence-activated cell sorting to reveal the cell origin of radioligand binding. *J Cereb Blood Flow Metab*. Jun 2020;40(6):1242-1255. doi:10.1177/0271678X19860408
193. Tournier BB, *et al*. Astrocytic TSPO Upregulation Appears Before Microglial TSPO in Alzheimer's Disease. *J Alzheimers Dis*. Aug 14 2020;doi:10.3233/JAD-200136

PART II

Multiple Sclerosis Pathology


6

Synaptic loss in multiple sclerosis spinal cord

Erik Nutma, Natalia Petrova, Daniele Carassiti, James R Newman, Sandra Amor, Daniel R Altmann, David Baker, Klaus Schmierer

Annals of Neurology 2020 88(3):619-625

Abstract

Disability in multiple sclerosis (MS) is considered primarily a result of axonal loss. However, correlation with spinal cord cross-sectional area-a predictor of disability-is poor, questioning the unique role of axonal loss. We investigated the degree of synaptic loss in postmortem spinal cords (18 chronic MS, 8 healthy controls) using immunohistochemistry for synaptophysin and synapsin. Substantial (58-96%) loss of synapses throughout the spinal cord was detected, along with moderate (47%) loss of anterior horn neurons, notably in demyelinating MS lesions. We conclude that synaptic loss is significant in chronic MS, likely contributing to disability accrual.

Introduction

Multiple sclerosis (MS) is an inflammatory demyelinating and degenerative disease of the central nervous system and a major cause of chronic disability in young adults[1]. Although 85% of people with MS (pwMS) initially experience a relapsing phenotype, most will develop chronic neurological dysfunction (progressive MS). Magnetic resonance imaging (MRI) is commonly used to support diagnosis and monitoring of pwMS. Although MRI lesion volume has been shown to be a useful predictor of disease activity, its value as an outcome is limited in people with progressive MS[2]. Volumetric indices of the whole brain, or segmented proportions thereof[3], as well as the spinal cord[4] appear to provide better outcome prediction. Given the reported correlation between indices of spinal cord cross-sectional area (CSA) and disability[5-7], and earlier evidence suggesting axonal loss as the key driver of chronic disability[8,9], we were surprised to find no correlation between axonal loss and CSA in a recent study of whole postmortem spinal cords[10]. Because synaptic damage has been recognized as an important feature of MS in the brain[11,12], we investigated whether such damage also occurs in the spinal cord, thereby potentially providing an additional substrate of chronic disease deterioration, and of CSA shrinkage. We addressed the following 3 questions: (1) What is the extent of synaptic loss in the MS spinal cord? (2) Does synaptic loss correlate with neuronal loss? (3) Do CSA and/or spinal cord gray matter (GM) area provide noninvasive substrates of synaptic damage?

Materials and methods

The protocol for this study received prior approval by the review board of the Multiple Sclerosis and Parkinson's Tissue Bank covered by Ethical Approval 08/MRE09/31+5 (Research Ethics Committee for Wales; Integrated Research Application System project ID 126869).

Tissue sampling and immunohistochemistry

Two blocks each of cervical, thoracic, and lumbar cord levels were selected, and serial 10µm-thick sections were cut using a Shandon Finesse ME+ microtome (Thermo Fisher Scientific, Dartford, UK), mounted on Superfrost+ slides (VWR, Lutterworth, UK) and left at 60°C overnight. Sections were stained with hematoxylin and eosin (H&E), and immunohistochemistry was undertaken using primary antibodies against myelin basic protein (MBP; SMI-94, mouse monoclonal, 1:100; Covance, Princeton, NJ), synapsin-1 (polyclonal rabbit, 1:100, NB300-104; Novus Biologicals, Littleton, CO), and synaptophysin (Dako Omnis FLEX Ready-to-Use monoclonal mouse anti-human, clone DAK-SYNAP; Agilent, Stockport, UK). Synapsin-1 immunostaining was done manually; for synaptophysin immunostaining, a Dako (Carpinteria, CA) autostainer was used (Figs 1 and 2).

Area measurements

The area of GM demyelination (if any) within the anterior horn boundaries was measured on MBP sections, whereas H&E sections were used to measure CSA and anterior horn GM area at low magnification (objective ×4). The total number of neurons within each anterior horn was counted at higher magnification (objective ×20) on H&E sections (see Fig 2).

Quantification of synapses

Sections immunostained for synaptophysin and synapsin-1 were scanned using a SlideScanner (C12000 NanoZoomer-XR Digital slide scanner; Hamamatsu Photonics, Welwyn Garden City, UK) and stored as Nanozoomer Digital Pathology image files. To assess transmittance (T),

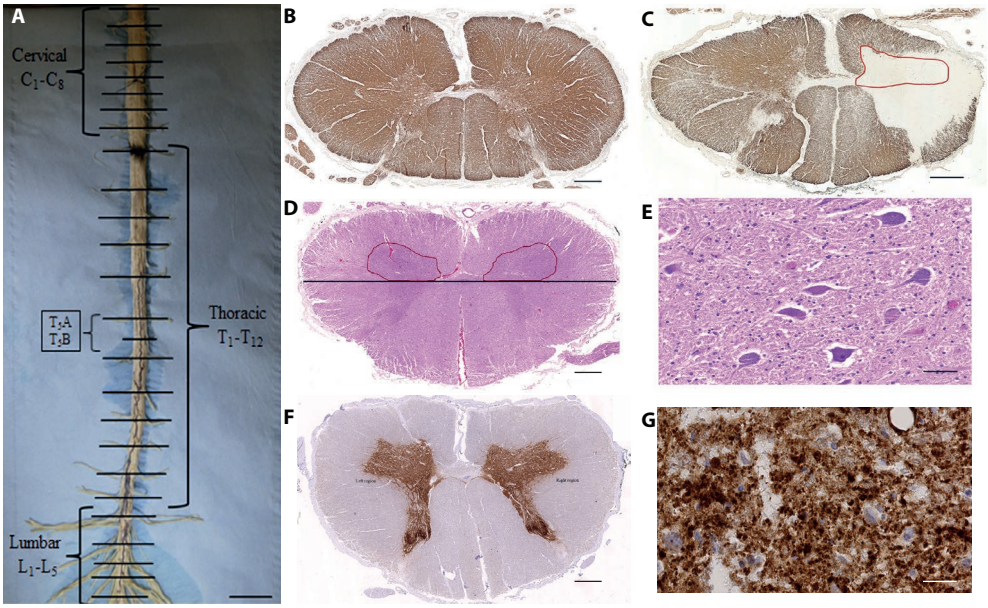

Figure 1. Spinal cord dissection and immunohistochemistry. (A) The distance between thoracic level 2 and lumbar level 5 was recorded after identifying all available spinal cord nerve roots, and axial blocks were dissected at each level. (B, C) Ten-micrometer-thick sections were immunostained for myelin basic protein on all available control (B) and multiple sclerosis sections (C). (D, E) Sequential sections were also stained with hematoxylin and eosin (D) and viewed at ×20 magnification (E) to count the number of neurons in each anterior horn. (G, H) Spinal cord sections were also immunostained for synaptophysin. Scale bar for spinal cord dissection (A), 1cm; scale bars for low-magnification images (B–D, F), 1mm; scale bars for high-magnification images (E, G), 50µm.

defined as the transmitted light divided by the incident light, synaptophysin images were opened using ONCOtopix software (Visiopharm, Hørsholm, Denmark) and measured in each anterior horn using the "intensity" tool. Light intensity is based on transformation of images into gray scale ranging from 0 to 255. Given that 0 represents absolute black and 255 represents white, low-intensity values represent the most intense staining. Thus, to render readings more intuitive (higher values meaning higher synaptic density) the results are reported as 1/T. To assess the synaptic bouton area, images of synaptophysin and synapsin-1 staining were opened using NDP.view2 (U12388-01NDP.view2, Hamamatsu Photonics) viewing software and inspected by zooming in from objective ×1.25 to ×80 magnification. Given the size of motor neurons, a ×20 objective was most suitable for assessment of synaptic bouton area. Using the "freehand region" selection tool, the total synaptic bouton area was outlined on a mean of 5 neurons (area size: at least 200µm2) per anterior horn (see Fig 2).

Statistics

Linear mixed models, with random subject intercepts to allow for within-subject dependency, were used both to compare measures between slice types and to examine association between measures. Where residuals suggested the possibility of heteroscedasticity or non-normality, robust standard errors or bootstrap was used to confirm or correct confidence intervals and p values.

Results

Clinicopathological data

A total of n = 154 tissue blocks from 26 subjects, 8 healthy controls (mean age = 82 ± 6 years), and 18 pwMS (mean age = 65 ± 11 years, disease duration = 29 ± 11 years) were included in the study. A total of n = 122 of 154 tissue blocks from 22 of 26 subjects, 7 healthy controls (mean age = 82 ± 7 years), and 15 pwMS (mean age = 69 ± 11 years, disease duration = 29 ± 11 years) were included for analysis of synaptophysin immunostaining.

To explore whether synaptic pathology is detectable using a different epitope, a total of n = 51 of 154 tissue blocks from 20 subjects, 7 healthy controls, and 13 pwMS were immunostained for synapsin. To explore the possible impact of the duration of fixation on the immunostaining in our samples, n = 9 tissue blocks from 9 subjects, 3 healthy controls, and 6 pwMS were used where tissue had been fixed in 10% neutral buffered formalin for 3 weeks, cryoprotected in 30% sucrose for 2 weeks, and then snap-frozen in isopentane cooled over dry ice. Mean time in these cases between death and tissue fixation was 18 ± 5 hours. All remaining blocks used in this study were from samples that had been fixed, following a mean time between death and tissue fixation of 36 ± 17 hours, in 4% formalin solution for a mean of 30 ± 24 months before processing.

In 3 of 154 blocks, mononuclear cells suggestive of inflammation were detected. For the remainder of tissue blocks, cellularity was decreased in areas of demyelination compared to the surrounding nonlesional tissue. However, cellularity in nonlesional tissue was indistinguishable from control tissue, with no changes suggestive of inflammation. Against this backdrop, no systematic assessment of inflammatory cells was undertaken.

Synaptic pathology is extensive in MS

Visual inspection of synaptophysin and synapsin immunostained sections revealed significant difference in staining intensity between MS and controls; 1/T was reduced by 54% in nonlesional GM ($p < 0.001$) and 58% in GM lesions ($p < 0.001$). Synaptophysin intensity in GM lesions was significantly less pronounced than in the nonlesional GM (9%, $p = 0.004$; Fig 3A, B, E). Using synaptophysin immunostained sections, the synaptic bouton area in MS was reduced by 92% in nonlesional GM and 96% in GM lesions ($p < 0.001$) compared to controls, with a moderate difference between nonlesional and lesional GM (42%, $p < 0.001$; see Fig 3C, D, F). In synapsin-1 immunostained sections, we detected a 58% lower synaptic bouton area in MS compared to controls ($p < 0.001$; see Fig 2J–L). In synaptophysin stained sections, short fixation time was associated with a nonsignificantly (7%) lower synaptic bouton area compared to sections of tissue that underwent a long fixation time. In synapsin-1 stained sections, short fixation time was associated with a nonsignificantly (2%) lower synaptic bouton area compared to sections of tissue that underwent a long fixation time.

Loss of synapses does not correlate with anterior horn area, or with the number of neurons

Using synaptophysin stained sections, strong correlation was detected between synaptic bouton and anterior horn GM area in controls ($p < 0.001$), but not in MS. Similarly, the

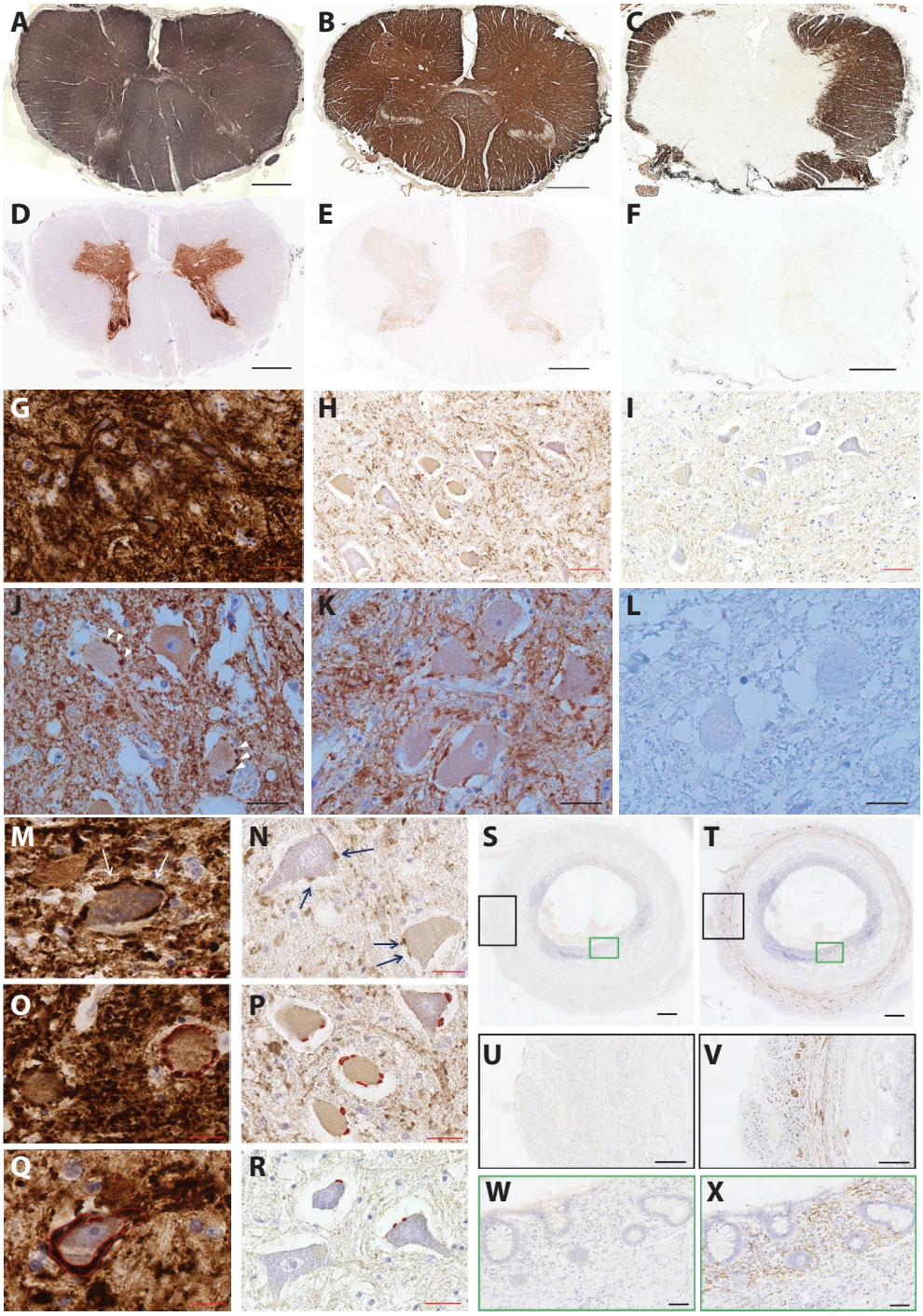
A
B
C
D
E
F
G
H
I
J
K
L
M
N
S
T
O
P
U
V
Q
R
W
X

Figure 2. Immunostaining for synaptic proteins, and synaptic bouton area quantification. (A–C) Myelin basic protein (MBP) immunostained sections from control (A) and multiple sclerosis (MS) cases (B, C) were reviewed. MS anterior horns were classified as nonlesional (B) or lesional (C) based on the presence of myelin on MBP sections. (D–I) Synaptophysin intensity was quantified in control (D, G), nonlesional (E, H), and lesional gray matter sections (F, I). (J, K, M–R) The area of synaptic boutons (white arrowheads in J, arrows in M and N) was assessed on high-magnification sections using (1) synapsin-1 in control (J) and MS sections (K), and (2) synaptophysin in control (M, O, Q) and MS sections (N, P, R). (M–R) The area of synaptic boutons around an average of 5 neurons was measured by outlining their boundaries, as shown in red. (L) Negative controls were run during synapsin-1 immunostaining. (S–X) Negative (S, U, W) and positive (T, V, X) controls were run for synaptophysin immunostaining. Scale bars = 1mm in A–F, 50µm in G–L, 10µm in J–R, 500µm in S and T, 100µm in U and V, and 50µm in W and X. Black rectangles in S and T are magnified in U and V; green rectangles in S and T are magnified in W and X.

relationship between synaptic bouton area and the number of neurons was significant ($p < 0.001$) in controls only. The relationship between synaptic bouton area and (1) GM area ($p < 0.001$) and (2) CSA ($p = 0.005$) was only significant in controls.

Discussion

Axonal loss has been considered the main substrate of chronic disability in pwMS[8], with approximately 60% of long spinal cord axons being lost approximately 30 years after diagnosis[10]. Although the figure of 60% indicates extensive axonal loss, comparison with other spinal cord pathologies raises important questions about additional factors involved in the progressive disability accrual of pwMS.

Animal models of traumatic spinal cord injury suggest preservation of as little as 8% of axons may enable useful limb movements[13], and the case of a 38-year-old man who regained lower limb control sufficient to walk (with assistance) after a near-complete traumatic spinal cord transection[14] indicates that a much smaller number of preserved long tract axons than the 40% detected in pwMS may suffice for meaningful leg function. The pwMS from which our samples were obtained, however, were invariably wheelchair bound due to loss of lower limb function. Thus, loss of long motor tracts is unlikely to fully explain the degree of motor dysfunction, particularly of the lower limbs, in pwMS. Given that synaptic loss was detectable throughout the cord, including the cervical level, which is associated with upper limb control, it is unlikely that this loss is solely due to a lack of sensory input and/or motor output secondary to immobility.

Synaptic loss in MS has previously been described in the cerebral GM, including the hippocampus, and the cerebellar dentate nucleus[11,12,15]. Although our results are not inconsistent with a possible effect of demyelination on synaptic survival, the key finding is of substantial synaptic loss throughout the spinal cord, corroborating recent work describing extensive synaptic spine density reduction in both myelinated and demyelinated neocortex[16].

We recently confirmed that CSA is not associated with axonal density[10]. Against this backdrop, the correlation between several measures of spinal cord area and synaptic bouton areas in control sections highlights the nature of the spinal cord as a self-regulatory network[17], rather than merely a conduit for long axonal tract fibers.

Neuronal damage and loss in pwMS can be extensive[11]. In a recent stereological study, we reported that after nearly 30 years disease duration, pwMS will have lost almost 40% of their neocortical neurons irrespective of the presence of demyelination[18]. The degree of neuronal loss in the current study (47%) is higher than previously reported[19], perhaps reflecting

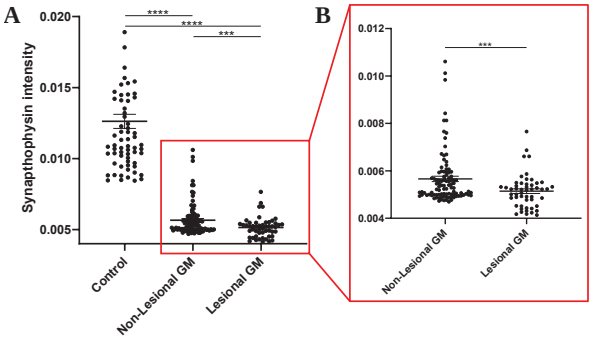

E

Synaptophysin intensity

	Absolute difference	% difference	P-value
Control - NLGM	0.006703	54	<0.001
Control - GML	0.007219	58	<0.001
NLGM - GML	0.000519	9	0.004

Synaptic bouton area (μm²)

	Absolute difference	% difference	P-value
Control - NLGM	282.6	92	<0.001
Control - GML	294.3	96	<0.001
NLGM - GML	11.7	42	<0.001

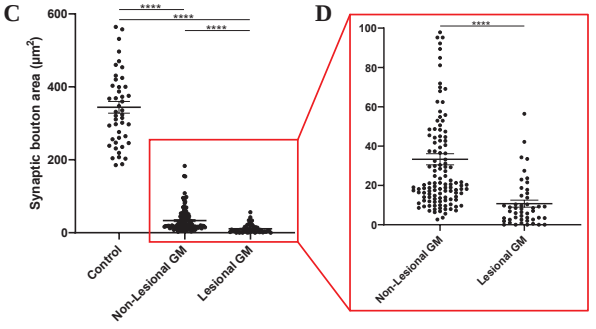

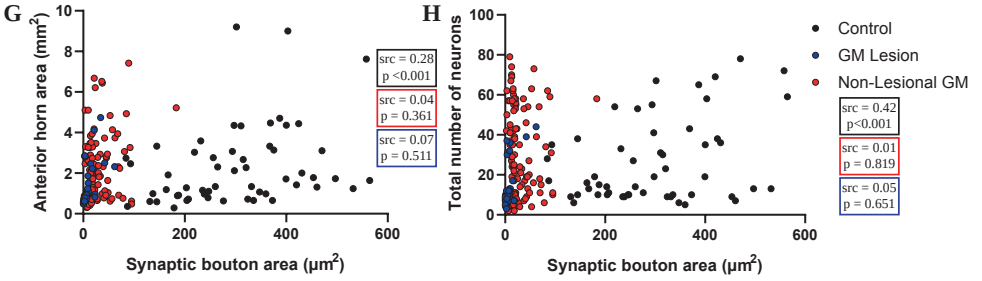

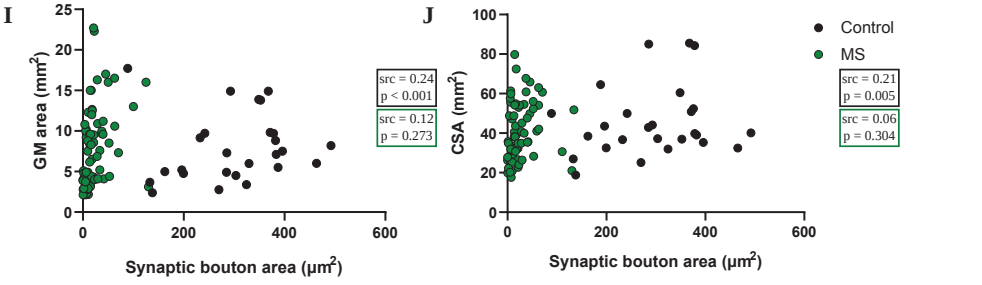

Figure 3. Synaptic change comparison between control, nonlesional, and lesional gray matter (GM). (A, B) The difference in synaptophysin intensity between control, nonlesional, and lesional anterior horns is shown in A, with the comparison between the 2 multiple sclerosis (MS) groups shown at higher magnification in B. (C, D) Synaptic bouton area differences between control and MS anterior horns are shown in C, whereas the high-magnification graph in D shows only data corresponding to the lesional and nonlesional anterior horns. (E) The absolute and percentage differences between groups. (F) The difference in the number of neurons between control and MS sections. (G, H) The relationship between synaptic bouton area and anterior horn area is shown in G, whereas the relationship between synaptic bouton area and number of neurons is shown in H separately for sections from control cases (black circles), and MS sections with nonlesional (red circles) and lesional anterior horns (blue circles). (I, J) The correlations show the relationship between synaptic bouton area and (1) GM (I) and (2) cross-sectional area (CSA; J). Two separate standardized regression coefficient (src) and p values are provided and correspond to control (black circles) and MS (green circles) sections, respectively. All p values are from linear mixed models allowing for multiple slices per patient and adjusting for side. Error bars represent standard deviation. **p <0.05, ***p <0.01, ****p <0.001. GML = lesional GM; NLGM = nonlesional GM.

differences in disease duration and/or severity between studies. Although the magnitude of neuronal loss detected is substantial, it is proportionally lower than the synaptic loss, certainly when synaptophysin is used as a marker. The difference in the magnitude of change in synaptophysin and synapsin immunostaining is likely explained by their differential expression and function[20].

Synapsin and synaptophysin are the most abundant synaptic vesicle proteins, with distinct functional roles. They are the most commonly used markers for presynaptic terminals, with synapsin being the most specific marker for presynaptic terminals[21]. Synapsin is the major peripheral membrane protein, accounting for 6% of the total synaptic vesicle protein[22]. It regulates the reserve pool of synaptic vesicles available for exocytosis[23], and maintains the organization and abundance of vesicles at presynaptic terminals[24]. Synaptophysin is the major integral membrane protein, accounting for 6 to 10% of total synaptic vesicle protein[25-27], regulating the kinetics of synaptic vesicle endocytosis[28], and synaptic vesicle retrieval through its interaction with synaptobrevin[29]. Synapsin is found at all glutamatergic and γ-aminobutyric acidergic (GABAergic) synaptic boutons, whereas synaptophysin levels are highest at glutamatergic and very low at GABAergic terminals[21,30]. Importantly, the development of both synapsin and synaptophysin expression is required for the maturation of presynaptic function and stabilization of presynaptic boutons[31]. Furthermore, the balance between these proteins will affect vesicle cycling and likely impact the probability of transmitter release, especially after strong or sustained stimulation.

The mechanisms and timing involved in synaptic injury and loss remain to be established. Studies using material of pwMS at earlier disease stages may allow establishing the sequence of events leading up to the extensive synaptic loss, which may have been partially confounded by lower limb inactivity.

In animal models of MS, synaptic loss has been shown to be associated with changes in the balance of inhibitory and excitatory neurotransmission as a consequence of inflammation[32]. However, analysis of the relationship between inflammation and synaptic damage was not possible due to the scarcity of inflammation in our tissue samples[10]. A cellular infiltrate suggestive of inflammatory activity was only detected in 3 of 154 blocks of our sample. Evidence suggests the main signature of inflammation in the spinal cord may be located in the meninges[33], which were not examined in this study. Although inflammation may contribute to synaptic damage/loss in the course of MS, it may not necessarily be involved in the initiation of the processes leading to connectivity breakdown in the spinal cord.

References

1. Mackenzie IS, *et al*. Incidence and prevalence of multiple sclerosis in the UK 1990-2010: a descriptive study in the General Practice Research Database. *J Neurol Neurosurg Psychiatry*. Jan 2014;85(1):76-84. doi:10.1136/jnnp-2013-305450
2. Fisniku LK, *et al*. Disability and T2 MRI lesions: a 20-year follow-up of patients with relapse onset of multiple sclerosis. *Brain*. Mar 2008;131(Pt 3):808-17. doi:10.1093/brain/awm329
3. Sormani MP, *et al*. Treatment effect on brain atrophy correlates with treatment effect on disability in multiple sclerosis. *Ann Neurol*. Jan 2014;75(1):43-9. doi:10.1002/ana.24018
4. Schlaeger R, *et al*. Spinal cord gray matter atrophy correlates with multiple sclerosis disability. *Ann Neurol*. Oct 2014;76(4):568-80. doi:10.1002/ana.24241
5. Losseff NA, *et al*. Spinal cord atrophy and disability in multiple sclerosis. A new reproducible and sensitive MRI method with potential to monitor disease progression. *Brain*. Jun 1996;119 (Pt 3):701-8. doi:10.1093/brain/119.3.701
6. Lin X, *et al*. Spinal cord atrophy and disability in multiple sclerosis over four years: application of a reproducible automated technique in monitoring disease progression in a cohort of the interferon beta-1a (Rebif) treatment trial. *J Neurol Neurosurg Psychiatry*. Aug 2003;74(8):1090-4. doi:10.1136/jnnp.74.8.1090
7. Kearney H, *et al*. Magnetic resonance imaging correlates of physical disability in relapse onset multiple sclerosis of long disease duration. *Mult Scler*. Jan 2014;20(1):72-80. doi:10.1177/1352458513492245
8. Bjartmar C, *et al*. Neurological disability correlates with spinal cord axonal loss and reduced N-acetyl aspartate in chronic multiple sclerosis patients. *Ann Neurol*. Dec 2000;48(6):893-901. doi:10.1002/1531-8249(200012)48:6<893::Aid-ana10>3.3.Co;2-2
9. DeLuca GC, *et al*. Axonal loss in multiple sclerosis: a pathological survey of the corticospinal and sensory tracts. *Brain*. May 2004;127(Pt 5):1009-18. doi:10.1093/brain/awh118
10. Petrova N, *et al*. Axonal loss in the multiple sclerosis spinal cord revisited. *Brain Pathol*. May 2018;28(3):334-348. doi:10.1111/bpa.12516
11. Wegner C, *et al*. Neocortical neuronal, synaptic, and glial loss in multiple sclerosis. *Neurology*. Sep 26 2006;67(6):960-7. doi:10.1212/01.wnl.0000237551.26858.39
12. Dutta R, *et al*. Demyelination causes synaptic alterations in hippocampi from multiple sclerosis patients. *Ann Neurol*. Mar 2011;69(3):445-54. doi:10.1002/ana.22337
13. Bradbury EJ, *et al*. Spinal cord repair strategies: why do they work? *Nat Rev Neurosci*. Aug 2006;7(8):644-53. doi:10.1038/nrn1964
14. Tabakow P, *et al*. Functional regeneration of supraspinal connections in a patient with transected spinal cord following transplantation of bulbar olfactory ensheathing cells with peripheral nerve bridging. *Cell Transplant*. 2014;23(12):1631-55. doi:10.3727/096368914X685131
15. Albert M, *et al*. Synaptic pathology in the cerebellar dentate nucleus in chronic multiple sclerosis. *Brain Pathol*. Nov 2017;27(6):737-747. doi:10.1111/bpa.12450
16. Jurgens T, *et al*. Reconstruction of single cortical projection neurons reveals primary spine loss in multiple sclerosis. *Brain*. Jan 2016;139(Pt 1):39-46. doi:10.1093/brain/awv353
17. Bourane S, *et al*. Identification of a spinal circuit for light touch and fine motor control. *Cell*. Jan 29 2015;160(3):503-15. doi:10.1016/j.cell.2015.01.011
18. Carassiti D, *et al*. Neuronal loss, demyelination and volume change in the multiple sclerosis neocortex. *Neuropathol Appl Neurobiol*. Jun 2018;44(4):377-390. doi:10.1111/nan.12405
19. Gilmore CP, *et al*. Spinal cord neuronal pathology in multiple sclerosis. *Brain Pathol*. Oct 2009;19(4):642-9. doi:10.1111/j.1750-3639.2008.00228.x
20. Pinto JG, *et al*. Comparing development of synaptic proteins in rat visual, somatosensory, and frontal cortex. *Front Neural Circuits*. May 2013;7:97. 97. doi:10.3389/fncir.2013.00097
21. Micheva KD, *et al*. Single-synapse analysis of a diverse synapse population: proteomic imaging methods and markers. *Neuron*. Nov 18 2010;68(4):639-53. doi:10.1016/j.neuron.2010.09.024
22. Huttner WB, *et al*. Synapsin I (protein I), a nerve terminal-specific phosphoprotein. III. Its association with synaptic vesicles studied in a highly purified synaptic vesicle preparation. *J Cell Biol*. May 1983;96(5):1374-88. doi:10.1083/jcb.96.5.1374
23. Bahler M, *et al*. The synapsins and the regulation of synaptic function. *Bioessays*. Jun 1990;12(6):259-63. doi:10.1002/bies.950120603
24. Bykhovskaia M. Synapsin regulation of vesicle organization and functional pools. *Semin Cell Dev Biol*. Jun 2011;22(4):387-92. doi:10.1016/j.semcdb.2011.07.003
25. Jahn R, *et al*. A 38,000-dalton membrane protein (p38) present in synaptic vesicles. *Proc Natl Acad Sci U S A*. Jun 1985;82(12):4137-41. doi:10.1073/pnas.82.12.4137
26. Wiedenmann B, *et al*. Identification and localization of synaptophysin, an integral membrane glycoprotein of Mr 38,000 characteristic of presynaptic vesicles. *Cell*. Jul 1985;41(3):1017-28. doi:10.1016/s0092-8674(85)80082-9
27. Takamori S, *et al*. Molecular anatomy of a trafficking organelle. *Cell*. Nov 17 2006;127(4):831-46.

doi:10.1016/j.cell.2006.10.030
28. Kwon SE*, et al*. Synaptophysin regulates the kinetics of synaptic vesicle endocytosis in central neurons. *Neuron*. Jun 9 2011;70(5):847-54. doi:10.1016/j.neuron.2011.04.001
29. Gordon SL*, et al*. Synaptophysin is required for synaptobrevin retrieval during synaptic vesicle endocytosis. *J Neurosci*. Sep 28 2011;31(39):14032-6. doi:10.1523/JNEUROSCI.3162-11.2011
30. Gronborg M*, et al*. Quantitative comparison of glutamatergic and GABAergic synaptic vesicles unveils selectivity for few proteins including MAL2, a novel synaptic vesicle protein. *J Neurosci*. Jan 6 2010;30(1):2-12. doi:10.1523/JNEUROSCI.4074-09.2010
31. Hopf FW*, et al*. Stability and plasticity of developing synapses in hippocampal neuronal cultures. *J Neurosci*. Feb 1 2002;22(3):775-81. doi:10.1523/jneurosci.22-03-00775.2002
32. Centonze D*, et al*. The link between inflammation, synaptic transmission and neurodegeneration in multiple sclerosis. *Cell Death Differ*. Jul 2010;17(7):1083-91. doi:10.1038/cdd.2009.179
33. Reali C*, et al*. B cell rich meningeal inflammation associates with increased spinal cord pathology in multiple sclerosis. *Brain Pathol*. Jul 2020;30(4):779-793. doi:10.1111/bpa.12841

PART III

Glia as Innate Immune Cells of the CNS

Astrocyte and oligodendrocyte cross-talk in the central nervous system

Erik Nutma, Démi van Gent, Sandra Amor, and Laura A. N. Peferoen

Cells 2020; 9(3):600

Abstract

Over the last decade knowledge of the role of astrocytes in central nervous system (CNS) neuroinflammatory diseases has changed dramatically. Rather than playing a merely passive role in response to damage it is clear that astrocytes actively maintain CNS homeostasis by influencing pH, ion and water balance, the plasticity of neurotransmitters and synapses, cerebral blood flow, and are important immune cells. During disease astrocytes become reactive and hypertrophic, a response that was long considered to be pathogenic. However, recent studies reveal that astrocytes also have a strong tissue regenerative role. Whilst most astrocyte research focuses on modulating neuronal function and synaptic transmission little is known about the cross-talk between astrocytes and oligodendrocytes, the myelinating cells of the CNS. This communication occurs via direct cell-cell contact as well as via secreted cytokines, chemokines, exosomes, and signalling molecules. Additionally, this cross-talk is important for glial development, triggering disease onset and progression, as well as stimulating regeneration and repair. Its critical role in homeostasis is most evident when this communication fails. Here, we review emerging evidence of astrocyte-oligodendrocyte communication in health and disease. Understanding the pathways involved in this cross-talk will reveal important insights into the pathogenesis and treatment of CNS diseases.

Introduction

Astrocytes, the most abundant glial cell type in the central nervous system (CNS), have long been considered to be cells that only respond to damage in CNS diseases. This view is gradually changing with the accumulating evidence that astrocytes fulfil many functions in health, during development and in response to damage[1]. Astrocytes regulate processes critical for cell-cell interactions and homeostasis such as ion and water transport, pH, neuroplasticity, synapse pruning and cerebral blood flow thus providing trophic and metabolic support to all cells in the CNS. Astrocytes also play a major role in maintaining the blood-brain barrier (BBB) and blood-cerebrospinal fluid barrier. During CNS injury, infection and inflammation astrocytes produce a wide range of pro-inflammatory factors including chemokines, cytokines, increased expression of innate immune receptors and molecules including MHC-II[2-5]. On the other hand, astrocytes produce anti-inflammatory cytokines, heat shock proteins and neuroprotective factors aiding in processes such as neuroregeneration and remyelination[2]. These different characteristics present the astrocyte as a versatile player in regulatory processes depending on context and time of injury and disease. While much of the knowledge of astrocytes relates to their interaction with neurons and neuronal functions astrocytes collaborate and impact on other cells within the CNS as well, such as endothelial cells and pericytes in BBB formation. They also share their lineage with oligodendrocytes and interact with these myelin forming cells by sharing gap junctions allowing passage of small metabolites and molecules for communication[6].

Oligodendrocytes have the highest metabolic rate of cells in the CNS, producing myelin up to three times their weight per day for up to 50 axons each. The myelin sheaths are critical for action potentials and need to be maintained constantly[7]. Additionally, oligodendrocytes provide axons with trophic support and are crucial for neuronal functionality[2,7]. Due to their high turnover of myelin oligodendrocytes are sensitive to reactive oxygen species and oxidative stress[7,8]. They have been shown to participate intricately in immune mediated processes by producing immune regulatory factors and expressing receptors to communicate with microglia[9]. As it becomes more apparent that astrocytes participate in immune mediated processes as well, their cross-talk with oligodendrocytes might elucidate new mechanisms in neuroinflammatory diseases.

The importance of astrocytes in oligodendrocyte functioning is exemplified in primary astrocytopathies such as Alexander disease (AxD) and vanishing white matter (VWM)[10] where astrocyte damage leads to demyelination and oligodendrocyte death. In osmotic demyelination syndrome astrocyte death is observed due to loss of gap junctions and proteostasis defects in astrocytes prior to oligodendrocyte loss and demyelination[11-13]. In addition, astrocyte dysfunction has been associated with many other neurological diseases including epilepsy[14], amyotrophic lateral sclerosis (ALS)[15], Huntington's disease (HD)[16], and Alzheimer's disease (AD)[17]. In neuroinflammatory diseases, such as multiple sclerosis (MS) oligodendrocyte loss might be a consequence of aberrant immune responses. MS is characterized by inflammatory lesions with demyelination, neurodegeneration, and astrogliosis, in which astrocytes and oligodendrocytes are damaged[18,19]. Similarly, numerous other white matter disorders also show important cross-talk between astrocytes and oligodendrocytes (Table 1)[10].

Here we review the evidence for cross-talk between astrocytes and oligodendrocytes demonstrating an emerging role for astrocytes in oligodendrocyte damage, as well as contributing to tissue regeneration and remyelination. Understanding how astrocytes

Table 1. Astrocyte involvement in white matter CNS diseases

	Disease	Pathology	Detrimental impact on astrocytes	Beneficial impact on astrocytes	Ref
Inflammatory	MS	Inflammation, myelin loss, neurodegeneration, astrogliosis, astrocyte damage.	BBB damage, impaired signal transduction and glutamate clearance. Reduced OPC proliferation	Gliosis may aid remyelination and regenerate integrity of BBB, aid remyelination and provide trophic support	5,23-26
	NMO	Inflammation, myelin loss in optic nerve and spinal cord. Reduction in AQP4 and GFAP. Decreased EAAT2.	Impaired water and ion homeostasis, impaired glutamate clearance	Stimulation of remyelination, trophic support	24, 27-29
	ADEM	Widespread CNS inflammation associated with infection.	Dependent on infectious agent	Infection may trigger protective response via TLR-dependent mechanism	30
	AHL	Perivascular demyelination, inflammation, oedema, haemorrhages. Hyper-reactive astrocytes.	Swelling of protoplasmic and fibrous astrocyte end-feet, beading consistent with degeneration.	Demyelination is secondary to astrocyte injury indicating a beneficial effect of astrocytes in early disease	31
Infectious	PML	Cytolytic JC virus induces oligodendrocytes death and focal myelin loss. Abnormal astrocytes with inclusion bodies.	Astrocytes aid the spread of JC virus to neighbouring oligodendrocytes	Unknown	32-34
	SSPE	Viral inclusion bodies in neurons, neuronal damage and loss. Virion inclusion in some astrocytes.	Infection of (perivascular) astrocytes may aid spread of virus	Reactive gliosis in longstanding disease may be beneficial	35,36
	Congenital CMV	Encephalitis, microglial activation.	CMV infection of astrocytes induces TGF-beta known to enhance productive infection. Infection of foetal astrocytes alters uptake and metabolism of glutamate	Unknown	37,38

Table 1. Astrocyte involvement in white matter CNS diseases *(continued)*

	Disease	Pathology	Detrimental impact on astrocytes	Beneficial impact on astrocytes	Ref
Toxic-metabolic	PNND	Depends on position and type of tumour.	Pathogenic antibodies and CD8+ T cells to astrocytic antigens expressed on tumour induces neurological damage	Unknown	39,40
Hypoxia-ischemia	Binswanger disease	Chronic microvascular leukoencephalopathy, white matter lesions, axonal damage.	Damage to BBB leads to peri-infarct reactive astrocytes	Unknown	41
	Cerebral hypoxia and ischemia in new-borns	Diffuse white matter damage, gliosis, decrease in oligodendrocytes.	Reactive astrocytes form a glia scar and secret inflammatory molecules e.g. ROS	Astrocytes produce PDGF, IGF-1, elevated levels of EAAT2 aid glutamate removal in response to hypoxia. VEGF production mobilises stem cells. BDNF reduces apoptosis.	42,43
TBI	Diffuse axonal injury	Axonal damage, tau accumulation, secondary white matter damage, astrogliosis.	Glial scar inhibits remyelination and axonal regrowth	Glial scar prevents spread of toxic molecules	2,44
Lysosomal storage	MLD	Accumulated sulfatides leads to demyelination, sparing of U-fibres. Eosinophilic granules in macrophages, metachromasia.	Sulfatide accumulates in astrocytes impairing differentiation	Unknown	45
Peroxisomal	X-linked ALD	Defective ABCD1 transport protein. Increased saturated VLCFA in serum. Progressive demyelination. VLCFA accumulate in glia.	Astrocyte stress prior to myelin damage due to accumulated VLCFA. Astrocytes produce ROS and have impaired oxidative ATP synthesis and decreased Ca^{2+} uptake capacity	Unknown	46,47

Table 1. Astrocyte involvement in white matter CNS diseases *(continued)*

	Disease	Pathology	Detrimental impact on astrocytes	Beneficial impact on astrocytes	Ref
Mitochondrial	Leber's hereditary optic neuropathy	Loss of retinal ganglion cells, optic nerve degeneration.	Unknown	Unknown	
DNA repair defects	Cockayne syndrome	Patchy myelin loss, neuronal loss, astrocytic gliosis, microglia nodules.	Multinucleated astrocytes	Unknown	[48]
Defects in myelin genes	PMD	PLP1 duplication or gene alterations, dysmyelination, failure to form myelin.	Increased astrocytic activity, astrogliosis.	Unknown	[49]
AA / organic acid metabolism disorders	Canavan disease	Mutations of aspartoacylase gene. Diffuse spongiform white matter degeneration, dysmyelination and intramyelinic oedema. Hypertrophy and hyperplasia of astrocytes.	Metabolic disturbance of mitochondria in abnormal astrocyte	Unknown	[50,51]
Miscellaneous	Alexander disease	Myelin damage, Rosenthal fibres, non-neoplastic astrocytes	Mutations in GFAP lead to diminished glutamate transporter, accumulation of CD44, and loss of EAAT-2. Loss of Cx43 and Cx30	Unknown	[52]
	VWM	Progressive demyelination, blunted dysmorphic astrocytes.	Failure to reach maturity of astrocytes. Overexpression of nestin and GFAPδ	Unknown	[53]
	CADASIL	Diffuse white matter lesions, subcortical infarcts. Granular osmiophilic material in small vessels	Astrocytes undergo autophagy-like cell death. Glia-vascular unit damaged, BBB disturbed	Unknown	[54]
	PMLD	Lack of the gap junction protein Cx47 leads to splitting and decompaction of myelin sheaths and axonal spheroids.	Gap junctions between astrocytes and oligodendrocytes are disturbed compromising oligodendrocyte survival and myelination.	Unknown	[55]

Abbreviations: ADEM, acute disseminated encephalomyelitis; AHL, acute haemorrhagic leukoencephalopathy; AQP4, Aquaporin-4; BBB, blood brain barrier; BDNF, Brain-derived neurotrophic factor; CMV, cytomegalovirus; CNS, central nervous system; EAAT, Excitatory amino acid transporter; GFAP, Glial fibrillary acidic protein; IGF, insulin-like growth factor; MLD, Metachromatic leukodystrophy; MS, multiple sclerosis; NMO, neuromyelitis optica; OPC, oligodendrocyte precursor cell; PDGF, platelet derived growth factor; PMD, Pelizaeus-Merzbacher disease; PMLD, Pelizae-

us-Merzbacher-like disease; PML, progressive multifocal leukoencephalopathy; PNND, paraneoplastic neurological disorders; ROS, Reactive oxygen species; SSPE, subacute sclerosing panencephalitis; TBI, traumatic brain injury; TGF, transforming growth factor; TLR, toll-like receptor; VEGF, vascular endothelial growth factor; VLCFA, very long chain fatty acid; VWM, vanishing white matter.

interact with oligodendrocytes will provide a deeper insight into the pathophysiology of neurological disorders that may elucidate new pathways to drug strategies for myelin damage in CNS diseases.

Astrocyte and oligodendrocyte cross-talk during brain development

In neurogenesis, a 'gliogenic switch' occurs and dividing neural stem cells develop into glial cells[20,21]. From these cells, both astrocyte precursor cells and oligodendrocyte progenitor cells (OPCs) arise[21,22]. Astrogenesis is mediated through cardiotrophin-1 (CT-1), a factor secreted by cortical neurons. CT-1 induces glial fibrillary acidic protein (GFAP) expression by immature astrocytes through activation of the janus kinase signal transducer and activator of transcription proteins (JAK-STAT). The importance of CT-1 is exemplified by the 50-80% decrease in GFAP expression in CT-1 knock-out mice[56]. Astrogenesis-related genes are silenced during the neurogenic period through epigenetic mechanisms[56-58]. Oligodendrogenesis, on the other hand, is subject to a morphogen gradient of Sonic hedgehog (Shh) and bone morphogenic protein (BMP) and OPCs arise on the ventral side of the neural tube[59,60]. Critical in proliferation and timing of oligodendrocyte maturation is secretion of platelet derived growth factor AA (PDGF-AA) by astrocytes[61]. Once generated, OPCs migrate due to chemokines and Shh signalling, all while being guided by astrocytes[62]. In the optic nerve, astrocytes transiently express high levels of the megalin receptor that regulates the availability of Shh in the microenvironment and thus guides OPC migration. Inhibition of the megalin receptor has been shown to result in impaired migration of OPCs to the optic nerve[63]. Furthermore, astrocytes tightly control release of BMPs and prevent maturation of OPCs into myelin-producing oligodendrocytes[64]. Clearly, cross-talk between astrocytes and oligodendrocytes during development is essential for migration and maturation of OPCs through the CNS.

Various areas in the brain give rise to different types of astrocytes. Fibrous astrocytes are located in the white matter while protoplasmic astrocytes are present in the grey matter. These phenotypes of astrocytes differ in morphology and expression patterns. One example is the expression of excitatory amino acid transporters (EAATs), which is higher in the white matter and results in extracellular glutamate levels being lower in white than in grey matter[3,5,65,66]. Additionally, the astrocytic syncytium formed by protoplasmic astrocytes is larger than that of fibrous astrocytes[66]. The differences observed in morphology and protein expression impact the way these cells interact with their environment and with other glia cells such as oligodendrocytes.

During development astrocytes provide critical metabolic support of oligodendrocytes by supplying e.g. sterol regulatory element-binding protein (SREBP) cleavage-activating protein, a protein essential in lipid production. Mice in which SREBP cleavage activating protein is conditionally knocked out in astrocytes, develop microcephaly and a decrease in white matter volume[67], indicating the importance of astrocyte-derived lipids in myelination. Astrocytes also provide cholesterol for myelin production, and since cholesterol cannot cross the BBB it has to be synthesized *de novo* in the CNS by astrocytes and oligodendrocytes[3,68,69]. However,

inhibition of the oligodendrocyte cholesterol synthesis pathway in mice leads to a delay in myelination suggesting cholesterol production by oligodendrocytes and astrocytes is critical for early myelination[69]. This suggests that cholesterol availability is a rate-limiting factor in myelin production. In experimental autoimmune encephalomyelitis (EAE), an animal model of MS, the cholesterol synthesis pathway is downregulated in astrocytes of the cerebellum and spinal cord[68]. Determining whether this is a cause of limited remyelination requires more investigation. The metabolite exchange between oligodendrocytes and astrocytes may be key for astrocytic leukodystrophies, as disturbed astrocyte function in these disorders may limit lipid exchange from astrocytes to oligodendrocytes.

Astrocytic communication with oligodendrocytes

Blood-brain barrier interactions

Astrocyte end-feet cover up to 90% of the brain vasculature and are exchange sites for nutrients, metabolites, and ions from the blood to the brain. BBB dysfunction is a key step in the pathogenesis of inflammatory and neurodegenerative CNS diseases[70].

Iron from the blood is provided by astrocytes to oligodendrocytes through endocytosis and transferred to the cells as protein-bound iron. Iron is essential for several enzymatic functions of oligodendrocytes, such as energy metabolism enzymes, including the mitochondrial respiratory chain protein complexes I-IV, which use it as a co-factor[4,71]. When oligodendrocytes are deprived of iron, proliferation and differentiation of OPCs is impaired as shown *in vitro*, leading to a delay in remyelination after injury *in vivo*[71,72]. The importance of iron in myelination is exemplified by prenatal iron deficiency in which abnormal oligodendrocyte distribution is observed[72]. Abnormalities in iron metabolism are also reported in MS[71] and HD[73] and restoration of normal metabolism is required for remyelination. Maintenance and development of the BBB is regulated by astrocytic Shh[74]. In MS, Shh acts as an anti-inflammatory molecule at the level of the neurovascular unit and is increased during neuroinflammation to promote BBB repair and integrity[74]. These examples underscore the critical role of astrocytes in BBB functioning in order to provide metabolic support to oligodendrocytes, essential in processes such as myelination.

While astrocytes are considered to be key players in maintaining BBB integrity, OPCs have also been shown to play a role in BBB integrity through TGF-β signalling[75]. Additionally, BBB integrity is enhanced by OPCs through PDGF-BB/PDGFRα signalling while oligodendrocytes control BBB integrity independent of this pathway[76]. Conversely, a recent study combining pathology, *in vivo* and *in vitro* cultures indicates that clusters of OPCs contribute to altered vascular permeability by impacting the astrocyte foot processes in MS[77]. OPCs require a vascular scaffold for migration throughout the CNS to repopulate demyelinated areas in MS but detachment of the vasculature fails which results in a disruption of the BBB integrity[77].

Gap junctions connect astrocytes and oligodendrocytes

Astrocytes are connected to other glial cells via gap junctions, allowing free flow of ions and small metabolites. Gap junctions between astrocytes are made up of connexin (Cx) 30 and/or 43 that forms either homotypic (Cx30:Cx30 or Cx43:Cx43) or heterotypic channels (Cx30:Cx43). Using these gap junctions, astrocytes form a syncytium with free flow of small molecules including gliotransmitters and lactate that aids buffering of K^+[23,78]. Astrocytes express Cx30 and Cx43 that couples to adjacent oligodendrocytes expressing Cx32 and Cx47

by forming heterotypic gap junctions respectively Cx30:Cx32 and Cx43:Cx47[6,78]. This physical contact is important in oligodendrocyte maturation and is often disrupted in demyelinating conditions. In EAE the reduction in Cx47 and Cx32 reduces oligodendrocyte-oligodendrocyte and astrocyte-oligodendrocyte interactions[23]. This reduction is also observed in active and chronic lesions in MS, neuromyelitis optica (NMO) and Baló's disease[79]. Absence of Cx47 or Cx32 in oligodendrocytes exacerbates clinical EAE in mice associated with increased myelin loss but does not affect Cx30 and Cx43 expression in astrocytes[80]. Pathogenic mutations in Cx32 also contribute to Charcot-Marie-Tooth disease characterized by peripheral demyelination and neuropathy[79]. In contrast, Cx43 is upregulated in remyelinating MS lesions, emphasizing the importance of communication via gap junctions in remyelination[79]. The detrimental effect of Cx loss on remyelination may be attributed to the necessity of trophic support of oligodendrocytes by astrocytes, although whether the loss of Cx in gap junctions is the cause or consequence of myelin damage is unclear[81].

Astrocytes and oligodendrocytes play active roles in immune responses

Emerging studies have changed the perception that astrocytes and oligodendrocytes are solely bystanders in inflammatory processes. In infectious and inflammatory CNS diseases oligodendrocytes have been reported to act as antigen presenting cells and produce immune molecules[9] (Table 2). In neuroinflammation oligodendrocytes express many factors known to activate astrocytes[82,83] (Figure 1). For example, *in vitro* astrocytes express receptors for e.g. CCL2 and CXCL10 which are mostly secreted to attract monocytes and macrophages[84-87]. In MS lesions oligodendrocyte and astrocyte expression of IL-17 suggests that glia, as well as T cells, promote the pro-inflammatory environment that attracts macrophages to the lesion[88]. In mice, administration of cuprizone, that damages and ablates oligodendrocytes, both oligodendrocytes and OPCs secrete IL-1β, a known pro-inflammatory cytokine[89-91]. CXCL1, CXCL2, CXCL3, CXCL5, and CXCL6 all bind the CXCR2 receptor, which is constitutively expressed on oligodendrocytes, but not present on astrocytes[87,92]. The CXCR2 receptor is upregulated in response to these cytokines that are secreted by oligodendrocytes, supporting autocrine regulation. Several CXCR2 ligands have previously been associated with OPC proliferation and differentiation[93], indicating that oligodendrocytes regulate their own proliferation. Granulocyte macrophage colony stimulating factor (GM-CSF) is upregulated in resting oligodendrocytes[92] which has been found to be anti-apoptotic for neurons and neuroprotective in models of stroke.

Additionally, astrocytes secrete CXCL1 in spinal cord injury and in MS lesions, both *in vivo* and *in vitro,* which may act to recruit oligodendrocytes[87,94]. Gap junctions are also reported to play an immunoregulatory role for example Cx43 loss in astrocytes increases recruitment of immune cells in the brain as well as inducing an atypical reactive astrocyte phenotype that secretes both pro- and anti-inflammatory factors[81,117,118].

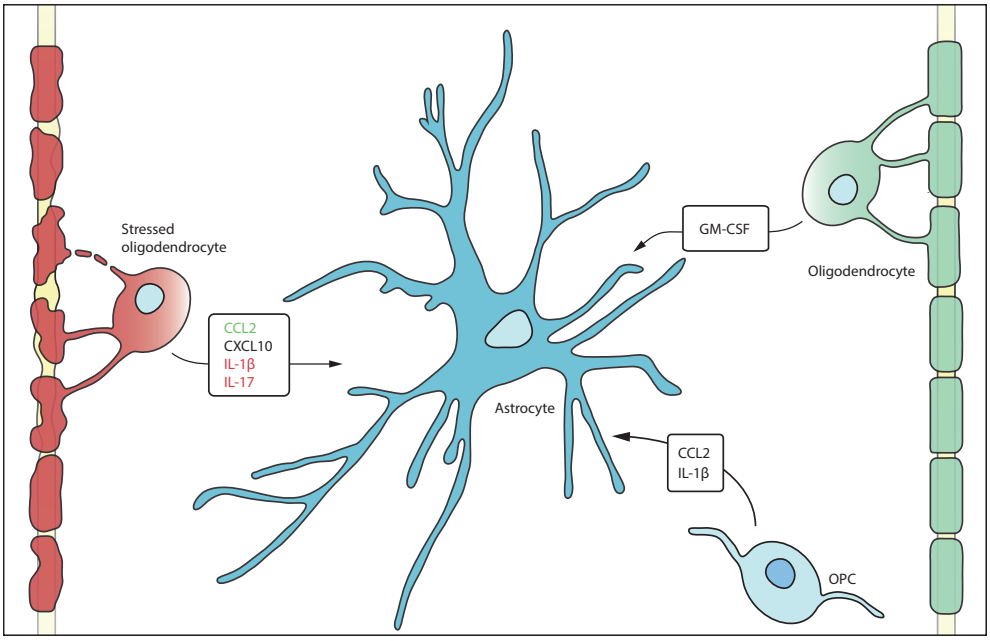

Figure 1. Oligodendrocytes secrete factors that impact on astrocytes. Stressed oligodendrocytes release factors that have beneficial effects (green) on astrocytes such as CCL2 to reduce inflammation. In contrast detrimental factors (red) such as IL-1β exacerbates inflammation. Healthy oligodendrocytes and OPCs also interact with astrocytes by secretion of GM-CSF and CCL2 as well as IL-1β.

Many immune factors are secreted by both oligodendrocytes and astrocytes *in vitro* i.e. IL-1β, CXCL10 and IL17, underscoring a possible immune function of these cells[89]. In addition, astrocytes also secrete tumour necrosis factor-α (TNF-α), IL-1β, interferon-γ (IFN-γ), fibroblast growth factor-2 (FGF-2), PDGF, and BMPs, factors known to influence oligodendrocytes and OPCs[3,119] (Figure 2, Table 2). TNF-α is recognized by TNFR1 and induces pro-inflammatory effects, while binding to TNF-αR2 induces anti-inflammatory effects. Both TNFR1 and TNFR2 are expressed on oligodendrocytes[9], and both are upregulated during inflammation[8] indicating that oligodendrocytes could trigger both pro- and anti-inflammatory responses. Likewise, astrocytes express predominantly TNFR1 but are capable of upregulating TNFR2 after stimulation by TNF-α[3,120], suggesting an autocrine feedback loop. While inhibition of TNF-α is an effective therapy in autoimmune diseases such as rheumatoid arthritis, this approach has been less straightforward in MS[121], recent data shows that selective modulation of TNFRs by activating TNFR2 and/or silencing TNFR1 might have therapeutic potential[122]. IL-1β is expressed by astrocytes during ischemic stroke, as well as neuroinflammatory disease although the precise mechanisms of IL-1β remain unclear[100,123]. IL-1β was also found in active MS lesions in reactive astrocytes and in pre-active lesions where it might act on oligodendrocytes and astrocytes in lesion formation[124]. IFN-γ has both pro- and anti-inflammatory effects, as treatment with IFN-γ exacerbates MS pathology, but also induces neurotrophic factor production in astrocytes, which are also able to produce IFN-γ[104,107]. FGF-2 is secreted by astrocytes after focal demyelination in mice, and has been shown to promote OPC proliferation yet inhibit their differentiation to oligodendrocytes[4,24]. BMPs are upregulated in EAE, and direct OPC differentiation into the astrocyte lineage[24]. Lastly, insulin-like growth factor-1 (IGF-1) also induces OPC maturation[109].

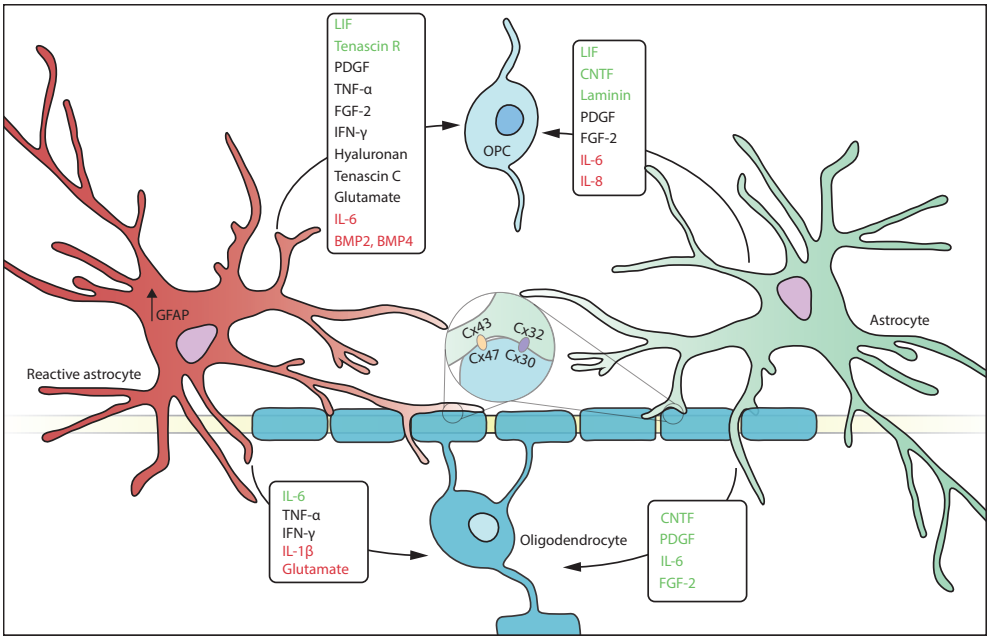

Figure 2. Astrocytes release a wide variety of molecules that impact oligodendrocyte functioning. Reactive and homeostatic astrocytes can release both beneficial (green) as well as detrimental (red) molecules. Most molecules that are secreted by astrocytes have a context dependent effect as well as a differential effect on oligodendrocytes and OPCs.

Astrocyte – oligodendrocyte interplay in disease

Reactive gliosis and glial scar formation

Reactive astrocytes are a hallmark of many CNS diseases for example in MS lesions[3,25,28,125], around the injured site during spinal cord injury (SCI)[44], within Rosenthal fibres in AxD[126], after ischemic stroke[127], and near amyloid plaques in AD[128], indicating their importance in both classic white matter and grey matter disease. Reactive gliosis is a spectrum rather than an all-or-nothing reaction, and the severity may differ between diseases, patients, or even within a patient. Mildly reactive astrocytes are associated with milder CNS injury or inflammation, and do not proliferate, showing only moderate changes in gene expression. Severely reactive astrocytes are characterized by upregulation of GFAP, hypertrophy and proliferation, and are present in severe injury and infection, as well as in chronic neurodegenerative disease. The most severe reaction is the glial scar, where astrocytes proliferate and intertwine to form a physical barrier that surrounds injured CNS tissue and isolates it from healthy tissue. It is associated with severe necrosis or inflammation[129]. In the acute stages of CNS damage, glial scarring is essential to prevent more widespread inflammation and the spread of toxic factors, protecting neurons from secondary degeneration[130]. An astrocyte-specific STAT3 knock-out inhibits formation of the glial scar, and leads to increased inflammation and motor dysfunction in mice after SCI[2,4,119]. On the other hand, in an AD mouse model, inhibition of the JAK2-STAT3 pathway leads to reduced astrocyte reactivity and increased learning abilities[131]. Glial scars are also involved in restoration of BBB integrity in inflammatory CNS disorders[23,130]. However, in the chronic stages, the glial scars inhibit OPC migration and differentiation and is thus considered to be detrimental blocking tissue repair[3,4,65,123]. This is observed in ischemic

Table 2. Immunologic interplay between astrocytes and oligodendrocytes.

	Detrimental	Beneficial	Refs
Astrocyte mediator	Impact on oligodendrocytes		
TNF-α	Induces demyelination and oligodendrocyte necrosis	Induces PDGF, and LIF on astrocytes which enhances OPC survival and differentiation	3,95-99
IL-1β	Induces oligodendrocyte apoptosis and hypomyelination		100
IFN-γ	Reversibly reduces OPC proliferation	Limits inflammation, limits Th17 activation, limits IL-1β signalling, protects oligodendrocytes from endoplasmic reticulum stress	101-104
FGF-2	Induces loss of myelin and myelin-producing oligodendrocytes	Induces proliferation of OPCs	4,105
BMP	BMPs induce OPC differentiation into the astrocyte lineage		24,106
CNTF		Induces proliferation and differentiation of OPCs	24,107
IGF-1		Induces OPC differentiation	24,108,109
Oligodendrocyte mediator	Impact on astrocytes		
CCL2		Reduces IL-6 expression in astrocytes, leading to a less inflammatory environment	91,110,111
CXCL10	Induces CXCR3 receptor expression		110,112
IL-17	Induces GFAP, IL-1β, and VEGF, reduces BBB integrity Induces astrogliosis		88,113
IL-1β	Induces IL-1β and NF-κB, and $P2X_7$ receptor.		89,91,114,115
GM-CSF		Inhibits glial scar formation. Induces proliferation, and migration of astrocytes	92,116

Abbreviations: BMP, bone morphogenic protein, CNTF, ciliary neurotrophic factor; FGF, Fibroblast growth factor; IFN, interferon; IGF, insulin-like growth factor; LIF, Leukaemia inhibitory factor; OPC, oligodendrocyte precursor cell; PDGF, Platelet-derived growth factor; TNF, tumour necrosis factor.

stroke, where the glial scar secretes growth inhibiting factors that prevent axonal regrowth[127], and in MS, where OPC migration into demyelinated lesions is inhibited[25].

Astrocytes become reactive in response to both direct and indirect activation; indirect activation is mediated by cytokines secreted by microglia, while direct activation is mediated by damage or pathogen associated molecular patterns that are released by pathogens or during cell death, oxidative stress, or chemical stress[3,25]. This implies that oligodendrocyte

injury induces astrocyte reactivity. Upon activation, astrocytes secrete factors e.g. TNF-α, IL-1β, IL-6, brain derived neurotrophic factor (BDNF), leukemia inhibitory factor (LIF), CCL2, and CXCL10[3,25,119,123,132]. These factors play a critical role in generating the immune responses during infection or damage, but also lead to collateral damage of oligodendrocytes and OPCs. The glial scar is essential to keep these factors isolated in the acute phase of disease, and abolishing it is adverse to recovery, while modulation of the glial scar in the chronic phase of disease may stimulate remyelination in white matter disorders.

Astrocytes in neuroinflammation

The NF-κB pathway is a major inflammatory pathway involved in activation of the innate and adaptive immune responses essential for e.g. generation of T-cell and B-cells. The pathway is constitutively active in many inflammatory disorders of the white matter[89,133]. *In vitro,* astrocytes upregulate NF-κB in response to pro-inflammatory cytokines such as IL-17, IL-1β, and TNF-α[89,134]. In vivo, overexpression of the NF-κB inhibitor IκBα in astrocytes results in protection of oligodendrocytes via reduced leukocyte infiltration and lower levels of chemokines during EAE[135]. NF-κB is also relevant in other CNS disorders that are not classically seen as white matter disorders, including AD, where amyloid-β plaques induce NF-κB activation in an astrocyte-specific manner[136]. In SOD1 mice, a mouse model of ALS, astrocytic NF-κB promotes degeneration of motor neurons and accelerates disease progression[137]. Subtle white matter changes are found in neurodegenerative diseases as early as pre-clinical AD where the NF-κB pathway could play a role in exacerbating inflammatory signaling[138]. Intervention in this pathway is effective, as demonstrated by the MS drug laquinimod, which inhibits astrocytic NF-κB expression[4,133]. NF-κB signalling represents an important inflammatory pathway in various neurological disorders that is frequently used by astrocytes to exacerbate inflammation. Alleviation of oligodendrocyte pathology via astrocytic NF-κB targeting may be relevant in more white matter disorders, and its use in MS treatment is proof of concept for the relevance of cross-talk in white matter disease therapy.

Excitotoxicity

Oligodendrocytes are sensitive to excitotoxic damage due to their expression of α-amino-3-hydroxy-5-methyl-4-isoxazolepropionic acid (AMPA) and kainate receptors. In EAE, treatment with AMPA and kainate antagonists significantly reduces oligodendrocyte death and disease severity, suggesting a role for excitotoxic cell death in MS[25,139]. Moreover, TNF-α triggers astrocytic upregulation of prostaglandin-E2 *in vitro*, which induces release of glutamate into the extracellular space[140], indicating that neuroinflammation exacerbates excitotoxic damage, leading to oligodendrocyte death. Excitotoxicity is further facilitated by downregulation of EAATs, which occurs in the senile plaques in AD, and in ALS[128,136]. Excitotoxicity in oligodendrocytes is not just glutamate-mediated, but also ATP-mediated, via overstimulation of the P2X purinoreceptor-7 (P2X7) ATP receptors. Similar to the AMPA and kainate receptors, the P2X7 receptor is Ca2+ permeable, and the intracellular Ca2+ damages oligodendrocytes.

Studies by Matute and colleagues show that in mice P2X7 antagonists prevent ATP toxicity in oligodendrocytes [7]. P2X7 receptors are significantly increased in oligodendrocytes in the optic nerves of people with MS compared to healthy controls, indicating that ATP toxicity might be a relevant pathogenic mechanism in disease[141]. ATP toxicity is also pathogenic after SCI, increasing demyelination and neuronal death after injury[142]. In support of this, treatment of rats with P2X7 antagonists increases neuronal survival and functional recovery after SCI[142]. Stimulation of the P2X7 receptor of neonatal rat-derived astrocytes results in

glutamate release, supplying the environment with more excitotoxic molecules[141]. Astrocytic overexpression of P2X7 was also found in the white and grey matter in secondary progressive MS[143] as well as upon stimulation with IL-1β[114], suggesting that this signalling pathway is especially relevant during inflammation.

P2X7 is also of importance in epilepsy, since sufferers have higher P2X7 expression than healthy controls in the neocortical nerve terminals. P2X7 antagonist treatment decreases the severity and number of epileptic seizures in rats[144]. Excitotoxicity is a relevant mechanism of cell death in many disorders, and astrocyte-oligodendrocyte cross-talk plays an important role here, as astrocytes are able to create a hostile environment with glutamate and ATP which then damages oligodendrocytes. Inhibition of astrocytic glutamate release or increasing the activity of the EAAT receptors may thus be a relevant treatment mechanism in epilepsy or white matter diseases.

Astrocyte control of remyelination and the extracellular matrix

The white matter of the brain primarily consists of myelinated axons formed by oligodendrocytes, after differentiating from OPCs[4]. In demyelinating diseases such as MS and NMO, functional recovery requires remyelination. Although in these diseases astrocytes are known to be detrimental to oligodendrocytes and OPCs, they also promote and mediate remyelination[7,44]. For example, in vivo ablation of astrocytes results in impaired recovery from SCI[2]. In MS or SCI remyelination occurs but often fails despite the presence of significant numbers of OPCs suggesting the lack of remyelination is likely due to a failure in OPC differentiation rather than migration[23,145,146]. However, migration failure and clustering of OPCs at astrocyte endfeet indicates that astrocytes may also play a role in restricting migration of OPCs[77]. Recruitment of OPCs to the demyelinating area occurs through astrocyte chemokine signalling of IL-1β and CCL2, confirming the necessity of cellular cross-talk in remyelination[23,147]. After migration, OPCs exit the cell cycle and differentiate into oligodendrocytes through stimulation of PDGF and FGF-2[146]. FGF-2 is highly upregulated by astrocytes in remyelinating spinal cord lesions where it acts on oligodendrocytes as well as in autocrine fashion on astrocytes[148]. Recently, a new study has found that OPCs might not be as important for remyelination as previously thought. Remyelination was found to be mainly dependent on the pool of surviving mature oligodendrocytes present in the lesions based on carbon dating of oligodendrocytes[149].

Astrocytes influence oligodendrocytes via modification of the extracellular matrix (ECM). A major ECM component secreted by astrocytes is hyaluronan, which acts on T-cells and OPCs, blocking OPC differentiation into oligodendrocytes and promoting astrocytic differentiation[44]. Hyaluronan is especially abundant in white matter lesions of MS patients[24], as well as patients with rare familial leukodystrophies VWM[53] and AxD[126]. Exaggerated hyaluronan secretion is a common feature of leukodystrophies, and likely has a role in neurological pathogenesis. Another astrocytic ECM factor is laminin that controls the differentiation and migration of OPCs, and promotes their survival by binding integrin and dystroglycan receptors. Mutations in laminin result in profound muscular and white matter abnormalities[150-152]. In inflammatory conditions, reactive astrocytes also produce tenascin C and R. Tenascin C is linked to inhibition of OPC migration, but tenascin R induces myelin gene expression and OPC differentiation. In chronic MS plaques, both tenascin C and R were shown to be upregulated in reactive astrocytes[152]. Lastly, astrocytes secrete proteoglycans that inhibit remyelination in high concentrations[153]. Proteoglycans also capture chemokines and growth factors, localizing them and targeting immune cells to the area of inflammation. This helps to

prevent immune-mediated collateral damage[130]. These studies underscore the importance of the ECM in providing a healthy environment for remyelination. If disrupted, a remyelination promoting environment turns inhibitory, leading to impaired differentiation and proliferation of OPCs. Astrocytes are an important source of many ECM factors, and communicate with and influence OPCs and oligodendrocytes via secretion of ECM factors.

In inflammatory CNS conditions infiltration of immune cells is a hallmark of disease and heavily dependent on the breakdown of the ECM. MMP2 and 9 are important in degradation of the *lamina basalis*, as well as infiltration of immune cells into the brain parenchyma. The activity of these proteins is regulated by tissue inhibitors of metalloproteinases (TIMPs). Although astrocytes express MMP2 and 9 both *in vivo* and *in vitro*, they also produce TIMP-1[123]. Astrocytes promote oligodendrogenesis during and after injury through secretion of BDNF and TIMP-1[154,155]. This is also shown in TIMP-1 deficient mice that exhibit defective myelin repair[23], indicating the importance of the ECM in remyelination. Another MMP that is active in remyelination is MMP7, which cleaves fibronectin aggregates present in demyelinating lesions in MS. These aggregates prevent OPC maturation and remyelination. Secreted proMMP7 is activated by astrocytic MMP3, indicating that astrocytes assist in this cleavage[156]. This shows that astrocytes are not only involved in the building of the ECM, but also in its breakdown and maintenance.

In summary, astrocytic dysfunction results in a toxic extracellular environment with high levels of excitotoxic molecules and pro-inflammatory cytokines such as IL-1β and TNF-α. On the other hand, their basal functions are essential in maintaining a healthy brain microenvironment where oligodendrocytes thrive and remyelinate the CNS. Although astrocytes can be detrimental in neurological disease they are also essential for the recovery from damage. Astrocytes are particularly important in early recovery by supporting oligodendrocyte migration and OPC differentiation. However, astrocytes become pathological in the chronic phase, exemplified by the glial scar formation in SCI or MS, in which hypertrophic astrocytes produce many factors that induce a harmful environment for mature oligodendrocytes and inhibit OPC differentiation[44,130].

Conclusion

Astrocyte and oligodendrocyte interactions in healthy conditions and disease are complex and multifaceted. The widely considered view that astrocytes only react to damage in neurological diseases is changing to embrace the emerging evidence that these cells are essential to the development of the healthy CNS. On the other hand astrocytes are involved in the pathogenesis of several CNS diseases since loss of normal trophic functions of astrocytes results in damage to neurons and oligodendrocytes thereby exacerbating pathology. Furthermore, astrocytes are important for the regenerative capacities of the brain aiding oligodendrocyte proliferation, maturation and migration – a key step in repair in diseases such as MS and other demyelinating diseases. There is also a growing awareness that astrocytes and oligodendrocytes are not only targets for autoimmune responses in the context of neuroinflammation. Astrocytes play an important role as innate immune cells, e.g. by secreting chemokines, and as such influence other glia cells. Future studies into the communication between astrocytes and oligodendrocytes as well as their impact on other CNS cell types will provide new clues for controlling innate immunity and aiding repair in the CNS.

References

1. Colombo E, *et al*. Astrocytes: Key Regulators of Neuroinflammation. *Trends Immunol*. Sep 2016;37(9):608-620. doi:10.1016/j.it.2016.06.006
2. Gaudet AD, *et al*. Glial Cells Shape Pathology and Repair After Spinal Cord Injury. *Neurotherapeutics*. Jul 2018;15(3):554-577. doi:10.1007/s13311-018-0630-7
3. Kiray H, *et al*. The multifaceted role of astrocytes in regulating myelination. *Exp Neurol*. Sep 2016;283(Pt B):541-9. doi:10.1016/j.expneurol.2016.03.009
4. Li J, *et al*. Astrocytes in Oligodendrocyte Lineage Development and White Matter Pathology. *Front Cell Neurosci*. 2016/05/10 2016;10:119. doi:10.3389/fncel.2016.00119
5. Seth P, *et al*. Astrocyte, the star avatar: redefined. *J Biosci*. Sep 2008;33(3):405-21. doi:10.1007/s12038-008-0060-5
6. Orthmann-Murphy JL, *et al*. Gap junctions couple astrocytes and oligodendrocytes. journal article. *J Mol Neurosci*. May 2008;35(1):101-16. doi:10.1007/s12031-007-9027-5
7. McTigue DM, *et al*. The life, death, and replacement of oligodendrocytes in the adult CNS. *J Neurochem*. Oct 2008;107(1):1-19. doi:10.1111/j.1471-4159.2008.05570.x
8. Patel J, *et al*. Molecular mechanisms of oligodendrocyte injury in multiple sclerosis and experimental autoimmune encephalomyelitis. *Int J Mol Sci*. 2012/08/23 2012;13(8):10647-59. doi:10.3390/ijms130810647
9. Peferoen L, *et al*. Oligodendrocyte-microglia cross-talk in the central nervous system. *Immunology*. Mar 2014;141(3):302-13. doi:10.1111/imm.12163
10. van der Knaap MS, *et al*. Leukodystrophies: a proposed classification system based on pathological changes and pathogenetic mechanisms. *Acta Neuropathol*. Sep 2017;134(3):351-382. doi:10.1007/s00401-017-1739-1
11. Bouchat J, *et al*. Regional oligodendrocytopathy and astrocytopathy precede myelin loss and blood-brain barrier disruption in a murine model of osmotic demyelination syndrome. *Glia*. Mar 2018;66(3):606-622. doi:10.1002/glia.23268
12. Gankam Kengne F, *et al*. Astrocytes are an early target in osmotic demyelination syndrome. *Journal of the American Society of Nephrology : JASN*. Oct 2011;22(10):1834-45. doi:10.1681/ASN.2010111127
13. Gankam-Kengne F, *et al*. Osmotic Stress-Induced Defective Glial Proteostasis Contributes to Brain Demyelination after Hyponatremia Treatment. *Journal of the American Society of Nephrology : JASN*. Jun 2017;28(6):1802-1813. doi:10.1681/ASN.2016050509
14. Coulter DA, *et al*. Astrocytic regulation of glutamate homeostasis in epilepsy. *Glia*. Aug 2012;60(8):1215-26. doi:10.1002/glia.22341
15. Seifert G, *et al*. Astrocyte dysfunction in neurological disorders: a molecular perspective. *Nat Rev Neurosci*. Mar 2006;7(3):194-206. doi:10.1038/nrn1870
16. Faideau M, *et al*. In vivo expression of polyglutamine-expanded huntingtin by mouse striatal astrocytes impairs glutamate transport: a correlation with Huntington's disease subjects. *Hum Mol Genet*. Aug 1 2010;19(15):3053-67. doi:10.1093/hmg/ddq212
17. Simpson JE, *et al*. Astrocyte phenotype in relation to Alzheimer-type pathology in the ageing brain. *Neurobiol Aging*. Apr 2010;31(4):578-90. doi:10.1016/j.neurobiolaging.2008.05.015
18. Reich DS, *et al*. Multiple Sclerosis. *N Engl J Med*. Jan 11 2018;378(2):169-180. doi:10.1056/NEJMra1401483
19. Thompson AJ, *et al*. Multiple sclerosis. *The Lancet*. 2018/04 2018;391(10130):1622-1636. doi:10.1016/s0140-6736(18)30481-1
20. Sloan SA, *et al*. Mechanisms of astrocyte development and their contributions to neurodevelopmental disorders. *Curr Opin Neurobiol*. Aug 2014;27:75-81. doi:10.1016/j.conb.2014.03.005
21. Zuchero JB, *et al*. Glia in mammalian development and disease. *Development*. Nov 15 2015;142(22):3805-9. doi:10.1242/dev.129304
22. Noble M, *et al*. Precursor cell biology and the development of astrocyte transplantation therapies: lessons from spinal cord injury. *Neurotherapeutics*. Oct 2011;8(4):677-93. doi:10.1007/s13311-011-0071-z
23. Domingues HS, *et al*. Oligodendrocyte, Astrocyte, and Microglia Crosstalk in Myelin Development, Damage, and Repair. *Front Cell Dev Biol*. 2016/06/28 2016;4:71. doi:10.3389/fcell.2016.00071
24. Moore CS, *et al*. How factors secreted from astrocytes impact myelin repair. *J Neurosci Res*. Jan 2011;89(1):13-21. doi:10.1002/jnr.22482
25. Ponath G, *et al*. The Role of Astrocytes in Multiple Sclerosis. *Front Immunol*. 2018/02/19 2018;9:217. doi:10.3389/fimmu.2018.00217
26. Torkildsen O, *et al*. Disease-modifying treatments for multiple sclerosis - a review of approved medications. *Eur J Neurol*. Jan 2016;23 Suppl 1:18-27. doi:10.1111/ene.12883
27. Hostenbach S, *et al*. Astrocyte loss and astrogliosis in neuroinflammatory disorders. *Neurosci Lett*. Apr 17 2014;565:39-41. doi:10.1016/j.neulet.2013.10.012
28. Popescu BF, *et al*. Pathology of demyelinating diseases. *Annu Rev Pathol*. 2012/02/28 2012;7(1):185-217. doi:10.1146/annurev-pathol-011811-132443
29. Uzawa A, *et al*. Cytokine and chemokine profiles in neuromyelitis optica: significance of interleukin-6. *Mult Scler*. Dec 2010;16(12):1443-52. doi:10.1177/1352458510379247

30. Vitturi BK, *et al*. Multiphasic disseminated encephalomyelitis associated with herpes virus infection in a patient with TLR3 deficiency. *Mult Scler Relat Disord*. Nov 2019;36:101379. doi:10.1016/j.msard.2019.101379
31. Robinson CA, *et al*. Early and widespread injury of astrocytes in the absence of demyelination in acute haemorrhagic leukoencephalitis. *Acta Neuropathol Commun*. May 8 2014;2:52. doi:10.1186/2051-5960-2-52
32. Bauer J, *et al*. Progressive multifocal leukoencephalopathy and immune reconstitution inflammatory syndrome (IRIS). *Acta Neuropathol*. Dec 2015;130(6):751-64. doi:10.1007/s00401-015-1471-7
33. Gheuens S, *et al*. Progressive multifocal leukoencephalopathy: why gray and white matter. *Annu Rev Pathol*. Jan 24 2013;8(1):189-215. doi:10.1146/annurev-pathol-020712-164018
34. Langer-Gould A, *et al*. Progressive multifocal leukoencephalopathy in a patient treated with natalizumab. *N Engl J Med*. Jul 28 2005;353(4):375-81. doi:10.1056/NEJMoa051847
35. Lewandowska E, *et al*. Ultrastructural changes in neuronal and glial cells in subacute sclerosing panencephalitis: correlation with disease duration. *Folia Neuropathol*. 2001;39(3):193-202.
36. Mesquita R, *et al*. Measles virus antigen in macrophage/microglial cells and astrocytes of subacute sclerosing panencephalitis. *APMIS*. May 1998;106(5):553-61. doi:10.1111/j.1699-0463.1998.tb01384.x
37. Kossmann T, *et al*. Cytomegalovirus production by infected astrocytes correlates with transforming growth factor-beta release. *J Infect Dis*. Feb 15 2003;187(4):534-41. doi:10.1086/373995
38. Zhang L, *et al*. HCMV induces dysregulation of glutamate uptake and transporter expression in human fetal astrocytes. *Neurochem Res*. Dec 2014;39(12):2407-18. doi:10.1007/s11064-014-1445-5
39. Banjara M, *et al*. Detection of brain-directed autoantibodies in the serum of non-small cell lung cancer patients. *PLOS ONE*. 2017;12(7):e0181409. doi:10.1371/journal.pone.0181409
40. Fang B, *et al*. Autoimmune Glial Fibrillary Acidic Protein Astrocytopathy: A Novel Meningoencephalomyelitis. *JAMA Neurol*. Nov 1 2016;73(11):1297-1307. doi:10.1001/jamaneurol.2016.2549
41. Rosenberg GA. Binswanger's disease: biomarkers in the inflammatory form of vascular cognitive impairment and dementia. *J Neurochem*. Mar 2018;144(5):634-643. doi:10.1111/jnc.14218
42. Pregnolato S, *et al*. Glutamate Transport and Preterm Brain Injury. *Front Physiol*. 2019;10:417. doi:10.3389/fphys.2019.00417
43. Revuelta M, *et al*. Ischemic stroke in neonatal and adult astrocytes. *Mech Ageing Dev*. Oct 2019;183:111147. doi:10.1016/j.mad.2019.111147
44. Wang HF, *et al*. Effect of glial cells on remyelination after spinal cord injury. *Neural Regen Res*. Oct 2017;12(10):1724-1732. doi:10.4103/1673-5374.217354
45. Frati G, *et al*. Human iPSC-based models highlight defective glial and neuronal differentiation from neural progenitor cells in metachromatic leukodystrophy. *Cell Death Dis*. Jun 13 2018;9(6):698. doi:10.1038/s41419-018-0737-0
46. Kruska N, *et al*. Astrocytes and mitochondria from adrenoleukodystrophy protein (ABCD1)-deficient mice reveal that the adrenoleukodystrophy-associated very long-chain fatty acids target several cellular energy-dependent functions. *Biochim Biophys Acta*. May 2015;1852(5):925-36. doi:10.1016/j.bbadis.2015.01.005
47. Gortz AL, *et al*. Heat shock protein expression in cerebral X-linked adrenoleukodystrophy reveals astrocyte stress prior to myelin loss. *Neuropathol Appl Neurobiol*. Jun 2018;44(4):363-376. doi:10.1111/nan.12399
48. Weidenheim KM, *et al*. Neuropathology of Cockayne syndrome: Evidence for impaired development, premature aging, and neurodegeneration. *Mech Ageing Dev*. Sep 2009;130(9):619-36. doi:10.1016/j.mad.2009.07.006
49. Takanashi J, *et al*. Brain N-acetylaspartate is elevated in Pelizaeus-Merzbacher disease with PLP1 duplication. *Neurology*. Jan 22 2002;58(2):237-41. doi:10.1212/wnl.58.2.237
50. Adachi M, *et al*. Spongy degeneration of the central nervous system (van Bogaert and Bertrand type; Canavan's disease). A review. *Hum Pathol*. Sep 1973;4(3):331-47. doi:10.1016/s0046-8177(73)80098-x
51. Baslow MH, *et al*. Are astrocytes the missing link between lack of brain aspartoacylase activity and the spongiform leukodystrophy in Canavan disease? *Neurochem Res*. Sep 2009;34(9):1523-34. doi:10.1007/s11064-009-9958-z
52. Borrett D, *et al*. Alexander's disease. A disease of astrocytes. *Brain*. Jun 1985;108 (Pt 2):367-85. doi:10.1093/brain/108.2.367
53. Bugiani M, *et al*. Vanishing white matter: a leukodystrophy due to astrocytic dysfunction. *Brain Pathol*. May 2018;28(3):408-421. doi:10.1111/bpa.12606
54. Hase Y, *et al*. Severe white matter astrocytopathy in CADASIL. *Brain Pathol*. Nov 2018;28(6):832-843. doi:10.1111/bpa.12621
55. Orthmann-Murphy JL, *et al*. Loss-of-function GJA12/Connexin47 mutations cause Pelizaeus-Merzbacher-like disease. *Mol Cell Neurosci*. Apr 2007;34(4):629-41. doi:10.1016/j.mcn.2007.01.010
56. Molofsky AV, *et al*. Astrocytes and disease: a neurodevelopmental perspective. *Genes Dev*. May 1

2012;26(9):891-907. doi:10.1101/gad.188326.112
57. Miller FD, *et al*. Timing is everything: making neurons versus glia in the developing cortex. *Neuron*. May 3 2007;54(3):357-69. doi:10.1016/j.neuron.2007.04.019
58. Yang Y, *et al*. Developmental maturation of astrocytes and pathogenesis of neurodevelopmental disorders. *J Neurodev Disord*. Aug 29 2013;5(1):22. doi:10.1186/1866-1955-5-22
59. Naruse M, *et al*. Origin of oligodendrocytes in mammalian forebrains: a revised perspective. *J Physiol Sci*. Jan 2017;67(1):63-70. doi:10.1007/s12576-016-0479-7
60. Rowitch DH, *et al*. Developmental genetics of vertebrate glial-cell specification. *Nature*. Nov 11 2010;468(7321):214-22. doi:10.1038/nature09611
61. Durand B, *et al*. A cell-intrinsic timer that operates during oligodendrocyte development. *Bioessays*. Jan 2000;22(1):64-71. doi:10.1002/(SICI)1521-1878(200001)22:1<64::AID-BIES11>3.0.CO;2-Q
62. Ortega MC, *et al*. Megalin mediates the influence of sonic hedgehog on oligodendrocyte precursor cell migration and proliferation during development. *Glia*. May 2012;60(6):851-66. doi:10.1002/glia.22316
63. Clemente D, *et al*. The effect of glia-glia interactions on oligodendrocyte precursor cell biology during development and in demyelinating diseases. *Front Cell Neurosci*. Dec 20 2013;7:268. doi:10.3389/fncel.2013.00268
64. See J, *et al*. Oligodendrocyte maturation is inhibited by bone morphogenetic protein. *Mol Cell Neurosci*. Aug 2004;26(4):481-92. doi:10.1016/j.mcn.2004.04.004
65. Lanciotti A, *et al*. Astrocytes: Emerging Stars in Leukodystrophy Pathogenesis. *Transl Neurosci*. Jun 1 2013;4(2)doi:10.2478/s13380-013-0118-1
66. Lundgaard I, *et al*. White matter astrocytes in health and disease. *Neuroscience*. Sep 12 2014;276:161-73. doi:10.1016/j.neuroscience.2013.10.050
67. Camargo N, *et al*. Oligodendroglial myelination requires astrocyte-derived lipids. *PLoS Biol*. May 2017;15(5):e1002605. doi:10.1371/journal.pbio.1002605
68. Itoh N, *et al*. Cell-specific and region-specific transcriptomics in the multiple sclerosis model: Focus on astrocytes. *Proc Natl Acad Sci U S A*. Jan 9 2018;115(2):E302-E309. doi:10.1073/pnas.1716032115
69. Liu JP, *et al*. Cholesterol involvement in the pathogenesis of neurodegenerative diseases. *Mol Cell Neurosci*. Jan 2010;43(1):33-42. doi:10.1016/j.mcn.2009.07.013
70. Sweeney MD, *et al*. The role of brain vasculature in neurodegenerative disorders. *Nat Neurosci*. Oct 2018;21(10):1318-1331. doi:10.1038/s41593-018-0234-x
71. Stephenson E, *et al*. Iron in multiple sclerosis: roles in neurodegeneration and repair. *Nat Rev Neurol*. Aug 2014;10(8):459-68. doi:10.1038/nrneurol.2014.118
72. Morath DJ, *et al*. Iron deficiency during embryogenesis and consequences for oligodendrocyte generation in vivo. *Dev Neurosci*. 2002;24(2-3):197-207. doi:10.1159/000065688
73. Heneka MT, *et al*. Innate immune activation in neurodegenerative disease. *Nat Rev Immunol*. Jul 2014;14(7):463-77. doi:10.1038/nri3705
74. Alvarez JI, *et al*. The Hedgehog pathway promotes blood-brain barrier integrity and CNS immune quiescence. *Science (New York, NY)*. 2011;334(6063):1727-1731. doi:10.1126/science.1206936
75. Seo JH, *et al*. Oligodendrocyte precursor cells support blood-brain barrier integrity via TGF-beta signaling. *PLOS ONE*. 2014;9(7):e103174. doi:10.1371/journal.pone.0103174
76. Kimura I, *et al*. Oligodendrocytes upregulate blood-brain barrier function through mechanisms other than the PDGF-BB/PDGFRalpha pathway in the barrier-tightening effect of oligodendrocyte progenitor cells. *Neurosci Lett*. Jan 10 2020;715:134594. doi:10.1016/j.neulet.2019.134594
77. Niu J, *et al*. Aberrant oligodendroglial-vascular interactions disrupt the blood-brain barrier, triggering CNS inflammation. *Nat Neurosci*. May 2019;22(5):709-718. doi:10.1038/s41593-019-0369-4
78. Giaume C, *et al*. Connexins, gap junctions, and glia. *Wiley Interdisciplinary Reviews: Membrane Transport and Signaling*. 2013/05/07 2013;2(4):133-142. doi:10.1002/wmts.87
79. Masaki K. Early disruption of glial communication via connexin gap junction in multiple sclerosis, Balo's disease and neuromyelitis optica. *Neuropathology*. Oct 2015;35(5):469-80. doi:10.1111/neup.12211
80. Papaneophytou CP, *et al*. Regulatory role of oligodendrocyte gap junctions in inflammatory demyelination. *Glia*. Dec 2018;66(12):2589-2603. doi:10.1002/glia.23513
81. Boulay AC, *et al*. Immune quiescence of the brain is set by astroglial connexin 43. *J Neurosci*. Mar 11 2015;35(10):4427-39. doi:10.1523/JNEUROSCI.2575-14.2015
82. Darbinyan A, *et al*. Polyomavirus JC infection inhibits differentiation of oligodendrocyte progenitor cells. *J Neurosci Res*. Jan 2013;91(1):116-27. doi:10.1002/jnr.23135
83. Ramesh G, *et al*. A possible role for inflammation in mediating apoptosis of oligodendrocytes as induced by the Lyme disease spirochete Borrelia burgdorferi. *J Neuroinflammation*. Apr 23 2012;9(1):72. doi:10.1186/1742-2094-9-72
84. Andjelkovic AV, *et al*. Functional expression of CCR2 by human fetal astrocytes. *J Neurosci Res*. Oct 15 2002;70(2):219-31. doi:10.1002/jnr.10372
85. Ashutosh, *et al*. CXCL8 protects human neurons

from amyloid-beta-induced neurotoxicity: relevance to Alzheimer's disease. *Biochem Biophys Res Commun*. Sep 9 2011;412(4):565-71. doi:10.1016/j.bbrc.2011.07.127
86. Hsu MP*, et al*. Analysis of IL-6/gp130 family receptor expression reveals that in contrast to astroglia, microglia lack the oncostatin M receptor and functional responses to oncostatin M. *Glia*. Jan 2015;63(1):132-41. doi:10.1002/glia.22739
87. Omari KM*, et al*. Role for CXCR2 and CXCL1 on glia in multiple sclerosis. *Glia*. Jan 1 2006;53(1):24-31. doi:10.1002/glia.20246
88. Tzartos JS*, et al*. Interleukin-17 production in central nervous system-infiltrating T cells and glial cells is associated with active disease in multiple sclerosis. *Am J Pathol*. Jan 2008;172(1):146-55. doi:10.2353/ajpath.2008.070690
89. Choi SS*, et al*. Human astrocytes: secretome profiles of cytokines and chemokines. *PLOS ONE*. 2014/04/01 2014;9(4):e92325. doi:10.1371/journal.pone.0092325
90. Moynagh PN. The interleukin-1 signalling pathway in astrocytes: a key contributor to inflammation in the brain. *J Anat*. Sep 2005;207(3):265-9. doi:10.1111/j.1469-7580.2005.00445.x
91. Moyon S*, et al*. Demyelination causes adult CNS progenitors to revert to an immature state and express immune cues that support their migration. *J Neurosci*. Jan 7 2015;35(1):4-20. doi:10.1523/JNEUROSCI.0849-14.2015
92. Kim WK*, et al*. Secretome analysis of human oligodendrocytes derived from neural stem cells. *PLOS ONE*. 2014/01/02 2014;9(1):e84292. doi:10.1371/journal.pone.0084292
93. Kadi L*, et al*. Differential effects of chemokines on oligodendrocyte precursor proliferation and myelin formation in vitro. *J Neuroimmunol*. May 2006;174(1-2):133-46. doi:10.1016/j.jneuroim.2006.01.011
94. Zhang ZJ*, et al*. Chemokine contribution to neuropathic pain: respective induction of CXCL1 and CXCR2 in spinal cord astrocytes and neurons. *Pain*. Oct 2013;154(10):2185-2197. doi:10.1016/j.pain.2013.07.002
95. Chang R*, et al*. Tumor necrosis factor alpha Inhibition for Alzheimer's Disease. *J Cent Nerv Syst Dis*. 2017/01 2017;9:1179573517709278. doi:10.1177/1179573517709278
96. Fischer R*, et al*. Astrocyte-specific activation of TNFR2 promotes oligodendrocyte maturation by secretion of leukemia inhibitory factor. *Glia*. Feb 2014;62(2):272-83. doi:10.1002/glia.22605
97. Hofman FM*, et al*. Tumor necrosis factor identified in multiple sclerosis brain. *J Exp Med*. Aug 1 1989;170(2):607-12. doi:10.1084/jem.170.2.607
98. Selmaj K*, et al*. Cytokine cytotoxicity against oligodendrocytes. Apoptosis induced by lymphotoxin. *J Immunol*. Sep 1 1991;147(5):1522-9.
99. Selmaj K*, et al*. Tumor necrosis factor mediates myelin damage in organotypic cultures of nervous tissue. *Ann N Y Acad Sci*. 1988/11 1988;540(1 Advances in N):568-70. doi:10.1111/j.1749-6632.1988.tb27175.x
100. Deng Y*, et al*. Astrocyte-derived proinflammatory cytokines induce hypomyelination in the periventricular white matter in the hypoxic neonatal brain. *PLOS ONE*. 2014/01/31 2014;9(1):e87420. doi:10.1371/journal.pone.0087420
101. Agresti C*, et al*. Reversible inhibitory effects of interferon-gamma and tumour necrosis factor-alpha on oligodendroglial lineage cell proliferation and differentiation in vitro. *Eur J Neurosci*. Jun 1996;8(6):1106-16. doi:10.1111/j.1460-9568.1996.tb01278.x
102. Hindinger C*, et al*. IFN-gamma signaling to astrocytes protects from autoimmune mediated neurological disability. *PLOS ONE*. 2012/07/27 2012;7(7):e42088. doi:10.1371/journal.pone.0042088
103. LaFerla FM*, et al*. Regional hypomyelination and dysplasia in transgenic mice with astrocyte-directed expression of interferon-gamma. *J Mol Neurosci*. Aug 2000;15(1):45-59. doi:10.1385/JMN:15:1:45
104. Panitch HS*, et al*. Treatment of multiple sclerosis with gamma interferon: exacerbations associated with activation of the immune system. *Neurology*. Jul 1987;37(7):1097-102. doi:10.1212/wnl.37.7.1097
105. Butt AM*, et al*. Fibroblast growth factor 2 induces loss of adult oligodendrocytes and myelin in vivo. *Exp Neurol*. Mar 2005;192(1):125-33. doi:10.1016/j.expneurol.2004.11.007
106. Gross RE*, et al*. Bone morphogenetic proteins promote astroglial lineage commitment by mammalian subventricular zone progenitor cells. *Neuron*. Oct 1996;17(4):595-606. doi:10.1016/s0896-6273(00)80193-2
107. Hesp ZC*, et al*. Chronic oligodendrogenesis and remyelination after spinal cord injury in mice and rats. *J Neurosci*. Jan 21 2015;35(3):1274-90. doi:10.1523/JNEUROSCI.2568-14.2015
108. Clarner T*, et al*. Corticosteroids impair remyelination in the corpus callosum of cuprizone-treated mice. *J Neuroendocrinol*. Jul 2011;23(7):601-11. doi:10.1111/j.1365-2826.2011.02140.x
109. McMorris FA*, et al*. Insulin-like growth factor I/somatomedin C: a potent inducer of oligodendrocyte development. *Proc Natl Acad Sci U S A*. Feb 1986;83(3):822-6. doi:10.1073/pnas.83.3.822
110. Balabanov R*, et al*. Interferon-gamma-oligodendrocyte interactions in the regulation of experimental autoimmune encephalomyelitis. *J Neurosci*. Feb 21 2007;27(8):2013-24. doi:10.1523/JNEUROSCI.4689-06.2007
111. Semple BD*, et al*. CCL2 modulates cytokine production in cultured mouse astrocytes. *J*

Neuroinflammation. Oct 14 2010;7(1):67. doi:10.1186/1742-2094-7-67
112. Goldberg SH, *et al*. CXCR3 expression in human central nervous system diseases. *Neuropathol Appl Neurobiol*. Apr 2001;27(2):127-38. doi:10.1046/j.1365-2990.2001.00312.x
113. You T, *et al*. IL-17 induces reactive astrocytes and up-regulation of vascular endothelial growth factor (VEGF) through JAK/STAT signaling. *Sci Rep*. Mar 10 2017;7(1):41779. doi:10.1038/srep41779
114. Narcisse L, *et al*. The cytokine IL-1beta transiently enhances P2X7 receptor expression and function in human astrocytes. *Glia*. Jan 15 2005;49(2):245-58. doi:10.1002/glia.20110
115. Zeis T, *et al*. The immunomodulatory oligodendrocyte. *Brain Res*. Jun 15 2016;1641(Pt A):139-148. doi:10.1016/j.brainres.2015.09.021
116. Choi JK, *et al*. GM-CSF reduces expression of chondroitin sulfate proteoglycan (CSPG) core proteins in TGF-beta-treated primary astrocytes. *BMB Rep*. Dec 2014;47(12):679-84. doi:10.5483/bmbrep.2014.47.12.018
117. Boulay AC, *et al*. Immunoregulation at the gliovascular unit in the healthy brain: A focus on Connexin 43. *Brain Behav Immun*. Aug 2016;56:1-9. doi:10.1016/j.bbi.2015.11.017
118. Boulay AC, *et al*. Connexin 43 Controls the Astrocyte Immunoregulatory Phenotype. *Brain sciences*. Mar 22 2018;8(4):50. doi:10.3390/brainsci8040050
119. Allaman I, *et al*. Astrocyte-neuron metabolic relationships: for better and for worse. *Trends Neurosci*. Feb 2011;34(2):76-87. doi:10.1016/j.tins.2010.12.001
120. Choi SJ, *et al*. Differential expression, shedding, cytokine regulation and function of TNFR1 and TNFR2 in human fetal astrocytes. *Yonsei Med J*. Dec 31 2005;46(6):818-26. doi:10.3349/ymj.2005.46.6.818
121. Kemanetzoglou E, *et al*. CNS Demyelination with TNF-alpha Blockers. *Curr Neurol Neurosci Rep*. Apr 2017;17(4):36. doi:10.1007/s11910-017-0742-1
122. Pegoretti V, *et al*. Selective Modulation of TNF-TNFRs Signaling: Insights for Multiple Sclerosis Treatment. *Front Immunol*. 2018;9:925. doi:10.3389/fimmu.2018.00925
123. Miljkovic D, *et al*. Astrocytes in the tempest of multiple sclerosis. *FEBS Lett*. Dec 1 2011;585(23):3781-8. doi:10.1016/j.febslet.2011.03.047
124. Burm SM, *et al*. Expression of IL-1beta in rhesus EAE and MS lesions is mainly induced in the CNS itself. *J Neuroinflammation*. Jun 6 2016;13(1):138. doi:10.1186/s12974-016-0605-8
125. Prins M, *et al*. Pathological differences between white and grey matter multiple sclerosis lesions. *Ann N Y Acad Sci*. Sep 2015;1351(1):99-113. doi:10.1111/nyas.12841
126. Sosunov A, *et al*. Alexander disease: an astrocytopathy that produces a leukodystrophy. *Brain Pathol*. May 2018;28(3):388-398. doi:10.1111/bpa.12601
127. Huang L, *et al*. Glial scar formation occurs in the human brain after ischemic stroke. *Int J Med Sci*. 2014;11(4):344-8. doi:10.7150/ijms.8140
128. Verkhratsky A, *et al*. Glia in the pathogenesis of neurodegenerative diseases. *Biochem Soc Trans*. Oct 2014;42(5):1291-301. doi:10.1042/BST20140107
129. Anderson MA, *et al*. Heterogeneity of reactive astrocytes. *Neurosci Lett*. Apr 17 2014;565:23-9. doi:10.1016/j.neulet.2013.12.030
130. Rolls A, *et al*. The bright side of the glial scar in CNS repair. *Nat Rev Neurosci*. Mar 2009;10(3):235-41. doi:10.1038/nrn2591
131. Ceyzeriat K, *et al*. Modulation of astrocyte reactivity improves functional deficits in mouse models of Alzheimer's disease. *Acta Neuropathol Commun*. Oct 16 2018;6(1):104. doi:10.1186/s40478-018-0606-1
132. Ludwin SK, *et al*. Astrocytes in multiple sclerosis. *Mult Scler*. Aug 2016;22(9):1114-24. doi:10.1177/1352458516643396
133. Leibowitz SM, *et al*. NF-kappaB Pathways in the Pathogenesis of Multiple Sclerosis and the Therapeutic Implications. *Front Mol Neurosci*. 2016/09/15 2016;9:84. doi:10.3389/fnmol.2016.00084
134. Yi H, *et al*. IL-17A induces MIP-1alpha expression in primary astrocytes via Src/MAPK/PI3K/NF-kB pathways: implications for multiple sclerosis. *J Neuroimmune Pharmacol*. Dec 2014;9(5):629-41. doi:10.1007/s11481-014-9553-1
135. Brambilla R, *et al*. Transgenic inhibition of astroglial NF-kappa B improves functional outcome in experimental autoimmune encephalomyelitis by suppressing chronic central nervous system inflammation. *J Immunol*. Mar 1 2009;182(5):2628-40. doi:10.4049/jimmunol.0802954
136. Gonzalez-Reyes RE, *et al*. Involvement of Astrocytes in Alzheimer's Disease from a Neuroinflammatory and Oxidative Stress Perspective. *Front Mol Neurosci*. 2017/12/19 2017;10:427. doi:10.3389/fnmol.2017.00427
137. Ouali Alami N, *et al*. NF-kappaB activation in astrocytes drives a stage-specific beneficial neuroimmunological response in ALS. *EMBO J*. Aug 15 2018;37(16):e98697. doi:10.15252/embj.201798697
138. Butt AM, *et al*. Oligodendroglial Cells in Alzheimer's Disease. *Adv Exp Med Biol*. 2019;1175:325-333. doi:10.1007/978-981-13-9913-8_12
139. Matute C, *et al*. P2X(7) receptor blockade prevents ATP excitotoxicity in oligodendrocytes and ameliorates experimental autoimmune encephalomyelitis. *J Neurosci*. Aug 29 2007;27(35):9525-33. doi:10.1523/JNEUROSCI.0579-07.2007
140. Bezzi P, *et al*. CXCR4-activated astrocyte glutamate release via TNFalpha: amplification by

microglia triggers neurotoxicity. *Nat Neurosci*. Jul 2001;4(7):702-10. doi:10.1038/89490

141. Jeremic A*, et al*. ATP stimulates calcium-dependent glutamate release from cultured astrocytes. *J Neurochem*. Apr 2001;77(2):664-75. doi:10.1046/j.1471-4159.2001.00272.x
142. Wang X*, et al*. P2X7 receptor inhibition improves recovery after spinal cord injury. *Nat Med*. Aug 2004;10(8):821-7. doi:10.1038/nm1082
143. Amadio S*, et al*. Modulation of P2X7 Receptor during Inflammation in Multiple Sclerosis. *Front Immunol*. 2017;8:1529. doi:10.3389/fimmu.2017.01529
144. Beamer E*, et al*. The ATP-Gated P2X7 Receptor As a Target for the Treatment of Drug-Resistant Epilepsy. *Front Neurosci*. 2017/02/02 2017;11:21. doi:10.3389/fnins.2017.00021
145. Olsen JA*, et al*. Remyelination in multiple sclerosis: cellular mechanisms and novel therapeutic approaches. *J Neurosci Res*. May 2015;93(5):687-96. doi:10.1002/jnr.23493
146. Van Strien ME*, et al*. Tissue transglutaminase activity is involved in the differentiation of oligodendrocyte precursor cells into myelin-forming oligodendrocytes during CNS remyelination. *Glia*. Nov 2011;59(11):1622-34. doi:10.1002/glia.21204
147. Franklin RJM*, et al*. Regenerating CNS myelin - from mechanisms to experimental medicines. *Nat Rev Neurosci*. Nov 16 2017;18(12):753-769. doi:10.1038/nrn.2017.136
148. Albrecht PJ*, et al*. Astrocytes produce CNTF during the remyelination phase of viral-induced spinal cord demyelination to stimulate FGF-2 production. *Neurobiol Dis*. Jul 2003;13(2):89-101. doi:10.1016/s0969-9961(03)00019-6
149. Yeung MSY*, et al*. Dynamics of oligodendrocyte generation in multiple sclerosis. *Nature*. Feb 2019;566(7745):538-542. doi:10.1038/s41586-018-0842-3
150. Lau LW*, et al*. Pathophysiology of the brain extracellular matrix: a new target for remyelination. *Nat Rev Neurosci*. Oct 2013;14(10):722-9. doi:10.1038/nrn3550
151. Mohassel P*, et al*. Extracellular matrix-driven congenital muscular dystrophies. *Matrix Biol*. Oct 2018;71-72:188-204. doi:10.1016/j.matbio.2018.06.005
152. van Horssen J*, et al*. The extracellular matrix in multiple sclerosis pathology. *J Neurochem*. Nov 2007;103(4):1293-301. doi:10.1111/j.1471-4159.2007.04897.x
153. Lau LW*, et al*. Chondroitin sulfate proteoglycans in demyelinated lesions impair remyelination. *Ann Neurol*. Sep 2012;72(3):419-32. doi:10.1002/ana.23599
154. Jiang P*, et al*. Human iPSC-Derived Immature Astroglia Promote Oligodendrogenesis by Increasing TIMP-1 Secretion. *Cell Rep*. May 10 2016;15(6):1303-15. doi:10.1016/j.celrep.2016.04.011
155. Miyamoto N*, et al*. Astrocytes Promote Oligodendrogenesis after White Matter Damage via Brain-Derived Neurotrophic Factor. *J Neurosci*. Oct 14 2015;35(41):14002-8. doi:10.1523/JNEUROSCI.1592-15.2015
156. Wang P*, et al*. MMP7 cleaves remyelination-impairing fibronectin aggregates and its expression is reduced in chronic multiple sclerosis lesions. *Glia*. Aug 2018;66(8):1625-1643. doi:10.1002/glia.23328

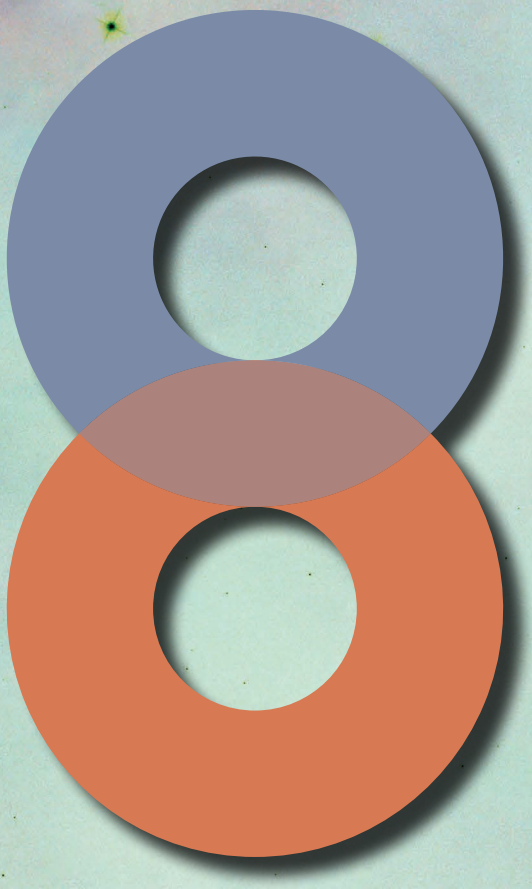

White matter microglia heterogeneity in the CNS

Sandra Amor, Niamh B. McNamara, Emma Gerrits, Manuel C. Marzin, Susanne M. Kooistra, Veronique E. Miron, Erik Nutma

Acta Neuropathologica 2022; 143(2):124-141

Abstract

Microglia, the resident myeloid cells in the central nervous system (CNS) play critical roles in shaping the brain during development, responding to invading pathogens, and clearing tissue debris or aberrant protein aggregations during ageing and neurodegeneration. The original concept that like macrophages, microglia are either damaging (pro-inflammatory) or regenerative (anti-inflammatory) has been updated to a kaleidoscope view of microglia phenotypes reflecting their wide-ranging roles in maintaining homeostasis in the CNS and, their contribution to CNS diseases, as well as aiding repair. The use of new technologies including single cell/nucleus RNA-sequencing has led to the identification of many novel microglia states, allowing for a better understanding of their complexity and distinguishing regional variations in the CNS. This has also revealed differences between species and diseases, and between microglia and other myeloid cells in the CNS. However, most of the data on microglia heterogeneity has been generated on cells isolated from the cortex or whole brain, whereas white matter changes and differences between white and grey matter have been relatively understudied. Considering the importance of microglia in regulating white matter health, we provide a brief update on the current knowledge of microglia heterogeneity in the white matter, how microglia are important for the development of the CNS, and how microglial ageing affects CNS white matter homeostasis. We discuss how microglia are intricately linked to the classical white matter diseases such as multiple sclerosis and genetic white matter diseases, and their putative roles in neurodegenerative diseases in which white matter is also affected. Understanding the wide variety of microglial functions in the white matter may provide the basis for microglial targeted therapies for CNS diseases.

Introduction

Microglia, the resident macrophages in the central nervous system (CNS), were discovered over 100 years ago by Pío del Río-Hortega, and have since been the focus of many studies. While historically microglia have been described as the phagocytes of the CNS, advancements in research techniques over the last few decades have shown that microglia have diverse roles (Fig. 1). Their main functions are to protect the CNS parenchyma by constantly scanning their surroundings for potential harm[1] and to regulate CNS homeostasis[2]. Microglia comprise roughly 10% of the total glial population, but unlike astrocytes or oligodendrocytes, microglia are derived from yolk sac progenitors that populate the CNS during embryonic development[3].

Throughout life, microglia have the ability to self-renew through proliferation, while during disease this process shifts towards clonal expansion depending on the local need for microglia[4]. Such proliferation of microglia is associated with apoptosis that removes excess numbers of microglia to keep the cell numbers in check[5]. This self-renewal capacity indicates that microglia are subject to constant changes independent of disease or homeostatic activities. Following injury, microglia undergo morphological and transcriptional changes to adapt their behaviour in response to the type of injury. The versatile nature of microglia also proves to be one of major the challenges in microglia research – *ex vivo* culturing of microglia leads to fast and extensive downregulation of microglia-specific genes and upregulation of genes associated with acute inflammatory responses and immune functions[6], making it difficult to decipher their roles solely using *in vitro* approaches.

While microglia are often considered as drivers of CNS pathology (Fig. 2), leukodystrophies and myelin damage are associated with loss of microglial functions and decrease in microglial numbers[7]. Microglia are thus essential for normal functioning of the CNS white matter. Additionally, white matter integrity is essential for cognitive, sensory, and motor functions, throughout the lifespan ranging from development to ageing[8-12]. Aberrations in myelin structure are observed in neurodegenerative diseases such as amyotrophic lateral sclerosis (ALS), Alzheimer's disease (AD), and viral encephalitis. These findings indicate a strong link between white matter integrity and neuronal health and function. As white matter is increasingly implicated in a range of CNS functions, the need to elucidate the roles of microglia within the white matter, and their heterogeneous functions in health and disease, is critical. Here, we review the current knowledge of microglia heterogeneity in the white matter during development and ageing, and their roles in white matter diseases and neurodegenerative diseases in which white matter is affected. Finally, we discuss potential therapeutic avenues for microglial targeting in these diseases.

Microglia heterogeneity in the CNS

Historically, microglia have been compared to peripheral blood derived macrophages, and consequently, classifications used to describe macrophage activation states in non-CNS tissue were applied to microglia. Initially, microglia were categorised as 'resting' under homeostatic conditions, M1 under pro-inflammatory conditions ('classically activated') or M2 under anti-inflammatory conditions ('alternatively activated')[13,14]. However, *in vivo*, microglia adopt intermediate phenotypes expressing both pro-inflammatory and anti-inflammatory markers[15,16], suggesting a more complex profile. Additionally, it is unclear as to whether M1 or M2 microglia states exist *in vivo*[17]. Proteomics and single cell/nucleus RNA-seq analyses have supported the concept that microglia heterogeneity is far more diverse, and that this heterogeneity is influenced by regional differences in the CNS, age, and the type of injury.

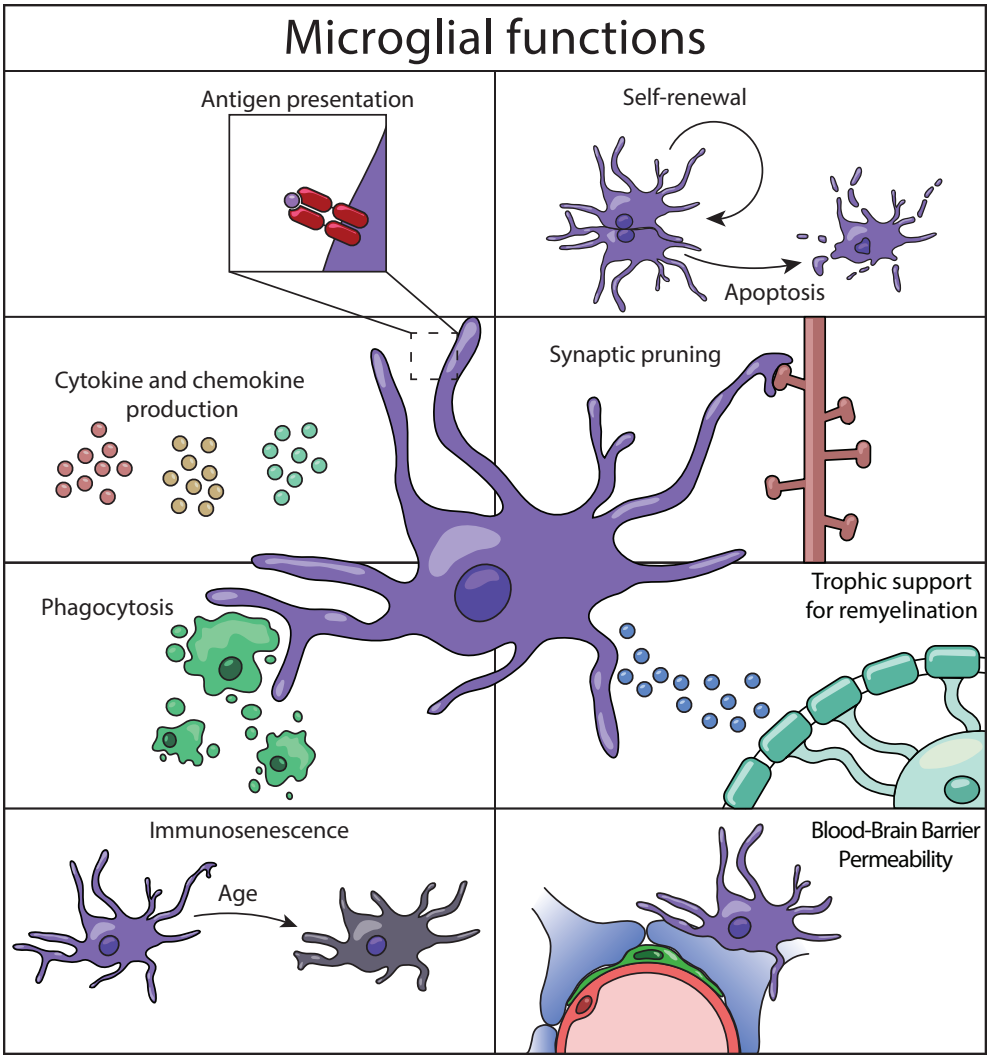

Figure 1. Microglial functions in the central nervous system. Microglia have many immunological functions in the central nervous system by presenting antigens, secreting cytokines and chemokines and by phagocytosing myelin debris or dead cells. Microglia also self-renew the microglia pool through coordinated proliferation and apoptosis. During development, microglia are important for neuronal development by synaptic pruning. Microglia provide trophic support for maintaining myelin integrity as well as remyelination. During ageing microglia adopt a more pro-inflammatory profile. Microglia also play a role in maintaining and influencing the permeability of the blood–brain barrier.

Frequently used markers to detect homeostatic or activated microglia are the ionized calcium binding adapter molecule 1 (IBA1), MHC class II cell surface receptor human leukocyte antigen DR (HLA-DR), CX3CR1 (fractalkine receptor), and cluster of differentiation (CD) markers, CD68, CD40, CD206, CD163, and CD11b[18-20]. However, these proteins are not unique to microglia as other macrophage populations, such as infiltrating monocyte-derived macrophages present during neuroinflammation and CNS-associated macrophages (CAMs), have also been reported to express these markers[21-24]. In addition, combinations of markers, such as

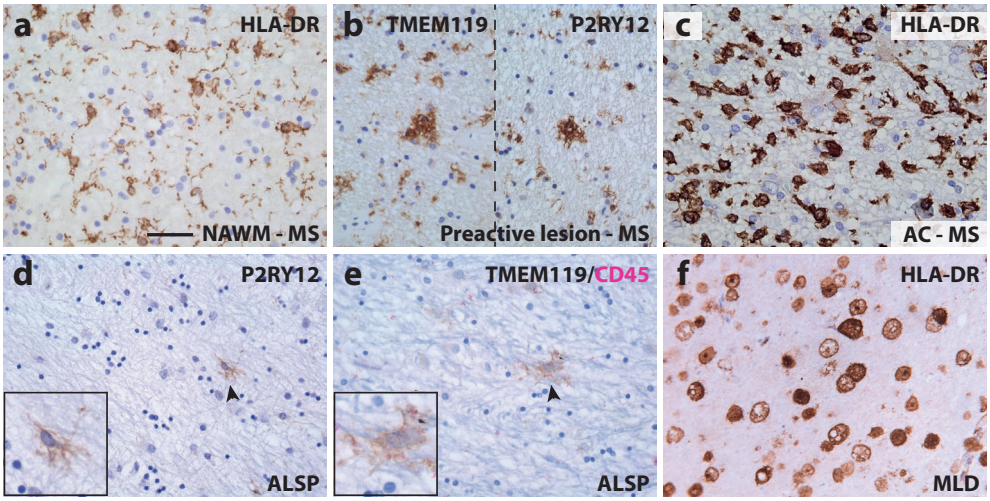

Figure 2. Microglia involvement in CNS diseases. Microglia are involved in CNS white matter diseases. Microglia in the normal appearing white matter (NAWM) in multiple sclerosis (MS) show ramified morphology similar to healthy controls (a). Clustering of microglia may represent preactive lesions in MS, but these cells still express homeostatic markers TMEM119 and P2RY12 (b). In active MS lesions microglia undergo transcriptional and morphological changes associated with phagocytosis and display an amoeboid morphology (c). In leukodystrophies, white matter in ALSP (in the frontal lobe) is almost devoid of microglia and only few cells express the homeostatic microglia markers TMEM119 and P2RY12 (d, e). Highly activated and amoeboid microglia are a key characteristic of the pathology of the leukodystrophy MLD (f). Scale bar=50 µm. ALSP = adult-onset leuko-encephalopathy with axonal spheroids and pigmented glia, MLD = metachromatic leukodystrophy.

CD45 and CD11b, have been used to differentiate microglia from other macrophages using flow cytometry[25]. Unlike CD11b-high monocytes and macrophages, microglia do not require Myb but depend on factors such as Pu.1 and Irf8 for their development[26,27]. Recently, microglia specific markers were identified- transmembrane protein 119 (TMEM119) and P2Y purinoreceptor 12 (P2RY12) - which distinguish microglia from invading myeloid cells and CAMs[28,29]. However, both TMEM119 and P2RY12 are downregulated in neurodegenerative diseases including AD[30] and active multiple sclerosis (MS)[18]. Conversely, *Hexb*, which encodes for the beta subunit of the lysosomal enzyme hexosaminidase B, is a recently discovered microglia-enriched gene which is stably expressed even under neuroinflammatory or demyelinating conditions. In addition, *Hexb* is only faintly detected in CAMs and circulating myeloid cells indicating that *Hexb* can be used for specific microglia detection in the CNS[31].

Approaches to determine heterogeneity

To study the roles of microglia in health and disease, several reporter mouse models have been developed. While mouse models do not always represent the full complexity of the human CNS[32,33], they do provide the opportunity to study specific microglia states *in vivo* and to target microglia genes in a temporally-controlled manner in development, homeostasis, ageing and following injury. One such model, the CX3CR1^{GFP} mouse, tracks cells expressing CX3CR1- a chemokine receptor involved in chemotaxis and cell survival during homeostasis and inflammation[34]. CX3CR1 is abundantly expressed by homeostatic microglia[35], and promoter-driven GFP expression allows tracking of microglia. However, this does not distinguish between microglia and CAMs and also detects other macrophages, dendritic cells and natural killer cells under pathological conditions[36,37]. Nevertheless, tamoxifen inducible

CX3CR1^{CreER} mice have greatly contributed to our understanding of microglia by identifying critical pathways that underlie microglial activation during neuroinflammation[38,39]. To discriminate between microglia and macrophages, *Tmem119*^{EGFP}, *Tmem119*^{CreERT2}, *P2ry12*^{CreER}, *Hexb*^{tdT} and *Hexb*^{CreERT2} models have recently been developed[31,40,41]. Among these models, *Hexb* transgenic lines have the advantage of stable *Hexb* expression following CNS damage, allowing microglia tracking or manipulation in these contexts[31,42].

Cytometry by time-of-flight (CyTOF) mass spectrometry, has allowed for the identification of macrophage subsets in the CNS which shift in the context of pathology[23,43]. While these elegantly developed techniques provide great insight into microglial heterogeneity, they have yet to be specifically applied to white matter microglia. A more recent advanced technique, single cell RNA-sequencing (scRNA-seq), allows the gathering of transcriptional profiles of thousands of cells from one sample to identify gene expression at a single cell level. This makes scRNA-seq an outstanding tool to investigate the heterogeneity of microglia across different brain regions and/or different cellular development stages. scRNA-seq has already progressed to allow more detailed studies to generate full-length cDNA (e.g. SMART-seq2) or cDNA with an unique molecular identifier (UMI) at the 5' or 3' end (e.g. MARS-seq, 10X Genomics). SMART-seq2 covers the entire transcriptome and has a very high accuracy and sensitivity[44]. MARS-seq, while less accurate than SMART-seq2, is less expensive and allows multiplexing of samples via molecular tagging[45]. Both full-length and tag-based methods are used for various fundamental applications such as cell-type discovery, gene expression analysis, tissue composition assessment and to investigate microglial heterogeneity in the CNS. Using SMART-seq2, a microglial gene signature for cell cycle phases of dividing microglia was found[46]. Additionally, MARS-seq was used to identify different phases of regulatory networks in microglia[47]. While scRNA-seq studies have identified heterogeneity of microglia, combining this advanced technique with spatial transcriptomics[48] will help elucidate microglia heterogeneity in the context of pathology or cellular interactions, as has recently been reported in a mouse model of AD[49], and in astrocytes in the context of neuroinflammation[50]. These advanced tools allow us to identify more diverse microglia states than possible with classical methods, revealing the full complement of microglial heterogeneity (Fig. 3).

Regional and morphological differences of microglia

Microglia numbers and morphology vary between brain regions in humans and mice although species differences are observed. For example, human microglia density is higher in white matter compared to grey matter (Table 1), converse to that observed in rodents[5,51]. Microglial density might reflect regional requirements for microglial support or surveillance[52,53]. Indeed, regional differences in expression of cell surface proteins related to environmental scanning have been documented in mice[54]. Furthermore, genes related to immune signalling, dampening of microglial activation, metabolism and the sensome are differentially expressed between the cortex, cerebellum, hippocampus and striatum of mice[54]. Despite this regional heterogeneity microglia retain a specific signature that distinguishes them from peripheral macrophages[29,54-56]. A recent study utilising bulk RNA-seq found distinct microglial signatures in the white matter compared to the grey matter in both MS brain and healthy controls, irrespective of disease[57]. For example, the NF-κB pathway was found to be engaged at a higher level in white matter microglia compared to their grey matter counterparts, possibly providing an explanation as to why microglial inflammation is increased in the former[58].

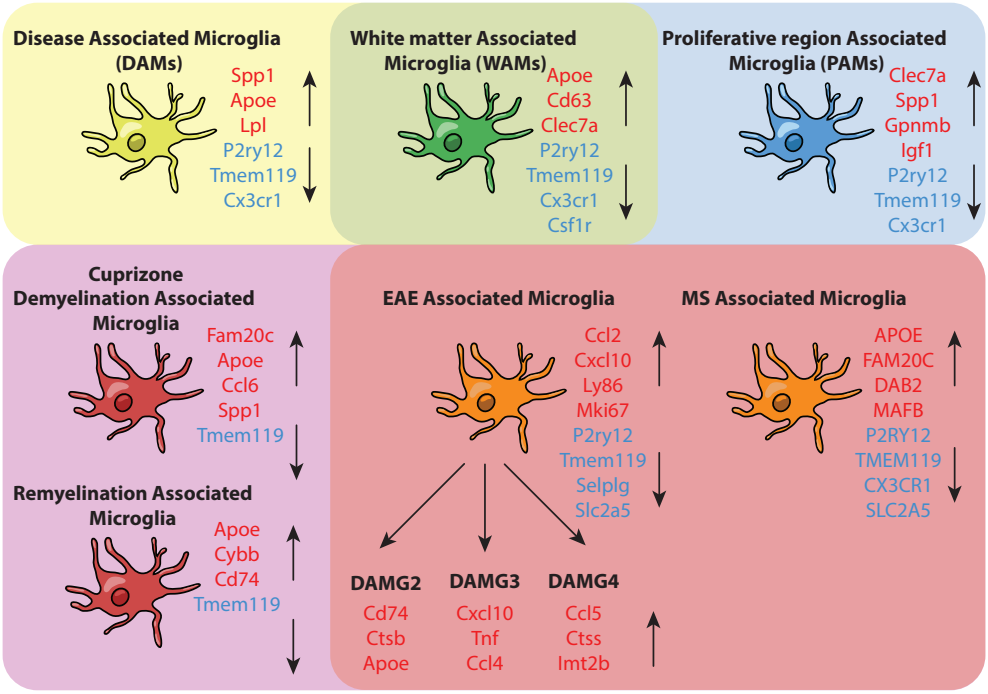

Figure 3. Microglia states in development and disease. Multiple microglia states have been identified in mice throughout development, ageing and disease, some of which have partially overlapping signatures. Similarly, microglia expression profiles in mouse models of MS, cuprizone and experimental autoimmune encephalomyelitis (EAE), only partially overlap with that of MS-associated microglia, likely reflecting species differences

Additionally, white matter microglia have higher elasticity and viscosity, compared to grey matter microglia[59], which might impact microglial ability to phagocytose[60]. A subset of macrophages has also been identified lining the apical surface of the choroid plexus epithelium, also known as Kolmer's epiplexus cells. These epiplexus macrophages share microglial signature genes such as *Sall1* and have a transcriptional signature reminiscent of 'damage/disease-associated microglia' (DAM) under homeostatic conditions, suggesting possible roles in responses to pathology[24]. Overall, white matter microglia appear to have properties and engage pathways involved in inflammation, more so than those in the grey matter (Table 1).

Microglia heterogeneity in development and ageing

Development

Regional and temporal heterogeneity of microglia are observed during development[46,61-63]. Developmental white matter microglia exhibit a more activated profile compared to those in the cortex, as defined by expression of genes associated with activated microglia including *Spp1*, *Itgax*, *Gpnmb*, *Igf1* and *Clec7a*[64]. Regional heterogeneity is further indicated by the more pronounced depletion of white matter microglia in mice deficient in the CSF1R ligand CSF-1, particularly in the spinal cord[65,66]. Indeed, differential expression of *Csf-1* and *IL-34* between the white and grey matter has recently been shown, with white matter microglia depending more on *Csf-1* for their development/maintenance potentially explaining this heterogeneity[66]. Single-cell sequencing studies have characterised the heterogeneity of

Table 1. Microglia differences in white and grey matter

	White matter	Grey matter	Ref
Healthy conditions			
Microglial density	High	Low	5,51
Biomechanical properties (viscoelasticity)	High, decreased in inflammation and after uptake in of myelin	Low, increased in inflammation, decreased after myelin intake	59
Nf-κB pathway expression	Enriched		58
Type-1 interferon pathway expression	Enriched during remyelination	Enriched	58,62, 67,68
Marker expression for Antigen presentation, phagocytosis and cholesterol transport	High	Low	69,70
TREM2-dependent white matter associated microglia (WAMs)	Present	Absent	71
Expression of Sall1 (loss of Sall1 results in inflammation)	Enriched		72
Disease / Ageing			
SPP1 expression in ageing	Enriched		69
Lipid metabolism in MS	High	Low	58
Glycolysis and iron homeostasis in MS	Low	High	58
Expression of Sall1	Reduced	Enriched	72
Microgliosis after cuprizone administration	Severe	Mild	73

microglial gene expression during development. By sequencing the whole brain, Hammond *et al.*[62] and Li *et al.*[46] found that postnatal microglia (postnatal day (P) 4/5 and P7 respectively) display marked transcriptomic heterogeneity in contrast to adult microglia. Of particular interest, both studies identified a microglial state associated with the developing white matter, sometimes referred to as the proliferative-region-associated microglia (PAM) state. While the role of this developmental white matter microglial state is not fully understood, it appears to represent highly phagocytic cells as ~13% of *Clec7a*+ microglia contain *Mbp* transcripts, and CLEC7A+ microglia in the corpus callosum and cerebellum phagocytose beads and nuclei[46]. While *CX3CR1*-eGFP+ microglia phagocytose apoptotic oligodendrocytes (cleaved caspase-3+ MBP+) in the developing white matter[46] whether these represent the CLEC7A+ state remains to be determined. Although these studies have identified a white matter-associated microglia state by sequencing the whole brain, the heterogeneity of microglia specifically in the white matter during development has yet to be resolved.

These studies complement previous work identifying a microglia state associated with developing white matter identified by expression of CD11c (*Itgax*)[64,74], which appears transiently in the corpus callosum and cerebellar white matter of mice during the early postnatal period[74]. Not all microglia in the white matter express CD11c, indicating heterogeneity within white matter during development. CD11c-driven knockout of the gene encoding the growth factor insulin-like growth factor (IGF)-1 causes a reduction in myelinated axons and alters myelin thickness, suggesting a role of CD11c+ cells in regulating developmental myelination[74]. Whether the CD11c+ and CLEC7A+ microglia represent the same or distinct states within the

developing white matter is unclear. However, there is an overlap in genes expressed by both microglial states including *Spp1*, *Apoe*, and *Lpl,* which are also expressed by DAMs and are re-expressed following white matter injury[30,46,62,63]. Similarly, *Ccl4*-expressing microglia peak at P5 and are expanded in the ageing mouse brain and following demyelination in the mouse and in humans[62]. DAM signatures were also found in the developing human foetal CNS, and increasingly resemble adult homeostatic microglia throughout development[63]. Importantly, shared expression of one or several genes does not necessarily translate to function. For instance, CD11c+ microglia that re-emerge in the adult CNS following autoimmune-mediated demyelination have a distinct gene signature to neonatal CD11c+ microglia, indicating that this marker may be expressed by distinct microglial states throughout the lifespan[74]. Nevertheless, Hammond and colleagues found that while microglia are most diverse in the developing brain and this diversity decreases in adulthood, they become more heterogeneous again in the aged or injured brain[62].

Ageing

A plethora of studies support microglia heterogeneity in the ageing and diseased CNS. Microglia in the aged brain are characterised by expression of inflammatory genes, including chemokines *Ccl3* and *Ccl4*, *Cst7* and *IL1b*[62,75], and those involved in immunoregulatory function, such as the interferon pathway[54,62,76]. In human microglia, ageing induces downregulation of genes associated with TGF-β signalling, suggesting a reduction in their homeostatic signature, while amyloid fibre formation pathway-associated genes are upregulated[77]. Grabert *et al.* reported regional heterogeneity in mouse microglia ageing profiles, with cerebellar microglia showing accelerated ageing in their transcriptomic signature compared to other brain regions[54]. This raises the important question of the effect of ageing on microglia in the white matter specifically.

While the majority of studies involved sequencing of microglia from the whole brain, a recent report shed light on microglia heterogeneity in the ageing white matter[69]. Sankowski *et al*. compared human microglia in grey versus white matter of the temporal lobe across various ages, by combining scRNA-sequencing and multiplexed mass cytometry (cyTOF). Microglia in the white matter showed enriched expression of HLA-DR, CD68 and APOE compared to grey matter microglia, pointing to differential roles in antigen presentation, phagocytosis and cholesterol transport. Interestingly, an increase in osteopontin+ (SPP1+) microglia/macrophages (IBA1+) during ageing was reported, with higher percentages in the white matter compared to grey matter[69,75]. SPP1 is a pro-inflammatory cytokine upregulated by microglia in aged mice and mouse models of AD[78], although its precise function remains unclear in this context.

Heterogeneity of microglia specifically in the aged mouse white matter was reported using two sequencing approaches, SmartSeq2 for higher gene depth and Drop-Seq for greater cell coverage, revealing four major microglia populations in the white matter of 18–24-month-old mice[71]. Two homeostatic microglial states were found in both grey and white matter, and two populations were exclusive to white matter: an activated microglia cluster and 'white matter-associated microglia' (referred to as WAMs). Both white matter-specific states were dependent on TREM2 for their development, in common with the previously identified DAM population. TREM2 signalling is also required for driving macrophage cell states outside of the CNS, for example in lipid-associated macrophages (LAM)[79], which may point to roles of DAM and WAM in lipid metabolism. Reanalysis of previously published scRNA-seq aged mouse

microglial datasets revealed that the WAMs were also present in these studies[62,80]. WAMs had depleted expression of microglial homeostatic genes, including *P2ry12*, *Tmem119*, *Csf1r* and *Cx3cr1*, and enriched expression of *Apoe*, *Cd63* and *Clec7a*, some of which are associated with DAM and microglia in the developing white matter. Comparing genes that were differentially expressed in Cd11b+ cells (microglia and CNS-resident macrophages) in aged (21 month) versus young (4 month) mouse corpus callosum revealed that the top enriched pathways in aged white matter were related to immune cell function. WAM signature genes were present, including *Spp1*, *Clec7a*, *Itgax* and *Apoe*, again showing similarity to genes expressed by the developmental white matter state. Precisely when these pathway changes are initiated in white matter microglia with ageing is not known. Between 10-30% of IBA1+ cells in the *corpus callosum* expressed a WAM marker (CLEC7A, AXL, LGALS3, *Itgax*) and notably, these cells were almost absent from the cortex. It is not clear, however, what proportion of the IBA1+ cells co-express WAM markers, nor how many markers constitute a WAM state. WAM were found to group together in clusters or "nodules" of 3-5 cells, with distinctly thick processes and large cell bodies, reminiscent of previously documented microglia clusters considered to precede CNS demyelination in MS[81]. Using *Trem2*$^{-/-}$ mice and *in vitro* studies, WAMs were found to be involved in digestion of phagocytosed myelin debris, suggesting a protective function that avoids the build-up of degenerating myelin during ageing[71]. In several mouse models of AD, the WAM population appeared before the DAM state, and both states share part of their gene signature[71]. Interestingly, DAM rely on APOE for their development whereas WAM do not, indicating dissimilarities between the two states[71]. The conversion of WAM into DAM may be a mechanism by which normal brain ageing switches to a neurodegenerative state, with the WAM potentially pivoting from a protective function. Further work is required to understand if, why and how this conversion could occur. While it is still unclear whether DAM are protective or detrimental, elucidating the mechanisms underlying potential microglia state conversion represents a promising avenue to prevent disease in the ageing brain.

Microglia heterogeneity in CNS diseases

Inflammatory white matter diseases

MS is a prototypical inflammatory white matter disease in which microglia are considered to contribute to myelin damage, and remyelination. Microglia activation and myelin loss also occur in the grey matter in MS[82], preceding the neuronal and synaptic loss which are key determinants of disease progression[83,84]. The aetiology of MS and mechanisms leading to chronic disease likely involves interactions between environmental factors, the immune system, and neurons and glia. Studies in a model of autoimmune-mediated demyelination (experimental autoimmune encephalomyelitis- EAE) led to the widely held concept that MS is a T-cell-mediated disease, however, the efficacy of B-cell targeting (anti-CD20) therapies in MS has challenged this hypothesis[85-88]. Nevertheless, microglia are likely key players in MS lesion formation and MS disease progression. Studies using scRNA-seq and immunohistochemistry have identified a wide range of MS-associated microglia gene transcripts[22,61,89]. During EAE, microglia showed reduced expression of core signature genes *P2RY12*, *Tmem119*, and *Selplg*[22]. Jordao *et al.* identified four disease linked microglia states showing similarities with the DAM signature, and although all had reduced expression of *P2RY12, Maf*, and *Slc2a5,* differential up- and down-regulation of genes distinguished the disease-associated states, possibly related to stage of activation of microglia. Nevertheless, DAM did not change expression of the genes *Olfml3* and *Sparc*, indicating that these might serve as robust markers of microglia in health and disease[22]. Microglia states related to de- and remyelination were

reported in the cuprizone-mediated demyelination mouse model, which induces oxidative damage and mitochondrial dysfunction with selective damage to oligodendrocytes[61], where microglia showed long lasting gene changes after cuprizone had been removed from the diet when remyelination proceeds. Signatures associated with both de- and remyelination revealed enriched expression of *Apoe*, *Axl*, *Igf*, *Lyz2* and reduced *Tmem119* expression[61]. Microglia states that were more enriched during demyelination or remyelination were in part recapitulated in biopsied MS lesions[61]. Recently, DAM-like signatures were identified in MS white matter lesions[90,91]. Additionally, two clusters of microglia were identified, one associated with myelin phagocytosis and clearance, while the other showed enrichment in iron related genes, antigen presentation and complement C1-complex genes[90]. Microglia are the primary source of C1q in the CNS[92,93], and a conditional knockout of C1q in microglia resulted in reduced microglial activity after EAE induction[90]. Unlike comparative studies on microglia isolated from EAE and cuprizone models, human microglia studies revealed a greater microglia diversity in which gene expression only partially overlaps with mouse data[75], likely reflecting species differences. However, this may also be due to differing age, regional variations or comorbidities.

Studies on MS post-mortem tissues assessing single microglia transcriptomes identified several microglia clusters, reflecting the wide variation in microglia and macrophage profiles in MS lesions[18,89]. One must consider, however, that profiles of isolated microglia may also be influenced by cause of death, disease activity or stage, post-mortem interval, age or cell isolation protocols. Pathology studies reveal that macrophages and microglia in MS lesions were not solely pro- or anti-inflammatory, but rather demonstrated an intermediate profile[15,94]. Additionally, microglia in the white matter of MS showed a gene signature associated with increased lipid metabolism, while grey matter microglia had enriched expression of genes associated with glycolysis and iron homeostasis[57]. Furthermore, microglia in white matter MS lesions had significantly reduced expression of P2RY12 and TMEM119, while grey matter microglia did not[95]. However, TMEM119 was seen to be expressed in preactive MS lesions (that lack evidence of BBB disruption and T cells), and early active lesions, while macrophages were found to dominate developed lesions[18,96]. Likewise, in EAE, microglia activation preceded clinical disease in the CNS[97] and depletion or inactivation of microglia and macrophages delayed disease onset and decreased clinical disease[98].

Changes in microglia states have also been observed in a mouse model of *neuromyelitis optica* spectrum disorder (NMOSD). NMOSD is a chronic immune-mediated inflammatory disease of the CNS characterised by optic neuritis and transverse myelitis[99] caused by loss of AQP4 and GFAP due to the presence of autoantibodies targeting AQP4. While microglia in NMOSD showed enriched expression of genes associated with innate immune responses compared to controls, CD11c- microglia had enriched expression of genes related to mitosis, while CD11c+ microglia had enriched genes related to migration and antigen presentation[100].

Microglia in inflammatory white matter diseases, and those associated with demyelination and remyelination, show similarities in gene enrichment profiles. However, as these microglia states also have distinct enough signatures to distinguish them, it appears that microglia may have context-dependent transcriptomes and function.

Leukodystrophies

Leukodystrophies have recently been classified based on the pathological changes and mechanisms driving disease and its progression[101]. Until recently, only a few leukodystrophies had been discovered based on gene mutations affecting microglia development/behaviour, also known as microgliopathies.

Adult-onset leukoencephalopathy with axonal spheroids and pigmented glia (ALSP), previously known as hereditary diffuse leukoencephalopathy with spheroids (HDLS) or pigmentary orthochromatic leukodystrophy (POLD)[102], is a leukoencephalopathy caused by heterozygous mutations in the colony stimulating factor-1 receptor gene (CSF1R). CSF1R is a cell-surface receptor regulating survival, proliferation, and differentiation of macrophages, including microglia. ALSP presents with progressively altered microglia morphology and reduced microglia density, particularly in the white matter[103]. In ALSP, microglial expression of CD68, CD163 and CD204 was found to precede loss of axons and axonal swelling[103] suggesting that microglia undergo changes in immune sensing and initiate phagocytosis. Experimental models lacking expression of, or inhibiting the function of CSF1R, have revealed its importance in maintaining microglia numbers[3,104-106]. Additionally, while microglia were seen to retain their specific microglial signature in zebrafish with *csf1r* mutations[106], this was not found in humans, where microglia in the white matter lose their homeostatic signature and expression of IBA-1 and P2RY12[107]. Furthermore, Kempthorne *et al* showed that, in humans, white matter closer to the cortex was less affected than the deep white matter, indicating regional differences in response to microglial changes . Additionally, white matter in the frontal lobe was found to be more affected than white matter elsewhere in the brain in ALSP, and is associated with increased expression of 75 genes including *APOE, CCL4, JUN, and HEXB*[107]. Reduced microglia numbers were also found in brain tissue with no apparent myelin damage, suggesting changes in microglia function could also underpin white matter degeneration, leading to regional heterogeneity in white matter vulnerability.

Another microgliopathy is Nasu-Hakola disease (NHD)[108-111], also known as polycystic lipomembraneous osteodysplasia with sclerosing leukoencephalopathy (PLOSL). NHD is an autosomal recessive disorder caused by genetic mutations in either *TREM2* or *TYROBP* (DAP12) resulting in loss of function[112]. TREM2 and TYROBP encode for different subunits of the same receptor-signalling complex[113] involved in regulating microglial activity in immune processes[114]. While NHD shows widespread activation of microglia due to lack of TREM2 signalling[115], damage to the white matter is most prominent in the frontotemporal lobe and basal ganglia, while subcortical arcuate fibres are more preserved[115,116]. This suggests that regional heterogeneity in the brain influences microglial function, resulting in differences in white matter damage. Clinical and pathological presentation of the disease might also be dependent on the type and severity of the mutation. Overall, these findings demonstrate that mutations in microglia-associated genes result in aberrant function and myelin damage, underlining the importance of microglial homeostasis for normal CNS function.

Another likely microgliopathy is pseudo-TORCH syndrome, which develops due to genetic loss-of-function mutations in USP18[117-119], which dampens microglial activation in the context of upregulation of type I interferon genes. USP18 is highly enriched in white matter microglia and in pseudo-TORCH syndrome associated with microgliosis and calcifications in the white matter[118,120]. How or why USP18 expression is differentially regulated in white and grey matter is unknown, further investigation may reveal regional heterogeneity in microglial function.

Microglial activation has also been reported in other leukodystrophies[121-123] such as in X-linked adrenoleukodystrophy (X-ALD) where prelesional areas with intact myelin are demarcated by loss of microglial TMEM119 and P2RY12 expression. Additionally, in metachromatic leukodystrophy (MLD) patches of amoeboid microglia that downregulate TMEM119 and P2RY12 show evidence of myelin phagocytosis in the normal appearing white matter (NAWM)[121]. Both MLD and X-ALD show overall loss of microglia and microglial death prior to major myelin breakdown[121]. Interestingly, there is a loss of microglial markers and altered microglial morphology in MLD, but not in X-ALD[121]. In Krabbe's disease, also known as globoid cell leukodystrophy, microglia activation is the first pathological hallmark observed prior to astrocyte activation or oligodendrocyte pathology, possibly due to TLR2 mediated signalling[123]. Taken together, microglial activation has been implicated in driving pathology in several leukodystrophies through dysregulation of several pathways[124]. The regional and disease specific-manifestations might in future be explained by microglial heterogeneity.

Neurodegenerative diseases

The role of white matter microglia in neurodegenerative diseases is relatively understudied, as the main pathological hallmarks usually relate to neuronal cell bodies in the grey matter. One of the most prevalent neurodegenerative diseases is AD, characterized by deposition of extracellular amyloid-β plaques and intracellular tau tangles. AD is associated with genetic mutations in genes encoding for APP, PS1 and PS2 (early-onset AD; EOAD), or can occur sporadically (late-onset AD; LOAD). Neuroimaging studies have shown white matter changes associated with cognitive changes in EOAD, but whether white matter changes also occur in LOAD is still a matter of debate[125-127]. A role for microglia in AD has been implicated by genome wide association studies (GWAS)[128], and microglia are affected particularly in relation to amyloid-β pathology[129,130]. The TgAPP21 rat model of AD does not spontaneously develop amyloid-β plaques but is vulnerable to plaque formation, making it an interesting model to study the pre-plaque phase. In this model, IBA1 immunoreactivity is increased in white matter tracts (corpus callosum, cingulum and internal capsule), correlated with impaired behavioral flexibility[131], linking microglia with impairments of executive dysfunction prior to amyloid-β plaque formation. Similarly, in humans, increased IBA1 reactivity is present in the white matter of aged versus young individuals[132]. When comparing EOAD tissues with age-matched controls, a similar increase in IBA1 activity was observed, but not in LOAD tissues. These data suggest that ageing and AD-related pathology may affect white matter microglia in a similar way, but that the combined effect is not additive. With the advent of single-cell/nucleus RNA sequencing techniques, significant progress has been made in understanding the potential role of microglia in AD, both in mouse models and human brain tissue[129,130,133]. However, so far only studies using grey matter tissue[129], or a mixture of cortical grey and white matter[133], have been performed.

Neuroinflammation and microglia have been increasingly implicated in the pathology of amyotrophic lateral sclerosis (ALS), characterised by progressive degeneration of motor neurons. ALS exists in a genetic form (fALS), often caused by mutations in *C9orf72*, *SOD1*, *FUS* or *TARDBP*, and a sporadic form (sALS). White matter damage in ALS may occur prior to the death of motor neurons[134]. Several bulk RNAseq studies of sALS tissue showed an enrichment of microglia gene expression in the ventral horn of the spinal cord[135] and the motor cortex[136]. Several studies reported microgliosis in white matter of ALS and associated mouse models. In a SOD1 (G93A) mouse model of ALS, decreased grey and white matter volumes were

observed in the spinal cords in association with increased apoptosis, astrogliosis and microgliosis[137]. In the human corticospinal tract in ALS, microgliosis correlated with axonal loss in white matter adjacent to the motor cortex, being most pronounced in cases with fast disease progression[138]. Spatial transcriptomics showed enrichment of a gene expression module relating to microglia homeostasis in the white matter of control and presymptomatic SOD1 mice compared to the terminal end stage disease of both ALS and SOD1 mice[72]. At end stage disease in mice, a reactive microglial gene expression module was also enriched in the grey matter, yet was attenuated in the white matter of the spinal cord, although microglia-associated changes in ALS spinal cord were not reported.

In *C9orf72*$^{-/-}$ mice, another mouse model of ALS, expression of genes associated with activated microglia (DAM-like) were downregulated, while expression of interferon associated genes were upregulated[139]. These changes did not result in differential abundance of microglia states, indicating that the gene expression differences observed did not drive microglial heterogeneity. Microglia in a double transgenic mouse model, *C9orf72*$^{-/-}$ and amyloid-β (5xFAD), showed enhanced engagement with and clearance of plaques, but also enhanced synaptic pruning resulting in memory deficits and neuronal injury. These data suggest that microglia in *C9orf72*$^{-/-}$ mice have both beneficial and detrimental functions in the context of neurodegeneration. However, whether these changes are associated with white or grey matter microglia is not yet known.

Taken together, these studies reveal that white matter microglia are affected and contribute to neurodegenerative diseases such as AD and ALS. Although heterogeneity of microglia has been identified in the grey matter, further research is needed to establish the presence and contribution of white matter microglia heterogeneity in these diseases.

Therapeutic approaches

Despite the implication of microglia in CNS pathology and repair, there are no approved therapies specifically aimed at targeting microglia behaviour for the treatment of neurological conditions or disease. This may reflect in part the challenge imposed by microglial heterogeneity in state and function, and the missing link between the two. Drug development is further complicated by the dynamic changes microglia undergo over time following CNS insult, as observed during white matter damage and repair[55,61,62,140]. Nonetheless, pre-clinical studies have revealed several promising therapeutic strategies which regulate microglia function in the white matter. For instance, phagocytosis of myelin debris by microglia consequent to demyelination is required for efficient remyelination, and is encouraged in microglia/macrophages by *in vivo* exposure to vitamin B3 (niacin)[141], an agonist of retinoid-X-receptors (RXR)[142], and immuno-modulatory drugs (fingolimod, glatiramer acetate)[143]. Promotion of myelin debris clearance and remyelination has also been achieved through increased physical activity following demyelination[144], pointing to exercise as a potential drug-free treatment strategy. In addition, dampening the microglial pro-inflammatory responses that occur with ageing and disease may prevent neural cell damage. The expression of inflammatory mediators by microglia/macrophages is reduced by treatment with the antibiotic minocycline, the mood disorder drug quetiapine fumarate, and the muscarinic receptor antagonist clemastine, the latter currently being trialled for its ability to promote remyelination[143].

Another potential therapeutic option is the replacement of damaging microglia for restoration of normal microglia function. For instance, in MS, the reduced remyelination

observed with age[145], may result from compromised function of microglia/macrophages[146]. Here, rejuvenation of microglia to restore remyelination capacity could provide a valuable tool to halt, or at the least, slow disease progression. Several microglial depletion and repopulation strategies have been developed in recent years: genetic, toxin-based and pharmacological[147,148], with the latter having potential translational value. Experimentally eliminating the majority of microglia using orally administered inhibitors of the pro-survival receptor CSF1R has been shown to improve clinical or neuropathological outcomes in various models of CNS disease and dysfunction (reviewed in[149]), including in the white matter[150,151]. A clinical trial of the CSF1R inhibitor pexidartinib for the treatment of glioma demonstrated that the drug was well tolerated in humans, although post-mortem brain tissue analysis indicated variable impact on CNS IBA1+ cells[152]. In mice, removal of CSF1R inhibitor from the diet induces microglia repopulation and can in some contexts be associated with altered transcriptomes and improved outcome[153-155], which may point to expansion of protective or regenerative microglia states. Clinical outcome would likely be influenced by timing and dosing of depletion in relation to the occurrence of pathology, whether microglial repopulation occurs, and whether repopulated microglia have altered function[149]. Interestingly, depletion/repopulation of microglia in aged mice does appear to have a rejuvenating effect on their transcriptome, associated with improved cognition[153]. However, potential off-target effects of CSF1R inhibition on other CNS macrophages or receptors may need to be taken into account[156], in addition to avoiding microglia depletion in contexts where they are protective[157-160].

Altogether, these studies provide an encouraging prospect of therapeutically targeting microglia in the injured CNS. Future work is needed to determine the differential impact of drugs on specific microglia states, and whether this is influenced by CNS region and timing of treatment post-insult.

Conclusions and future aspects

Microglia have regionally defined functions in the CNS relating to development, homeostasis, ageing, and response to injury, reflecting the local needs of the CNS parenchyma. Indeed, microglia show regional differences in density, morphology, and transcriptome between white and grey matter. In addition, heterogeneity of white matter microglial responses has been observed in development, ageing, inflammatory white matter diseases, leukodystrophies and neurodegenerative diseases (Fig. 4). Furthermore, transcriptomic and proteomic approaches have identified microglial states in the white matter in development and ageing, and during de- and re-myelination.

There are however key questions that need to be addressed to fully understand white matter microglial heterogeneity and its relevance to CNS health. Firstly, *'how similar are mouse (or other animals) and human white matter microglia?*' Although recent studies have shown some similarities in mouse versus human transcriptomic states, differences have also been observed which may be important for CNS health, disease, or recovery. For example, DAM signatures found in mouse models do not completely overlap with signatures in human AD brains[129], nor in MS lesions[90,91]. One must take into account confounding factors when comparing mouse to human microglia, such as species differences regarding expression of key genes regulating microglia, differences in age, environmental exposures (e.g. infection and vaccination status), genetic variability, and CNS regions assessed. Secondly, *'what is the function of specific microglial states in the white matter?'* Recent work has implicated phagocytosis as an important function of white matter microglia in development and ageing,

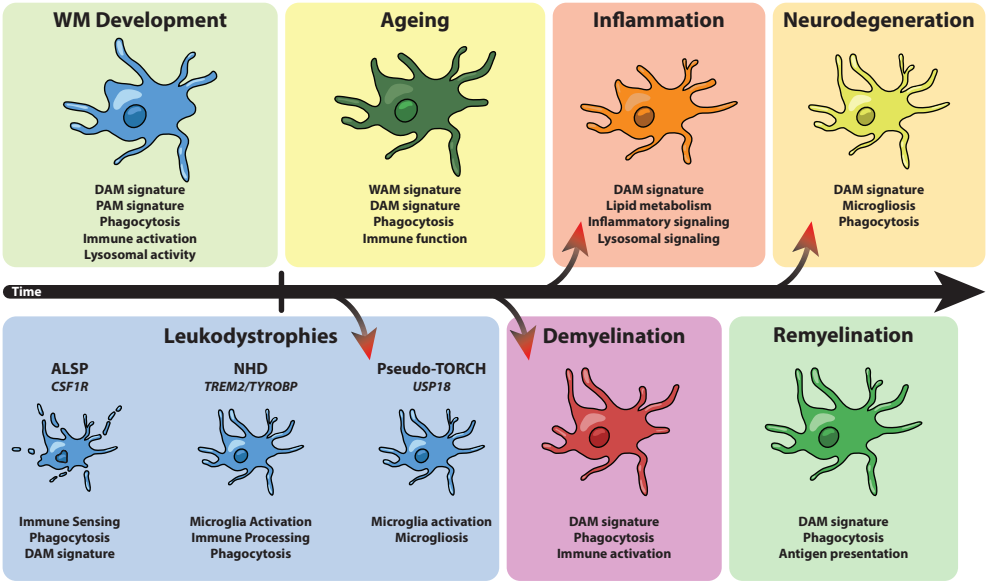

Figure 4. Heterogeneity of microglia in the white matter. Heterogeneity in white matter microglia is present from the early stages of development, as microglia states in the developing CNS show gene enrichment related to phagocytosis and proliferation. Mutations that impact on microglial function in the CNS give rise to leukodystrophies where microglia exhibit heterogeneity in their response depending on the mutation. During ageing, microglia states show similarities with disease associated microglia (DAM) that are also present in inflammation, neurodegeneration, demyelination and remyelination. Nevertheless, although similarities in gene enrichment are found in CNS diseases in which white matter is affected, many microglia states show distinct context-specific profiles and functions

yet other functions may be equally important in influencing CNS health. Thirdly, *'how stable are white matter microglial states?'* Understanding whether and/or how microglia are able to transition from one state to another could shed light on disease-triggering processes, and may point to potential therapeutic strategies to switch microglia state/function in disease. Fourthly, *'how can we therapeutically target microglia states specifically, for instance in white matter disease, and detect the impact of drugs?'* The ease by which microglia adapt could prove to be beneficial for developing therapeutic strategies, either in alleviating disease progression by aiding white matter repair or restoration of homeostasis. In addition, development of targeting drug-encapsulating nanocapsules and microglia specific positron emission tomography tracers may facilitate therapeutic progress. In summary, the importance of microglia in white matter health together with the emerging importance of microglial states in CNS health and disease point to the importance of understanding the full spectrum and relevance of white matter microglia heterogeneity.

Acknowledgements

We thank Prof. Dr. M.S. van der Knaap, Prof. Dr. N. Wolf., and Dr. M. Bugiani for supplying tissue from ALSP and MLD for the pathology figure.

References

1. Thomas WE. Characterization of the dynamic nature of microglial cells. *Brain Res Bull*. Aug 1990;25(2):351-4. doi:10.1016/0361-9230(90)90083-c
2. Yin J*, et al*. The Role of Microglia and Macrophages in CNS Homeostasis, Autoimmunity, and Cancer. *J Immunol Res*. 2017/12/19 2017;2017:5150678. doi:10.1155/2017/5150678
3. Ginhoux F*, et al*. Fate mapping analysis reveals that adult microglia derive from primitive macrophages. *Science*. Nov 5 2010;330(6005):841-5. doi:10.1126/science.1194637
4. Tay TL*, et al*. A new fate mapping system reveals context-dependent random or clonal expansion of microglia. *Nat Neurosci*. Jun 2017;20(6):793-803. doi:10.1038/nn.4547
5. Askew K*, et al*. Coupled Proliferation and Apoptosis Maintain the Rapid Turnover of Microglia in the Adult Brain. *Cell Rep*. Jan 10 2017;18(2):391-405. doi:10.1016/j.celrep.2016.12.041
6. Gosselin D*, et al*. An environment-dependent transcriptional network specifies human microglia identity. *Science*. Jun 23 2017;356(6344):eaal3222. doi:10.1126/science.aal3222
7. Tada M*, et al*. Characteristic microglial features in patients with hereditary diffuse leukoencephalopathy with spheroids. *Ann Neurol*. Oct 2016;80(4):554-65. doi:10.1002/ana.24754
8. Chen JF*, et al*. Enhancing myelin renewal reverses cognitive dysfunction in a murine model of Alzheimer's disease. *Neuron*. Jul 21 2021;109(14):2292-2307 e5. doi:10.1016/j.neuron.2021.05.012
9. McKenzie IA*, et al*. Motor skill learning requires active central myelination. *Science*. Oct 17 2014;346(6207):318-22. doi:10.1126/science.1254960
10. Steadman PE*, et al*. Disruption of Oligodendrogenesis Impairs Memory Consolidation in Adult Mice. *Neuron*. Jan 8 2020;105(1):150-164 e6. doi:10.1016/j.neuron.2019.10.013
11. Wang F*, et al*. Myelin degeneration and diminished myelin renewal contribute to age-related deficits in memory. *Nat Neurosci*. Apr 2020;23(4):481-486. doi:10.1038/s41593-020-0588-8
12. Xiao L*, et al*. Rapid production of new oligodendrocytes is required in the earliest stages of motor-skill learning. *Nat Neurosci*. Sep 2016;19(9):1210-1217. doi:10.1038/nn.4351
13. Colton CA. Heterogeneity of microglial activation in the innate immune response in the brain. *J Neuroimmune Pharmacol*. Dec 2009;4(4):399-418. doi:10.1007/s11481-009-9164-4
14. Wynn TA*, et al*. Macrophage biology in development, homeostasis and disease. *Nature*. Apr 25 2013;496(7446):445-55. doi:10.1038/nature12034
15. Vogel DY*, et al*. Macrophages in inflammatory multiple sclerosis lesions have an intermediate activation status. *J Neuroinflammation*. Mar 4 2013;10:35. doi:10.1186/1742-2094-10-35
16. Kim CC*, et al*. Brain trauma elicits non-canonical macrophage activation states. *J Neuroinflammation*. May 24 2016;13(1):117. doi:10.1186/s12974-016-0581-z
17. Ransohoff RM. A polarizing question: do M1 and M2 microglia exist? *Nat Neurosci*. Jul 26 2016;19(8):987-91. doi:10.1038/nn.4338
18. Zrzavy T*, et al*. Loss of 'homeostatic' microglia and patterns of their activation in active multiple sclerosis. *Brain*. Jul 1 2017;140(7):1900-1913. doi:10.1093/brain/awx113
19. Bottcher C*, et al*. Human microglia regional heterogeneity and phenotypes determined by multiplexed single-cell mass cytometry. *Nat Neurosci*. Jan 2019;22(1):78-90. doi:10.1038/s41593-018-0290-2
20. Jurga AM*, et al*. Overview of General and Discriminating Markers of Differential Microglia Phenotypes. Review. *Front Cell Neurosci*. 2020-August-06 2020;14(198):198. doi:10.3389/fncel.2020.00198
21. Amici SA*, et al*. Molecular Mechanisms Modulating the Phenotype of Macrophages and Microglia. Review. *Front Immunol*. 2017-November-10 2017;8(1520):1520. doi:10.3389/fimmu.2017.01520
22. Jordao MJC*, et al*. Single-cell profiling identifies myeloid cell subsets with distinct fates during neuroinflammation. *Science*. Jan 25 2019;363(6425):eaat7554. doi:10.1126/science.aat7554
23. Mrdjen D*, et al*. High-Dimensional Single-Cell Mapping of Central Nervous System Immune Cells Reveals Distinct Myeloid Subsets in Health, Aging, and Disease. *Immunity*. Feb 20 2018;48(2):380-395 e6. doi:10.1016/j.immuni.2018.01.011
24. Van Hove H*, et al*. A single-cell atlas of mouse brain macrophages reveals unique transcriptional identities shaped by ontogeny and tissue environment. *Nat Neurosci*. Jun 2019;22(6):1021-1035. doi:10.1038/s41593-019-0393-4
25. Martin E*, et al*. Analysis of Microglia and Monocyte-derived Macrophages from the Central Nervous System by Flow Cytometry. *J Vis Exp*. Jun 22 2017;2017(124):1-7. doi:10.3791/55781
26. Kierdorf K*, et al*. Microglia emerge from erythromyeloid precursors via Pu.1- and Irf8-dependent pathways. *Nat Neurosci*. Mar 2013;16(3):273-80. doi:10.1038/nn.3318
27. Schulz C*, et al*. A lineage of myeloid cells independent of Myb and hematopoietic stem cells. *Science*. Apr 6 2012;336(6077):86-90. doi:10.1126/science.1219179

28. Bennett ML, *et al*. New tools for studying microglia in the mouse and human CNS. *Proc Natl Acad Sci U S A*. Mar 22 2016;113(12):E1738-46. doi:10.1073/pnas.1525528113
29. Butovsky O, *et al*. Identification of a unique TGF-beta-dependent molecular and functional signature in microglia. *Nat Neurosci*. Jan 2014;17(1):131-43. doi:10.1038/nn.3599
30. Keren-Shaul H, *et al*. A Unique Microglia Type Associated with Restricting Development of Alzheimer's Disease. *Cell*. Jun 15 2017;169(7):1276-1290 e17. doi:10.1016/j.cell.2017.05.018
31. Masuda T, *et al*. Novel Hexb-based tools for studying microglia in the CNS. *Nat Immunol*. Jul 2020;21(7):802-815. doi:10.1038/s41590-020-0707-4
32. Baker D, *et al*. Mouse models of multiple sclerosis: lost in translation? *Curr Pharm Des*. 2015;21(18):2440-52. doi:10.2174/1381612821666150316122706
33. Dawson TM, *et al*. Animal models of neurodegenerative diseases. *Nat Neurosci*. 2018/10/01 2018;21(10):1370-1379. doi:10.1038/s41593-018-0236-8
34. White GE, *et al*. Fractalkine: a survivor's guide: chemokines as antiapoptotic mediators. *Arterioscler Thromb Vasc Biol*. Mar 2012;32(3):589-94. doi:10.1161/ATVBAHA.111.237412
35. Harrison JK, *et al*. Role for neuronally derived fractalkine in mediating interactions between neurons and CX3CR1-expressing microglia. *Proc Natl Acad Sci U S A*. Sep 1 1998;95(18):10896-901. doi:10.1073/pnas.95.18.10896
36. Garcia JA, *et al*. Analyses of microglia effector function using CX3CR1-GFP knock-in mice. *Methods Mol Biol*. 2013;1041(4):307-17. doi:10.1007/978-1-62703-520-0_27
37. Jung S, *et al*. Analysis of fractalkine receptor CX(3) CR1 function by targeted deletion and green fluorescent protein reporter gene insertion. *Mol Cell Biol*. Jun 2000;20(11):4106-14. doi:10.1128/MCB.20.11.4106-4114.2000
38. Goldmann T, *et al*. A new type of microglia gene targeting shows TAK1 to be pivotal in CNS autoimmune inflammation. *Nat Neurosci*. Nov 2013;16(11):1618-26. doi:10.1038/nn.3531
39. Yona S, *et al*. Fate mapping reveals origins and dynamics of monocytes and tissue macrophages under homeostasis. *Immunity*. Jan 24 2013;38(1):79-91. doi:10.1016/j.immuni.2012.12.001
40. Kaiser T, *et al*. Tmem119-EGFP and Tmem119-CreERT2 Transgenic Mice for Labeling and Manipulating Microglia. *eNeuro*. Jul/Aug 2019;6(4) doi:10.1523/ENEURO.0448-18.2019
41. McKinsey GL, *et al*. A new genetic strategy for targeting microglia in development and disease. *Elife*. Jun 23 2020;9:e54590. doi:10.7554/eLife.54590
42. Dubbelaar ML, *et al*. The Kaleidoscope of Microglial Phenotypes. Review. *Front Immunol*. 2018-July-31 2018;9(1753):1753. doi:10.3389/fimmu.2018.01753
43. Ajami B, *et al*. Single-cell mass cytometry reveals distinct populations of brain myeloid cells in mouse neuroinflammation and neurodegeneration models. *Nat Neurosci*. Apr 2018;21(4):541-551. doi:10.1038/s41593-018-0100-x
44. Svensson V, *et al*. Power Analysis of Single Cell RNA-Sequencing Experiments Europe PMC Funders Group. *Nat Methods*. 2017;14(4):381-387. doi:10.1038/nmeth.4220.Power
45. See P, *et al*. A Single-Cell Sequencing Guide for Immunologists. *Front Immunol*. 2018;9(OCT):2425. doi:10.3389/fimmu.2018.02425
46. Li Q, *et al*. Developmental Heterogeneity of Microglia and Brain Myeloid Cells Revealed by Deep Single-Cell RNA Sequencing. *Neuron*. Jan 16 2019;101(2):207-223 e10. doi:10.1016/j.neuron.2018.12.006
47. Matcovitch-Natan O, *et al*. Microglia development follows a stepwise program to regulate brain homeostasis. *Science*. Aug 19 2016;353(6301):aad8670. doi:10.1126/science.aad8670
48. Stahl PL, *et al*. Visualization and analysis of gene expression in tissue sections by spatial transcriptomics. *Science*. Jul 1 2016;353(6294):78-82. doi:10.1126/science.aaf2403
49. Chen WT, *et al*. Spatial Transcriptomics and In Situ Sequencing to Study Alzheimer's Disease. *Cell*. Aug 20 2020;182(4):976-991 e19. doi:10.1016/j.cell.2020.06.038
50. Hasel P, *et al*. Neuroinflammatory astrocyte subtypes in the mouse brain. *Nat Neurosci*. Oct 2021;24(10):1475-1487. doi:10.1038/s41593-021-00905-6
51. De Biase LM, *et al*. Region-Specific Phenotypes of Microglia: The Role of Local Regulatory Cues. *Neuroscientist*. Aug 2019;25(4):314-333. doi:10.1177/1073858418800996
52. von Bartheld CS, *et al*. The search for true numbers of neurons and glial cells in the human brain: A review of 150 years of cell counting. *J Comp Neurol*. Dec 15 2016;524(18):3865-3895. doi:10.1002/cne.24040
53. Lawson LJ, *et al*. Heterogeneity in the distribution and morphology of microglia in the normal adult mouse brain. *Neuroscience*. 1990;39(1):151-70. doi:10.1016/0306-4522(90)90229-w
54. Grabert K, *et al*. Microglial brain region-dependent diversity and selective regional sensitivities to aging. *Nat Neurosci*. Mar 2016;19(3):504-16. doi:10.1038/nn.4222
55. Yamasaki R, *et al*. Differential roles of microglia and monocytes in the inflamed central nervous system. *J Exp Med*. Jul 28 2014;211(8):1533-49. doi:10.1084/jem.20132477
56. Cronk JC, *et al*. Peripherally derived macrophages

can engraft the brain independent of irradiation and maintain an identity distinct from microglia. *J Exp Med*. Jun 4 2018;215(6):1627-1647. doi:10.1084/jem.20180247
57. van der Poel M*, et al*. Transcriptional profiling of human microglia reveals grey-white matter heterogeneity and multiple sclerosis-associated changes. *Nat Commun*. Mar 13 2019;10(1):1139. doi:10.1038/s41467-019-08976-7
58. Peterson JW*, et al*. Transected neurites, apoptotic neurons, and reduced inflammation in cortical multiple sclerosis lesions. *Ann Neurol*. Sep 2001;50(3):389-400. doi:10.1002/ana.1123
59. van Wageningen TA*, et al*. Viscoelastic properties of white and gray matter-derived microglia differentiate upon treatment with lipopolysaccharide but not upon treatment with myelin. *J Neuroinflammation*. Mar 29 2021;18(1):83. doi:10.1186/s12974-021-02134-x
60. Agarwal M*, et al*. Reactive oxygen species-mediated cytoplasmic stiffening impairs the phagocytic ability of the macrophage. *J Cell Sci*. Mar 2 2020;133(5) doi:10.1242/jcs.236471
61. Masuda T*, et al*. Spatial and temporal heterogeneity of mouse and human microglia at single-cell resolution. *Nature*. Feb 2019;566(7744):388-392. doi:10.1038/s41586-019-0924-x
62. Hammond TR*, et al*. Single-Cell RNA Sequencing of Microglia throughout the Mouse Lifespan and in the Injured Brain Reveals Complex Cell-State Changes. *Immunity*. Jan 15 2019;50(1):253-271 e6. doi:10.1016/j.immuni.2018.11.004
63. Kracht L*, et al*. Human fetal microglia acquire homeostatic immune-sensing properties early in development. *Science*. Jul 31 2020;369(6503):530-537. doi:10.1126/science.aba5906
64. Hagemeyer N*, et al*. Microglia contribute to normal myelinogenesis and to oligodendrocyte progenitor maintenance during adulthood. *Acta Neuropathol*. Sep 2017;134(3):441-458. doi:10.1007/s00401-017-1747-1
65. Kondo Y*, et al*. Selective reduction in microglia density and function in the white matter of colony-stimulating factor-1-deficient mice. *J Neurosci Res*. Sep 2009;87(12):2686-95. doi:10.1002/jnr.22096
66. Badimon A*, et al*. Negative feedback control of neuronal activity by microglia. *Nature*. Oct 2020;586(7829):417-423. doi:10.1038/s41586-020-2777-8
67. Lloyd AF*, et al*. Central nervous system regeneration is driven by microglia necroptosis and repopulation. *Nat Neurosci*. Jul 2019;22(7):1046-1052. doi:10.1038/s41593-019-0418-z
68. Plemel JR*, et al*. Microglia response following acute demyelination is heterogeneous and limits infiltrating macrophage dispersion. *Sci Adv*. Jan 2020;6(3):eaay6324. doi:10.1126/sciadv.aay6324
69. Sankowski R*, et al*. Mapping microglia states in the human brain through the integration of high-dimensional techniques. *Nat Neurosci*. Dec 2019;22(12):2098-2110. doi:10.1038/s41593-019-0532-y
70. Zrzavy T*, et al*. Dominant role of microglial and macrophage innate immune responses in human ischemic infarcts. *Brain Pathol*. Nov 2018;28(6):791-805. doi:10.1111/bpa.12583
71. Safaiyan S*, et al*. White matter aging drives microglial diversity. *Neuron*. Apr 7 2021;109(7):1100-1117 e10. doi:10.1016/j.neuron.2021.01.027
72. Maniatis S*, et al*. Spatiotemporal dynamics of molecular pathology in amyotrophic lateral sclerosis. *Science*. Apr 5 2019;364(6435):89-93. doi:10.1126/science.aav9776
73. Gudi V*, et al*. Regional differences between grey and white matter in cuprizone induced demyelination. *Brain Research*. Aug 4 2009;1283:127-138. doi:10.1016/j.brainres.2009.06.005
74. Wlodarczyk A*, et al*. A novel microglial subset plays a key role in myelinogenesis in developing brain. *EMBO J*. Nov 15 2017;36(22):3292-3308. doi:10.15252/embj.201696056
75. Masuda T*, et al*. Microglia Heterogeneity in the Single-Cell Era. *Cell Rep*. Feb 4 2020;30(5):1271-1281. doi:10.1016/j.celrep.2020.01.010
76. Gyoneva S*, et al*. Cx3cr1-deficient microglia exhibit a premature aging transcriptome. *Life Sci Alliance*. Dec 2019;2(6)doi:10.26508/lsa.201900453
77. Olah M*, et al*. A transcriptomic atlas of aged human microglia. *Nat Commun*. Feb 7 2018;9(1):539. doi:10.1038/s41467-018-02926-5
78. Kang SS*, et al*. Microglial translational profiling reveals a convergent APOE pathway from aging, amyloid, and tau. *J Exp Med*. Sep 3 2018;215(9):2235-2245. doi:10.1084/jem.20180653
79. Jaitin DA*, et al*. Lipid-Associated Macrophages Control Metabolic Homeostasis in a Trem2-Dependent Manner. *Cell*. Jul 25 2019;178(3):686-698 e14. doi:10.1016/j.cell.2019.05.054
80. Sala Frigerio C*, et al*. The Major Risk Factors for Alzheimer's Disease: Age, Sex, and Genes Modulate the Microglia Response to Abeta Plaques. *Cell Rep*. Apr 23 2019;27(4):1293-1306 e6. doi:10.1016/j.celrep.2019.03.099
81. Singh S*, et al*. Microglial nodules in early multiple sclerosis white matter are associated with degenerating axons. *Acta Neuropathol*. Apr 2013;125(4):595-608. doi:10.1007/s00401-013-1082-0
82. Kutzelnigg A*, et al*. Cortical demyelination and diffuse white matter injury in multiple sclerosis. *Brain*. Nov 2005;128(Pt 11):2705-12. doi:10.1093/brain/awh641
83. Petrova N*, et al*. Synaptic Loss in Multiple Sclerosis Spinal Cord. *Ann Neurol*. Sep 2020;88(3):619-625. doi:10.1002/ana.25835
84. Werneburg S*, et al*. Targeted Complement Inhibition at Synapses Prevents Microglial Synaptic Engulfment and Synapse Loss in Demyelinating

Disease. *Immunity*. Jan 14 2020;52(1):167-182 e7. doi:10.1016/j.immuni.2019.12.004
85. Baker D, *et al*. Both cladribine and alemtuzumab may effect MS via B-cell depletion. *Neurology-Neuroimmunology Neuroinflammation*. 2017;4(4)
86. Gelfand JM, *et al*. Ocrelizumab and Other CD20(+) B-Cell-Depleting Therapies in Multiple Sclerosis. *Neurotherapeutics*. Oct 2017;14(4):835-841. doi:10.1007/s13311-017-0557-4
87. Li R, *et al*. Reassessing B cell contributions in multiple sclerosis. *Nat Immunol*. Jul 2018;19(7):696-707. doi:10.1038/s41590-018-0135-x
88. Greenfield AL, *et al*. B-cell Therapy for Multiple Sclerosis: Entering an era. *Ann Neurol*. Jan 2018;83(1):13-26. doi:10.1002/ana.25119
89. Schirmer L, *et al*. Neuronal vulnerability and multilineage diversity in multiple sclerosis. *Nature*. Sep 2019;573(7772):75-82. doi:10.1038/s41586-019-1404-z
90. Absinta M, *et al*. A lymphocyte-microglia-astrocyte axis in chronic active multiple sclerosis. *Nature*. Sep 2021;597(7878):709-714. doi:10.1038/s41586-021-03892-7
91. Miedema A, *et al*. Brain macrophages acquire distinct transcriptomes prior to demyelination in multiple sclerosis. *bioRxiv*. 2021:2021.10.27.465877. doi:10.1101/2021.10.27.465877
92. Fonseca MI, *et al*. Cell-specific deletion of C1qa identifies microglia as the dominant source of C1q in mouse brain. *J Neuroinflammation*. Mar 6 2017;14(1):48. doi:10.1186/s12974-017-0814-9
93. Stephan AH, *et al*. A dramatic increase of C1q protein in the CNS during normal aging. *J Neurosci*. Aug 14 2013;33(33):13460-74. doi:10.1523/JNEUROSCI.1333-13.2013
94. Peferoen LA, *et al*. Activation status of human microglia is dependent on lesion formation stage and remyelination in multiple sclerosis. *J Neuropathol Exp Neurol*. Jan 2015;74(1):48-63. doi:10.1097/NEN.0000000000000149
95. van Wageningen TA, *et al*. Regulation of microglial TMEM119 and P2RY12 immunoreactivity in multiple sclerosis white and grey matter lesions is dependent on their inflammatory environment. *Acta Neuropathol Commun*. Dec 11 2019;7(1):206. doi:10.1186/s40478-019-0850-z
96. van Horssen J, *et al*. Clusters of activated microglia in normal-appearing white matter show signs of innate immune activation. *Journal of neuroinflammation*. 2012;9(1):1-9.
97. Allen SJ, *et al*. Isolation and characterization of cells infiltrating the spinal cord during the course of chronic relapsing experimental allergic encephalomyelitis in the Biozzi AB/H mouse. *Cell Immunol*. Feb 1993;146(2):335-50. doi:10.1006/cimm.1993.1031
98. Bauer J, *et al*. The role of macrophage subpopulations in autoimmune disease of the central nervous system. *Histochem J*. Feb 1996;28(2):83-97. doi:10.1007/BF02331413
99. Trebst C, *et al*. Update on the diagnosis and treatment of neuromyelitis optica: recommendations of the Neuromyelitis Optica Study Group (NEMOS). *J Neurol*. Jan 2014;261(1):1-16. doi:10.1007/s00415-013-7169-7
100. Wlodarczyk A, *et al*. Type I interferon-activated microglia are critical for neuromyelitis optica pathology. *Glia*. Apr 2021;69(4):943-953. doi:10.1002/glia.23938
101. van der Knaap MS, *et al*. Leukodystrophies: a proposed classification system based on pathological changes and pathogenetic mechanisms. *Acta Neuropathol*. Sep 2017;134(3):351-382. doi:10.1007/s00401-017-1739-1
102. Adams SJ, *et al*. Adult-onset leukoencephalopathy with axonal spheroids and pigmented glia (ALSP): Integrating the literature on hereditary diffuse leukoencephalopathy with spheroids (HDLS) and pigmentary orthochromatic leukodystrophy (POLD). *J Clin Neurosci*. Feb 2018;48:42-49. doi:10.1016/j.jocn.2017.10.060
103. Oyanagi K, *et al*. Adult onset leukoencephalopathy with axonal spheroids and pigmented glia (ALSP) and Nasu-Hakola disease: lesion staging and dynamic changes of axons and microglial subsets. *Brain Pathol*. Nov 2017;27(6):748-769. doi:10.1111/bpa.12443
104. Dai XM, *et al*. Targeted disruption of the mouse colony-stimulating factor 1 receptor gene results in osteopetrosis, mononuclear phagocyte deficiency, increased primitive progenitor cell frequencies, and reproductive defects. *Blood*. Jan 1 2002;99(1):111-20. doi:10.1182/blood.v99.1.111
105. Erblich B, *et al*. Absence of colony stimulation factor-1 receptor results in loss of microglia, disrupted brain development and olfactory deficits. *PLOS ONE*. 2011;6(10):e26317. doi:10.1371/journal.pone.0026317
106. Oosterhof N, *et al*. Colony-Stimulating Factor 1 Receptor (CSF1R) Regulates Microglia Density and Distribution, but Not Microglia Differentiation In Vivo. *Cell Rep*. Jul 31 2018;24(5):1203-1217 e6. doi:10.1016/j.celrep.2018.06.113
107. Kempthorne L, *et al*. Loss of homeostatic microglial phenotype in CSF1R-related Leukoencephalopathy. *Acta Neuropathol Commun*. May 19 2020;8(1):72. doi:10.1186/s40478-020-00947-0
108. Hakola HP, *et al*. Osteodysplasia polycystica hereditaria combined with sclerosing leucoencephalopathy, a new entity of the dementia praesenilis group. *Acta Neurol Scand*. 1970;46(S43):79-80.
109. Hakola HPA. Neuropsychiatric and genetic aspects of a new herediary disease characterized by progressive dementia and lipomembranous polycytic osteodysplasia. *Acta Psychiatr Scand Suppl*. 1972;232:1-173.
110. Nasu T, *et al*. A lipid metabolic disease—

"membranous lipodystrophy"—an autopsy case demonstrating numerous peculiar membrane-structures composed of compound lipid in bone and bone marrow and various adipose tissues. *Pathology International*. 1973;23(3):539-558.
111. Oda M. Familial sudanophilic leukodystrophy with multiple and semisystematic spongy foci: Autopsy report of three adult females. International Symposium on the Leukodystrophy and Allied Diseases. *Neuropathology*. 1983:173-185.
112. Dardiotis E*, et al*. A novel mutation in TREM2 gene causing Nasu-Hakola disease and review of the literature. *Neurobiol Aging*. May 2017;53:194 e13-194 e22. doi:10.1016/j.neurobiolaging.2017.01.015
113. Paloneva J*, et al*. Mutations in two genes encoding different subunits of a receptor signaling complex result in an identical disease phenotype. *Am J Hum Genet*. Sep 2002;71(3):656-62. doi:10.1086/342259
114. Mecca C*, et al*. Microglia and Aging: The Role of the TREM2-DAP12 and CX3CL1-CX3CR1 Axes. *Int J Mol Sci*. Jan 22 2018;19(1)doi:10.3390/ijms19010318
115. Paloneva J*, et al*. CNS manifestations of Nasu-Hakola disease: a frontal dementia with bone cysts. *Neurology*. Jun 12 2001;56(11):1552-8. doi:10.1212/wnl.56.11.1552
116. Tanaka J. Nasu-Hakola disease: a review of its leukoencephalopathic and membranolipodystrophic features. *Neuropathology*. Sep 2000;20 Suppl:S25-9. doi:10.1046/j.1440-1789.2000.00297.x
117. Schwabenland M*, et al*. Loss of USP18 in microglia induces white matter pathology. *Acta Neuropathol Commun*. Jul 4 2019;7(1):106. doi:10.1186/s40478-019-0757-8
118. Meuwissen ME*, et al*. Human USP18 deficiency underlies type 1 interferonopathy leading to severe pseudo-TORCH syndrome. *J Exp Med*. Jun 27 2016;213(7):1163-74. doi:10.1084/jem.20151529
119. Goldmann T*, et al*. USP 18 lack in microglia causes destructive interferonopathy of the mouse brain. *The EMBO journal*. 2015;34(12):1612-1629.
120. Takata K*, et al*. Poised for action: USP18 restrains microglial activation in the white matter. *EMBO J*. Jun 12 2015;34(12):1603-5. doi:10.15252/embj.201591899
121. Bergner CG*, et al*. Microglia damage precedes major myelin breakdown in X-linked adrenoleukodystrophy and metachromatic leukodystrophy. *Glia*. Jun 2019;67(6):1196-1209. doi:10.1002/glia.23598
122. Marteyn A*, et al*. Is involvement of inflammation underestimated in Pelizaeus-Merzbacher disease? *J Neurosci Res*. Dec 2016;94(12):1572-1578. doi:10.1002/jnr.23931
123. Snook ER*, et al*. Innate immune activation in the pathogenesis of a murine model of globoid cell leukodystrophy. *Am J Pathol*. Feb 2014;184(2):382-96. doi:10.1016/j.ajpath.2013.10.011
124. Garcia LM*, et al*. Glial cells in the driver seat of leukodystrophy pathogenesis. *Neurobiol Dis*. Dec 2020;146:105087. doi:10.1016/j.nbd.2020.105087
125. Hirono N*, et al*. Impact of white matter changes on clinical manifestation of Alzheimer's disease: A quantitative study. *Stroke*. Sep 2000;31(9):2182-8. doi:10.1161/01.str.31.9.2182
126. Jang H*, et al*. Correlations between Gray Matter and White Matter Degeneration in Pure Alzheimer's Disease, Pure Subcortical Vascular Dementia, and Mixed Dementia. *Sci Rep*. Aug 25 2017;7(1):9541. doi:10.1038/s41598-017-10074-x
127. Stout JC*, et al*. Association of dementia severity with cortical gray matter and abnormal white matter volumes in dementia of the Alzheimer type. *Arch Neurol*. Aug 1996;53(8):742-9. doi:10.1001/archneur.1996.00550080056013
128. Jansen IE*, et al*. Genome-wide meta-analysis identifies new loci and functional pathways influencing Alzheimer's disease risk. *Nat Genet*. Mar 2019;51(3):404-413. doi:10.1038/s41588-018-0311-9
129. Gerrits E*, et al*. Distinct amyloid-beta and tau-associated microglia profiles in Alzheimer's disease. *Acta Neuropathol*. May 2021;141(5):681-696. doi:10.1007/s00401-021-02263-w
130. Sierksma A*, et al*. Novel Alzheimer risk genes determine the microglia response to amyloid-beta but not to TAU pathology. *EMBO Mol Med*. Mar 6 2020;12(3):e10606. doi:10.15252/emmm.201910606
131. Levit A*, et al*. Impaired behavioural flexibility related to white matter microgliosis in the TgAPP21 rat model of Alzheimer disease. *Brain Behav Immun*. Aug 2019;80:25-34. doi:10.1016/j.bbi.2019.02.013
132. Raj D*, et al*. Increased White Matter Inflammation in Aging- and Alzheimer's Disease Brain. *Front Mol Neurosci*. 2017;10:206. doi:10.3389/fnmol.2017.00206
133. Mathys H*, et al*. Single-cell transcriptomic analysis of Alzheimer's disease. *Nature*. Jun 2019;570(7761):332-337. doi:10.1038/s41586-019-1195-2
134. Zhou T*, et al*. Implications of white matter damage in amyotrophic lateral sclerosis (Review). *Mol Med Rep*. Oct 2017;16(4):4379-4392. doi:10.3892/mmr.2017.7186
135. D'Erchia AM*, et al*. Massive transcriptome sequencing of human spinal cord tissues provides new insights into motor neuron degeneration in ALS. *Sci Rep*. Aug 30 2017;7(1):10046. doi:10.1038/s41598-017-10488-7
136. Dols-Icardo O*, et al*. Motor cortex transcriptome reveals microglial key events in amyotrophic lateral sclerosis. *Neurol Neuroimmunol Neuroinflamm*. Sep 2020;7(5):e829. doi:10.1212/NXI.0000000000000829
137. Petrik MS*, et al*. Magnetic resonance microscopy and immunohistochemistry of the CNS of the mutant SOD murine model of ALS reveals

widespread neural deficits. *Neuromolecular Med*. 2007/08/14 2007;9(3):216-29. doi:10.1007/s12017-007-8002-1

138. Brettschneider J*, et al*. Microglial activation correlates with disease progression and upper motor neuron clinical symptoms in amyotrophic lateral sclerosis. *PLOS ONE*. 2012;7(6):e39216. doi:10.1371/journal.pone.0039216
139. Lall D*, et al*. C9orf72 deficiency promotes microglial-mediated synaptic loss in aging and amyloid accumulation. *Neuron*. Jul 21 2021;109(14):2275-2291 e8. doi:10.1016/j.neuron.2021.05.020
140. Miron VE*, et al*. M2 microglia and macrophages drive oligodendrocyte differentiation during CNS remyelination. *Nat Neurosci*. Sep 2013;16(9):1211-1218. doi:10.1038/nn.3469
141. Rawji KS*, et al*. Niacin-mediated rejuvenation of macrophage/microglia enhances remyelination of the aging central nervous system. *Acta Neuropathol*. May 2020;139(5):893-909. doi:10.1007/s00401-020-02129-7
142. Natrajan MS*, et al*. Retinoid X receptor activation reverses age-related deficiencies in myelin debris phagocytosis and remyelination. *Brain*. Dec 2015;138(Pt 12):3581-97. doi:10.1093/brain/awv289
143. Lloyd AF*, et al*. The pro-remyelination properties of microglia in the central nervous system. *Nat Rev Neurol*. Aug 2019;15(8):447-458. doi:10.1038/s41582-019-0184-2
144. Jensen SK*, et al*. Multimodal Enhancement of Remyelination by Exercise with a Pivotal Role for Oligodendroglial PGC1alpha. *Cell Rep*. Sep 18 2018;24(12):3167-3179. doi:10.1016/j.celrep.2018.08.060
145. Franklin RJM*, et al*. Regenerating CNS myelin - from mechanisms to experimental medicines. *Nat Rev Neurosci*. Nov 16 2017;18(12):753-769. doi:10.1038/nrn.2017.136
146. Baror R*, et al*. Transforming growth factor-beta renders ageing microglia inhibitory to oligodendrocyte generation by CNS progenitors. *Glia*. Jul 2019;67(7):1374-1384. doi:10.1002/glia.23612
147. Elmore MR*, et al*. Colony-stimulating factor 1 receptor signaling is necessary for microglia viability, unmasking a microglia progenitor cell in the adult brain. *Neuron*. Apr 16 2014;82(2):380-97. doi:10.1016/j.neuron.2014.02.040
148. Parkhurst CN*, et al*. Microglia promote learning-dependent synapse formation through brain-derived neurotrophic factor. *Cell*. Dec 19 2013;155(7):1596-609. doi:10.1016/j.cell.2013.11.030
149. Green KN*, et al*. To Kill a Microglia: A Case for CSF1R Inhibitors. *Trends Immunol*. Sep 2020;41(9):771-784. doi:10.1016/j.it.2020.07.001
150. Gibson EM*, et al*. Methotrexate Chemotherapy Induces Persistent Tri-glial Dysregulation that Underlies Chemotherapy-Related Cognitive Impairment. *Cell*. Jan 10 2019;176(1-2):43-55 e13. doi:10.1016/j.cell.2018.10.049
151. Beckmann N*, et al*. Brain region-specific enhancement of remyelination and prevention of demyelination by the CSF1R kinase inhibitor BLZ945. *Acta Neuropathol Commun*. Feb 15 2018;6(1):9. doi:10.1186/s40478-018-0510-8
152. Butowski N*, et al*. Orally administered colony stimulating factor 1 receptor inhibitor PLX3397 in recurrent glioblastoma: an Ivy Foundation Early Phase Clinical Trials Consortium phase II study. *Neuro Oncol*. Apr 2016;18(4):557-64. doi:10.1093/neuonc/nov245
153. Elmore MRP*, et al*. Replacement of microglia in the aged brain reverses cognitive, synaptic, and neuronal deficits in mice. *Aging Cell*. Dec 2018;17(6):e12832. doi:10.1111/acel.12832
154. Henry RJ*, et al*. Microglial Depletion with CSF1R Inhibitor During Chronic Phase of Experimental Traumatic Brain Injury Reduces Neurodegeneration and Neurological Deficits. *J Neurosci*. Apr 1 2020;40(14):2960-2974. doi:10.1523/JNEUROSCI.2402-19.2020
155. Willis EF*, et al*. Repopulating Microglia Promote Brain Repair in an IL-6-Dependent Manner. *Cell*. Mar 5 2020;180(5):833-846 e16. doi:10.1016/j.cell.2020.02.013
156. Miron VE*, et al*. Investigating Microglia in Health and Disease: Challenges and Opportunities. *Trends Immunol*. Sep 2020;41(9):785-793. doi:10.1016/j.it.2020.07.002
157. Bellver-Landete V*, et al*. Microglia are an essential component of the neuroprotective scar that forms after spinal cord injury. *Nat Commun*. Jan 31 2019;10(1):518. doi:10.1038/s41467-019-08446-0
158. Szalay G*, et al*. Microglia protect against brain injury and their selective elimination dysregulates neuronal network activity after stroke. *Nat Commun*. May 3 2016;7:11499. doi:10.1038/ncomms11499
159. Jacobs AJ*, et al*. Microglial Depletion Causes Region-Specific Changes to Developmental Neuronal Cell Death in the Mouse Brain. *Dev Neurobiol*. Aug 2019;79(8):769-779. doi:10.1002/dneu.22706
160. Sariol A*, et al*. Microglia depletion exacerbates demyelination and impairs remyelination in a neurotropic coronavirus infection. *Proc Natl Acad Sci U S A*. Sep 29 2020;117(39):24464-24474. doi:10.1073/pnas.2007814117


g

General Discussion

Adapted from:

Imaging immunological processes from blood to brain in amyotrophic lateral sclerosis

Sandra Amor, Erik Nutma, Manuel Marzin, Fabiola Puentes

Clinical and Experimental Immunology 2021 206(3):301-313

Visualising neuroinflammation in the CNS

Neuroinflammation, associated with neuropathology of neuroinflammatory and neurodegenerative diseases is one of the many complex multicellular processes that occurs behind the 'closed borders' within the CNS. Two key innate immune cells that contribute to damage as well as repair are microglia and astrocytes. Given their importance in many diseases there is an urgent clinical need to monitor glial cell activity during disease as well as assess the impact of medical intervention on innate immune responses during diseases. One of the most common modalities to monitor neuroinflammation and pathological changes in neurodegenerative diseases and experimental animal models is PET imaging, which has the advantage of being able to interrogate various disease mechanisms by quantifying specific molecular targets to directly study the CNS[1-3]. Even though PET imaging is expensive, it can be a valuable tool to generate knowledge on the efficacy of drugs in a preclinical setting before translating to the clinic. PET imaging can also provide insights into the therapeutic effects in the CNS of patients *in vivo*. PET allows direct visualization of neuroinflammation in early stages of disease as well as recurrent analysis to monitor disease progression. Importantly, this approach lends itself to study the efficacy of therapies targeting molecular pathways that can be visualized by specific ligands[3]. PET imaging may thus serve as a tool to study disease progression or as prognostic or predictive biomarker, while allowing a detailed analysis of molecular alterations key to the pathogenesis of neurodegenerative diseases, such as cerebral blood flow, glucose metabolism, neuroinflammation, neuronal dysfunction and oxidative stress[4]. TSPO PET imaging is a promising molecular imaging technique that has been used over the last decades as a measurement of activated microglia in the CNS.

In this thesis we examined the cellular distribution of TSPO in CNS resident cells in neurodegenerative diseases to identify whether TSPO is indeed a marker of activated microglia as has been reported by many studies (reviewed by Guilarte[2]). Initial reports on animal models of neuroinflammatory diseases showed that TSPO is also expressed by other cell types than microglia[5-18] but these findings have been largely ignored by PET studies, and the early human studies were qualitative rather than quantitative[19-21]. Recently, it was shown *in vitro* that while primary rodent microglia upregulate TSPO expression in a pro-inflammatory environment, primary human microglia do not[22]. Thus, findings of the triggers of TSPO, and the cellular expression of TSPO in the CNS in animal models may not translate to human disease. To investigate the cellular distribution and understand the triggers of TSPO we have performed in-depth studies of TSPO expression in MS, AD and ALS and their respective animal models. In addition, we have utilised publicly available databases on TSPO regulation on multiple molecular levels (e.g. epigenetic, protein and RNA). Together, these studies have allowed a more detailed understanding of the role of microglia and astrocytes as innate immune cells of the CNS.

Is TSPO a marker of only activated microglia?

Early TSPO PET studies used the first-generation TSPO ligand [11C]-PK11195, while more recent studies use second-generation TSPO tracers such as [11C]-PBR28 and [18F]-DPA-714, which have improved uptake and binding affinity compared to older tracers[23]. Surprisingly, very little data is available on the precise origin of TSPO in CNS cells, on which to base interpretations of TSPO PET. Due to the fast pace of research and increasing advances in the development of radiotracers for TSPO PET, often times there is a lack of appreciation for the neurobiology of TSPO and conclusions are made about its cellular origin without proper

investigation of its response to injury and neuroinflammation. Knowledge of the cellular and phenotypic correlates of the TSPO PET signal is important to understand the clinical meaningfulness of TSPO PET as a diagnostic tool. For example, there is heterogeneity in the radioligand uptake of T2-hyperintense lesion in MS before and after initiation of disease modifying therapies[24]. However, before the relevance of such TSPO PET expression can be explored we need to know where the signal is coming from. Many studies have largely ignored the possible contribution of cell types other than microglia to the TSPO PET signal[25-41], either by not investigating expression by cell types than microglia, or not performing quantitative experiments at all. Together, the previously published studies has created the foundation for the misconception that TSPO is almost exclusively present in microglia with almost no association with astrocytes – even though the first study showing TSPO in astrocytes is over two decades old[42]. Fortunately, emerging studies have reported TSPO in astrocytes in animal models of neurodegenerative diseases[5-18] and a few studies show astrocytic TSPO in human disease[19-21].

TSPO is widely considered as a marker for neuroinflammation, and thus many studies on TSPO PET have been performed in MS, where neuroinflammation, a prominent hallmark of disease is associated with demyelination[43], as well as neuronal damage and synaptic loss (**Chapter 6**). Many studies find increases in TSPO PET signal in active and chronic active lesions in MS[40,44-47] and overall the increased TSPO PET signal in the brain predicts disease progression of MS regardless of relapses[48]. However, as mentioned above this increase in TSPO PET was widely regarded to originate in pathogenic activated microglia[2]. In **Chapter 2** we show that while microglia are the main cells expressing TSPO in MS lesions there is also a significant contribution of astrocytes present in the centre of chronic active and inactive lesions. The finding that in the centre of chronic active and inactive MS lesions the contribution of TSPO is significantly higher in astrocytes, as compared to microglia, is consistent with reports of newer generation ligands for TSPO that bind to reactive astrocytes[6,49]. Autoradiography with 3H-PBR28 and 3H-PK11195 revealed a strong association between TSPO+ cells and radioligand binding across all cell subtypes. Increased TSPO expression was present not only in white matter lesions but also in leukocortical lesions, lesions that comprise both white and grey matter. The more inflammatory component of the white matter in leukocortical lesions might influence the adjoining grey matter in terms of inflammation. Indeed, purely cortical grey matter lesions show little to no inflammation[50-52]. These findings indicate that TSPO PET signal must be interpreted in a context-dependent manner.

Next, we performed a detailed neuropathological studies to investigate whether TSPO expression was limited to activated microglia – the widely accepted view. In contrast to this view, we showed that TSPO in microglia in MS lesions was present in microglia that expressed anti- and pro-inflammatory markers. Additionally, homeostatic microglia were also found to express TSPO, indicating that while increased TSPO PET signal is a marker of microglia it should not be used as a marker for a change in the activation state of microglia. Additionally, as autoradiography correlated with the number of TSPO+ cells in active MS lesions this indicates that TSPO PET could be a used to identify the microglial density, rather than activation state. A smaller portion of cells did not show colocalisation with GFAP (a marker for astrocytes) or HLA-DR (a marker used to identify activated myeloid cells), but showed strong microglial morphology. In **Chapter 3** we thus investigated the possibility of TSPO+ microglia that colocalised with other microglial markers than HLA-DR - a proportion of microglia was found to express either HLA-DR or IBA-1 in the MS brain[53]. MS lesions were stained for

combinations of microglial markers and TSPO. This study showed that the majority of cells expressing TSPO in control, NAWM, and active lesions are likely to be microglia/macrophages as the majority colocalised with either HLA-DR, IBA-1 or CD68. We also confirmed that in the centre of chronic active lesions and inactive lesions up to 70% of the cells expressing TSPO did not express microglia/macrophage markers and were thus considered to be astrocytes based on their morphology and this was investigated in **Chapter 2**. Additionally, our studies showed that in control and NAWM tissue TSPO+ microglia primarily express IBA-1 or CD68, indicating that microglia HLA-DR expression arises during microglial activation under neuroinflammatory conditions. Some TSPO+ microglia expressed both markers of homeostasis (P2ry12 and TMEM119) and HLA-DR suggesting that some microglia might be in a transitional state towards activation or vice versa.

To extend the findings from the neuropathology study in MS to other neurodegenerative and neuroinflammatory diseases we performed a similar in-depth study in ALS. In ALS, a higher TSPO PET signal in motor cortex, supplementary motor and temporal cortex in ALS patients with bulbar onset compared to healthy controls using [18F]-DPA-714 has been reported[54]. In addition a study using [11C]-PK11195 showed increased binding in motor cortex, pons, frontal lobe regions and the thalamus in ALS patients compared to healthy controls, regardless of bulbar or limb onset[38]. More recent studies utilizing [11C]-PBR28 report increased binding of TSPO PET in the motor cortex, but also in upper regions of the corticospinal tracts[55-57]. More specifically, increased binding was found in precentral gyri for limb-onset ALS patients and in the brain stem for bulbar-onset ALS patients, indicating that glial activation is present in clinically relevant neuroanatomical areas[55,56] and providing an atlas of the disease neuropathology with a close relationship to the clinical phenotype. Correlating altered PET binding with MRI has shown that increased binding in the precentral gyri was associated with cortical thinning, reduced fractional anisotropy (FA) and higher diffusivity[58,59]. Overall, PET studies have found similar affected regions in ALS patients (motor cortex and the upper corticospinal tracts), and there is some evidence that astrocytes are also affected in ALS patients[60]. Furthermore, while there is no lack of PET studies in ALS[4] most do not focus on glial cells and have limitations that restrict the ability to draw strong conclusions about the immunopathology in ALS. In addition, few studies involve large sample sizes or follow their subjects longitudinally. In **Chapter 4** we found that while microglia express TSPO in ALS, most of the TSPO expression was originating in astrocytes in the spinal cord. This finding was consistent when looking at short and medium disease duration and was present regardless of looking at the ventral horn or lateral columns – indicating a widespread increase of TSPO+ astrocytes in the ALS spinal cord. Additionally, also in ALS, we found both homeostatic and activated microglia expressing TSPO, indicating that TSPO expression in multiple microglia states is most likely not MS-specific.

To further extend our neuropathology studies in MS and ALS we also examined the common neurodegenerative disease AD. In AD, the hippocampus is one of the most affected regions[61,62]. When looking at TSPO PET studies investigating the hippocampus in AD there are conflicting findings. Some studies have found increases in TSPO PET, while some studies have found no differences. These discrepancies might be due to differences in cohort size, methodology, disease duration, radioligands, or therapeutics of the patients. In **Chapter 4** we show that there no differences in the numbers of TSPO+ cells either homeostatic or activated microglia or astrocytes in the hippocampus compared to control cases. In addition, classical amyloid plaques in AD were not associated with a high number of TSPO+ microglia.

In summary, this thesis shows that microglia are not the only source of TSPO in the CNS when interpreting TSPO PET. In **Chapter 5** we have summarised the current findings on the cellular sources of TSPO in the healthy and disease brain in humans and in rodents. We show that there are many studies hinting towards a more complex profile of TSPO expression than just the presence of TSPO in activated microglia. We argue that the clinical interpretation of TSPO PET signal should be disease and context-dependent, as differences are observed between different neurodegenerative diseases, in terms of cellular origin of the TSPO (e.g. microglia for MS lesions but astrocytes in the ALS spinal cord). Furthermore, TSPO PET might be more a measurement of cell proliferation/cell density rather than the activation state of the cell, as many homeostatic, and intermediate activated microglia are TSPO+ as well in the CNS.

Is TSPO expression and regulation similar in human CNS diseases versus their respective animal models?

One of the advantages of using PET imaging is the possibility to monitor ongoing biological processes in vivo. TSPO PET creates opportunities to monitor neuroinflammation after therapeutic intervention in humans, but it could also allow us to investigate the neuroinflammatory effects of therapeutics in a preclinical setting in experimental animal models. However, to utilise TSPO PET for this purpose, meaningful quantitative data on the origin of TSPO in animal models is essential given that biological pathways and drug therapies for neuroinflammatory and neurodegenerative diseases are tested in the animal models. Of relevance to this study and PET imaging in humans we thus need to know whether TSPO is expressed and regulated in a similar manner in rodents versus humans. There are reports that this might not be the case[22]. Pro-inflammatory stimulation of primary human microglia did not result in increased production of *TSPO*, and stimulation of human monocyte-derived macrophages was even associated with a reduction of *TSPO* expression and a reduction of TSPO binding sites (Figure 1). Contrastingly, pro-inflammatory stimulation of the equivalent rodent cells results in increases, of up to 10-fold, in both TSPO gene and protein expression[22,63-66]. These findings hint towards species differences in the regulation of TSPO. In **Chapter 4** we have investigated the single cell TSPO expression by measuring TSPO in microglia and astrocytes in MS, ALS, and AD and their respective animal models (EAE, $SOD1^{G93A}$, APP^{NLGF}, and TAU^{P301S}). In human CNS diseases we did not find evidence of increased TSPO protein expression in microglia and astrocytes in the brain parenchyma. In contrast, we did find TSPO expression was increased in all the respective animal models. In support of our findings, a meta-analysis of pro-inflammatory stimulated myeloid cells in humans and rodents showed a similar finding that *TSPO* is not upregulated in human myeloid cells after stimulation while *Tspo* is upregulated in rodent cells – confirming previous findings[22]. We also investigated whether these findings were consistent for microglial cells, and utilised publicly available single-cell RNAseq databases of MS, AD and their respective animal models. Unfortunately, only single-cell RNA-seq databases were available as TSPO gene expression is not picked up with single-nucleus RNAseq despite TSPO being a nuclear encoded protein[67]. We found that activated microglia do not upregulate *TSPO* gene expression in MS and AD: no single-cell RNAseq data was available for ALS. Additionally, similar to the meta-analysis of myeloid cells, activated microglia in animal models of MS and AD did upregulate *Tspo* expression. Interestingly, a paired CHIPseq and RNAseq database was available allowing us to investigate the regulation of the TSPO gene on an epigenetic level after pro-inflammatory stimulation. These studies showed that TSPO gene is methylated to a greater extent in humans after pro-inflammatory stimulation compared to mice.

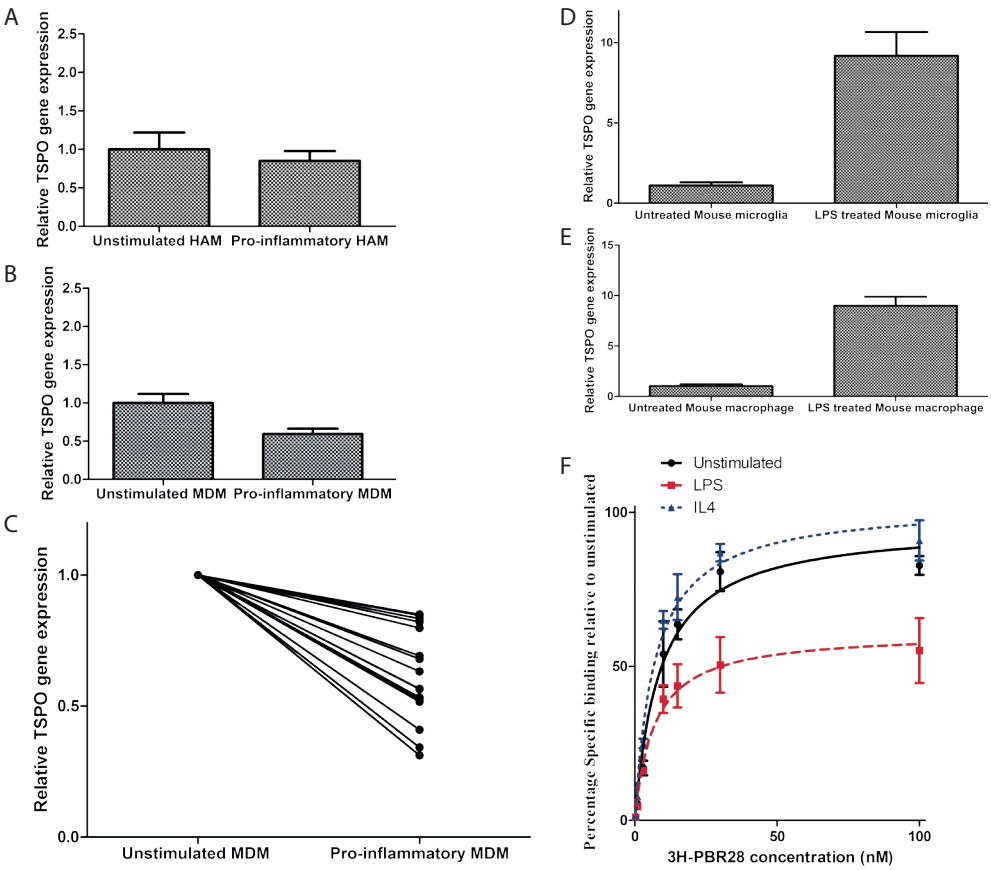

Figure 1. Pro-inflammatory activation of primary microglia and macrophages increases 18 kDa TSPO expression in rodents but not humans (Adapted from Owen et al.,[22]). Human microglia show no increase in TSPO after proinflammatory stimulation (A). Human macrophages show a reduction in relative TSPO expression after pro-inflammatory stimulation (B,C). Contrastingly, mouse microglia and macrophages show a significant upregulation of TSPO after pro-inflammatory stimulation ($p < 0.001$, D,E). Radioligand binding of 3H-PBR28 decreases after pro-inflammatory stimulation of macrophages (F).

This points towards a significant phylogenetic diversification of the regulation of the TSPO gene and perhaps a different role of the TSPO gene in humans versus rodents – possibly also related to the availability of the binding site of the PU.1 enhancer region in the TSPO gene which we found to be less accessible in humans compared to rodents in a pro-inflammatory environment.

In summary, our studies, and the publicly available datasets on single cell expression of TSPO suggest a phylogenetic difference in the regulation of the TSPO gene. How, or why this diversification has taken place warrants more research into the function and role of the TSPO gene in inflammatory conditions. TSPO expression in humans does not increase when microglia adopt a pro-inflammatory state and thus TSPO PET signal reports on microglial density rather than phenotype. TSPO PET signal also is confounded by astrocytic TSPO expression under some conditions (e.g. inactive lesions in MS) and must thus be interpreted accordingly.

Microglia and astrocytes as CNS innate immune cells

Another goal of the thesis was to investigate the role of microglia and astrocytes as innate immune cells of the CNS as they are becoming increasingly implicated in having diverse functions and heterogeneous states in many CNS diseases. While historically, microglia were considered as the phagocytes of the brain and astrocytes as responders to damage, the rise in advanced technologies such as single cell and single nucleus RNAseq, as well as detailed pathology studies made available by a plethora of antibodies and probes has shown that microglia and astrocytes have diverse and complex functions in the CNS. In **Chapter 8** we discussed the role of microglia and their heterogeneity in the white matter of the CNS. We report that microglia have regionally defined functions in the CNS which relate to development, homeostasis, ageing, and response to injury. These functions are dependent on the local needs of the CNS parenchyma and are reflected in differential transcriptomes, morphology and density of microglia numbers in the brain.

Over the last years astrocytes have been recognised as critical for cell-cell interactions, homeostasis, synapse pruning and cerebral blood flow providing trophic and metabolic support for all CNS resident cells. Since many of the studies on astrocytes focus on their interactions with neurons, in **Chapter 7** we have investigated the role of astrocytes as innate immune cells in the brain and their interactions with oligodendrocytes, as oligodendrocytes are essential for white matter health and homeostasis. Indeed, astrocytes produce a wide range of pro-inflammatory factors including chemokines, cytokines, increased expression of innate immune receptors and molecules[68-71]. We report that interactions between astrocytes and oligodendrocytes have many immunological functions where both astrocytes and oligodendrocytes are capable of secreting cytokines and reacting to them during reactive gliosis, oligodendrocyte damage, excitotoxicity and remyelination. There is a growing awareness that astrocytes are not only targets for autoimmune responses but can also initiate them in the context of neuroinflammation.

Concluding remarks

The objective of this thesis was to identify TSPO expression in the CNS in neurodegenerative and neuroinflammatory diseases. Identifying the cellular origin of TSPO expression in CNS diseases and investigating the role of microglia and astrocytes as innate immune cells aids in uncovering the clinical use of TSPO PET as a non-invasive biomarker for neuroinflammation.

By using post-mortem studies, we characterised the cellular expressing of TSPO in the neuroinflammatory and neurodegenerative diseases MS, ALS, and AD, and their respective animal models. Our main findings of are summarised in **Box 1**. We hypothesised that TSPO expression is not exclusive to activated microglia but is present in a wide variety of microglia states. Additionally, we hypothesised that TSPO is also expressed by other cell types such as astrocytes in the CNS.

We showed that TSPO expression in CNS diseases is a complex combination of expression by multiple cell types and states, and that TSPO PET most likely reflects a multi-cellular neuroinflammatory reaction which is disease and context-dependent, with potential use as pharmacodynamic biomarker for therapies[60,72]. For example, in MS, the results emphasise that precise interpretations depend on the specific pathological context.

We also hypothesised that TSPO is not upregulated in microglia once they are activated / in

Box 1 Conclusions of the studies performed in this thesis

Chapter 2
Microglia but also astrocytes express TSPO in MS lesions, TSPO PET reports on cell density rather than activation state.

Chapter 3
TSPO is not upregulated in activated microglia in MS lesions compared to homeostatic microglia in the NAWM and in control white matter.

Chapter 4
Regulation of TSPO is phylogenetically diverse between humans and rodents, resulting in differential regulation of the TSPO gene in humans. TSPO is not increased in activated microglia and astrocytes in human CNS diseases.

Chapter 5
TSPO binding, cellular origin, and functional significance is dependent on many factors such as the pathology or the experimental animal model.

Chapter 6
Microglial activation in the MS spinal cord is associated with synaptic loss, resulting in progressive clinical disability.

Chapter 7
Astrocytes and oligodendrocytes produce and respond to many immunomodulatory factors playing critical roles in immune responses in the CNS.

Chapter 8
Microglia have regionally defined functions in the CNS relating to development, homeostasis, ageing, neuroinflammation and in response to injury, reflecting the local needs of the CNS parenchyma.

a pro-inflammatory environment. Our studies consistently show that human microglia do not upregulate expression of TSPO upon activation in neuro-inflammatory and-degenerative diseases, both *in vitro* and *in vivo*. Contrastingly, rodent microglia quite easily start upregulating TSPO in pro-inflammatory environments *in vitro* and *in vivo*, possibly due to phylogenetic differences in the regulation of the TSPO gene.

While TSPO PET has many advantages, there are some perceived difficulties that need to be overcome to use TSPO PET as a reliable marker. First generation TSPO ligands had difficulties with specificity while second generation TSPO ligands were sensitive to genetic polymorphisms that altered binding affinity. However, there are new reports indicating that significant advances are being made in generating TSPO radioligands with improved pharmacokinetics and low levels of non-specific binding[73-75]. There might even be some new radioligands that show low sensitivity towards the TSPO polymorphism[76-78]. Development of these radiotracers provide a promising prospect to what TSPO PET might contribute towards making more informed decisions for diagnoses and therapeutic strategies for clinical therapies in the future.

References

1. Trias E, *et al*. Mast cells and neutrophils mediate peripheral motor pathway degeneration in ALS. *JCI Insight*. Oct 4 2018;3(19)doi:10.1172/jci.insight.123249
2. Guilarte TR. TSPO in diverse CNS pathologies and psychiatric disease: A critical review and a way forward. *Pharmacol Ther*. Feb 2019;194:44-58. doi:10.1016/j.pharmthera.2018.09.003
3. Kreisl WC, *et al*. PET imaging of neuroinflammation in neurological disorders. *Lancet Neurol*. Nov 2020;19(11):940-950. doi:10.1016/S1474-4422(20)30346-X
4. Chew S, *et al*. Positron Emission Tomography Molecular Imaging Biomarkers for Amyotrophic Lateral Sclerosis. Mini Review. *Front Neurol*. 2019-March-01 2019;10(135):135. doi:10.3389/fneur.2019.00135
5. Arlicot N, *et al*. Evaluation of CLINDE as potent translocator protein (18 kDa) SPECT radiotracer reflecting the degree of neuroinflammation in a rat model of microglial activation. *Eur J Nucl Med Mol Imaging*. Dec 2008;35(12):2203-11. doi:10.1007/s00259-008-0834-x
6. Dickens AM, *et al*. Detection of microglial activation in an acute model of neuroinflammation using PET and radiotracers 11C-(R)-PK11195 and 18F-GE-180. *J Nucl Med*. Mar 2014;55(3):466-72. doi:10.2967/jnumed.113.125625
7. Domene A, *et al*. Expression of Phenotypic Astrocyte Marker Is Increased in a Transgenic Mouse Model of Alzheimer's Disease versus Age-Matched Controls: A Presymptomatic Stage Study. *Int J Alzheimers Dis*. 2016;2016:5696241. doi:10.1155/2016/5696241
8. Israel I, *et al*. Combined [(18)F]DPA-714 micro-positron emission tomography and autoradiography imaging of microglia activation after closed head injury in mice. journal article. *J Neuroinflammation*. Jun 7 2016;13(1):140. doi:10.1186/s12974-016-0604-9
9. Ji B, *et al*. Imaging of peripheral benzodiazepine receptor expression as biomarkers of detrimental versus beneficial glial responses in mouse models of Alzheimer's and other CNS pathologies. *J Neurosci*. Nov 19 2008;28(47):12255-67. doi:10.1523/JNEUROSCI.2312-08.2008
10. Lavisse S, *et al*. Reactive astrocytes overexpress TSPO and are detected by TSPO positron emission tomography imaging. *J Neurosci*. Aug 8 2012;32(32):10809-18. doi:10.1523/JNEUROSCI.1487-12.2012
11. Lavisse S, *et al*. [18F]DPA-714 PET imaging of translocator protein TSPO (18 kDa) in the normal and excitotoxically-lesioned nonhuman primate brain. *Eur J Nucl Med Mol Imaging*. Mar 2015;42(3):478-94. doi:10.1007/s00259-014-2962-9
12. Maeda J, *et al*. Phase-dependent roles of reactive microglia and astrocytes in nervous system injury as delineated by imaging of peripheral benzodiazepine receptor. *Brain Res*. Jul 9 2007;1157:100-11. doi:10.1016/j.brainres.2007.04.054
13. Mattner F, *et al*. Evaluation of [(1)(2)(3)I]-CLINDE as a potent SPECT radiotracer to assess the degree of astroglia activation in cuprizone-induced neuroinflammation. *Eur J Nucl Med Mol Imaging*. Aug 2011;38(8):1516-28. doi:10.1007/s00259-011-1784-2
14. Nguyen DL, *et al*. Longitudinal positron emission tomography imaging of glial cell activation in a mouse model of mesial temporal lobe epilepsy: Toward identification of optimal treatment windows. *Epilepsia*. Jun 2018;59(6):1234-1244. doi:10.1111/epi.14083
15. Rojas S, *et al*. Imaging brain inflammation with [(11)C]PK11195 by PET and induction of the peripheral-type benzodiazepine receptor after transient focal ischemia in rats. *J Cereb Blood Flow Metab*. Dec 2007;27(12):1975-86. doi:10.1038/sj.jcbfm.9600500
16. Serriere S, *et al*. Amyloid load and translocator protein 18 kDa in APPswePS1-dE9 mice: a longitudinal study. *Neurobiol Aging*. Apr 2015;36(4):1639-1652. doi:10.1016/j.neurobiolaging.2014.11.023
17. Wang Y, *et al*. PET imaging of neuroinflammation in a rat traumatic brain injury model with radiolabeled TSPO ligand DPA-714. *Eur J Nucl Med Mol Imaging*. Jul 2014;41(7):1440-9. doi:10.1007/s00259-014-2727-5
18. Daugherty DJ, *et al*. A TSPO ligand is protective in a mouse model of multiple sclerosis. *EMBO Mol Med*. Jun 2013;5(6):891-903. doi:10.1002/emmm.201202124
19. Cosenza-Nashat M, *et al*. Expression of the translocator protein of 18 kDa by microglia, macrophages and astrocytes based on immunohistochemical localization in abnormal human brain. *Neuropathol Appl Neurobiol*. Jun 2009;35(3):306-28. doi:10.1111/j.1365-2990.2008.01006.x
20. Liu B, *et al*. In Vivo Detection of Age- and Disease-Related Increases in Neuroinflammation by 18F-GE180 TSPO MicroPET Imaging in Wild-Type and Alzheimer's Transgenic Mice. *J Neurosci*. Nov 25 2015;35(47):15716-30. doi:10.1523/JNEUROSCI.0996-15.2015
21. Maeda J, *et al*. In vivo positron emission tomographic imaging of glial responses to amyloid-beta and tau pathologies in mouse models of Alzheimer's disease and related disorders. *J Neurosci*. Mar 23 2011;31(12):4720-30. doi:10.1523/JNEUROSCI.3076-10.2011
22. Owen DR, *et al*. Pro-inflammatory activation of primary microglia and macrophages increases

18 kDa translocator protein expression in rodents but not humans. *J Cereb Blood Flow Metab*. Aug 2017;37(8):2679-2690. doi:10.1177/0271678X17710182
23. Kreisl WC, *et al*. Comparison of [11C]-(R)-PK 11195 and [11C] PBR28, two radioligands for translocator protein (18 kDa) in human and monkey: implications for positron emission tomographic imaging of this inflammation biomarker. *Neuroimage*. 2010;49(4):2924-2932.
24. Datta G, *et al*. (11)C-PBR28 and (18)F-PBR111 Detect White Matter Inflammatory Heterogeneity in Multiple Sclerosis. *J Nucl Med*. Sep 2017;58(9):1477-1482. doi:10.2967/jnumed.116.187161
25. Banati RB, *et al*. The peripheral benzodiazepine binding site in the brain in multiple sclerosis: quantitative in vivo imaging of microglia as a measure of disease activity. *Brain*. Nov 2000;123 (Pt 11)(11):2321-37. doi:10.1093/brain/123.11.2321
26. Cagnin A, *et al*. In vivo visualization of activated glia by [11C] (R)-PK11195-PET following herpes encephalitis reveals projected neuronal damage beyond the primary focal lesion. *Brain*. Oct 2001;124(Pt 10):2014-27. doi:10.1093/brain/124.10.2014
27. Debruyne JC, *et al*. PET visualization of microglia in multiple sclerosis patients using [11C]PK11195. *Eur J Neurol*. May 2003;10(3):257-64. doi:10.1046/j.1468-1331.2003.00571.x
28. Gerhard A, *et al*. [11C](R)-PK11195 PET imaging of microglial activation in multiple system atrophy. *Neurology*. Sep 9 2003;61(5):686-9. doi:10.1212/01.wnl.0000078192.95645.e6
29. Gerhard A, *et al*. In vivo imaging of microglial activation with [11C](R)-PK11195 PET in idiopathic Parkinson's disease. *Neurobiol Dis*. Feb 2006;21(2):404-12. doi:10.1016/j.nbd.2005.08.002
30. Gerhard A, *et al*. In vivo imaging of microglial activation with [11C](R)-PK11195 PET in progressive supranuclear palsy. *Mov Disord*. Jan 2006;21(1):89-93. doi:10.1002/mds.20668
31. Gerhard A, *et al*. In vivo imaging of microglial activation with [11C](R)-PK11195 PET in corticobasal degeneration. *Mov Disord*. Oct 2004;19(10):1221-6. doi:10.1002/mds.20162
32. Ghadery C, *et al*. Microglial activation in Parkinson's disease using [(18)F]-FEPPA. *J Neuroinflammation*. Jan 11 2017;14(1):8. doi:10.1186/s12974-016-0778-1
33. Groom GN, *et al*. PET of peripheral benzodiazepine binding sites in the microgliosis of Alzheimer's disease. *J Nucl Med*. Dec 1995;36(12):2207-10.
34. Henkel K, *et al*. Imaging of activated microglia with PET and [11C]PK 11195 in corticobasal degeneration. *Mov Disord*. Jul 2004;19(7):817-821. doi:10.1002/mds.20040
35. Politis M, *et al*. Increased central microglial activation associated with peripheral cytokine levels in premanifest Huntington's disease gene carriers. *Neurobiol Dis*. Nov 2015;83:115-21. doi:10.1016/j.nbd.2015.08.011
36. Tai YF, *et al*. Imaging microglial activation in Huntington's disease. *Brain Res Bull*. Apr 30 2007;72(2-3):148-51. doi:10.1016/j.brainresbull.2006.10.029
37. Tomasi G, *et al*. Novel reference region model reveals increased microglial and reduced vascular binding of 11C-(R)-PK11195 in patients with Alzheimer's disease. *J Nucl Med*. Aug 2008;49(8):1249-56. doi:10.2967/jnumed.108.050583
38. Turner MR, *et al*. Evidence of widespread cerebral microglial activation in amyotrophic lateral sclerosis: an [11C](R)-PK11195 positron emission tomography study. *Neurobiol Dis*. Apr 2004;15(3):601-9. doi:10.1016/j.nbd.2003.12.012
39. Venneti S, *et al*. PK11195 labels activated microglia in Alzheimer's disease and in vivo in a mouse model using PET. *Neurobiol Aging*. Aug 2009;30(8):1217-26. doi:10.1016/j.neurobiolaging.2007.11.005
40. Vowinckel E, *et al*. PK11195 binding to the peripheral benzodiazepine receptor as a marker of microglia activation in multiple sclerosis and experimental autoimmune encephalomyelitis. *Journal of Neuroscience Research*. Oct 15 1997;50(2):345-353. doi:Doi 10.1002/(Sici)1097-4547(19971015)50:2<345::Aid-Jnr22>3.0.Co;2-5
41. Yankam Njiwa J, *et al*. Quantitative longitudinal imaging of activated microglia as a marker of inflammation in the pilocarpine rat model of epilepsy using [(11)C]-(R)-PK11195 PET and MRI. *J Cereb Blood Flow Metab*. Apr 2017;37(4):1251-1263. doi:10.1177/0271678X16653615
42. Kuhlmann AC, *et al*. Cellular and subcellular localization of peripheral benzodiazepine receptors after trimethyltin neurotoxicity. *J Neurochem*. Apr 2000;74(4):1694-704. doi:10.1046/j.1471-4159.2000.0741694.x
43. van der Valk P, *et al*. Staging of multiple sclerosis (MS) lesions: pathology of the time frame of MS. *Neuropathol Appl Neurobiol*. Feb 2000;26(1):2-10. doi:10.1046/j.1365-2990.2000.00217.x
44. Versijpt J, *et al*. Microglial imaging with positron emission tomography and atrophy measurements with magnetic resonance imaging in multiple sclerosis: a correlative study. *Mult Scler*. Apr 2005;11(2):127-34. doi:10.1191/1352458505ms1140oa
45. Oh U, *et al*. Translocator protein PET imaging for glial activation in multiple sclerosis. *J Neuroimmune Pharmacol*. Sep 2011;6(3):354-61. doi:10.1007/s11481-010-9243-6
46. Rissanen E, *et al*. In Vivo Detection of Diffuse Inflammation in Secondary Progressive Multiple Sclerosis Using PET Imaging and the Radioligand (1)(1)C-PK11195. *J Nucl Med*. Jun 2014;55(6):939-44. doi:10.2967/jnumed.113.131698
47. Datta G, *et al*. Translocator positron-emission tomography and magnetic resonance spectroscopic

imaging of brain glial cell activation in multiple sclerosis. *Mult Scler*. Oct 2017;23(11):1469-1478. doi:10.1177/1352458516681504
48. Sucksdorff M*, et al*. Brain TSPO-PET predicts later disease progression independent of relapses in multiple sclerosis. *Brain*. Dec 5 2020;143(11):3318-3330. doi:10.1093/brain/awaa275
49. Kaunzner UW*, et al*. Quantitative susceptibility mapping identifies inflammation in a subset of chronic multiple sclerosis lesions. *Brain*. Jan 1 2019;142(1):133-145. doi:10.1093/brain/awy296
50. Bo L*, et al*. Magnetic resonance imaging as a tool to examine the neuropathology of multiple sclerosis. *Neuropathol Appl Neurobiol*. Apr 2004;30(2):106-17. doi:10.1111/j.1365-2990.2003.00521.x
51. Brink BP*, et al*. The pathology of multiple sclerosis is location-dependent: no significant complement activation is detected in purely cortical lesions. *J Neuropathol Exp Neurol*. Feb 2005;64(2):147-55. doi:10.1093/jnen/64.2.147
52. van Horssen J*, et al*. The blood-brain barrier in cortical multiple sclerosis lesions. *J Neuropathol Exp Neurol*. Apr 2007;66(4):321-8. doi:10.1097/nen.0b013e318040b2de
53. Hendrickx DAE*, et al*. Staining of HLA-DR, Iba1 and CD68 in human microglia reveals partially overlapping expression depending on cellular morphology and pathology. *J Neuroimmunol*. Aug 15 2017;309:12-22. doi:10.1016/j.jneuroim.2017.04.007
54. Corcia P*, et al*. Molecular imaging of microglial activation in amyotrophic lateral sclerosis. *PLOS ONE*. 2012;7(12):e52941. doi:10.1371/journal.pone.0052941
55. Zurcher NR*, et al*. Increased in vivo glial activation in patients with amyotrophic lateral sclerosis: assessed with [(11)C]-PBR28. *Neuroimage Clin*. 2015;7:409-14. doi:10.1016/j.nicl.2015.01.009
56. Ratai EM*, et al*. Integrated imaging of [(11)C]-PBR28 PET, MR diffusion and magnetic resonance spectroscopy (1)H-MRS in amyotrophic lateral sclerosis. *Neuroimage Clin*. 2018/01/01/2018;20:357-364. doi:10.1016/j.nicl.2018.08.007
57. Albrecht DS*, et al*. Pseudoreference Regions for Glial Imaging with (11)C-PBR28: Investigation in 2 Clinical Cohorts. *J Nucl Med*. Jan 2018;59(1):107-114. doi:10.2967/jnumed.116.178335
58. Alshikho MJ*, et al*. Integrated magnetic resonance imaging and [(11) C]-PBR28 positron emission tomographic imaging in amyotrophic lateral sclerosis. *Ann Neurol*. Jun 2018;83(6):1186-1197. doi:10.1002/ana.25251
59. Alshikho MJ*, et al*. Glial activation colocalizes with structural abnormalities in amyotrophic lateral sclerosis. *Neurology*. Dec 13 2016;87(24):2554-2561. doi:10.1212/WNL.0000000000003427
60. Johansson A*, et al*. Evidence for astrocytosis in ALS demonstrated by [11C](L)-deprenyl-D2 PET. *J Neurol Sci*. Apr 15 2007;255(1-2):17-22. doi:10.1016/j.jns.2007.01.057
61. Lane CA*, et al*. Alzheimer's disease. *Eur J Neurol*. Jan 2018;25(1):59-70. doi:10.1111/ene.13439
62. Tiwari S*, et al*. Alzheimer's disease: pathogenesis, diagnostics, and therapeutics. *Int J Nanomedicine*. 2019;14:5541-5554. doi:10.2147/IJN.S200490
63. Bae KR*, et al*. Translocator protein 18 kDa negatively regulates inflammation in microglia. *J Neuroimmune Pharmacol*. Jun 2014;9(3):424-37. doi:10.1007/s11481-014-9540-6
64. Gottfried-Blackmore A*, et al*. Brain microglia express steroid-converting enzymes in the mouse. *J Steroid Biochem Mol Biol*. Mar 2008;109(1-2):96-107. doi:10.1016/j.jsbmb.2007.12.013
65. Karlstetter M*, et al*. Translocator protein (18 kDa) (TSPO) is expressed in reactive retinal microglia and modulates microglial inflammation and phagocytosis. *J Neuroinflammation*. Jan 8 2014;11:3. doi:10.1186/1742-2094-11-3
66. Wang M*, et al*. Macroglia-microglia interactions via TSPO signaling regulates microglial activation in the mouse retina. *J Neurosci*. Mar 5 2014;34(10):3793-806. doi:10.1523/JNEUROSCI.3153-13.2014
67. Rone MB*, et al*. Targeting and insertion of the cholesterol-binding translocator protein into the outer mitochondrial membrane. *Biochemistry*. Jul 28 2009;48(29):6909-20. doi:10.1021/bi900854z
68. Gaudet AD*, et al*. Glial Cells Shape Pathology and Repair After Spinal Cord Injury. *Neurotherapeutics*. Jul 2018;15(3):554-577. doi:10.1007/s13311-018-0630-7
69. Kiray H*, et al*. The multifaceted role of astrocytes in regulating myelination. *Exp Neurol*. Sep 2016;283(Pt B):541-9. doi:10.1016/j.expneurol.2016.03.009
70. Li J*, et al*. Astrocytes in Oligodendrocyte Lineage Development and White Matter Pathology. *Front Cell Neurosci*. 2016/05/10 2016;10:119. doi:10.3389/fncel.2016.00119
71. Seth P*, et al*. Astrocyte, the star avatar: redefined. *J Biosci*. Sep 2008;33(3):405-21. doi:10.1007/s12038-008-0060-5
72. Ghadery C*, et al*. PET Evaluation of Microglial Activation in Non-neurodegenerative Brain Diseases. *Curr Neurol Neurosci Rep*. May 28 2019;19(7):38. doi:10.1007/s11910-019-0951-x
73. Alam MM*, et al*. Recent Progress in the Development of TSPO PET Ligands for Neuroinflammation Imaging in Neurological Diseases. *Nucl Med Mol Imaging*. Dec 2017;51(4):283-296. doi:10.1007/s13139-017-0475-8
74. Werry EL*, et al*. Recent Developments in TSPO PET Imaging as A Biomarker of Neuroinflammation in Neurodegenerative Disorders. *Int J Mol Sci*. Jun 28 2019;20(13). doi:10.3390/ijms20133161
75. Zhang L*, et al*. Recent developments on PET radiotracers for TSPO and their applications in neuroimaging. *Acta Pharm Sin B*. Feb 2021;11(2):373-393. doi:10.1016/j.apsb.2020.08.006

76. Kim K*, et al*. [(18)F]CB251 PET/MR imaging probe targeting translocator protein (TSPO) independent of its Polymorphism in a Neuroinflammation Model. Research Paper. *Theranostics*. 2020;10(20):9315-9331. doi:10.7150/thno.46875
77. Mattner F*, et al*. Synthesis and pharmacological evaluation of [(18)F]PBR316: a novel PET ligand targeting the translocator protein 18 kDa (TSPO) with low binding sensitivity to human single nucleotide polymorphism rs6971. 10.1039/D1MD00035G. *RSC Med Chem*. Jul 21 2021;12(7):1207-1221. doi:10.1039/d1md00035g
78. Vo SV*, et al*. Reversing binding sensitivity to A147T translocator protein. 10.1039/C9MD00580C. *RSC Med Chem*. Apr 1 2020;11(4):511-517. doi:10.1039/c9md00580c

APPENDICES

Summary

Neuroinflammation in neuroinflammatory and neurodegenerative diseases is only one of the many complex multicellular processes that occurs behind the 'closed borders' within the central nervous system (CNS). Two important innate immune cells in the CNS that contribute to damage as well as repair are microglia and astrocytes. Given their importance in many diseases there is an urgent clinical need to monitor glial cell activity during disease as well as assess the impact of medical intervention on innate immune responses during diseases. Positron emission tomography (PET) is one of the modalities to monitor neuroinflammation and pathological changes in neurodegenerative diseases and experimental animal *in vivo.* PET has the advantage of being able to interrogate various disease mechanisms by quantifying specific molecular targets to directly study the CNS.

In this thesis we examined the cellular distribution and the regulation of the translocator protein (TSPO) in CNS resident cells in neurodegenerative diseases and their respective animal models. TSPO is generally through to be a marker of activated microglia and has been reported as such by many studies. Initial reports on animal models of neuroinflammatory diseases showed that TSPO is also expressed by other cell types than microglia but these findings have been largely ignored by PET studies, and the early human studies were qualitative rather than quantitative. Recently, it was shown *in vitro* that primary rodent microglia upregulate TSPO expression in a pro-inflammatory environment, while this is not the case in humans. Thus, findings of the triggers of TSPO, and the cellular expression of TSPO in the CNS in animal models may not translate to human disease. To investigate the cellular distribution and understand the triggers of TSPO we first performed in-depth studies of TSPO expression in MS to validate TSPO expression in glial cells and how the TSPO protein was regulated. Then we expanded our studies to other common neurodegenerative diseases such as AD and ALS and their respective animal models. In addition, we have utilised publicly available databases on TSPO regulation on multiple molecular levels.

Another goal of the thesis was to investigate the role of microglia and astrocytes as innate immune cells of the CNS as they are becoming increasingly implicated in having diverse functions and heterogeneous states in many CNS diseases. While historically, microglia were considered as the phagocytes of the brain and astrocytes as responders to damage, the rise in advanced technologies such as single cell and single nucleus RNAseq, as well as detailed pathology studies made available by a plethora of antibodies and probes has shown that microglia and astrocytes have diverse and complex functions in the CNS. Together, these studies have allowed a more detailed understanding of the role of microglia and astrocytes as innate immune cells of the CNS.

Chapter 2 describes the expression of the TSPO protein in MS compared to age-matched non-neurological controls. It features TSPO expression in glial cells in white and grey matter lesions in the brain and in the spinal cord. In this study we show that TSPO expression is not exclusive to activated microglia, as homeostatic microglia also express TSPO. Additionally we show that TSPO expression is not limited to microglia, but that astrocytes, and to a lower extent endothelial cells and oligodendroglia also are capable of TSPO expression in the CNS. We also show that TSPO expression is highly correlated with actual TSPO ligand binding that is used in the clinic for TSPO research and imaging neuroinflammation. The presence of TSPO in homeostatic microglia and astrocytes has implications for the interpretations of TSPO PET, and thus should be accounted for when interpreting this data.

Chapter 3 expands on the previous chapter and features an in-depth characterisation of TSPO expression in MS lesions using multiple markers of microglia (IBA1, HLA-DR, and CD68). We also investigated whether TSPO+ homeostatic microglia co-expressed markers of activation. Additionally, we investigated the amount of TSPO expressed by microglia in MS lesions and correlated this with morphological data. In this study, we replicated findings of chapter 2 but also found that almost all TSPO+ cells across a range of white matter regions were microglia, and that the phenotype in control and NAWM was homeostatic, and the phenotype in active and the rim of chronic active lesions was activated. More importantly we found no differences in the expression of TSPO in activated microglia when compared to microglia that were homeostatic in NAWM and control white matter nor did we find differences in morphology that indicated changes in TSPO expression. Overall, this indicates that TSPO PET could best be interpreted as a readout for total microglia count instead of the activation states of local microglia.

Chapter 4 investigates TSPO expression in glial cells in multiple neurodegenerative diseases, namely AD, ALS and MS and how TSPO is expressed in their commonly used rodent models. Since many studies have assumed TSPO PET to reflect an increase in TSPO in activated microglia we tested whether this assumption was holding true for these neurodegenerative diseases and rodent models. We performed a meta-analysis of publicly available expression array data and found that across a range of pro-inflammatory activation stimuli, TSPO expression is consistently and substantially increase in mouse, but not human macrophages and microglia in vitro. Afterwards we performed a comparative analysis of the TSPO promotor region in a range of mammalian species and found that the binding site for AP1 (a transcription factor which regulates macrophage activation) is present in and unique to a subset of species within the Muroidea superfamily of rodents and absent in humans. Consistent with the in vitro data we found that postmortem microglia in AD, ALS and MS, and in marmoset EAE do not increase TSPO expression when in a pro-inflammatory state. Contrastingly, TSPO expression is markedly increased in activated myeloid cells in all mouse models of these diseases. Lastly, we investigated relative expression of *TSPO* in publicly available single cell RNA sequencing datasets of the CNS of AD and MS and their respective animal models. Again we found no evidence for an increase of *TSPO* expression in the human CNS disease in activated microglia while mouse microglia did show an increase in *Tspo* expression. These data suggest that TSPO PET is sensitive to microglial activation is true only for a subset of species within the Muroidea superfamily of rodents. In contrast, in humans and other mammals, it simply reflects the local density of inflammatory cells irrespective of the disease context. The clinical interpretation of the TSPO PET signal therefore needs to be revised.

Chapter 5 summarises all the published studies on TSPO expression in the CNS in healthy and diseased brains. We provide an overview of TSPO expression in commonly used rodent models and in common human neurodegenerative and neuropsychiatric diseases. Based on the literature we conclude that the presence of TSPO in other cell types than microglia, such as astrocytes and endothelial cells is increasingly accepted. We find that the cellular TSPO is not only dependent on the pathology but also on the developmental stage and mode of cell activation. While monitoring TSPO levels in the CNS is now widely used as a readout of microglial activation and neuroinflammation more research is needed to better characterise the means and the cells involved in inflammatory processes and how these processes contribute to the TSPO signal. Future studies could also investigate the therapeutic potential of TSPO manipulation in the CNS.

Chapter 6 gives a short insight into the expansive effects of axonal loss on neurodegeneration and clinical disability in MS. We investigated the amount of axonal loss in the spinal cord of MS patients and correlated this with the presence of synapse proteins and the loss of local neurons. We found that the amount of synaptic pathology is extensive in MS spinal cord, the number of synaptic boutons, responsible for neuronal communication, were almost reduced to zero in lesional grey matter when compared to healthy spinal cord tissue. Additionally people with MS had a significant loss of spinal cord neurons. However, the loss of synaptic boutons did not correlate with the loss of neurons in the grey matter in the spinal cord. We concluded that axonal loss and neuronal loss in MS is extensive and higher than previously reported in the literature.

Chapter 7 explores the immunomodulatory roles of astrocytes and oligodendrocytes, glial cells that are not commonly seen as having immune functions. Astrocytes have long been seen as bystanders during immune-related events in the CNS. Oligodendrocytes have long been seen as the victims of neuroinflammation. An increasing body of literature is pointing towards more complex roles for glial cells during immune activation. We found that astrocytes and oligodendrocytes have important cell-to-cell communication during inflammation. Astrocyte and oligodendrocyte play active roles as innate immune cells by secreting chemokines, and thus can influence other glial cells as well as each other.

Chapter 8 is highlighting an important topic that is becoming increasingly important with the development of new technologies. Historically microglia are seen as the resident macrophages of the CNS, new techniques have highlighted diverse roles and their main functions in the CNS are to protect it from potential harm as well as regulate homeostasis. We show that microglia are diverse and have multifaceted roles in the white matter of the brain. Microglia have regionally defined functions related to development, homeostasis, ageing and in response to injury, reflecting the local need of the CNS parenchyma. This heterogeneity takes form in differences in density, morphology, and the transcriptome. We raise important questions that the field needs to take into account in future research while investigating microglia heterogeneity. Such as, '*How similar are mouse (or other animals) and human white matter microglia?*' and '*How stable are white matter microglial states?*'. By raising awareness for these important questions we hope to stimulate the field into investigating the diverse microglia functions to eventually develop microglial based therapies.

Overall, this thesis shows that TSPO is differently regulated in humans compared to mice and that all glial cells act as innate immune cells. The main conclusions per chapter are:

- Microglia but also astrocytes express TSPO in MS lesions, TSPO PET reports on cell density rather than activation state (**Chapter 2**)
- TSPO is not upregulated in activated microglia in MS lesions compared to homeostatic microglia in the NAWM and in control white matter (**Chapter 3**)
- Regulation of TSPO is phylogenetically diverse between humans and rodents, resulting in differential regulation of the TSPO gene in humans. TSPO is not increased in activated microglia and astrocytes in human CNS diseases (**Chapter 4**)
- TSPO binding, cellular origin, and functional significance is dependent on many factors such as the pathology or the experimental animal model (**Chapter 5**)
- Microglial activation in the MS spinal cord is associated with synaptic loss, resulting in progressive clinical disability (**Chapter 6**)

- Astrocytes and oligodendrocytes produce and respond to many immunomodulatory factors playing critical roles in immune responses in the CNS (**Chapter 7**)
- Microglia have regionally defined functions in the CNS relating to development, homeostasis, ageing, neuroinflammation and in response to injury, reflecting the local needs of the CNS parenchyma (**Chapter 8**)

Nederlandse samenvatting

Neuroinflammatie bij neuro-inflammatoire en neurodegeneratieve ziekten is slechts één van de vele complexe multicellulaire processen die plaatsvindt achter de bloed hersenbarrière in het centrale zenuwstelsel (CZS). Twee belangrijke aangeboren immuuncellen in het CZS die bijdragen aan schade en herstel zijn microglia en astrocyten. Gezien hun rol bij veel ziektes is er een dringende klinische behoefte om de activiteit van gliacellen tijdens ziekte te volgen maar ook om de impact van medische interventie op aangeboren immuunresponsen tijdens ziektes te kunnen volgen. Positronemissietomografie (PET) is een van de modaliteiten om neuroinflammatie en pathologische veranderingen in neurodegeneratieve ziekten en proefdieren in vivo te volgen. PET heeft het voordeel dat het verschillende ziektemechanismen kan ondervragen door specifieke moleculaire doelwitten te kwantificeren om het CZS direct te bestuderen.

In dit proefschrift hebben we de cellulaire distributie en de regulatie van het translocator eiwit (TSPO) in cellen in het CZS in neurodegeneratieve ziekten en hun respectievelijke diermodellen onderzocht. TSPO is over het algemeen een marker van geactiveerde microglia en is door veel onderzoeken als zodanig bestempeld. Eerste studies over diermodellen van neuro-inflammatoire ziekten toonden aan dat TSPO ook tot expressie wordt gebracht door andere celtypen dan microglia, maar deze bevindingen zijn grotendeels genegeerd door PET-onderzoeken, en de eerste onderzoeken bij mensen waren kwalitatief in plaats van kwantitatief. Onlangs is in vitro aangetoond dat primaire microglia van de muis TSPO meer tot expressie brengen in een pro-inflammatoire omgeving, terwijl dit bij primaire humane microglia niet het geval is. Nieuwe inzichten in de triggers van TSPO en de cellulaire expressie van TSPO in het CZS in diermodellen vertalen zich dus mogelijk niet naar menselijke ziekten. Om de cellulaire expressie te onderzoeken en de triggers van TSPO beter te begrijpen, hebben we eerst onderzoek uitgevoerd naar TSPO expressie in MS om TSPO-expressie in gliacellen te valideren en hoe het TSPO-eiwit werd gereguleerd. Daarna hebben we ons onderzoeksveld verbreed en hebben naar andere veelvoorkomende neurodegeneratieve ziekten zoals AD en ALS en hun respectievelijke diermodellen gekeken. Daarnaast hebben we gebruik gemaakt van openbaar beschikbare databases over TSPO-regulatie op meerdere moleculaire niveaus.

Een ander doel van het proefschrift was om de rol van microglia en astrocyten als aangeboren immuuncellen van het CZS te onderzoeken, aangezien blijkt dat ze meer betrokken zijn bij diverse functies in ziektes van het CZS. Hoewel historisch gezien microglia werden beschouwd als de fagocyten van de hersenen en astrocyten als omstanders in reactie op schade, heeft de opkomst van geavanceerde technologieën zoals single cell en single nucleus RNAseq, evenals gedetailleerde pathologiestudies die beschikbaar zijn gemaakt door een overvloed aan antilichamen aangetoond dat microglia en astrocyten diverse en complexe functies hebben in het CZS. Samen hebben deze onderzoeken geleid tot gedetailleerder begrip van de rol van microglia en astrocyten als aangeboren immuuncellen van het CZS.

Hoofdstuk 2 beschrijft de expressie van het TSPO eiwit in MS in vergelijking met niet-neurologische controles van dezelfde leeftijd. De TSPO expressie wordt onderzocht in gliacellen in witte en grijze stoflaesies in de hersenen en in het ruggenmerg. In deze studie laten we zien dat TSPO expressie niet exclusief aanwezig is in geactiveerde microglia, aangezien homeostatische microglia ook TSPO tot expressie brengen. Bovendien laten we zien dat TSPO expressie niet beperkt is tot microglia, maar dat astrocyten, en in mindere mate endotheelcellen en oligodendrocyten, ook in staat zijn TSPO tot expressie te brengen in het

CZS. We laten ook zien dat TSPO expressie sterk gecorreleerd is met de TSPO ligandbinding die in de kliniek wordt gebruikt voor TSPO onderzoek en beeldvorming van neuro-inflammatie. De aanwezigheid van TSPO in homeostatische microglia en astrocyten heeft implicaties voor de interpretaties van TSPO PET, en er moet dus rekening mee worden gehouden bij het interpreteren van deze gegevens.

Hoofdstuk 3 borduurt voort op het vorige hoofdstuk uit en bevat een karakterisering van TSPO expressie in MS-laesies met behulp van meerdere markers van microglia (IBA1, HLA-DR en CD68). We hebben ook onderzocht of TSPO+ homeostatische microglia markers van activatie tot expressie brachten. Daarnaast hebben we de hoeveelheid TSPO die tot expressie wordt gebracht door microglia in MS-laesies onderzocht en dit gecorreleerd met morfologische gegevens. In deze studie repliceerden we de bevindingen van hoofdstuk 2, maar ontdekten ook dat bijna alle TSPO+ cellen, in de witte stof, microglia waren. Daarnaast lieten we zien dat het fenotype van TSPO+ cellen in controle en NAWM homeostatisch was, en het fenotype in actieve en chronisch actieve laesies geactiveerd was. Wat nog belangrijker is, we vonden geen verschillen in de expressie van TSPO in geactiveerde microglia in vergelijking met microglia die homeostatisch waren in NAWM en controle witte stof, ook vonden we geen verschillen in morfologie die wijzen op veranderingen in TSPO expressie. Over het algemeen geeft dit aan dat TSPO PET het best kan worden geïnterpreteerd als het totale aantal microglia in plaats van het fenotype en de activatie van lokale microglia.

Hoofdstuk 4 onderzoekt TSPO expressie in gliacellen bij meerdere neurodegeneratieve ziekten, namelijk AD, ALS en MS, en hoe TSPO tot expressie komt in hun veelgebruikte muismodellen. Omdat in veel onderzoeken is aangenomen dat TSPO PET een toename van TSPO in geactiveerde microglia weerspiegelt, hebben we getest of deze wijdverbreide veronderstelling waar was voor deze neurodegeneratieve ziekten en muismodellen. We voerden een meta-analyse uit van openbaar beschikbare expressiedata en ontdekten dat TSPO expressie in een reeks van pro-inflammatoire activeringsstimuli consistent en aanzienlijk toeneemt in muizen, maar niet in humane macrofagen en microglia *in vitro*. Daarna voerden we een vergelijkende analyse uit van het TSPO promotorgebied in het DNA in een reeks zoogdiersoorten en ontdekten dat de bindingsplaats voor AP1 (een transcriptiefactor die macrofaagactivering reguleert) aanwezig is in en uniek is voor een subset van soorten binnen de Muroidea-superfamilie van knaagdieren en afwezig bij mensen. In overeenstemming met de in vitro gegevens vonden we dat postmortale microglia TSPO expressie niet verhogen wanneer ze in een pro-inflammatoire toestand zijn in AD, ALS en MS, en een primatenmodel van MS. Daarentegen is TSPO expressie aanzienlijk verhoogd in geactiveerde myeloïde cellen in alle muismodellen van deze ziekten. Ten slotte hebben we de relatieve expressie van TSPO onderzocht in openbaar beschikbare nucleus RNA-sequencing-datasets van het CZS van AD en MS en hun respectievelijke diermodellen. Opnieuw vonden we geen bewijs voor een toename van TSPO expressie in de humane CZS ziektes in geactiveerde microglia, terwijl microglia van muizen wel een toename in TSPO expressie vertoonden. Deze gegevens suggereren dat TSPO PET gevoelig is voor microglia activatie alleen in een subset van soorten binnen de Muroidea-superfamilie van knaagdieren. Daarentegen weerspiegelt het bij mensen en andere zoogdieren slechts de lokale dichtheid van ontstekingscellen, ongeacht de ziektecontext. De klinische interpretatie van het TSPO PET signaal moet daarom worden herzien.

Hoofdstuk 5 vat alle gepubliceerde studies over TSPO expressie in het CZS in gezonde en zieke hersenen samen. We bieden een overzicht van TSPO expressie in veelgebruikte diermodellen en in veel voorkomende humane neurodegeneratieve en psychiatrische ziekten. Op basis van de literatuur concluderen we dat de aanwezigheid van TSPO in andere celtypen dan microglia, zoals astrocyten en endotheelcellen, in toenemende mate wordt geaccepteerd. We laten zien dat de cellulaire TSPO niet alleen afhankelijk is van de pathologie, maar ook van het ontwikkelingsstadium en de mate van activatie van de cel. Hoewel het monitoren van TSPO levels in het CZS nu veel wordt gebruikt als een graadmeter voor microglia activatie en neuro-inflammatie, is er meer onderzoek nodig om de middelen en de cellen die betrokken zijn bij ontstekingsprocessen beter te karakteriseren en hoe deze processen bijdragen aan het TSPO PET signaal. Toekomstige studies zouden ook het therapeutische potentieel van TSPO manipulatie in het CZS kunnen onderzoeken.

Hoofdstuk 6 geeft een kort inzicht in de desastreuze effecten van verlies van axonen op neurodegeneratie en klinische invaliditeit bij MS. We onderzochten de hoeveelheid axonaal verlies in het ruggenmerg van MS patiënten en correleerden dit met de aanwezigheid van synaps-eiwitten en het verlies van lokale neuronen. We ontdekten dat de hoeveelheid synaptische pathologie in het ruggenmerg van MS zeer uitgebreid is, het aantal synaptische boutons, verantwoordelijk voor neuronale communicatie, was bijna tot nul teruggebracht in laesies in de grijze stof in vergelijking met gezond ruggenmergweefsel. Bovendien hadden mensen met MS een aanzienlijk verlies van neuronen in het ruggenmerg. Het verlies van synaptische boutons correleerde echter niet met het verlies van neuronen in de grijze stof in het ruggenmerg. We concludeerden dat axonaal verlies en neuronaal verlies bij MS uitgebreider is dan eerder gerapporteerd in de literatuur.

Hoofdstuk 7 onderzoekt de immunomodulerende rol van astrocyten en oligodendrocyten, gliacellen waarvan in het algemeen niet wordt aangenomen dat ze functies hebben als immuuncellen. Astrocyten werden lang gezien als omstanders tijdens immuungerelateerde gebeurtenissen in het CZS. Oligodendrocyten worden lang gezien als de slachtoffers van neuro-inflammatie. Een toenemend aantal studies wijst op meer complexe rollen voor gliacellen tijdens immuunactivatie. We ontdekten dat astrocyten en oligodendrocyten belangrijke cel-tot-cel communicatie hebben tijdens ontstekingen. Astrocyten en oligodendrocyten spelen een actieve rol als aangeboren immuuncellen door chemokines uit te scheiden en kunnen dus zowel andere gliacellen als elkaar beïnvloeden.

Hoofdstuk 8 belicht een belangrijk onderwerp dat met de ontwikkeling van nieuwe technologieën steeds belangrijker wordt. Historisch gezien worden microglia gezien als de macrofagen van het CZS, nieuwe technieken hebben verschillende rollen benadrukt. De belangrijkste functies in het CZS zijn de bescherming tegen mogelijke schade en om homeostase te reguleren. We laten zien dat microglia divers zijn en een veelzijdige rol spelen in de witte stof van de hersenen. Microglia hebben regionaal gedefinieerde functies die geassocieerd worden met ontwikkeling, homeostase, veroudering en in reactie op letsel, wat de lokale behoefte van het CZS-parenchym weerspiegelt. Deze heterogeniteit uit zich in verschillen in dichtheid, morfologie en de genen die microglia tot expressie brengen. We stellen belangrijke vragen waarmee het veld rekening moet houden in toekomstig onderzoek bij het onderzoeken van microglia-heterogeniteit. Zoals: ‘Hoe vergelijkbaar zijn muis (of andere dieren) en humane witte stof microglia?’ en ‘Hoe stabiel zijn microglia staten in de witte stof?’. Door het bewustzijn voor deze belangrijke vragen te vergroten, hopen we

het veld te stimuleren om de diverse microglia functies te onderzoeken om uiteindelijk op microglia gebaseerde therapieën te kunnen ontwikkelen.

Over het algemeen laat dit proefschrift zien dat TSPO bij mensen anders wordt gereguleerd dan bij muizen en dat alle gliacellen fungeren als aangeboren immuuncellen. De belangrijkste conclusies per hoofdstuk zijn:

- Microglia, maar ook astrocyten brengen TSPO tot expressie in MS-laesies, TSPO PET rapporteert eerder over cel dichtheid dan over activatiestatus (Hoofdstuk 2)
- TSPO wordt niet verhoogd in geactiveerde microglia in MS-laesies in vergelijking met homeostatische microglia in de NAWM en in controle witte stof (Hoofdstuk 3)
- De regulatie van TSPO is fylogenetisch divers tussen mensen en knaagdieren, wat resulteert in differentiële regulatie van het TSPO gen bij mensen. TSPO is niet verhoogd in geactiveerde microglia en astrocyten bij humane CZS-ziekten (Hoofdstuk 4)
- TSPO binding, cellulaire oorsprong en functionele significantie is afhankelijk van vele factoren, zoals de pathologie of het experimentele diermodel (hoofdstuk 5)
- Microglia activatie in het MS-ruggenmerg is geassocieerd met synaptisch verlies, resulterend in progressieve klinische invaliditeit (Hoofdstuk 6)
- Astrocyten en oligodendrocyten produceren en reageren op vele immunomodulerende factoren die een cruciale rol spelen bij immuunresponsen in het CZS (Hoofdstuk 7)
- Microglia hebben regionaal gedefinieerde functies in het CZS met betrekking tot ontwikkeling, homeostase, veroudering, neuro-inflammatie en als reactie op letsel, wat de lokale behoeften van het CZS-parenchym weerspiegelt (Hoofdstuk 8)

List of publications

Nutma E, Fancy N, Weinert M, Marzin MC, Tsartsalis S, Muirhead RCJ, Falk I, de Bruin J, Hollaus D, Pieterman R, Anink J, Story D, Chandran S, Tang J, Trolese MC, Saito T, Saido TC, Wiltshire K, Beltran-Lobo P, Philips A, Antel J, Healy L, Moore CS, Bendotti C, Aronica E, Radulescu CI, Barnes SJ, Hampton DW, van der Valk P, Jacobson S, Matthews PM, Amor S, Owen DR. Translocator protein is a marker ofa ctivated microglia in rodent models but not human neurodegenerative diseases. *bioRχiv.* May 2022

Macnair W, Calini D, Agirre E, Bryois J, Jakel S, Kukanja P, Stokar-Regenscheit N, Ott V, Foo L, Collin L, Schippling S, Urich E, **Nutma E**, Marzin M, Amor S, Magliozzi R, Heidari E, Robinson MD, French-Constant C, Castelo-Branco G, Williams A, Malhotra D. Single nuclei RNAseq stratifies multiple sclerosis patients into three distinct white matter glia responses. *bioRχiv.* April 2022

Vankriekelsvenne E, Chrzanowski U, Manzhula K, Greiner T, Wree A, Hawlitschka A, Llovera G, Zhan J, Joost S, Schmitz C, Ponsaerts P, Amor S, **Nutma E**, Kipp M, Kaddatz H. Transmembrane protein 119 is neither a specific nor a reliable marker for microglia. *Glia*. Mar 2022. Online ahead of print.

Amor S, McNamara NB, Gerrits E, Marzin MC, Kooistra SM, Miron VE, **Nutma E**. White matter microglia heterogeneity in the CNS. *Acta Neuropathol*. Feb 2022;143(2):125-141

Miedema A, Gerrits E, Brouwer N, Jiang Q, Kracht L, Meijer M, **Nutma E**, Peferoen-Baert R, Pijnacker ATE, Wesseling EM, Wijering MHC, Gabius H-J, Amor S, Eggen BJL, Kooistra SM. Brain macrophages acquire distinct transcriptomes prior to demyelination in multiple sclerosis. *Acta Neuropathol Comm*. Jan 2022;10(1):8

Amor S, **Nutma E**, Owen D. Imaging immune responses in neuroinflammatory diseases. *Clin Exp Immunol*. Dec 2021;206(3):248-250.

Amor S, **Nutma E**, Marzin MC, Puentes F. Imaging immunological processes from blood to brain in amyotrophic lateral sclerosis. *Clin Exp Immunol*. Dec 2021;206(3):301-313.

Nutma E, Ceyzeriat K, Amor S, Tsartsalis S, Millet P, Owen DR, Papadopoulos V, Tournier BB. Cellular sources of TSPO expression in healthy and diseased brain. *Eur J Nucl Med Mol Imaging*. Dec 2021;49(1):146-163.

Kotah JM, Hoeijmakers L, **Nutma E**, Lucassen PJ, Korosi A. Early-life stress does not alter spatial memory performance, hippocampal neurogenesis, neuroinflammation, or telomere length in 20-month-old male mice. *Neurobiol Stress*. Nov 2021;15:100379.

Bryois J, Calini D, Macnair W, Foo L, Urich E, Ortmann W, Iglesias VA, Selvaraj S, **Nutma E**, Marzin M, Amor S, Williams A, Castelo-Branco G, Menon V, De Jager P, Malhotra D. Cell-type cis-eQTLs in eight brain cell-types identifies novel risk genes for human brain disorders. *medRχiv*. Oct 2021

Zhu K, Wang Y, Salrus H, Geng K, **Nutma E**, Sun J, Kung SY, Bay C, Han J, Lund H, Amor S, Wang J, Zhang X, Kutter C, Guerreiro-Caicais AO, Hogberg B, Harris RA. Nanoengineered DNA origami with repurposed TOP1 inhibitors targeting myeloid cells for the midigation of neuroinflammation. *bioRχiv.* Oct 2021

Nutma E, Gebro E, Marzin MC, van der Valk P, Matthews PM, Owen DR, Amor S. Activated microglia do not increase 18 kDa translocator protein (TSPO) expression in the multiple sclerosis brain. *Glia*. Oct 2021;69(10):2447-2458.

Nutma E, Marzin MC, Cillessen SA, Amor S. Autophagy in white matter disorders of the CNS: mechanisms and therapeutic opportunities. *J Pathol*. Feb 2021;253(2):133-147.

Berglund R, Guerreiro-Cacais AO, Adzemovic MZ, Zeitelhofer M, Lund H, Ewing E, Ruhrmann S, **Nutma E**, Parsa R, Thessen-Hedreul M, Amor S, Harris RA, Olsson T, Jagodic M. Microglial autophagy-associated phagocytosis is essential for recovery from neuroinflammation. *Sci Immunol*. Oct 2020;5(52)

Petrova N*, **Nutma E***, Carassiti D, Rs Newman J, Amor S, Altmann DR, Baker D, Schmierer K. Synaptic Loss in Multiple Sclerosis Spinal Cord. *Ann Neurol*. Sep 2020;88(3):619-625.
*authors contributed equally

Baker D, **Nutma E**, O'Shea H, Cooke A, Orian JM, Amor S. Autoimmune encephalomyelitis in NOD mice is not initially a progressive multiple sclerosis model. *Ann Clin Transl Neurol*. Aug 2019;6(8):1362-1372.

Nutma E, van Gent D, Amor S, Peferoen LAN. Astrocyte and Oligodendrocyte Cross-Talk in the Central Nervous System. *Cells*. Mar 2020;9(3)

Gorter RP, Stephenson J, **Nutma E**, Anink J, de Jonge JC, Baron W, Jahreiss MC, Belien JAM, van Noort JM, Mijnsbergen C, Aronica E, Amor S. Rapidly progressive amyotrophic lateral sclerosis is associated with microglial reactivity and small heat shock protein expression in reactive astrocytes. *Neuropathol Appl Neurobiol*. Aug 2019;45(5):459-475.

Nutma E, Stephenson JA, Gorter RP, de Bruin J, Boucherie DM, Donat CK, Breur M, van der Valk P, Matthews PM, Owen DR, Amor S. A quantitative neuropathological assessment of translocator protein expression in multiple sclerosis. *Brain*. Nov 2019;142(11):3440-3455.

Nutma E, Willison H, Martino G, Amor S. Neuroimmunology- the past, present and future. *Clin Exp Immunol*. Sep 2019;197(3):278-293.

Gorter RP, **Nutma E**, Jahreiss MC, de Jonge JC, Quinlan RA, van der Valk P, van Noort JM, Baron W, Amor S. Heat shock proteins are differentially expressed in brain and spinal cord: implications for multiple sclerosis. *Clin Exp Immunol*. Nov 2018;194(2):137-152.

Stephenson J*, **Nutma E***, van der Valk P, Amor S. Inflammation in CNS neurodegenerative diseases. *Immunology*. Jun 2018;154(2):204-219.
*authors contributed equally

Bridel C, Koel-Simmelink MJA, Peferoen L, Derada Troletti C, Durieux S, Gorter R, **Nutma E**, Gami P, Iacobaeus E, Brundin L, Kuhle J, Vrenken H, Killestein J, Piersma SR, Pham TV, De Vries HE, Amor S, Jimenez CR, Teunissen CE. Brain endothelial cell expression of SPARCL-1 is specific to chronic multiple sclerosis lesions and is regulated by inflammatory mediators in vitro. *Neuropathol Appl Neurobiol*. Jun 2018;44(4):404-416.

Dankwoord

Nu op het bereiken van deze mijlpaal is het tijd voor een kleine terugblik op de reis naar dit moment. Vroeger was ik niet bepaald gemotiveerd om te leren en op de drempeltest van mijn basischool had ik dan ook een 1 voor leermotivatie, maar daar stond een 9 voor doorzettingsvermogen tegenover. En nu, tien jaar na het afronden van mijn middelbare school, mag ik mijn proefschrift verdedigen. Ik kan me nog goed herinneren dat ik biologie een van de stomste vakken vond. Toch werd mij geadviseerd om een keer te kijken naar de studie psychobiologie, omdat ik geïnteresseerd was in het brein. Na een dagje meekijken op de UVA was ik overtuigd, biologie was eigenlijk veel leuker dan ik tot dusver had begrepen, van daaruit is mijn passie voor het onderzoek naar het brein gegroeid. De reis naar dit moment, en het afronden van mijn tijd als PhD student is ook niet geweest zonder ups en downs. En ik heb heel veel te danken aan iedereen die mij heeft gesteund.

First off, dear **Sandra**, thank you for all the opportunities and space you have given me, not only to learn, but also to try my own things, which sometimes would fail. Your approach gave me room to become an independent researcher. Thank you for organising Christmas dinners, bringing me along to conferences, and letting me help in organising one. You have been wonderful in how you were always able to recruit more souls to help our research efforts. Unfortunately, all the social gatherings weren't always possible the last 2 years, but I will never forget that we went out for a wonderful dinner the day before the lockdown was announced in 2020 and you said that it could last until the summer. How wrong we were!

Beste **Paul**, dankjewel voor alle inzichten tijdens mijn PhD-traject, voor alle etentjes, bijeenkomsten en gezellige gesprekken over de afgelopen jaren.

Dear **Dave**, thank you for being a co-promotor on my thesis. Even though we have only met twice in real life during my time as a PhD student there were countless meetings, sometimes multiple times a week to discuss the papers that are in this thesis. You have always pushed me to get more out of the data I had gathered, and to put in extra bits of information that would convince the readers of our articles more.

Dan mijn rots in de branding, mijn Klaagmuur, en het lichtpuntje aan het einde van elke donkere tunnel en een zware werkdag. **Marjolein**, de vriendschap die we hebben opgebouwd over de afgelopen jaren is niet goed uit te drukken in woorden. Ik had hier niet gestaan, daar ben ik van overtuigd, zonder jou! De uren die we samen hebben geïnvesteerd in onderzoek en het uitwisselen van ideeën zijn ontelbaar. Om mislukte experimenten op te lossen konden we altijd bij elkaar terecht en samen ploegden we ons een baan door al ons labwerk heen. Ook al hebben we slechts co-auteurschap op één artikel, jij bent de grootste co-auteur van dit proefschrift en de afgelopen vier jaar van mijn leven. Daarnaast hebben we ook buiten werk heel wat uren samen doorgebracht, samen naar het tuincentrum, varen, bouwen, overleven, schilderen, eten, concerten. We delen heel veel interesses en voelen elkaar soms te goed aan! Mede door jou voel ik me thuis in Hoofddorp en ik kan me geen Hoofddorp voorstellen zonder jou. Bedankt voor elke lach en traan die we samen gelaten hebben, bedankt dat je me hebt betrokken met de creatieve activiteiten die je hier onderneemt, alleen en ook samen met Emma. Bedankt voor alle momenten tijdens onze bus of autoritjes naar werk en weer naar huis. Bedankt voor het zijn van jezelf en dat ik mezelf kan zijn bij jou! Er zijn zeker dingen die ik ben vergeten te noemen, maar ik weet zeker dat er nog genoeg momenten komen die we samen doorbrengen in te toekomst.

Beste **Manuel**, dank voor al je harde labwerk de afgelopen jaren. Mede dankzij jou inzet zijn de verschillende projecten tot een mooi einde gekomen. Het is me ook zeer bevallen dat we goed konden praten over andere onderwerpen dan werk. Nu de MS-groep op de neuropathologie verdwijnt moet ook jij op zoek naar een nieuwe plek en ik wil je daar heel veel succes mee wensen.

Beste leden van de comissie: prof. dr. Annemieke Rozemuller, prof. dr. David Baker, prof. dr. Elly Hol, prof. dr. Markus Kipp, dr. Marianna Bugiani, dr. Jeffrey Bajramovic, en dr. Wiep Scheper hartelijk dank voor het nemen van de tijd om mijn proefschrift te lezen en te beoordelen. Ik kijk er naar uit om met jullie van gedachten te wisselen over mijn onderzoek. / Dear members of the committee: prof. dr. Annemieke Rozemuller, prof. dr. David Baker, prof. dr. Elly Hol, prof. dr. Markus Kipp, dr. Marianna Bugiani, dr. Jeffrey Bajramovic, en dr. Wiep Scheper, thank you for taking the time to read and assess my thesis. I'm looking forward to exchange thoughts about my research.

Dear **Marianna**, thank you for your endless enthusiasm and all the scientific but also fun conversations over the past few years. I have learned a lot from your view on science. Thank you for incorporating me in the social activities with your group and your girls, it made my time in the neuropathology department memorable.

Beste **Bonnie**, **Jodie** en **Parand**, bedankt dat ik altijd welkom was bij jullie groep en dat we met elkaar konden praten over onze onderzoeken, samen inzichten en nieuwe bevindingen konden delen. Bedankt ook voor de leuke tijd die we hebben gehad samen in Dusseldorf en in de escape room.

Lieve **Kim**, ook al ben je al een tijdje weg, dankjewel voor de leuke tijd in het lab, de gesprekken en het samen lunchen op de kamer, waar we lief en leed met elkaar konden delen. We hadden altijd een leuke tijd samen en hebben veel gelachen over alle spannende ontwikkelingen op Lindanieuws. Ik denk altijd positief terug aan het moment dat ik spontaan met jou en Marjolein meeging naar het concert van Harry Styles. Nu bijna vier jaar later (waarvan 2 jaar uitstel) kunnen we deze zomer weer! Daarnaast heb ik er erg van genoten om mee te mogen maken dat Ivy onderdeel werd van jouw en Dennis zijn leven en dat deze prachtige dame er nu alweer dik twee jaar is.

Daarnaast wil ik graag alle andere (oud) collega's van de neuropathologie bedanken voor de prettige tijd, tijdens afdelingsuitjes en de samenwerking op het lab: **Tjado** bedankt voor alle hulp bij labwerk, het altijd meehelpen met de plakparty en voor de gezellige koffiepauzes op de kamer. **Jeroen**, **Baayla**, **Anna**, **Anke**, **Marlies**, **Priya**, **David**, **Andrea**, **Rianne** bedankt voor de leuke tijd die ik op de afdeling heb gehad de afgelopen jaren.

Mijn tijd als PhD-student ging ook gepaard met het begeleiden van studenten, die bijgedragen hebben aan het onderzoek in onze groep. Ik wil graag **Joy** en **Deirdre** in het bijzonder bedanken voor hun bijdrages aan het laatste project van dit proefschrift.

Dit proefschrift was niet mogelijk geweest zonder de eindeloze inzet van de **Nederlandse Hersenbank**, in het bijzonder **Michiel Kooreman**. Ook wil ik graag alle hersendonoren en hun families bedanken die dit bijzondere onderzoek mogelijk maken. Daarnaast wil ik ook graag de medewerkers van de **biobank** van het Amsterdam UMC bedanken.

Jinte, **Juliana**, **Loet** bedankt voor het fijne welkom in jullie groep en dat ik de laatste dingen van mijn PhD heb kunnen regelen. Ik kijk er erg naar uit om samen te werken en nieuwe projecten op te starten.

Vrienden, **familie**, en **schoonfamilie** wil ik ook graag bedanken voor alle leuke dingen die we hebben gedaan buiten het werk en voor jullie interesse in het onderzoek wat ik uitvoerde.

Lieve **Dirk** en **Hennie**, bedankt dat ik altijd welkom was in Wolvega en jullie mij met open armen en alle liefde altijd hebben ontvangen, ook in mijn jaar voor het studeren. Dat jaar heeft mij en DJ de ruimte gegeven om samen naar Amsterdam te verhuizen en heeft ook de basis gevormd voor waar we nu zijn.

Lieve **Papa**, **Mama**, en **Hedwig**: bedankt voor het altijd steunen van mijn ambities en jullie interesse in mijn werk. Papa en Mama, jullie warme thuishaven in Wytgaard heeft mede mogelijk gemaakt dat ik hier nu sta en mezelf heb mogen ontwikkelen tot de persoon die ik nu ben. Bedankt voor al jullie liefde, warmte en vertrouwen en dat ik altijd mezelf heb mogen zijn. Ik had het niet beter kunnen treffen dan met zulke lieve ouders. Lieve zus, bedankt dat we altijd welkom zijn op Ameland bij jou en Richard om te genieten van hoe mooi het daar is, bedankt dat we daar altijd tot rust konden komen. Wat ben ik trots op jou, en op onze lieve Elin, wat vind ik het fijn om oom te zijn!

Lieve **Dirk Jan**, wat een avontuur zijn de afgelopen jaren geweest. 10 jaar geleden zijn we samen verhuisd naar Amsterdam, en is dit allemaal begonnen. Inmiddels wonen we alweer een tijdje in Hoofddorp samen met Cosmo en Onyx. Bedankt voor alle steun en vertrouwen, tijdens het studeren maar ook tijdens mijn tijd als PhD-student. Ik kon altijd bij je terecht voor motivatie als ik er geen zin meer in had, dan herinnerde je me er aan dat ik het allemaal niet zo serieus hoefde te nemen. Bedankt voor alle leuke reizen de we gemaakt hebben en alle andere dingen die we samen hebben ondernomen. Ik ben erg dankbaar dat je ervoor hebt gekozen om jouw leven met die van mij te delen. Nu is het tijd voor onderzoek zonder de stress van een PhD. Bedankt voor alles en ik hou van je!

About the author

Erik was born on November 10, 1992. Although born prematurely, Erik was a lively, eager to learn and social child who loved action. At a young age Erik was interested in circus school and when he was 9 he went on tour through Scandinavia with Cirque Nouveau. After primary school Erik attended the Christian Gymnasium Beyers Naudé in Leeuwarden and his dean interested him in the study of Psychobiology. Because Erik did not have the right qualifications to study psychobiology, he obtained a physics diploma during a gap year in adult education. After that he was able to start studying at the University of Amsterdam.

Psychobiology was a great match with his interests because the study taught him a lot about how the human brain works and how little we often know about its mysteries. His studies went well and he managed to successfully complete his Bachelor's degree without delay after finishing an internship at the psychiatry department of the VU medical centre.

For his Master's degree he focused on psychopharmacology and pathophysiology of the central nervous system. He completed internships both at the UVA, studying the effects of early life stress on the immune landscape of the brain, as well as at the VU starting his research on TSPO. Obtaining his master's degree went well and after two years he received his diploma.

Immediately after graduating, he was able to start his PhD research at the Amsterdam UMC – Location VUmc. His research focuses on visualizing microglia in neurodegenerative disease using PET. Under the guidance of prof. dr. Paul van der Valk, prof. dr. Sandra Amor, and dr. David Owen he has further developed himself into a real scientific researcher, who has successfully completed his PhD.

He will continue to develop and chase his interests in the Neurobiology and Ageing group at the BPRC as a postdoctoral researcher.